RICE UNIVERSITY

Biomaterial-Based Strategies for Craniofacial Tissue Engineering

by

James D. Kretlow

A THESIS SUBMITTED
IN PARTIAL FULFILLMENT OF THE
REQUIREMENTS FOR THE DEGREE

Doctor of Philosophy

APPROVED, THESIS COMMITTEE:

Antonios G. Mikos, Professor (Chair)
Bioengineering, Rice University

K. Jane Grande-Allen, Associate Professor
Bioengineering, Rice University

F. Kurtis Kasper, Faculty Fellow
Bioengineering, Rice University

James M. Tour, Professor
Chemistry, Rice University

John A. Jansen, Professor
Chair, Periodontology and Biomaterials
Radboud University Nijmegen Medical Center

HOUSTON, TX
JANUARY, 2010

ABSTRACT

Biomaterial-Based Strategies for Craniofacial Tissue Engineering

by

James D. Kretlow

Damage to or loss of craniofacial tissues, often resulting from neoplasm, trauma, or congenital defects, can have devastating physical and psychosocial effects. The presence of many specialized tissue types integrated within a relatively small volume leads to difficulty in achieving complete functional and aesthetic repair. Tissue engineering offers a promising alternative to conventional therapies by potentially enabling the regeneration of normal native tissues. Initially, a stimulus responsive biomaterial designed for injectable cell delivery applications was investigated with the goal of providing a substrate for osteogenic differentiation of delivered cells. In order to enable faster clinical translation, later efforts focused on novel combinations of regulated materials. Most common approaches using cell delivery for bone tissue engineering involve the harvest and *ex vivo* expansion of progenitor cell populations over multiple weeks and cell passages. The effect of aging and passage on proliferation and differentiation were analyzed using murine mesenchymal stem cells as a model. These cells lose their ability to proliferate and differentiate with increases in donor age and

passages during cell culture. Delivery of uncultured bone marrow mononuclear cells was then investigated, and it was determined that when delivered to porous scaffolds these cells, which can be harvested, isolated, and returned to the body within the setting of a single operation, significantly increased bone regeneration *in vivo*. Finally, because these techniques of scaffold implantation and cell delivery would likely fail if delivered to an exposed or infected wound, a method of space maintenance was investigated. Space maintainers made of poly(methyl methacrylate) and having tunable porosity and pore interconnectivity were evaluated within a clean/contaminated mandibular defect. Low porosity space maintainers were found to prevent soft tissue collapse or contracture into the bony defect and allowed surrounding soft tissues to penetrate the pores of the implant, enabling healing over 12 weeks. The tissue response and wound healing characteristics of these implant was favorable when compared to solid or high porosity implants. Although optimization and further investigation of these techniques is necessary, in combination these approaches demonstrate one possible and translatable approach towards craniofacial tissue regeneration.

ACKNOWLEDGEMENTS

This work is dedicated to my family, Cindy, Bill, John, Betty, and Shahnaz.

The work presented in this thesis results from the direct and indirect contributions of many people, to all of whom I am indebted. I would first like to thank my Ph.D. advisor, Tony Mikos, for his support and guidance throughout my graduate studies. I am proud to call Dr. Mikos a mentor and friend, but without any frame of reference, it means little to say that he is the best Ph.D. advisor. I can say without hesitation that I was consistently challenged, given incredible opportunities, and amply rewarded for my work. I've benefitted from years of hard work by Dr. Mikos and the students who preceded me in his lab, and I have immensely enjoyed my time in his lab.

I would also like to thank the other members of my committee, Dr. Jane Grande-Allen, Dr. Kurt Kasper, Dr. James Tour, and Dr. John Jansen, for their time and guidance. Special thanks are also owed to Dr. Jansen and Dr. Wei Liu and Dr. Yilin Cao of the 9th People's Hospital in Shanghai, China, who were kind enough to allow me to visit their labs, interact with their students, and experience other parts of the world. Dr. Mark Wong of the University of Texas Health Science Center at Houston has also played an instrumental role in many of the projects on which I've been involved.

The National Institutes of Health and the Department of Defense funded most of the work presented in this thesis. Additionally, I've received personal funding through the Medical Scientist Training Program at Baylor College of

Medicine, the NIH Biotechnology Training Grant of the Institute of Biosciences and Bioengineering at Rice, and the Keck Center Nanobiology Training Program of the Gulf Coast Consortia.

I've had the pleasure and reaped the benefits of working with a number of talented people here at Rice. I've enjoyed interacting professionally and personally with all of the members of the Mikos Lab whose studies have coincided with mine. I was fortunate enough to join the lab at the same time as Leda Klouda; it has been incredibly valuable to go through my graduate studies with someone else to share the highs and lows. Also, Michael Hacker, Kurt Kasper, and Simon Young gave their friendship and took their time to teach me how to be a better student and person. During the later parts of my studies, Patrick Spicer gave me months of help and made many long days much more enjoyable.

At Baylor College of Medicine, Dr. Sharon Plon, Kathy Crawford, and Vanessa Hatfield have given me advice, guidance and assistance covering a broad range of topics.

Finally, my family has provided unwavering support of my academic pursuits. My parents and grandmother never discouraged questions and always did their best to answer "Why?", so I kept asking. My wife, Shahnaz, has given me love, friendship, and support that makes each day better than I could imagine.

Table of Contents

List of Figures

Chapter 1

Tissue Engineering: A Historical Perspective[†]

"Begin at the beginning and go on till you get to the end: then stop."

-Lewis Carroll, *Alice's Adventures in Wonderland*

1.1 Introduction

Tissue engineering and the synonymous or closely related field of regenerative medicine have drawn the widespread attention of clinicians, scientists, policy makers, investors, and the general public for over a decade dating back to the early to mid 1990s. Earlier, pioneering efforts in and related to the field of tissue engineering, including many of the key discoveries that later became the foundation for this field, were made long before this more generalized recognition and subsequent definition of this field. Because the field of tissue engineering, as recognized specifically by term itself, is relatively young but draws upon substantial, sometimes centuries old efforts in many related fields, adequately providing an overview of the history of tissue engineering is a difficult endeavor.

[†] Sections of this chapter will be published as the following book chapter: Kretlow JD and Mikos AG. Tissue Engineering: A Historical Perspective. *Tissue Engineering for the Hand: Research Advances and Clinical Applications*. Mountain View: World Scientific Publishing Co., Inc. (2010).

Providing a truly complete history of any field so closely tied to the understanding of biological processes, human physiology, materials science and engineering, and the practice of medicine within the confines of a single chapter or thesis would prove to be impractical due to the magnitude of existing and relevant knowledge within these fields. Conversely, a historical perspective that examines tissue engineering through some rigidly defined criteria such as recent definitions of the term tissue engineering, formulated only once the field has become well demarcated within related areas of science and engineering, would fail to give proper credit to nor engender any appreciation of the substantial efforts related to but not wholly within the present day confines of tissue engineering.

Because of this, we will first aim to provide a working definition of tissue engineering that somewhat limits our scope but allows for deviations into related fields where appropriate. Subsequent sections of this chapter will examine the history of the field within this context, organized broadly in chronological order but with an attempt to also look at certain key areas of scientific exploration within these chronological boundaries.

1.1.1 Defining tissue engineering

In the 1993 *Science* article that is often regarded as having brought tissue engineering into focus within the general scientific community, Robert Langer and Joseph Vacanti loosely defined the field as one that combines engineering and the life sciences towards developing biological tissue substitutes.[1] They went on

to identify cells and cell substitutes, growth factors and delivery vehicles, and cell-scaffold constructs as general strategies for tissue engineering. Today, researchers often refer to the tissue engineering paradigm when defining the field – some combination of bioactive factors, cells, and matrices for the generation or regeneration of living tissues.

Both definitions, while accurate and widely accepted today, prove too limiting within a historical context. Many seminal discoveries related to the field of tissue engineering were not aimed at conception towards generating tissue substitutes. Many of the earliest discoveries or observations also fail to appreciate or involve any of the critical aspects that now form the tissue engineering paradigm. Nonetheless, these efforts deserve mention.

For the sake of this chapter, tissue engineering can be defined as *an attempt, technique, or technology made or at some point applied towards the preternatural generation, regeneration, or restoration of native tissue structure and/or function using biological components.* This definition is purposefully broad, allowing for a wide contextual scope highlighting many predecessors to today's field of tissue engineering. This definition also includes the field of regenerative medicine, which, while often considered identical or overlapping with tissue engineering, is more correctly regarded by those in the field as the products and techniques developed through tissue engineering processes that are directly involved in the support and practice of medicine.[2]

1.1.2 Overview: why tissue engineering?

What can be gleaned from examining the history of tissue engineering, or rather, why should a historical perspective be of interest to those reading this thesis? First, even a cursory outline of tissue engineering in the historical sense provides strong evidence confirming the interdisciplinary nature of the field. Contributions from all areas of the natural sciences, engineering, and medicine will be presented both in this chapter and referred to in the rest of this thesis.

Second, the problems that today's tissue engineers seek to tackle have existed for thousands of years, and while etiologies may have changed and existing therapies have improved over time, the need for solutions has not. Slowly, some of these problems are being incrementally yet effectively addressed through tissue engineering approaches.

Finally, while specific and more recent advances will be covered in this chapter and others, historical perspectives are necessary to realize and appreciate that what may often be presented as seemingly science fiction is actually grounded in years, decades, and in some cases, centuries worth of scientific exploration. We do not aim to present tissue engineering as a panacea for the destruction or dysfunction of all tissues; it is not. Rather, we aim to provide some level of historical context such that, when considered along with the other knowledge presented within this thesis, one can examine recent advances and potential applications with a hopeful yet critical eye.

1.2 Conception to Birth

Adopting the definition laid out in section 1.1.1, one can loosely trace the early history of tissue engineering along a similar path as the history of surgery. Areas such as wound healing and organ transplantation are critical in both fields and played a large role in forming the foundations of tissue engineering. This section will highlight the earliest efforts related to tissue engineering and then examine in greater detail the advances of the 20th century and particularly the 1990s that led to the recognition of tissue engineering as a distinct field.

1.2.1 Ancient foundations

Beginning any discussion of tissue engineering with a section describing ancient history seems a bit exaggerated. Despite the fact that tissue engineering as a formal field is still relatively new, many principles of tissue engineering have been applied dating back to ancient times. Some authors have even noted that the first verse of Genesis in the Christian Bible mentions tissue engineering in the form of extraction and expansion of a man's rib resulting in a complete woman.[3] A brief examination highlighting some ancient predecessors to today's tissue engineers proves that while technologies and our understanding of biology and engineering have greatly expanded, many of the problems of the ancient time have persisted to become modern problems.

The Edwin Smith papyrus (Figure 1.1), an Egyptian text dating between 2600 – 2200 B.C., describes sutured closure of wounds allowing for subsequent healing by primary intention.[4] Although wound healing is of interest in many

fields, sutured closure of wound represents one of the earliest examples of tissue engineering. Because many of the wounds described would otherwise have healed by secondary intention, wound closure and healing represents a preternatural regeneration of native tissue structure/function as it minimizes scarring and thus improves the strength of the healed wound. Additionally, suturing with silk or linen/gum combinations was likely among the first successful uses of biomaterials. Despite a greater than four millennia history, wound healing remains a heavily investigated topic today as researchers and clinicians attempt to both gain improved understanding of its regulation[5, 6] and develop better therapies to aid in this process.[7, 8]

Working around 600 B.C., the Indian professor and clinician Sushruta provided the first written record of the use of rotational flaps to reconstruct amputated noses – the result of corporal punishment meted out in ancient India.[9] These early flaps, taken from the forehead with the angular artery serving as blood supply, used autologous tissue to restore the aesthetic function of the mutilated nose.[10] This technique also represents one of the earliest uses of autologous tissue for restorative purposes, and similar techniques remain the gold standards of treatment for many cases of tissue loss or dysfunction today.

A host of other important discoveries upon which today's field of tissue engineering lies began during antiquity. While significant efforts towards understanding anatomy, physiology, and various disease processes were made

during ancient times and are no doubt critical in modern tissue engineering, the scope of these subjects makes them best left to other, dedicated texts.

1.2.2 Renaissance through 19th century

The Renaissance period was not without contributions in the area of tissue engineering. Modified approaches to rhinoplasty, similar to those of Sushruta, emerged in Italy at the hands of the 15th century Branca and Viano families,[4, 11] followed by the 16th century efforts of Giulio Cesare Arantius (also referred to as Aranzio),[12] and finally popularized (and often solely attributed to) by the famous Renaissance surgeon Gaspare Tagliacozzi (Figure 1.2) in *De Curtorum Chirurgia per insitionem*, a 700-page surgical treatise published in 1597, two years before Tagliacozzi's death.[13] The technique used in these rhinoplasties, now referred to as surgical or vascular delay, at the time involved the elevation of a bipedicled flap from the forearm and later the anterior brachium. Medicated linen or cotton lint was then placed under the flap to prevent reattachment, and after two weeks to one month, the flap was attached to the patient's nose.

Delay represents a major step forward in the history of tissue engineering. Whereas wound edge approximation to allow for closure and healing by primary intention seems an obvious (although mechanistically complex) technique, delay represents one of the first non-obvious techniques resulting in tissue manipulation or truly engineering beyond that visible with the naked eye. Although the mechanism involved in delay was almost certainly not understood by its earliest practitioners, for one of the first times, autologous tissue was being

modified through a complex interplay between sympathetic tone, vascular tone, tissue metabolism, and ultimately neovascularization via endothelial progenitor cell recruitment.[14] It has taken nearly 500 years since Tagliacozzi's publication detailing these methods for them to be well understood, and vascular delay remains an accepted practice towards conditioning flaps today.[15, 16] For tissue engineering, vascularization of engineered tissues and angiogenic control remain one of the greatest and most unmet challenges facing the field.[17] Significant research efforts continue towards determining effective material and cellular parameters and growth factor regimes to induce neovascularization and angiogenesis such that *ex vivo* or *ex situ* engineered tissues of a clinically relevant size can be constructed.[18, 19]

Allograft transplantation was the next major historical step towards tissue engineering. Although evidence of allografts from earlier points in history are apparent, notably including a lower limb allograft transplanted by Saints Cosmas and Damian and captured in a famous painting by Fra Angelico (Figure 1.3), most early allografts were subject to rejection and disease transmission. The British surgeon John Hunter performed some of the first successful transplantations in the late 18th century. Hunter focused primarily on transplanting teeth, first using a rooster as an animal model but later transplanting human teeth between subjects.[20] This practice was short lived due to the spread of diseases such as syphilis through the practice rather than rejection.

Skin grafts were likely the first allografts to gain more widespread use. Giuseppe Baronio, a contemporary of John Hunter, published extensively on skin autografting in animals, likely paving the way for experiments with allografts.[4] Winston Churchill served as a skin graft donor for a fellow soldier in 1898,[21] although it would be nearly 50 years and two world wars before a better understanding of immune rejection existed.[22]

Corneal transplants were also investigated during the 19th century. Samuel Bigger performed a successful allograft cornea transplantation between gazelles while a prisoner in Egypt in 1837;[23] however, the first successful transplant in humans would not occur until the early 20th century.

Around this time, Nicholas Senn found that decalcified bone induced healing within bone cavities;[24] demineralized bone matrix is now a widely used product for bone healing and regeneration. The mechanism for this effect would not be known until the middle of the next century, and Senn's approach was impressive because, similar to that of Tagliacozzi's delay, he was modifying a human tissue to increase its effectiveness in regenerating an orthotopic defect. The next two sections will further discuss the use of the extracellular matrix and matrix components as powerful tissue engineering tools.

1.2.3 20th century advances

The 20th century saw significant advances in every area of science and technology, including tissue engineering. Progress in the first half of the century was similar to that of the decades before in that it was rooted deeply but

disparately in clinical medicine, biology, and engineering. During the second half of the century, however, important advances in a variety of fields began to be integrated in what would eventually lead to the birth of tissue engineering as a unique discipline.

Organ transplantation

In 1905, Austrian physician Eduard Zirm performed the first successful, full thickness human corneal allograft transplantation.[25] That same year, Alexis Carrel and Charles Guthrie reported a method to anastomose vessels,[26] a discovery that would lead to a Nobel Prize in 1912 for Carrel and that would later allow for solid organ transplants. In 1935, Carrel and aviator Charles Lindbergh published *The Culture of Whole Organs*, a book detailing *ex vivo* culture techniques to keep entire solid organs alive, including the use of a perfusion pump.[27]

Significant other contributions were made towards organ transplantation in the early and mid 20th century, including the first successful transplantations of many organs and the elucidation of many key aspects of immune tolerance and rejection. While undoubtedly these contributions are relevant and important within the field of medicine and tissue engineering, we will begin to limit our overview at this point to the first attempts towards tissue engineering in the sense that the term is used today. Organ transplants are a life saving therapy; however, persistent problems with organ shortages and immune rejection can be viewed as partially contributing to the development of tissue engineering.

In combination with medical advances, political and military events of the early 20th century also contributed to the rise of tissue engineering. Antibiotics, the use of plasma, and other life-saving medical and surgical techniques decreased mortality in the first two world wars relative to previous wars. As a result, soldiers were surviving previously fatal injuries but often at the cost of disfiguring tissue loss. Other authors have noted the increased importance of reconstructive surgeons following WWI due to the incidence of craniofacial injuries,[28] and this increased morbidity rather than mortality provided a nidus from which tissue engineering would later emerge.

Vascular grafts

Nearly 50 years after Carrel described vessel anastomosis, Arthur Voorhees made the first synthetic vascular graft, replacing aortic segments in dogs with a poly(vinyl chloride) based fabric.[29] Poly(methyl methacrylate) and other polymeric materials had been used previously in dental applications such as dentures, but Voorhees used a synthetic material to replace a tissue whose functionality was dependent on interactions with both adjacent vascular tissue and blood. Over the next 30 years, endothelial cell seeding of vascular grafts, resorbable graft materials, and finally *in vitro* graft engineering would be studied.

Bone and osteoinduction

Also in the 1950s, Marshall Urist began publishing studies on the phenomenon of bone induction using transplanted bone.[30, 31] Urist published groundbreaking papers that described in 1965 the differentiation of

osteoprogenitor cells in the presence of decalcified bone matrix[32] and later the isolation of osteoinductive bone morphogenetic proteins (BMPs),[33] confirming a preexisting hypothesis regarding the existence of an osteogenic substance within bone.[34] Sampath and Reddi were later able to isolate this osteogenic substance, bone morphogenetic protein 2 (BMP-2),[35] and it is now the basis for both commercially available products for bone regeneration and the focus of a wide variety of experimental applications within bone tissue engineering.[36-38]

Stem cells

Critical advances in cell biology were being made beginning in the 1960s that would later be integrated into tissue engineering approaches. Researchers were beginning to explore in depth the ability of terminally differentiated tissues to renew and regenerate.[39, 40] Recognition of a population of pluripotent circulating progenitor cells gave the first signs of the existence of marrow stromal or mesenchymal stem cells, a cell population that is potentially one of the most powerful tools at the disposal of today's tissue engineers.[41, 42] Following up the 1964 work of Kleinsmith and Peirce,[43] Gail Martin[44] and the team of Martin Evans and Matthew Kaufman[45] described in separate studies published in 1981 the first isolation of embryonic stem cells.

Other cell-based approaches

Pluripotent cells represent a promising technology for tissue engineering due to the ability to potentially harvest cells from the patient, then expand, differentiate and possibly form a functional tissue *in vitro*, followed by implantion

of the cellularized construct back into the patient with little risk of immune reaction. The use of differentiated cells has the disadvantage of possible lack of availability of autologous cells if an organ has been severely damaged or uniformly diseased. Nevertheless, tissues engineered using expanded allogeneic cells can be used to reduce the shortage of available donor tissue for transplantation or reconstruction.

The birth of tissue engineering

The field of tissue engineering as we know it today was eventually borne from efforts to combine differentiated somatic cells with biomaterials to form new living tissues either *in vitro* or *in vivo*. One such approach using endothelial cells to line synthetic vascular grafts was already, albeit briefly, mentioned. A similar approach towards replacing the function of the pancreas was taken by William Chick and his colleagues. Their approach involved seeding pancreatic beta cells on a semipermeable membrane to create a hybrid pancreas that combined living and artificial components.[46] This hybrid pancreas was used to successfully treat diabetes in rats[47] and later dogs[48] and in 1985 resulted in the formation of BioHybrid Technologies, an early tissue engineering company.

Following a similar path, W.T. Green investigated cartilage formation *in vitro* and *in vivo*.[49] His approach using cells implanted on a specifically tailored scaffold would years later be adopted as the fundamental technique in tissue engineering.[3] This same principal of using tailored scaffolds to support tissue growth was the idea behind the first tissue engineering company (although at the

time the founders referred to the idea as tissue gardening), Interpore Cross International, Inc., founded in 1975.[50]

In 1981, the cell-scaffold approach yielded reports of the first *in vitro* generated, full thickness skin grafts.[51, 52] One approach that resulted from collaboration between John Burke and Ioannis Yannas used a collagen and silicone based material that served as a dermal template, encouraging the ingrowth of native skin and vessels from surrounding skin. The approach taken by Eugene Bell and Howard Green used autologous dermal fibroblasts and epidermal keratinocytes, expanded *in vitro*, and a collagen matrix to generate a full thickness skin graft or living skin equivalent that can be sutured or stapled in place during surgery without the risk of rejection.

With the ability to grow functional, living tissues *in vitro*, the birth of tissue engineering was well underway. The first use of the term *tissue engineering* appears in a 1984 paper describing the macrophage mediated lining of a corneal prosthesis with a membrane.[53] One year later, in 1985, Y.C. Fung proposed that the NSF establish a new research center to be known as the "Center for the Engineering of Living Tissues".[50] His proposal was rejected, but tissue engineering, both the term and the field, was on the way to becoming established within the scientific community. In 1988, Joseph Vacanti and Robert Langer published what would be the first of many tissue engineering papers together – a study of cell transplantation using bioresorbable scaffold carriers.[54]

1.2.4 The 1990s: research, recognition, and general interest

Research in the early part of the 1990s continued along a similar path as that of the late 1980s. Groups were beginning to focus on biomaterial scaffold fabrication and to characterize the interaction between cells and these scaffolds,[55-58] an area that remains a critical component of tissue engineering research to this day. Publication of the article titled "Tissue Engineering" in the May 14, 1993 issue of *Science* is viewed as the introduction of the field to the broader scientific community.[1] This article helped define tissue engineering, describe critical areas for research within the new field, and also provided a glimpse into the significant potential held within the field.

It was also around this time that tissue engineering societies began emerging across the U.S. and the rest of the world.[59] The Tissue Engineering Society was launched in 1994 and later evolved into the Tissue Engineering Society International (TESI) and then TERMIS, the Tissue Engineering and Regenerative Medicine International Society. Charles A. Vacanti of the Massachusetts General Hospital and Harvard Medical School and Antonios G. Mikos of Rice University founded the journal Tissue Engineering, published by Mary Ann Liebert, Inc. Publishers, in 1994. The first issue was released in early 1995, and the journal remains the flagship journal dedicated solely to tissue engineering research. The journal now publishes in 3 parts, devoted to research, reviews, and methods, with Antonios Mikos now joined by co-editors-in-chief

Peter C. Johnson, who in the early 1990s had formed the Pittsburgh Tissue Engineering Initiative, along with John A. Jansen and John P. Fisher.

Research in the 1990s continued to expand the knowledge of biomaterial-cell interactions. Discoveries in other fields that would later become critical to tissue engineering applications, such as adult pluripotent stem cell characterization,[60, 61] were also made during this period.

In 1997, public interest in tissue engineering was sparked by major media outlets' coverage of what has become known as the "Vacanti mouse." A 1997 publication in *Plastic and Reconstructive Surgery* from the laboratory of Charles A. Vacanti described the fabrication of an ear shaped cartilage construct via transplantation of chondrocytes onto auricle-shaped poly(glycolic acid)-poly(lactic acid) fiber meshes that were implanted subcutaneously onto the backs of athymic mice (Figure 1.4).[62] Subsequent coverage of the story in the New York Times and later on the popular television series *Nip/Tuck* only increased public attention to this result and tissue engineering in general.

In reality, tissue engineering had been impacting patient care before the buzz from advances such as the Vacanti mouse. Charles Vacanti reports using a tissue engineering approach to regenerate a patient's sternum as early as 1991,[59] and FDA regulated tissue engineered procedures and products were available by the late 1990s as well in the form of Carticel®, a chondrocyte expansion procedure offered by Genzyme Biosurgery, and Apligraf®, a collagen

based full thickness skin equivalent from Organogenesis used to treat lower extremity diabetic and venous stasis ulcers.

1.3 Growth: The 21st century

The beginning of the 21st century has seen tremendous advances in tissue engineering. The field has established a role within clinical care, and recent advances in the laboratory and through *in vivo* testing using animals models point to exciting further developments over the course of the coming years and decades. A plethora of undeniably important advances in tissue engineering have been made thus far this decade, and for many of these advances, the true magnitude of their importance may not be fully realized for many more years. Many recent advances and the state of the art in most areas of tissue engineering will be discussed in the remaining chapters of this thesis; therefore, the next section will highlight a few select examples of clinically used tissue engineering strategies.

1.3.1 Continued advancement

Earlier this decade, a number of experimental techniques bridged the gap from laboratory to clinic. Reports of tissue engineered pulmonary arteries in the laboratory[63] quickly resulted in major publications reporting clinical use of these arteries.[64] At the same time, tissue engineering techniques were applied clinically to utilize autologous cells to regenerate bone.[65] More recently and based on work performed in the early 1990s,[66] autologous bone flaps have been created *in vivo*

using tissue engineering strategies and then used to engineer a functional hemimandible capable of accepting dental implants.[67] This technology eliminates the need to harvest the patient's fibula or rib to reconstruct the mandible but still relies on the use of autologous material, thus eliminating concern of disease transmission or rejection.

The use of biological scaffolds is an exciting technology that deserves special note in any discussion of recent tissue engineering trends and advances. While not a new idea, as demonstrated by the aforementioned studies by Nicholas Senn and Marshall Urist, the processing and use of the extracellular matrix has led to a number of exciting advances in tissue engineering this decade. Related to the work of Senn and Urist, a large number of decellularized, demineralized bone matrix products are commercially available and approved by regulatory agencies worldwide. Extracellular matrix based strategies are now expanding to include tissue engineering of other organs.

A group led by Anthony Atala published a landmark study in 2006 describing the use of tissue engineered autologous bladders to replace congenitally defective bladders in 7 patients.[68] The engineered bladders consisted of scaffolds made from decellularized bladder submucosa or a combination of collagen and poly(glycolic acid) seeded with autologous cells expanded *in vitro* from a punch biopsy taken from each patient's bladder (Figure 1.5). This study marked the first time a whole organ had been engineered for clinical use and garnered well-deserved attention and acclaim.

A related approach was used in 2008 to replace a patient's left bronchus using a tissue-engineered trachea.[69] The team of researchers, led by Paolo Macchiarini, used a bioreactor to culture autologous bone marrow derived mesenchymal stem cells seeded on a decellularized tracheal matrix taken from a donor. After 96 hours of culture within the bioreactor, the engineered trachea was surgically implanted to replace the patient's stenotic left main bronchus (Figure 1.6).

As a final example of the promising capabilities of the extracellular matrix, building on reports that transplanted hearts display donor-recipient chimerism indicating autologous seeding of the transplanted organs,[70] researchers have shown that decellularized cardiac matrices can be recellularized *in vitro* and can regain some of the pumping ability of functional hearts.

Commercial products that utilize extracellular matrices for tissue regeneration are also available. Two such products, Alloderm® and Strattice®, both manufactured by LifeCell, Inc., provide decellularized human and porcine matrices, respectively, for skin regeneration *in vivo*.

1.4 The Future and the Past

An attempt to predict the future of tissue engineering with any level of specificity or temporal conjecture would be foolish; the field continues to advance at a rapid but ever changing pace. As with any multidisciplinary field, advances will be predicated not only on the efforts of tissue engineers, but also on scientists from other fields, including chemists, materials scientists, molecular

and cell biologists, pharmaceutical engineers, and clinicians. Discernible trends, however, do exist within the field and shed possible light on future directions.

One such trend is the use of autologous cells to regenerate patient-specific tissues. While development of embryonic stem cell technology is hampered by ethical and political debates in the U.S., the identification and use of adult stem cells in tissue engineering research is becoming increasingly popular and promising. Stem cell populations in bone marrow, adipose tissue, dental tissues, and the skin represent potential targets upon which tissue engineering strategies will be based. While harvest and expansion of autologous, terminally differentiated cells is possible in many cases, in the future tissue engineering strategies may be used to address clinical problems for which no such tissue can safely be acquired. Thus tissue engineers have the need for a well-characterized, easily accessible stem cell population. Additionally, ideal growth factor or conditioning regimes for differentiation and maintenance of differentiation are necessary.

As previously mentioned, organ and tissue transplantation as long-term solutions to many clinical problems are limited due to the lack of supply of donor organs/tissues and also concern over rejection and long-term immunosuppression. Tissue engineering strategies will ideally overcome this hurdle. The use of autologous cells for tissue regeneration is one method to eliminate the need for immunosuppression. Antigen suppression or elimination is another potential solution to this problem. For strategies that rely on allogeneic

extracellular matrices, the supply of available materials is certainly greater than that of donor organs and tissues but still somewhat limited relative to solutions that use synthetic biomaterials. The continued development of methods to create functional synthetic extracellular matrices and to generate *de novo* allogeneic extracellular matrices, many of which already exist,[71-74] may further alleviate the need for donor tissues.

1.5 Conclusions

The common opinion of tissue engineering holds that it is a relatively new field within science. While this may be true of the name and more precise definition of the field, as with any multidisciplinary field, tissue engineering has roots that extend far into history. Early attempts at and advances in tissue engineering-related sciences were examined to establish the existence of this long history and also to exemplify the close relationship of tissue engineering to other fields within science and medicine. The defining studies of the 1980s and 1990s were discussed, as this can be viewed as the time period when the modern field of tissue engineering emerged. Highlights of more recent work were also provided as a means to justify the importance of tissue engineering within the scientific and medical communities and also to give some sense as to the possibilities that exist with the continued pursuit of research within the field.

1.6 Figures

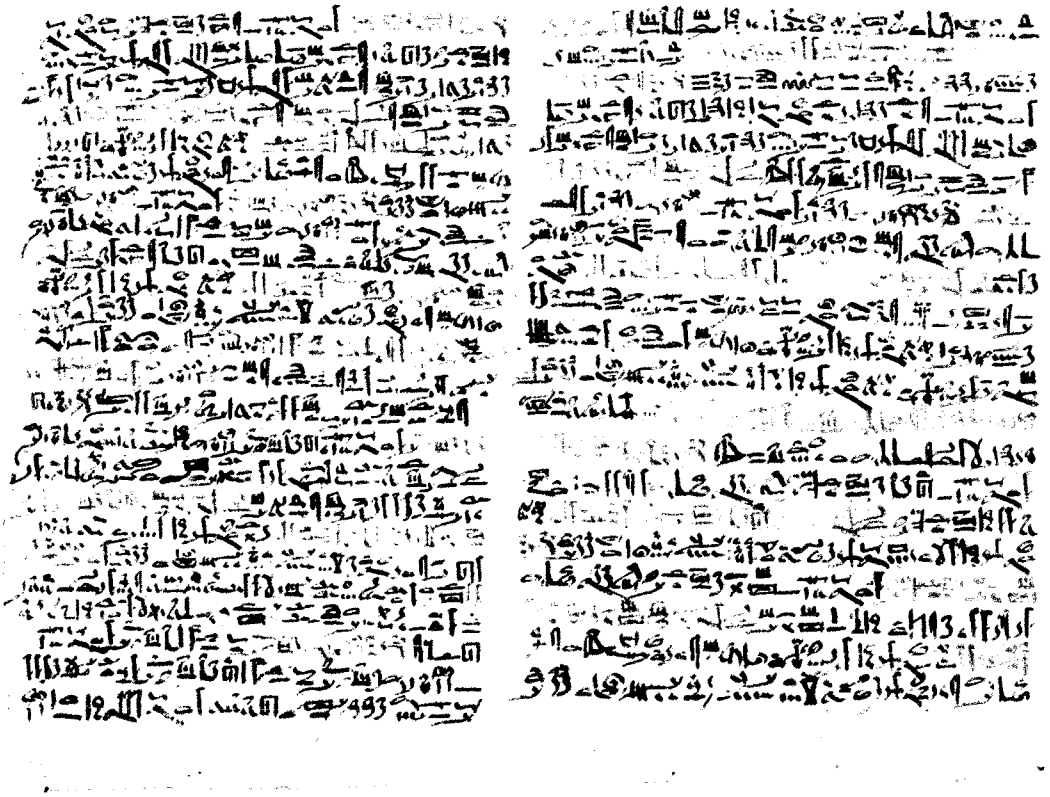

Figure 1.1. Plates vi and vii of the Edwin Smith Papyrus. Thought to be written by Imhotep, the document is the first known textbook of surgery and describes wound closure, one of the earliest forms of tissue engineering. Today the Edwin Smith Papyrus can be found at the New York Academy of Medicine.

Figure 1.2. A) Posthumously painted (1599) portrait of Gaspare Tagliacozzi from the University of Bologna. Gaspare Tagliacozzi, shown in a portrait painted posthumously in 1599 from the University of Bologna (A) advanced reconstructive surgery through techniques such as delay (B), where a flap is lifted and separated from the underlying tissue prior to reconstruction, enabling a complex but beneficial series of changes within the flap. (From *De Curtorum Chirurgia per insitionem*. Venice Italy: Bindoni, 1597)

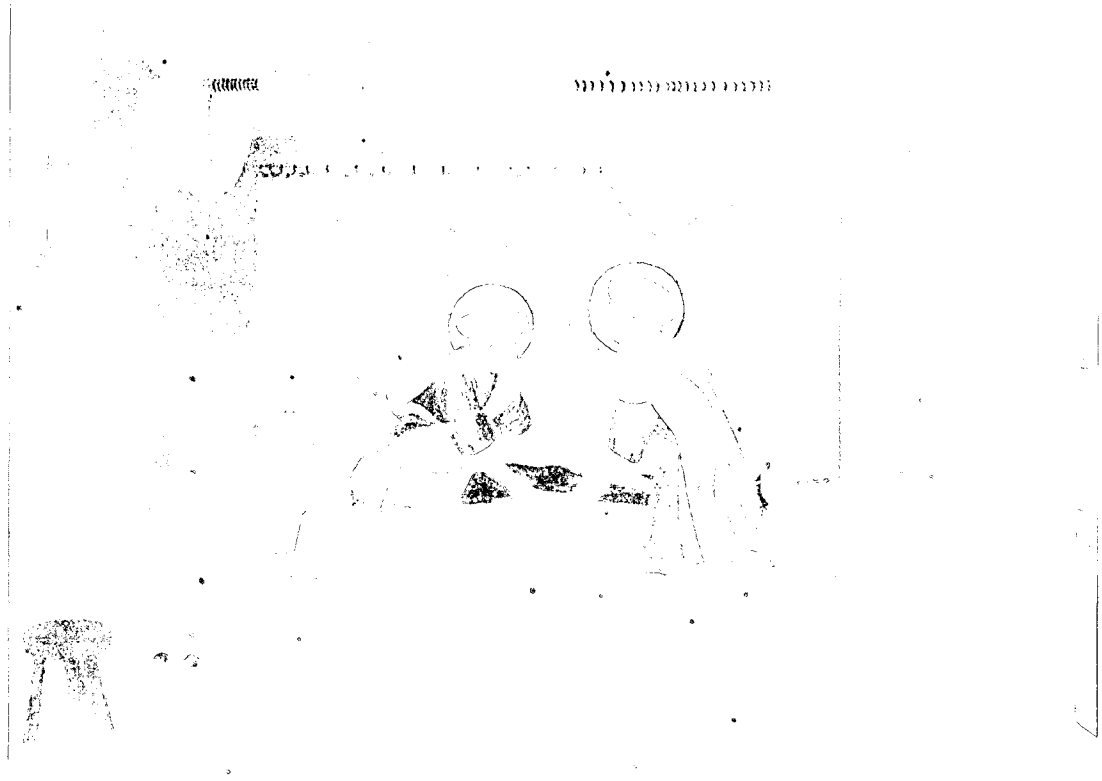

Figure 1.3. "The healing of Deacon Justinian" by Fra Angelico (ca. 1440) depicts the transplantation of a man's leg, taken from an Ethiopian donor, onto the injured deacon. (From *Museo di San Marco*, Florence, Italy)

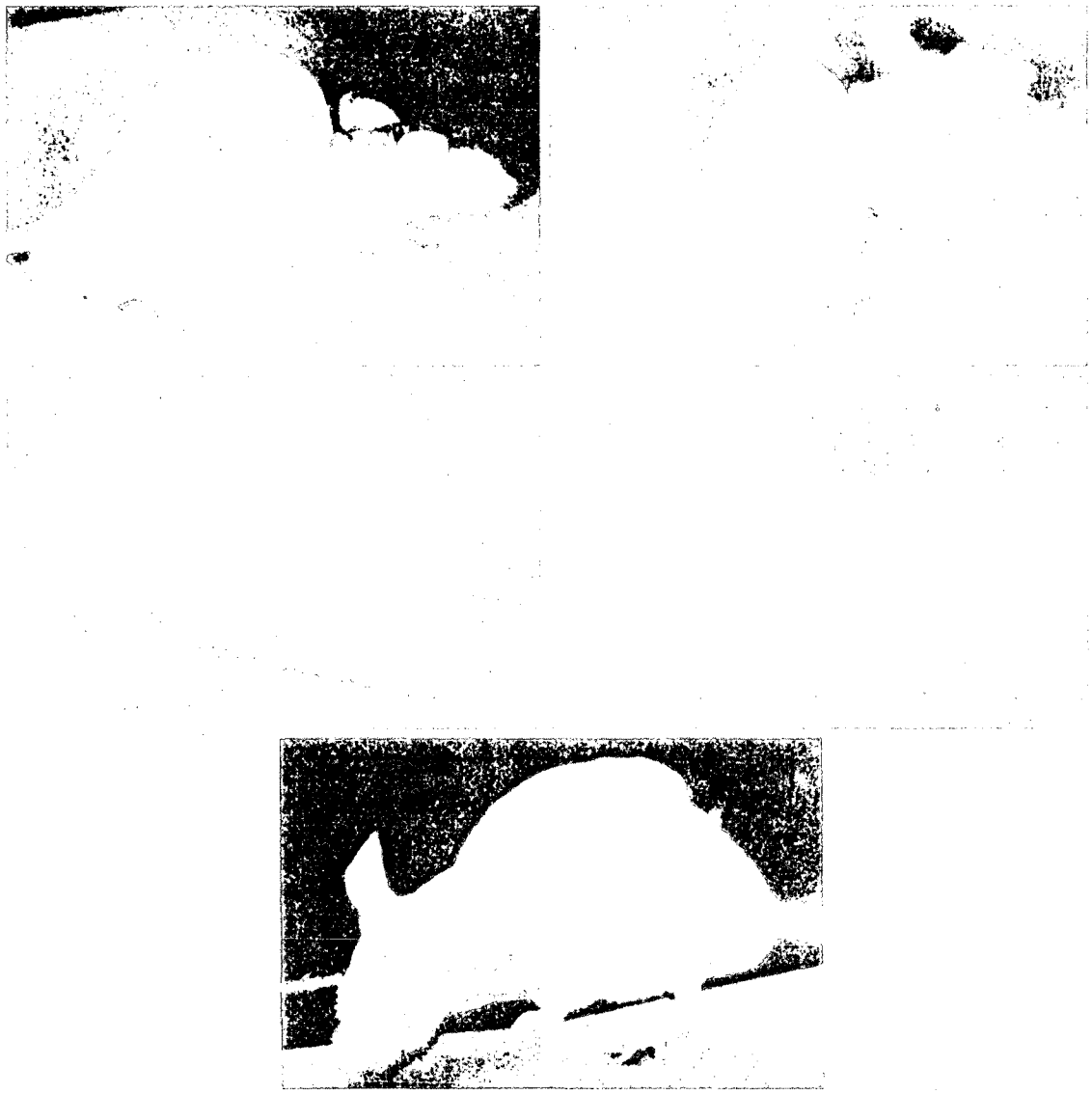

Figure 1.4. Gross appearance of a chondrocyte seeded-poly(glycolic acid)-poly(lactic acid) scaffold in the shape of a human ear, implanted subcutaneously on the dorsum of an athymic mouse for 12 weeks. Reproduced with permission from [62].

Figure 1.5. Generation and implantation of a tissue engineered bladder. A) Scaffold seeded with autologous cells. B) Tissue engineered bladder being *anastomosed to the remaining native bladder for reconstruction. C) Fibrin glue* and omentum covering the reconstructed bladder. Reproduced with permission from [68].

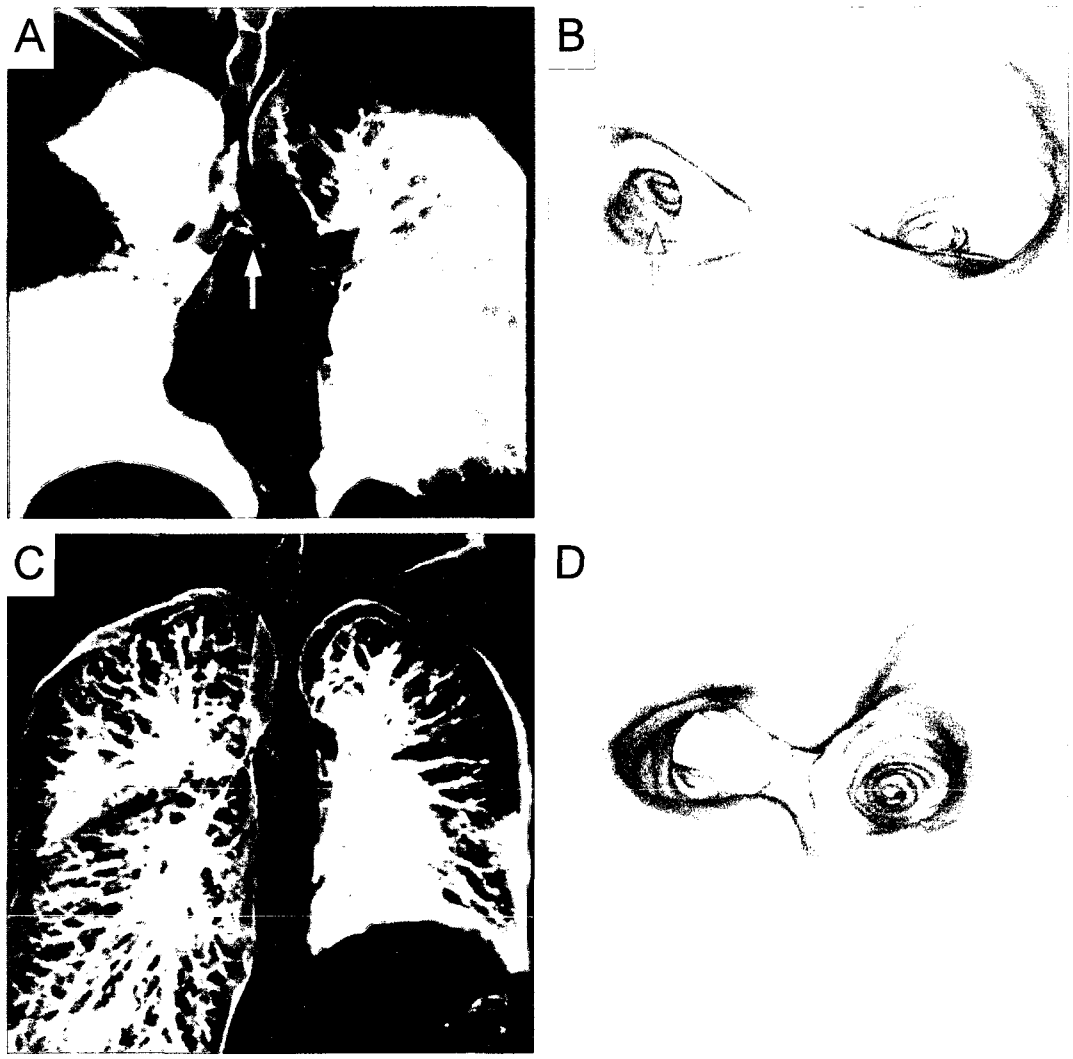

Figure 1.6. Computed tomography volume rendering (A and C) and bronchoscopic reconstructions (B and D) of a patient with left main bronchus stenosis (arrows) before (A and B) and 1 month after (C and D) resection of the bronchus and reconstruction with a tissue engineered trachea made using bone marrow mesenchymal stem cells seeded onto a decellularized tracheal matrix. Reproduced with permission from [69].

Chapter 2

Biomaterials for Regenerating Complex Craniofacial Tissues[†]

Abstract

Engineering complex tissues requires a precisely formulated combination of cells, spatiotemporally released bioactive factors, and a specialized scaffold support system. Injectable materials, particularly those delivered in aqueous solution, are considered ideal delivery vehicles for cells and bioactive factors and can also be delivered through minimally invasive methods and fill complex 3D shapes. In this review, we examine injectable materials that form scaffolds or networks capable of both replacing tissue function early after delivery and supporting tissue regeneration over a time period of weeks to months. The use of these materials for tissue engineering within the craniofacial complex is challenging but ideal as many highly specialized and functional tissues reside within a small volume in the craniofacial structures and the need for minimally invasive interventions is desirable due to aesthetic considerations. Current biomaterials and strategies used to treat craniofacial defects are examined, followed by a review of craniofacial tissue engineering, and finally an examination

[†] This chapter was published as: Kretlow JD, Young S, Klouda L, Wong M, Mikos AG. Injectable Biomaterials for Regenerating Complex Craniofacial Tissues. Adv Mat 2009;21(32-33):3368-93.

of current technologies used for injectable scaffold development and drug and cell delivery using these materials.

Abbreviations

ALT:	anterolateral thigh
APS:	ammonium persulfate
BAPO:	bis(2,4,6-trimethylbenzoyl) phenylphosphine oxide
BMP:	bone morphogenetic protein
BSE:	*bovine spongiform encephalopathy*
CaP:	calcium phosphate
CFC:	craniofacial complex
DBM:	demineralized bone matrix
DMAP:	2,2-dimethoxy-2-phenyl-acetophenone
DMSO:	dimethyl sulfoxide
ECM:	extracellular matrix
FDA:	Food and Drug Administration
FGF:	fibroblast growth factor
HDPE:	high-density polyethylene
HIV:	human immunodeficiency virus
HSC:	hematopoietic stem cell
HTV:	heat-vulcanizing
HUCM:	human umbilical cord matrix stem cell
IGF:	insulin-like growth factor
LCST:	lower critical solution temperature
MSC:	mesenchymal stem cell

NMP: N-methyl-2-pyrrolidone

OHNC: oral, head, and neck cancer

OPF: oligo(poly(ethylene glycol) fumarate)

PCL: poly(ε-caprolactone)

PDGF: platelet-derived growth factor

PDMS: polydimethylsiloxane

PEG: poly(ethylene glycol)

PEGDA: poly(ethylene glycol) diacrylate

PERVs: porcine endogenous retroviruses

PGA: poly(glycolic acid)

PLA: poly(lactic acid)

PLLA: poly(L-lactic acid)

PLGA: poly(lactic-*co*-glycolic acid)

PMMA: poly(methyl methacrylate)

PNIPAAm: poly(N-isopropyl acrylamide)

PPF: poly(propylene fumarate)

PTFE: poly(tetrafluoroethylene)

RFFF: radial forearm free flap

RTV: room-temperature vulcanizing

TE: tissue engineering

TEMED: N,N,N',N'-tetramethylethyldiamine

TGF-β: transforming growth factor-β

TMJ: temporomandibular joint

VEGF: vascular endothelial growth factor

β-TCP: beta-tricalcium phosphate

2.1 Introduction

Reconstruction of the oral and maxillofacial complex following traumatic insult, tumor ablation, or congenital deformities remains a formidable challenge for clinicians. A myriad of tissue types and morphologically complex structures are present in a relatively small area, with the consequence that defects often involve multiple tissue types including the facial skeleton, special sense organs, soft tissues (i.e. muscle, subcutaneous fat, skin, mucosa), salivary glands, cartilage, nerves, vessels, and teeth. Current clinical strategies designed to address such composite defects need to restore both the functional and aesthetic characteristics of the affected region. Additional considerations include the routine presence of bacterial contamination from the oral and sinus cavities, the ability to withstand the mechanical stresses imposed by masticatory function, and the special aesthetic challenges posed by the restoration of symmetric facial structures.

The morbidity and limitations associated with current surgical techniques and materials for oral and maxillofacial reconstruction has spurred the development of tissue engineering (TE) strategies to address these shortcomings. Injectable TE methods (with the ability to deliver both a therapeutic cell population and bioactive factors) are particularly attractive examples of how TE can be combined with minimally invasive techniques to reduce morbidity. The purpose of this review is to outline contemporary methods and materials in oral and maxillofacial reconstruction, describe currently available injectable tissue

engineering systems, and discuss the use of such systems for the delivery of cells and bioactive factors to regenerate complex tissues within the oral and maxillofacial region.

2.2 Reconstructive materials commonly used in the oral and maxillofacial region

Advances in surgical techniques, biomaterials science, and cell biology have established several approaches to the reconstruction of the oral and maxillofacial region depending upon certain characteristics of the defect such as size, shape, and vascularity. Autologous tissue remains the "gold standard" material, although associated harvesting procedures may result in donor site morbidity and require additional surgical time. Allograft or xenograft tissues do not require additional operative time and expense but may suffer from batch-to-batch variability and carry the risk of potential viral or bacterial transmission and immune-mediated regenerative compromise. Synthetic materials offer the ability to precisely control biologically important characteristics such as porosity or hydrophilicity/hydrophobicity through the manufacturing process, but they usually require the addition of bioactive factors or cells to promote tissue regeneration.

When complex, composite defects are encountered following treatment for neoplastic or cystic pathology and with high-velocity ballistic injuries, autologous tissue reconstruction using pre-vascularized hard and soft tissue grafts usually represents the technique of choice. However, for single tissue defects (i.e. solely bone or soft tissue regeneration), which are much, more common, the surgeon

can choose from a wide range of autograft, allograft, xenograft, and synthetic materials currently available (Table 2.1).

2.2.1 Osseous reconstruction

Autologous tissue

Many clinicians consider harvested autologous bone (i.e. taken from the same individual) as the "gold standard" material for the reconstruction of osseous defects. Autologous bone grafts by their very nature are able to deliver a physiologically optimized combination of osteogenic cells and growth factors in a mineralized scaffold. In 1956, Axhausen[75] described two "osteogenetic phases" of bone regeneration when using bone grafts. The first phase (i.e. osteogenesis) begins several days after the grafting procedure and is attributed to the activities of surviving, pre-existing osteogenic cells, which form osteoid within the transplanted bone. The second phase (i.e. osteoinduction) occurs several weeks later, particularly in response to the resorption and remodeling of the bone graft by osteoclasts resulting in exposure of invading host-site stem cells to osteoinductive factors such as bone morphogenetic proteins contained within the mineralized matrix of the original graft. An autologous graft is also capable of initiating bone formation through an osteoconductive mechanism, if it is placed in proximity to a well-vascularized bed and bone forming cells. With autologous bone grafts, immunologic rejection and disease transmission are absent.

Depending on the amount of bone graft required, the iliac crest, tibia, skull, and mandible[76, 77] are common areas in which particulate bone or blocks can be

harvested. However, the supply of donor tissue is limited and morbidity increases as larger amounts of bone are harvested. While the incidence is low, complications related to iliac crest bone harvesting such as persistent post-operative pain, nerve injury, arterial injury, scarring, hemorrhage, hematoma, infection, and gait disturbance have been reported.[78]

Non-vascularized autogenous bone grafts offer a relatively predictable means of filling osseous defects and inducing new bone growth. Following graft remodeling, complete integration into the host site occurs. Several parameters govern the success of such grafts including prevailing conditions within the host site and stability of the graft. Sufficient soft tissue bed vascularity and coverage of the non-vascularized bone graft are typically required to prevent healing complications such as wound dehiscence or infection[79] and allow for survival of the transplanted osteogenic cells within the graft. Rigid fixation of the graft allows rapid neovascularization of newly formed bone and survival of transplanted cells. In some cases, soft tissue bed vascularity may be compromised, as in patients who have undergone radiation therapy for malignant disease. A course of hyperbaric oxygen treatments can be undertaken to promote soft tissue oxygenation and neovascularization, optimizing the quality of the recipient tissue bed prior to receiving the non-vascularized bone graft.

Vascularized bone grafts are less dependent on the presence of an optimized soft tissue recipient bed, although their size and shape are largely dictated by the morphology of the donor site. Since vascularized bone must be

initially transferred with a peri-osseous cuff of soft tissue containing its blood supply, a second operation is frequently required to remove the excess soft tissue associated with the graft. Additional procedures may also be required to augment the volume of grafted bone to allow for dental implant rehabilitation. Nonetheless, despite the more technically demanding nature of microvascular free tissue transfer, vascularized bone and soft tissue grafts are now commonly used by experienced surgeons in the reconstruction of large composite tissue defects.

Allogeneic tissue

Allograft bone (i.e. harvested from an individual of the same species as the recipient) is typically derived from human cadavers and is available from bone banks and other commercial vendors. Donor site morbidity and limitations as to the quantity of graft are no longer considerations. Both cortical and cortico-cancellous allograft bone is available in the form of particulate, chips, and blocks. Large cortical allografts undergo minimal revascularization and remodeling leading to the accumulation of microfractures over time and the persistence of a non-vital graft incapable of physiological adaptation to functional loads.[80]

There is also a potential risk of bacterial, viral, or prion transmission with allograft bone, as well as immunologic rejection depending on the method adopted for bone preservation. To address these concerns, donor selection and screening (i.e. for human immunodeficiency viruses 1 and 2, and hepatitis B and C in the United States) combined with tissue processing (i.e. washing to ensure

blood component removal,[81] freeze-drying, or gamma irradiation[82]) are used by bone banks and vendors to increase the safety of allograft bone products. As a result of these measures, the risk of disease transmission has been calculated to be quite small (i.e. the risk of receiving allograft bone from an HIV-infected donor is approximately 1 in 1.6 million[83]).

Ideally, allograft processing should produce safe yet biologically active products for use in osseous reconstruction. However, some processing methods have been associated with detrimental effects on the mechanical and biological performance of allograft bone. Examples include the promotion of microcracks in cortical bone grafts with freeze-drying, increased brittleness of cortical bone with gamma irradiation, and a decrease in the osteoinductivity of demineralized bone allograft with higher levels of gamma irradiation or ethylene oxide sterilization.[84] As a result, current processing methods render mineralized allograft bone a predominantly osteoconductive material with minimal osteoinductivity and no osteogenicity.

The biological activity of allograft bone can be augmented by the addition of autogenous bone or platelet rich plasma.[85] Alternatively, treatment of mineralized allograft bone with hydrochloric acid (0.5 – 0.6 M) or a 1:1 formic acid-citric acid mixture yields demineralized bone matrix (DBM) which is less immunogenic[86] and possesses both osteoconductive and osteoinductive properties (through the exposure of bone morphogenetic proteins previously contained within the mineral component of the allograft).[84] The biological activity

of DBM is not consistent. Variations in growth factor content from lot-to-lot and between different commercial formulations of DBM have been reported[87] and confirmed by variations in osteoinductive potential between various products seen in animal studies.[88] To enhance intra-operative handling properties, DBM has been combined with carriers such as hyaluronate (i.e. DBX® from Synthes, USA), glycerol (Grafton® from Osteotech, USA), gelatin (Regenafil® from Regeneration Technologies, USA), poloxamer (Dynagraft® from GenSci Regeneration Sciences, Canada) and calcium sulfate (Allomatrix® from Wright Medical Technology, USA) by various commercial vendors.[89]

Xenogeneic tissue

Xenogeneic bone grafts (i.e. harvested from a different species) have the same potential advantages as allograft bone, in that virtually unlimited amounts can be procured without donor-site morbidity. As with the use of allografts, there is a small risk of pathogen transmission, although the risk of bovine spongiform encephalopathy (BSE) or the transmission of porcine endogenous retroviruses (PERVs) from xenogeneic products is low,[90] because unlike central nervous system tissues (i.e. brain and spinal cord), bone, skin, or skeletal muscle are not believed to contain infectious levels of transmissible spongiform encephalopathy agents.[91] The chemical and heat treatment of bovine bone to denature and remove proteins has also proven to be effective in the inactivation of prions.[92]

Although immunologic rejection of transplanted xenogeneic tissues is a possibility considering the large histocompatibility mismatch between animal and

human tissues, processed xenograft bone has been used (either alone or in combination with autograft bone) in numerous dental applications such as implantology,[93] maxillary sinus floor augmentation,[94] alveolar ridge preservation,[95] and periodontal regeneration without significant reaction.[96] Several commercial products available for dental and orthopedic bone regenerative applications include cross-linked bovine collagen I fibers coated in hydroxyapatite (Healos® Bone Graft replacement from DePuy Spine, USA), deproteinized bovine bone (Bio-Oss® from Osteohealth, USA), porcine collagen I and III resorbable membrane (Bio-Gide® from Osteohealth, USA), and a composite of 60% hydroxyapatite + 40% tricalcium phosphate ceramics in a bovine fibrillar collagen carrier (Collagraft® from Angiotech Pharmaceuticals, USA).[90]

Synthetic biomaterials

Ceramics

The extracellular matrix of bone has been described as a composite material composed of collagen type I fibrils mineralized with nanocrystals of hydroxyapatite.[97] Approximately 70% of bone by weight is composed of calcium salts, with hydroxyapatite ($Ca_{10}(PO_4)_6(OH)_2$) as the primary mineral constituent. Strictly speaking, bone mineral is not purely hydroxyapatite, and the presence of ion impurities has actually led to the consensus that a more accurate term for the inorganic component is carbonatehydroxyapatite with the formula $(Ca,Mg,Na)_{10}(PO_4HPO_4CO_3)_6(OH)_2$.[98] Devoid of an organic component, calcium

salts such as hydroxyapatite are biocompatible, non-immunogenic components of bone and are considered to be osteoconductive. Consequently, there has been much interest in designing synthetic osteoconductive grafting materials based on these naturally occurring calcium salts.

LeGeros[98] has characterized commercially available calcium phosphate (CaP) biomaterials as either hydroxyapatite of natural origin or synthetically produced CaP. The hydroxyapatite of natural origin is either obtained from bovine bone (as discussed above) or from certain species of coral. These naturally derived sources of hydroxyapatite are processed so that their macroporous, interconnected structure is maintained, allowing for in-growth of host tissue upon implantation, as well as the diffusion of nutrients throughout the graft material.

Coralline-derived ceramics are typically prepared in two ways. The first method involves a solid-state hydrothermal exchange reaction called the *Replamineform* process, in which the calcium carbonate-based coral skeleton is converted to a calcium phosphate-based material (while still maintaining its architecture), which is predominantly in the form of hydroxyapatite.[99] This material is marketed under the name Pro Osteon® (Interpore Cross International, USA). Since *Replamineform* grafting materials are nearly non-resorbable,[100] newer coralline ceramics that have undergone a partial *Replamineform* process have been developed, resulting in a material which is composed mainly of calcium carbonate with calcium phosphate present only on the internal and

external surfaces. This material is marketed as Biocoral® (Biocoral, USA) and has been shown to be resorbed and replaced by bone over time.[100]

Numerous synthetic CaP biomaterials are commercially available and have been classified according to their composition by LeGeros[98] as hydroxyapatite, unsintered calcium deficient apatite, beta-tricalcium phosphate, or biphasic calcium phosphate. Hydroxyapatite can be produced with either a dense or macroporous morphology, and is typically sintered at temperatures above 1000 °C in granular or block forms. The high heat of sintering produces a material that cannot be reshaped to fit into a bone defect (i.e. if in block form) and is non-resorbable.[101] Beta-tricalcium phosphate (β-TCP) has the formula $Ca_3(PO_4)_2$ and like hydroxyapatite is a brittle material with low fracture resistance. Both hydroxyapatite and β-TCP are biocompatible, osteoconductive, and bioactive (i.e. they develop a direct, adherent bond with bone).[98]

Under physiological conditions, hydroxyapatite is essentially a non-resorbable material, while on the other hand β-TCP has been shown to degrade within 6 weeks after implantation.[102] The dissolution of CaP biomaterials is dependent on composition (hydroxyapatite vs. β-TCP ratio), surface area of the implant (particulate vs. block form), porosity, and crystallinity (sintering creates larger, slower dissolving crystals).[98] Biphasic CaP products which contain hydroxyapatite and β-TCP in various ratios (the higher the β-TCP content, the greater the resorbability[103]) are aimed at the provision of a bone grafting material which is able to degrade within a physiologically optimized time frame, while

providing some measure of mechanical stability until sufficient bone in-growth has occurred.[102]

CaP cements are also available, and these combine a dry powder (CaP) and a liquid component (i.e. an inorganic or organic acid, or sodium phosphate solutions) in a setting reaction that occurs under physiologic pH and temperatures.[98] Examples include Norian® (Synthes Craniomaxillofacial, USA), BoneSource® (Stryker Leibinger, Germany), and Mimix® (Walter Lorenz Surgical, USA). A variety of CaP compounds have been used for the solid phase such as dicalcium phosphate, dicalcium phosphate dihydrate, calcium-deficient hydroxyapatite, and amorphous calcium phosphate.[101] These cements are injectable and able to be molded for variable periods before hardening. They are also described as resorbable, though clinical experience has demonstrated retention of the material over extended periods. While CaP cements have been successfully used for clinical applications such as vertebroplasty[104] and cranial defect repair,[105] they are brittle and contraindicated for use in areas of mobility, active infection, or in situations where they directly contact the sinuses or dura.[101]

Synthetic polymers

The long and successful history of synthetic polymers in medicine combined with the ability to control their material properties has generated much interest in their use for bone regeneration strategies. Polymers currently used for oral and maxillofacial osseous reconstruction/augmentation include silicones, poly(lactic acid) (PLA), poly(glycolic acid) (PGA), poly(lactic-*co*-glycolic acid)

(PLGA), poly(ethylene), poly(caprolactone) (PCL) and poly(methyl methacrylate) (PMMA). These materials are biologically inert and do not possess osteogenic, osteoconductive, or osteoinductive properties. Hence, none of these materials have been incorporated into commercial bone grafting products as of yet. However, the biocompatibility of many synthetic polymers, combined with the ability to reproducibly control their composition, rate of degradation, pore size, porosity, interconnectivity, hydrophobicity/hydrophilicity, ability for cell attachment, morphology, and handling properties has made them attractive materials for investigation as scaffolds and delivery vehicles of cells, drugs, and growth factors in tissue engineering.

Currently, the most common synthetic absorbable polymers available for oral and maxillofacial applications include the poly(alpha-hydroxy esters) PGA, PLA, and their copolymer, PLGA. Once implanted, these materials slowly degrade through hydrolysis and the by-products (lactic acid from PLA and glycolic acid from PGA) are incorporated into the Krebs cycle and eventually eliminated as carbon dioxide and water.[106] They have been used as resorbable sutures for the past 40 years, and recently as degradable plates and screws for bone fixation following craniofacial surgery,[107] orthognathic surgery,[108] and trauma.[109, 110] Advantages of these devices over traditional titanium plates and screws include elimination of long-term palpable devices and continued skull growth in the pediatric population once they have degraded.[107] Resorbable membranes made of PLA and PLGA have also been successfully used as

barriers for use in guided tissue regeneration procedures to treat periodontal defects.[111]

The biocompatibility of non-degradable synthetic polymers has led to their commercialization as permanent implants for craniofacial augmentation or reconstruction. Solid facial implants made from silicone elastomer have been used for almost 50 years, and are available for skeletal augmentation of the malar eminence, zygomatic arch, and chin.[112] These implants are available in various pre-contoured forms and can be carved intra-operatively to customize the shape for implantation in a particular area. Once implanted, the smooth-surfaced silicone implants are encapsulated by an avascular fibrous capsule, although initial fixation of the implant is important to prevent displacement or subsequent mobility which can lead to complications.[112] Porous high-density polyethylene (HDPE) (MedPor®, from Porex Industries, USA) is also available as a customizable pre-fabricated porous implant and has found applications as a skeletal augmentation material, a space maintainer following globe exenteration, and as a structural support for orbital reconstruction following trauma and tumor resection.[113]

Another non-degradable polymer commonly used in craniofacial osseous reconstruction is PMMA. The biocompatibility of PMMA, established over a 50 year history of clinical use, has led to it being the most frequently used synthetic material for skull reconstruction in the world.[114] *In situ* curing PMMA cement is available as a two-phase system, in which a powder (consisting of PMMA

polymer particles and a polymerization catalyst) is mixed with a liquid (consisting of MMA monomer). The combination produces a moldable, putty-like material that polymerizes into a rigid, high strength solid within 10-15 minutes. The exothermic nature of the setting reaction and the leaching of unreacted monomer from the implanted PMMA has been shown to cause bone necrosis and inflammation.[115] Consequently, PMMA cement is usually polymerized extra-corporeally before insertion into the defect. PMMA can also be obtained as a pre-formed implant, whose shape is customized to fit a patient's bone defect through the use of computed tomography stereolithographic models.[116]

Since PMMA does not bond directly to the surrounding hard and soft tissues, techniques have been developed to allow better fixation of the material, such as the incorporation of titanium mesh scaffolding in cranioplasty[117] or by combining PMMA with carboxymethylcellulose gel to generate surface porosity.[118] PMMA is considered to be the alloplastic material of choice for cranioplasty in adults with good soft tissue quality and no frontal sinus exposure or previous history of infection. It should be used with caution in children since this essentially "permanent" and rigid material cannot adapt to a growing craniofacial skeleton.[114]

Recombinant growth factors

In view of the biological limitations associated individually with autograft, allograft, and synthetic materials, surgeons have attempted to augment the activity and physical properties with composite grafts combining several different

materials. For example, particulate allograft bone can be used as an "expander" for autograft bone, resulting in less bone having to be harvested from a donor site, but still allowing for a grafting material which is osteoinductive, osteoconductive, and osteogenic. Recently, the commercial availability of recombinant growth factor products has given oral and maxillofacial surgeons an additional option for the reconstruction of bony defects. In the United States, recombinant human bone morphogenetic protein-2 (BMP-2) in an absorbable collagen sponge carrier (Infuse® from Medtronic, USA) has been approved for maxillary sinus augmentation and localized alveolar ridge augmentation in the oral and maxillofacial region. Orthopedic procedures approved by the United States Food and Drug Administration (FDA) for the use of Infuse® bone graft include spinal fusion and open tibia fractures. Platelet-derived growth factor (PDGF) in a β-TCP carrier (GEM 21S® from Osteohealth, USA) has been approved in the United States as well for the treatment of bone defects and gingival tissue recession associated with advanced periodontal disease.

The use of recombinant growth factor products for bone regeneration is appealing since they reduce the need for bone harvesting, are readily available, and contain high concentrations of a purified biological agent involved in the bone healing process. The implantation of such factors into a bone defect and the controlled release of the factor over time should promote the proliferation and differentiation of osteogenic stem cells within the wound, accelerating the healing process. Thus, products such as Infuse® contain the osteoinductivity of autograft

bone, combined with the convenience of "off the shelf" demineralized bone matrix, without the concerns of pathogen transmission or batch-to-batch variations in potency. These advantages have already spurred surgeons to find "off-label" uses of BMP-2 such as the reconstruction of mandibular continuity defects following tumor resection, the grafting of maxillary clefts, and the reconstruction of hard tissue avulsion defects following trauma.[119]

Since our clinical experience with such technology is relatively new, issues such as: 1) the long-term effects of implanting materials containing supra-physiologic doses of growth factors and, 2) the use of growth factors for the reconstruction of defects associated with neoplasms, remain unresolved. In addition, the potential efficacy of these materials and their ability to reduce operating time and donor site morbidity will have to be weighed against their relatively high cost.

2.2.2 Soft tissue reconstruction

Autologous tissue

Similar to osseous reconstruction, autologous tissue is the standard for reconstruction of oral and maxillofacial soft tissue defects. Small to medium-sized superficial defects can be repaired with skin grafts, which can be harvested as either "full-thickness" or "partial-thickness". Both types of skin graft contain the entire epidermis, but full-thickness grafts incorporate the entire dermal component (including dermal appendages such as hair follicles or sweat glands if present), while partial-thickness grafts are harvested at the level of the more

superficial papillary dermis, leaving the deeper reticular dermis in place. Autologous grafts can also be harvested from various regions of the oral cavity, including the free gingiva, buccal mucosa, and palate. During the first 2-3 days of transplantation, nutrient exchange to the graft occurs through serum imbibition, after which the graft becomes revascularized through anastomoses between the host and donor vessels. Thus, the survival of both types of skin grafts relies on a recipient site that is well vascularized and immobility of the graft against its nutrient bed.

Unlike free grafts, soft tissue flaps are prepared in such a way that their blood supply is maintained following transfer to the recipient site. The donor tissue for local flaps is located close to the recipient site so that the tissue can be advanced or rotated into position while retaining a nerve and blood supply through its pedicle. A number of local flaps have been used for reconstruction of oral and facial defects including those involving the lip (i.e. Abbe flap)[120] and oral cavity (i.e. palatal flaps and tongue flaps).[121] Larger oral and maxillofacial soft tissue defects require more tissue and can be reconstructed with regional flaps. Like local flaps, regional flaps rely on an intact vascular pedicle for their blood supply, although the donor site is more distant. Examples of regional flaps include the pectoralis major, deltopectoral, and temporalis flaps. The pectoralis major flap can be used to transfer both muscle and skin (hence its classification as a "myocutaneous" flap) to large oral and maxillofacial defects.[122] The temporalis muscle flap is another regional flap which can be used for soft tissue

reconstruction of oral defects. It is elevated from the temple and rotated into the orbit or oral cavity. Regional flaps for closure of palatal defects are reliable and versatile, but create cosmetic defects at the donor site and often require secondary procedures to remove excess tissue.[123] Such flaps are also unable to transfer bone along with the soft tissue and cannot address the comprehensive needs of a composite defect.

The advent of microvascular surgical techniques in the 1980s allowed the development of a new way to transfer soft and hard tissue together in the form of vascularized free flaps. These flaps are harvested from distant sites along a dominant arterial supply and venous system and re-anastomosed to vessels at the recipient site, providing an instantaneous vascular system. A variety of free flaps have been described for oral and maxillofacial reconstruction, and they can be harvested with soft tissue alone (i.e. fascio-cutaneous or fascial flaps) or with a combination of hard and soft tissue (i.e. osseo-fascio-cutaneous flaps). A review by Gonzalez-Garcia *et al.*[124] lists numerous vascularized free flaps available for such purposes, with donor sites such as the radius, fibula, iliac crest, deltoid, anterolateral thigh (ALT), and scapula. The authors also describe the versatility of the radial forearm free flap (RFFF) in particular, which can be used to cover defects involving any location within the oral cavity including the floor of the mouth, tongue, gingiva, buccal mucosa, soft palate, and retromolar area. In skilled hands, the overall failure rates of vascularized free flaps for soft tissue reconstruction in the head and neck region are relatively low, ranging from

5.5-8.8%,[124] indicating that this versatile technique is predictable and an important technique for the reconstruction of composite defects or those where vascular compromise of the recipient bed is an issue.

Aside from the reconstruction of soft tissue defects, autologous soft tissue has also been used for cosmetic facial augmentation. Composite grafts such as dermofat or adipofascial grafts from the ALT region have been used for this purpose,[125] as well as local flaps such as the buccal fat pad flap.[126] "Microfat" grafting has also been described,[127] in which adipose tissue is harvested atraumatically by suctioning or direct excision and then injected into the subcutaneous or intramuscular layers of the deficient site. While the supply of donor site adipose tissue is generally abundant, substantial over-filling of a defect is required due to the unpredictable stability and longevity of the injected fat over time.

The *ex vivo* expansion of harvested autologous cells for dermal augmentation has also been attempted commercially. Isolagen® (from Isolagen Technologies, USA) is a product currently in Phase 3 clinical trials within the United States where it is being investigated for the treatment of wrinkles.[128] The process involves harvesting skin from the post-auricular region using a 3 mm biopsy punch, and sending the specimen to the manufacturer to isolate and culture dermal fibroblasts. 4-6 weeks later, an autologous expanded explant is ready for use as an injectable dermal filler. Two to four treatments are typically required to obscure a wrinkle. As growth factors are used during the culturing

process, this product is considered a "medical device" and requires additional safety testing prior to approval by the United States FDA.

Allogeneic tissue

Autologous skin grafts are the preferred method for the treatment of burns. Patients with extensive burns, however, often lack sufficient donor tissue. The temporary use of allograft skin for third-degree facial burn coverage has been reported,[129] where it was used to promote initial vascularization of the wound bed following debridement, then removed 6 days later prior to the placement of a split-thickness skin autograft. Allograft skin usually undergoes rejection within 2 weeks, although there are reports of skin allografts persisting in non-immunosuppressed burn patients for up to 7 weeks, possibly due to the repopulation of the allograft by host cells.[130] Skin grafting involving the entire face is associated with poor aesthetic and functional results, since multiple grafts are required, producing a patchwork appearance.[131]

One of the most spectacular and controversial solutions to the problem of total facial reconstruction is the use of allograft transplantation of a composite flap containing all the soft tissue structures: skin, fat, muscle, and nerves. The first human partial face transplant was completed in 2005.[132] Apart from difficult ethical and psychological issues involved with such a procedure, patients must be placed on immunosuppressive drugs for life.[133] The initial outcome of such work appears promising, and satisfactory functional and aesthetic results have been observed 18 months post-transplantation.[134]

A more biocompatible allogeneic grafting material for soft tissue reconstruction is freeze-dried, de-epithelialized, acellular dermal graft (Alloderm® from LifeCell, USA). The removal of all cellular components from the graft reduces the potential for pathogen transmission while also decreasing the immunogenicity of the material. The resulting product is an acellular dermal matrix which can be used as sheets or as an injectable particulate. Both formulations undergo rapid vascularization and repopulation of the graft material with host cells derived from the wound site.[135, 136] Alloderm® sheets have been used for the treatment of acute burns[137] and the reconstruction of eyelids[138] and buccal mucosal defects,[139] while the injectable material Cymetra® has been described for use in lip augmentation procedures.[140]

Xenogeneic tissue

One of the most commonly used dermal fillers is bovine collagen. Commercial preparations such as Zyderm® (from Allergan, USA) are composed of purified, fibrillar collagen type I and III and are approved for cosmetic procedures for the treatment of wrinkles, frown lines, crow's feet, and acne scars. A related product called Zyplast® (from Allergan, USA) is composed of cross-linked bovine collagen which is less prone to enzymatic degradation after injection, but is recommended for injection into deeper defects because it may result in a beaded appearance.[141] While these materials have variable rates of degradation depending on the area of injection, collagen fillers typically last 2-4 months in duration. One of the main drawbacks to the use of bovine collagen is

the risk of a severe allergic reaction, thus a skin test should be performed on all patients prior to treatment. Approximately 3-10% of patients will display a positive response such as redness, itching, tenderness, or firmness at the test site, and should not undergo grafting with this material.[141]

Hyaluronic acid is a glycosaminoglycan that forms a major non-structural component of the connective tissue extracellular matrix and aids the skin in maintaining its turgor through its hydrophilicity. Since the hyaluronic acid moiety is identical across all species, xenogeneic hyaluronic acid is not immunogenic in humans.[142] Cross-linked hyaluronic acid derivatives are commercially available as soft tissue fillers, including Hylaform® (from Biomatrix, USA) which is derived from rooster combs, and Restylane® (from Medicis Aesthetics, USA) or Juvéderm® (from Allergan, USA) which are produced through bacterial fermentation. Like the bovine collagen fillers, these hyaluronic acid-derived products are approved by the FDA as injectable materials for soft tissue augmentation. While allergic skin testing is not necessary prior to treatment, rare allergic reactions have been known to occur to the residual avian/bacterial proteins in these materials.[142] The dermal augmentation achieved with hyaluronic acid-derived products has been reported to persist for longer periods compared with bovine collagen (up to 6 months) and longevity can be extended up to 9 months with the concomitant use of botulinum toxin to reduce recipient site mobility around the filler material.[143]

Synthetic biomaterials

Up to this point, the injectable materials discussed for soft tissue augmentation have all been "temporary" in nature, with the results generally lasting less than one year. Although some permanent injectable dermal fillers are available, Homicz and Watson[144] caution that changes in facial form or adverse reactions to injected materials may actually warrant the use of temporary fillers.

One of the most controversial permanent soft tissue fillers is liquid silicone, which has been used by physicians for more than 50 years. Currently the FDA approves medical-grade liquid silicone injections solely for ophthalmologic use to tamponade retinal detachments. However, some physicians have also used it off-label for soft tissue augmentation using a "microdroplet" technique, in which the silicone is injected in 0.01 ml increments, 1 mm apart in the sub-dermal layer.[145] Over several weeks, the injected silicone droplets produce a granulomatous reaction in the host tissues, and are encapsulated as foreign bodies within fibrous tissue. While some clinicians prefer the more natural feeling augmentation which can be achieved with silicone, the injection of large volumes has sometimes led to severe local and system reactions.[144]

Another permanent injectable dermal filler material is ArteFill® (from Arte Medical, USA) which is a FDA-approved combination of PMMA microspheres suspended in a solution of 3.5% ultrapurified bovine collagen and 0.3% lidocaine.[146] The manufacturer recommends the injection of small quantities of

ArteFill® every 1-3 months to minimize the chances of severe inflammatory reactions. Following injection, the bovine collagen is degraded and each microsphere is encapsulated in a fibrous sheath with minimal foreign body reaction, although some authors have reported the induction of foreign body granulomas following ArteFill® injections for lip augmentation.[147]

In an effort to address the need for a temporary material with longer lasting results, a new product called Sculptra® (from Dermik Laboratories, USA) has recently been approved by the FDA for the treatment of HIV-associated facial lipatrophy. Sculptra® is an injectable filler composed of freeze-dried, crystalline, irregularly sized microparticles of poly-L-lactic acid (PLLA) combined with sodium carboxymethylcellulose as a delivery vehicle.[148] PLLA is a well-known biocompatible and biodegradable polymer which has been used in numerous medical technologies ranging from resorbable sutures and plates and screws to drug delivery vehicles. To minimize the risk of complications from aggressive use of Sculptra® injections (such as the formation of nodules and granulomas), recommendations include limiting the volume of each injection, placing the material subcutaneously and not intradermally, post-injection massage of the area, and a delay of 6 weeks between treatment sessions.[148] Some authors have reported results lasting up to 18-24 months, fulfilling its promise as a longer-lasting yet non-permanent dermal filler material.

2.2.3 Composite tissue reconstruction

Severe traumatic insults and the surgical treatment of extensive oral and maxillofacial pathology can involve a considerable loss of facial tissues. Local control of disease requires complete removal without regard for aesthetically sensitive areas and may produce defects which are disfiguring and impose significant emotional stress on the patient. While tissue engineering holds promise for the future, the current mainstay of reconstruction and rehabilitation in patients with large composite tissue deformities remains with a combination of microvascular free tissue transfers and maxillofacial prosthetics.

Since vascularized free flaps have already been discussed, this section will focus on the use of maxillofacial prosthetics for the restoration of complex defects involving the loss of multiple tissues.

Commonly used polymeric materials for maxillofacial prostheses

Acrylic resins

Polymethylmethacrylate is the most widely used acrylic polymer in health care. Variations in the molecular structure produces hard polymethacrylates used for dentures and orthopedic bone cement while various soft polyacrylates (i.e. ethyl or butyl acrylates) are used in contact lenses.[149]

Methyl methacrylate resins are readily available and the durability and color stability of PMMA make it an excellent material for facial prostheses. The strength of PMMA enables the clinician to thin the exposed margins of the

prosthesis, improving the aesthetic result. In addition, benefits to the patient include compatibility with most adhesive systems and easily cleaning.[150]

Acrylic resins are most successfully employed in specific types of facial defects, namely those in which minimal movement of the underlying tissue bed occurs during function (i.e. prosthetic eyes). If placed in an inappropriate location, rigid PMMA facial prostheses can be uncomfortable and erosion may occur through the soft tissue.

Polyetherurethane elastomers

Polyetherurethanes have a variety of commercial uses and have also become popular for biomedical applications. In general, polyetherurethanes possess a number of favorable characteristics making them suitable for restoring defects with mobile tissue beds.[151] Polyurethanes can be made flexible without compromising edge strength, allowing the clinician to thin the margins giving the prosthesis a lifelike appearance and feel. In addition, when processed properly these elastomers are chemically inert, abrasion-resistant, and do not require the use of plasticizers to attain their flexibility.

A serious drawback to the use of polyurethanes in maxillofacial prosthetics is the difficulty in processing these materials consistently. A precise, stoichiometric admixing of all the components is necessary, with little margin for error. Furthermore, the toxic and hazardous diisocyanate component is moisture sensitive, as water contamination will cause gas bubble formation resulting in poor curing of the material with defects. As a consequence, either specially

prefabricated metal molds must be utilized for the polymerization reaction or if stone molds are employed, they must be thoroughly dehydrated prior to use. In addition, facial prostheses fabricated from polyurethane are not color-stable, possibly due to the effects of ultraviolet light and surface oxidation.[150] From the patient perspective, additional problems with polyurethane prostheses are their poor compatibility with adhesive systems and difficulty to clean.[152]

Silicone elastomers

Technically called polydimethylsiloxane (PDMS), the silicones are probably the most widely used materials in maxillofacial prostheses.[150] Silicone elastomers are formed by cross-linking the PDMS chains into a network, a process which is also referred to as vulcanization. Compounding the material with silica fillers typically provides additional strength.

The numerous silicone elastomers used for maxillofacial prostheses have been classified into two general categories based on the type of cross-linking reaction used to form the final shape of the device: room-temperature vulcanizing (RTV) and heat-vulcanizing (HTV). Thus, vulcanization can occur both with and without the application of heat, and depends on the specific catalysts and cross-linking agents utilized by the two general types of silicone elastomers.

Although HTV silicone elastomers have been shown to have excellent thermal stability, color stability upon ultraviolet light exposure, and biologic inertness, they do not possess sufficient flexibility to function well on moveable tissue beds. Clinically, the aesthetics of this material have been criticized for their

opacity and lifeless appearance.[150] Nonetheless, when compared to their RTV silicone counterparts, HTV silicone elastomers exhibit better physical and mechanical properties, partly by overcoming the problem of hand-mixing pigments as typically used for fabricating prostheses from viscous RTV silicones.[149]

Designed for cross-linking at room temperature, RTV silicone elastomers are composed of relatively short-chain silicone polymers which are partially end-blocked with hydroxyl groups.[151] In general, some limiting aspects of RTV silicone elastomers include air entrapment from mixing the various components prior to cross-linking.[149] These voids persist in the finished prosthesis, which may lower tear resistance and help accumulate skin exudates. Silica fillers are used to enhance tensile strength as well as mask discoloration of the material, although a considerable amount of translucency is lost, thus compromising the ability to achieve optimal intrinsic coloration of the material through the incorporation of pigments.

An improved alternative is MDX 4-4210® (from Dow Corning, USA), a Medical Grade RTV silicone elastomer which is the most commonly used material in clinical practice for the fabrication of maxillofacial prostheses.[153] This material has a chloroplatinic acid catalyst and a hydro-methylsiloxane cross-linking agent, allowing for curing to take place through an addition-type reaction, and hence a lack of reaction by-products.[150] MDX 4-4210® has been reported to address the general limitations of RTV silicone elastomers with superior

coloration qualities and edge strength,[154] reducing the need for tear repair which typically requires the skilled application of additional PDMS or reinforcement of the edge with fabric. Although MDX 4-4210® does not possess all the characteristics of an ideal maxillofacial polymer, it has many desirable properties as discussed. Nonetheless, efforts continue to improve the material properties of this popular maxillofacial prosthetic material by increasing tear strength[155] and surface wettability.[156]

2.2.4 Tissue engineering approaches for composite tissue regeneration

Up until 2004, autologous tissue remained the only source for transferring viable hard and soft tissue simultaneously. From vascularized osseo-fascio-cutaneous free flaps for craniofacial reconstruction, to simple, non-vascularized costo-chondral grafts used for the reconstruction of the mandibular condyle, an allogeneic, xenogeneic, or alloplastic material does not exist which can match the characteristics of composite tissue grafts/flaps.

Recently however, a tissue engineering approach for mandibular regeneration in a patient was reported by Warnke *et al.*,[157] in which a custom, vascularized bone graft was used to restore masticatory function and aesthetic form to a patient who had undergone subtotal mandibulectomy 8 years prior. The patient had received post-surgical radiation treatment, decreasing the probability for a successful non-vascularized bone graft. He was also on anti-coagulation therapy for an aortic valve replacement which increased his risk of severe post-operative bleeding following a large bone harvest.

Thus, a tissue engineering strategy was selected, in which a titanium mesh tray was custom designed for the mandibular defect and then filled with blocks of Bio-Oss® (deproteinized bovine bone) coated with recombinant BMP-7 in a bovine collagen type 1 carrier. In addition, 20 mL of bone marrow was aspirated from the patient's right iliac crest and mixed with Bio-Oss® particulate as a "grout" between the Bio-Oss® blocks of the construct. This approach utilized all the components of a tissue engineering strategy: cells (from the bone marrow), growth factors (the recombinant BMP-7 and endogenous growth factors in the marrow aspirate), and a scaffold (both the titanium mesh for the overall morphology of the implant and Bio-Oss® blocks providing an osteoconductive material).

To overcome the problem of transplanting this construct into the poorly vascularized tissue bed of the residual mandible, it was instead placed within the latissmus dorsi muscle of the patient for 7 weeks to allow for revascluarization of the construct. In this way, a vascularized free flap transfer of the TE construct and its accompanying soft tissue envelope was possible, whereby the thoracodorsal artery and vein of the latissmus dorsi were anastomosed to vessels of the neck. Warnke *et al.* were able to follow the patient for 15 months until he passed away from cardiac arrest, but during that time the patient's quality of life improved dramatically as his ability to eat and speak had improved.[158]

This brief overview of conventional treatments for disfiguring and large composite tissue defects using vascularized free flaps and prostheses illustrates

the fact that all of the materials and methods currently in clinical use fall short of providing complete aesthetic and functional regeneration of lost tissues. The following sections will provide an overview of current research in craniofacial tissue engineering which has the potential to revolutionize the clinical methods of reconstruction we know today.

2.3 Engineering multiple craniofacial tissues

Tissue engineering strategies rely on the use of cells, bioactive factors, and scaffolds or combinations thereof. The scaffold serves the purpose of a delivery vehicle, a space-filling and structurally supportive agent, and can be designed to be biointeractive, i.e. to guide tissue regeneration. The field of tissue engineering has made significant advances over the past 15 years. Interdisciplinary research spanning basic cell biology to nanotechnology has deepened our understanding of nature and enabled methods of biomimicry to augment or replace tissue or even organ function. Research on the regeneration of virtually all types of tissues is being conducted, and products for cartilage, bone, and skin regeneration are already approved for commercial use by the United States FDA. The engineering of more complex tissues remains a challenge, but encouraging advances in the form of a tissue engineered bladder[68] and an increased focus on issues specific to engineering complex tissues[159] have recently appeared in the literature.

The coordinated regeneration of multiple tissues in the complex craniofacial environment requires a deep understanding of their physiology and

remodeling characteristics. Complex tissues must be engineered with the structural and functional characteristics of native tissue in a process that is not only biocompatible but also interactive and integrative with neighboring tissues simultaneously. Another challenge lies in that one type of tissue can be found in various structures that serve different functions and have therefore different properties. For example, the cartilaginous structures found in the craniofacial region have very distinct characteristics. A specifically tailored approach may be required to regenerate the weight-bearing, dense, and bilaminar cartilage found in the temporomandibular joint (TMJ) and a quite different approach required to create the delicate elastic cartilage found in the ears or nose.[160]

Tissues of the craniofacial region include skin, bone, muscle, cartilage, adipose tissue, tendons, ligaments, salivary glands, blood vessels, nerves, and teeth (Figure 2.1). Extensive research is conducted on each of these tissues and the need for them well established,[161] but few studies focus on regenerating multiple tissues in tandem. Recent advances in craniofacial tissue engineering, as summarized by Mao *et al.*,[162] include integrated bone and cartilage layers for the TMJ condyle, various elements of the periodontium, craniofacial bone, cranial suture-like structures as well as adipose tissue. Tissue engineering of skin is not always reported in articles reviewing craniofacial tissue regeneration; however, skin regeneration is an important aspect to consider, as trauma is one of the major causes of tissue loss. Trauma affects both hard and soft tissues, damaging the skin and severely compromising its protective barrier function.

The next sections will focus on briefly reviewing the distinct anatomical and physiological properties of craniofacial and oral components, as well as progress towards engineering these tissues. Finally, the parameters that will allow for tissue engineering of complex structures will be discussed.

2.3.1 Bone

Tissue engineering of the cranial and facial bones holds great potential towards the functional and aesthetic restoration of this tissue. Craniofacial bone serves as a protective barrier to the intracranial structures and maintains the shape of the head and face. Bone loss results in severe functional and aesthetic consequences such as problems in mastication and compromised head and facial contour with collapse of the surrounding soft tissues. Bone is a highly vascularized and cellular tissue. The inorganic mineral component of bone extracellular matrix (ECM) provides the mechanical strength of the matrix.[163] Approaches towards bone tissue engineering are numerous, and much progress has been reported towards that goal. Desirable bone tissue engineering constructs are osteoconductive and osteoinductive. Review articles on bone tissue engineering considerations have been extensively published.[164-169] Our group and other researchers have been using synthetic biomaterials in conjunction with growth factors and/or cellular delivery to regenerate bone. Synthetic polymers, ceramics, or composites thereof are biomaterials commonly investigated for bone tissue engineering; many of these systems are injectable as well and will be discussed in subsequent sections.

Osteogenesis is likely very strongly dependent on angiogenesis.[159] Besides the facilitated transport of nutrients, oxygen, and minerals, blood vessels stimulate bone morphogenesis due to the osteogenic effects of vascular cells.[170] This association has led many researchers to investigate the incorporation of angiogenic growth factors into bone tissue engineering models.[19, 171, 172] Potent osteogenic factors such as BMP-2 have been shown to induce ectopic bone formation, i.e. in sites where bone would not normally grow.[173, 174] As our understanding of bone biology and development deepens, potential frontiers open within tissue engineering. One such breakthrough was the isolation and identification of mesenchymal stem cells (MSCs), a class of bone tissue progenitor cells. Biomechanical and biochemical factors that enhance the bone-forming capacity of these cells are currently heavily examined.[175-178]

2.3.2 Skin

The skin is the largest organ in the body. Its barrier function protects the internal organs from the external environment, maintains water and temperature homeostasis and provides communication with the immune system. Skin consists of two main layers, the epidermis and the dermis, the latter being vascularized. Bell *et al.*[51] and Burke *et al.*[179] reported some of the first attempts to create a full thickness, tissue engineered skin graft. Natural polymers such as collagen gels have been widely used as matrices for skin tissue engineering.[51, 179, 180] Vascularization is critical for success of engineered skin, and room for improvement in this area exists for current tissue engineered skin[181]. This has

been addressed by various techniques such as seeding skin cells together on a scaffold with endothelial cells that can then form new vessels.[180, 182] The potential role of growth factors in skin tissue engineering is reviewed elsewhere.[181] Skin tissue engineering has been largely successful relative to other tissues and must now be performed in combination with tissue engineering of other less superficial tissues such as bone and muscle for the treatment of deep wounds or for regeneration following aggressive tumor resections.

2.3.3 Cartilaginous structures

Cartilage regeneration *in vivo* seldom occurs due to the avascular nature and relatively sparse cellularity of native cartilage. Therefore, tissue engineering strategies employing scaffolds, cells and bioactive factors represent one of the only methods to regenerate or repair cartilage following injury. In craniofacial structures, cartilage is mainly found in the ear, the nasal tip, and the TMJ. As mentioned before, the cartilage in these structures has distinct characteristics and serves different functions that are reflected by differences in the composition and architecture of the various cartilage types. In the first two organs, cartilage provides shape and flexibility but has no load-bearing properties. In order to increase ECM production and considering the relatively low number of chondrocytes in cartilage, cell transplantation is one of the most common approaches in cartilage regeneration. Much research has been devoted in identifying the right cell source and culture conditions for cartilage tissue engineering and for auricular and nasal tissues in particular.[183, 184] Kamil *et al.*[185]

were able to engineer full-sized human cartilaginous skeletons for the external ear and the nasal tip *in vitro* by seeding chondrocytes on prefabricated, biodegradable scaffolds. Even though injectable hydrogels that mimic the cartilaginous matrix have been used extensively as models for articular cartilage regeneration, there has been limited use of these systems in nasal and auricular cartilage tissue engineering. The TMJ is another distinct, cartilaginous structure within the joint connecting the mandible to the temporal bone; TMJ cartilage can be found on the surface of the mandibular condyle, as a layer lining the temporal bone, and as the TMJ disc positioned between the two bone surfaces.[186, 187] These load-bearing structures lubricate the surface between the bones and may have shock-absorbing and load-distributing properties.[186] The TMJ disc is composed of fibrocartilage, a type of cartilage characterized by high collagen fiber content in its matrix.

Review articles summarizing TMJ properties and design parameters using the tissue engineering paradigm of cells, scaffolds and stimuli, are available.[186-188] Tissue engineering of the mandibular condyle needs to account for its distinct architecture, consisting of a cartilage layer and the underlying subchondral bone. Successful attempts towards regeneration of that complex structure have been performed using pre-differentiated, osteogenic and chondrogenic, cell populations,[189] although no consistently successful tissue engineering solution is clinically available.

2.3.4 Oral and dental tissues: periodontium and teeth

The oral cavity represents a unique environment for tissue regeneration as there is widespread need to develop functional tooth replacements with proper attachment, and healing within the oral cavity must occur in the presence of the oral flora, which creates a "contaminated" environment.[159] Engineering a whole tooth is a difficult task due to the complexity of the teeth, which are mineralized, multi-layered matrices. Enamel, dentin, and cementum layers form the hard tissue part of teeth, whereas dental pulp forms the soft tissue in the central core. An additional hurdle in tooth tissue engineering is the creation of appropriate innervation and vasculature.[190] Other common dental conditions include diseases of the periodontium, which can lead to tooth loss. The periodontium is comprised of cementum, the periodontal ligament, which is the fibrous connective tissue surrounding the root of a tooth, and the attached alveolar bone. Approaches towards the regeneration of the periodontal ligament and surrounding osseous defects with growth factors, gene and cellular delivery have been reviewed elsewhere.[162]

2.3.5 Muscle and adipose tissue

The treatment of craniofacial injuries or anomalies often requires the regeneration of soft tissues such as skeletal muscle and adipose tissue. Skeletal muscle directly attaches to bone and, in the craniofacial region, allows for mastication, respiration, eye movement, and facial expression.[191] Skeletal muscle tissue engineering is still at an early stage. Results from *in vitro* studies have

shed light on the extracellular matrix remodeling of muscle[192-194] and identified conditions for increased skeletal muscle differentiation and growth.[195, 196] Shah *et al.*[191] have investigated the potential of a three-dimensional phosphate glass fiber scaffold for craniofacial muscle engineering. Human muscle-derived cells seeded on these scaffolds and cultured *in vitro* with insulin-like growth factor 1 (IGF-1) were able to proliferate and produce prototypical muscle fibers.

Adipose tissue regeneration is needed for the reconstruction of craniofacial structures such as the cheek, chin and jaw.[197, 198] There have been several studies that demonstrated the potential for *in vivo* adipose tissue regeneration. MSCs isolated from the bone marrow[199-201] or adipose tissue[200] have been shown to be promising candidates for adipose tissue engineering. Conditions that promote differentiation of these uncommitted progenitor cells to adipose cells, such as adipogenic culture media[199, 200, 202] and growth factor regimes,[201] have been reported. An interesting approach towards the creation of vascularized adipose tissue was recently suggested by Marra *et al.*[203] Particles of the small intestinal submucosa were used as a carrier for the delivery of progenitor fat cells. The cells attached and proliferated on these particles, and cell survival *in vivo* was noted for a period of 14 days. This injectable vehicle allowed also for the incorporation of PLGA microspheres loaded with fibroblast growth factor 2 (FGF-2), which enhanced vascularization.

2.3.6 Future directions and considerations

Tissue engineering of complex tissues such as these found in the craniofacial region is a demanding task. One needs to account for multiple cellular phenotypes and find ways to enhance cellular interactions towards tissue repair, possibly stimulating their behavior by supplying bioactive factors. Furthermore, the problem of insufficient vascularization must be overcome since most tissues are strongly dependent on blood supply for growth. Creating stratified tissue architectures and recreating the physiological structure-function properties of the native tissues is the ultimate goal. The choice of a tissue engineering scaffold can significantly aid in this process, not only by serving as a delivery vehicle for cells and bioactive factors but also by providing the ability to interact with and guide tissue growth. Cell-material interactions and mass transport are only some of the important parameters that need to be incorporated into the design. Additionally, one needs to consider that the location and form of craniofacial tissues requires special treatment. For this delicate region, aesthetic considerations are important and there should ideally be minimal scar formation. All these parameters will be further examined in the next sections where the use of injectable systems for multiple tissue regeneration is discussed.

2.4 Injectable systems in tissue engineering

As highlighted in the previous sections, technologies and strategies in tissue engineering, and in particular those designed for engineering multiple functional tissues, utilize the delivery of cells and bioactive factors in combination

with the placement of a support structure or scaffold. Injectable systems, particularly aqueous systems, hold great promise in tissue engineering applications as they can potentially deliver water soluble drugs and growth factors in combination with cells to a tissue defect in a manner that provides an adequate environment for long term cell survival, proliferation, and differentiation.

In the clinical setting, particularly when considering surgical repair, revisions, and/or subsequent reconstruction/regeneration of tissue defects, injectable materials at present hold the most immediate promise in treating defects for which minimally invasive strategies already exist. The delivery of cells, bioactive factors, and support materials via an injectable system within the context of an endoscopic, arthroscopic, laparoscopic, or radiologically guided procedure is feasible given the current state of the art. Within the craniofacial complex (CFC), however, most current surgical techniques towards the treatment of traumatic injury, tumor resection, or congenital deformity are somewhat more invasive than those previously mentioned. Injectable systems are attractive in this setting due to the ability of these systems to conform to complex craniofacial shapes, contours, and defects without the need for extensive presurgical modeling. Additionally, due to the close proximity of multiple tissue types within the CFC, injectable systems containing multi- or totipotent cell populations and growth factors will potentially allow for more natural remodeling and regeneration of damaged, diseased, and excised tissues. In the case of a staged surgical intervention, the use of injectable systems to aid tissue regeneration may avoid

the need for multiple invasive operations, thus reducing the morbidity and negative aesthetic effects associated with these repeated procedures. Finally, and as mentioned previously, there are many aesthetic cases where the use of injectable materials is already widespread due to the requirement in these cases for no incision as to minimize potential scarring. As described before, these materials are however not used for tissue engineering purposes but are rather volume fillers with biological activity that is often limited to being encapsulated as part of the foreign body response.

While the ability to deliver cells and bioactive factors make injectable systems attractive alternatives to the preformed implant materials currently used, the success of any injectable system will largely be determined by the support system or framework the system provides. This scaffold must provide early mechanical support commensurate to that of the tissue it replaces, allow cells to survive, proliferate, and differentiate, and it must provide for the controlled release of any drugs or growth factors delivered simultaneously. Above all, this matrix must be biocompatible and ideally will be biodegradable such that with time regenerated tissue will replace the biomaterial component of the system, resulting in functional, healthy tissues approximating those of the premorbid individual and avoiding long term implant failure requiring subsequent retrieval (Figure 2.2).[204] A large number of materials have been developed and applied *in vitro* and in animal models towards this end; we will highlight a number of those materials in the next section to introduce promising materials and

fabrication/synthetic strategies for creating injectable tissue engineering scaffolds.

2.5 Injectable scaffolds

2.5.1 Requirements

In addition to the basic requirements for any biomaterial to be considered in clinical applications (biocompatibility of the material and subsequent degradation products, handling characteristics allowing achievement of any necessary processing and end functions, etc.), a number of unique requirements exist for complex tissue engineering within the CFC. Three fundamental requirements for biomaterial scaffolds used in the CFC include the ability to fit complex anatomical defects, provide mechanical support for regenerating and surrounding tissues, and deliver bioactive factors to aid tissue regeneration.[205]

The following sections of this chapter will demonstrate the ability of injectable biomaterial scaffolds to fit complex defects, given that the defects have well defined borders or given the incorporation of a rigid template to define the shape as well as the well documented delivery of bioactive factors and cells with injectable material scaffolds. Mechanical requirements for biomaterials in the CFC vary widely based on tissue type and location. Within a human mandible, for example, significant regional variation has been found for cortical bone thickness and the direction of maximum stiffness, with maximum elastic moduli exceeding 30 GPa.[206, 207] Similarly, the cranial vault and zygoma exhibit high levels of

anisotropy and elastic properties based on regional and functional character.[208] Facial muscles have wide variations in tensile properties as well,[209] thus making it apparent that a single material without variable properties will not likely be successful for applications in which multiple tissues or large portions of one structure are to be regenerated. For such applications, combinations of materials or materials with varying mechanical and biological properties must be investigated. Therefore, in addition to those requirements laid out previously, any injectable biomaterial to be used for complex tissue engineering in the CFC must either have tunable mechanical properties or be able to be integrated into a delivery system or scheme that involves the use of other biomaterials. An ideal system will also degrade in a manner so that the degradation rate is proportional to the rate with which tissue ingrowth or differentiation occurs into or within the scaffold and the extent of mechanical support needed by that specific tissue.

The following section provides examples of injectable materials. These materials, selected from amongst a multitude of injectable materials currently being studied as biomaterials for tissue engineering and other applications, have been chosen to highlight different classes of materials and different methods that are commonly used or promising in their potential for future use and development in making the transition from an injectable material to a tissue engineering scaffold.

2.5.2 Injectable scaffold materials

Calcium phosphate cements

As described earlier, there are a number of CaP cement-based injectable biomaterials that are currently used and regulated in clinical applications. While these materials have achieved widespread success for bone defect repair and regeneration, concerns about degradation and the brittle mechanical profile of these materials limits their successful usage in many applications.[210] Most commonly used for bone related applications, CaP composites have also been used as soft tissue fillers, demonstrating the potential versatility of these materials.[211]

CaP composites have been studied to alleviate some of the negative properties of materials based solely on CaP cement. Macroporous CaP materials are more favorable for tissue engineering applications than nonporous implants.[212] PLGA microparticles incorporated within an injectable CaP formulation can, upon degradation of the PLGA, yield macroporosity for tissue ingrowth and, possibly through a lowered local pH upon degradation of the PLGA, can accelerate degradation of the CaP phase.[213-216] The incorporation of other degradable particles such as poly(trimethyl carbonate) and gelatin microparticles has yielded similar favorable results within injectable formulations,[217, 218] and the potential for drug or growth factor release from these systems has been well demonstrated.[38, 213, 219-221] Including a water soluble porogen such as mannitol can both improve the injectability of CaP cement while

also improving the flexural strength and toughness of the resulting scaffold.[222] Although not part of an injectable system, the incorporation of an absorbable polymer mesh within a CaP cement can also significantly increase the flexural strength and toughness of the material while resulting in macroporosity upon degradation of the network.[223, 224] CaP composite systems that utilize an injectable CaP cement with a porogen have distinct advantages over CaP cements alone and will likely, once gaining final regulatory approval, be counted among the preferred choices of clinicians for bone regeneration and tissue engineering applications.

A second class of composite scaffolds uses CaP granules within water soluble carriers. These materials, which among others can use modified[225, 226] or unmodified[227-229] hydroxy-propyl-methyl-cellulose as the polymer carrier, have resulted in faster initial osteoconduction *in vivo* when compared to other macroporous CaP cements. If achieved rapidly enough, this early bony apposition could potentially ameliorate any mechanical deficiencies in the material, facilitating its use in load bearing tissue applications. Smaller, nanosized CaP crystals have been incorporated into other injectable biomaterials,[230] and coating of mesenchymal stem cells with CaP nanorods enhances osteoblastic differentiation and extracellular matrix production of the cells,[231] indicating that CaP materials, at least in some forms or as composites, may be suitable carriers for the injection and induction of stem cells.

In situ polymerizable and crosslinkable materials

Polymeric biomaterials are the most widely studied class of biomaterials investigated for use as injectable scaffolds. *In situ* solidification of polymeric systems is typically achieved either through phase separation or via polymerization or crosslinking of reactive monomers and macromer chains. Systems that utilize phase separation to solidify or harden *in situ* will be considered along with other self-assembling systems in a subsequent section.

Both *in situ* polymerization and crosslinking often use a radical initiator that, through interactions with reactive functional groups such as the double bond within a vinyl or acrylic moiety, results in enhanced mechanical properties and shape definition of the scaffold. Photopolymerization using ultraviolet light-activated initiators is one method by which biomaterials can be crosslinked *in situ.* One such radical initiator is bis(2,4,6-trimethylbenzoyl) phenylphosphine oxide (BAPO), a molecule that is activated by long wavelength ultraviolet light and has been successfully used to crosslink networks of poly(propylene fumarate) (PPF).[232, 233] Photopolymerizable interpenetrating networks of poly(ethylene glycol) (PEG) and poly(ethylene glycol) diacrylate (PEGDA) have been used to encapsulate human MSCs, and the network mechanical properties can influence extracellular matrix (ECM) deposition and cellular differentiation.[234] A similar PEG network used photoinitiation to pattern the hydrogel surface.[235] Successful encapsulation of and differentiation of MSCs into osteoblast-like cells

on poly(D,L lactide-*co*-ε caprolactone) photocrosslinked injectable scaffolds has also been demonstrated.[236, 237]

Transdermal photopolymerization has been successfully performed using ultraviolet light;[238, 239] however, most clinical applications using ultraviolet-activated photocrosslinkable or photopolymerizable systems will require an open defect to allow for penetration of light to the material, a potential drawback in the clinical setting. Using a near IR light source would however allow deeper tissue and material penetration such that larger material volumes could be polymerized/crosslinked, and the use of such a light source also allows for three-dimensional patterning of the material.[240] Similar to three-dimensional patterning, Sun *et al.* demonstrated microstructural control of polymer nanocomposites with tunable physical characteristics based on crosslinking density as influenced through crosslinker and photoinitiator concentrations.[241] Similarly, Burdick *et al.* utilized a microfluidic approach to create surface peptide gradient hydrogels via photopolymerization.[242]

Thermal initiators are perhaps more amenable to minimally invasive delivery and *in situ* formation of an injectable scaffold. Systems that are activated near or at body temperature (37 °C) are ideal as they utilize normal *in vivo* conditions to initiate scaffold or network formation. Ammonium persulfate/N,N,N',N'-tetramethylethyldiamine (APS/TEMED) is a water soluble thermal initiator system with demonstrated cytocompatibility that has been studied as part of an *in situ* crosslinkable oligo(poly(ethylene glycol) fumarate)

(OPF) hydrogel.[243] One of the main problems with radically initiated systems is that, although tolerated at low concentrations, high initiator concentrations can be cytotoxic to encapsulated cells,[244] thus limiting the amount of initiator that can be included for *in situ* forming systems and subsequently limiting the range of control over important parameters such as formation kinetics and material mechanical properties.

In addition to free radical initiation, a variety of chemical crosslinking or polymerization strategies for the *in situ* formation of biomaterial scaffolds exist. *In situ* crosslinkable PEGDA gels were fabricated using a reverse emulsion and Michael-type addition, resulting in materials with an ultimate compressive strength of nearly 7 MPa and making them potential scaffolds for load bearing soft tissue regeneration.[245] Nano- and microscale control of scaffold architecture has been demonstrated for *in situ* prepared nanocomposites and microspheres using a condensation reaction and interfacial polymerization, respectively.[246, 247]

More biologically motivated systems for *in situ* scaffold formation also exist. Enzymatic methods for chemically crosslinking polymer chains *in situ* have been used to fabricate matrices composed of peptide modified synthetic polymers[248, 249] and natural polymers.[250-252] Transglutaminases, which naturally crosslink blood clots and other biological structures, are commonly used to crosslink protein scaffolds or peptide modified scaffolds as the enzyme facilitates an acyl transfer reaction between a free amine group and a γ-carboxyamide.[253, 254]

Stimulus responsive systems

Materials that undergo physical gelation rather than chemical crosslinking are also being explored for use as injectable scaffold materials for tissue engineering. These materials can undergo physical gelation in response to one or multiple changes in their surrounding environment including changes in temperature, pH, ions, and pressure or the presence of electrical and/or magnetic fields.[255-257]

Thermogelling materials, which undergo entropically driven phase separation above their lower critical solution temperature (LCST), are widely investigated for use in drug delivery and tissue engineering applications.[258] For *in situ* gel formation following injection, water-soluble materials with LCSTs at or below normal body temperature are desirable as they rapidly gel following injection and can then encapsulate cells and bioactive factors within a well-hydrated network. Poly(N-isopropylacrylamide) (PNIPAAm) has a LCST of 32 °C; however, when copolymerized with hydrophilic molecules, PNIPAAm containing materials with LCSTs closer to physiological temperature and thus undergoing less syneresis at 37 °C have been synthesized.[259-262] Other synthetic thermogelling polymers that have been studied as tissue engineering scaffolds and cell delivery vehicles include block copolymers of poly(ethylene oxide) and poly(propylene oxide)[263-265] as well as copolymers of PEG with PPF,[266] poly(organophosphazenes),[267] and PLA.[268] Natural polymers and associated composites also demonstrate thermogelling character and have been explored

as injectable tissue engineering matrices.[269-271] The use of tandem gelation combining physical and chemical gelation techniques has led to materials that undergo rapid thermogelation and subsequent chemical crosslinking, yielding injectable materials that combine the favorable kinetics associated with physical gelation with the mechanical characteristics and stability of covalently crosslinked materials.[272-275]

Self assembling materials

Similar to stimulus responsive materials, injectable self-assembling materials undergo gelation or precipitation, often with the ability to form precise nano- or microscale structures without the need for chemical crosslinking or initiating agents. Many such systems use hydrophobicity, either of the bulk material for phase segregation or of certain molecular domains for amphiphiles, as the key means by which self-assembly occurs.

Injectable materials that self assemble *in situ* via phase segregation are often delivered in the form of a water insoluble polymer injected in solution with a water miscible solvent. Following injection, the solvent diffuses into the tissue space, allowing the polymer component to precipitate within the aqueous environment of the injection site. The solvent must thus be biocompatible to surrounding tissues and cytocompatible if cellular delivery is to be achieved; dimethyl sulfoxide (DMSO) and N-methyl-2-pyrrolidone (NMP) are two such solvents. Phase separating systems based on PLGA have been studied for nearly 20 years,[276] and continuing recent research has been directed at

optimizing PLGA and other polymeric systems by better controlling the solvent removal rate and drug release kinetics *in vivo*.[277, 278]

Tisseel® (Baxter Biosciences, USA), one of the earliest developed and clinically most successful of these phase separation systems uses a dual injection of fibrinogen and thrombin to form a fibrin clot or scaffold. Thrombin cleaves soluble fibrinogen into insoluble fibrin that then self assembles into fibrils resulting in, in combination with platelets, a clot. These fibrin clots, formed from the same biomolecules as used for natural clotting *in vivo* but at higher relative concentrations, are widely used as an adhesive sealant to achieve hemostasis during surgical procedures. Although Tisseel® as packaged for current clinical applications is not an ideal scaffold material because the high crosslinking density of the fibrin network prevents cell migration into and throughout the clot,[279] more dilute fibrinogen and thrombin solutions can support stem cell proliferation[280, 281] and with appropriate mechanical properties can also induce stem cell differentiation.[282] Fibrin-based systems have also been modified, resulting in promising materals for engineering specific tissue types. Research has yielded engineered BMP-2 fusion proteins that incorporate into fibrin matrices and enhance bone regeneration[283] and fibrin gels with incorporated ECM peptides that enhance key aspects of nerve regeneration (Figure 2.3).[284] Although not truly self assembling systems, as mentioned previously biomaterials such as PEG can also be modified with peptides so that they can be crosslinked using similar thrombin/clotting factor systems, eliminating the need for soluble

synthetic initiators that may be cytotoxic to encapsulated cells or surrounding host tissue.[249]

Self-assembling amphiphiles are another promising class of injectable materials for tissue engineering. A recently developed self-assembling peptide hydrogel undergoes shear thinning, such that when an appropriate shear stress is applied, the material thins into a low viscosity gel allowing for injection.[285] After injection, the gel recovers its initial mechanical rigidity, making it a promising candidate for injectable applications. Peptide amphiphiles that self assemble with nanostructural organization in aqueous solution can be modified with peptide sequences to influence cell behavior, leading to increased cellular adhesion (Figure 2.4)[286, 287] or guided axonal regeneration within an injured spinal cord.[288] Kirkham *et al.* have investigated similarly functional self assembling peptide amphiphiles that nucleate mineralization in physiological conditions, an effect that has applications in dental and other hard tissue engineering applications.[289, 290] Self-assembling peptide amphiphiles modified with heparin have been used to stimulate angiogenesis[291] and, within a titanium scaffold, to aid in bone regeneration;[292] these applications demonstrate the ability of modified peptide amphiphiles to aid in regeneration of multiple tissue types, making them ideal candidates for complex tissue engineering.

Other promising self-assembly strategies for injectable scaffold fabrication exist. Micro- and nanosphere injection for use as drug delivery vehicles and scaffolds is possible;[293, 294] however, simple injection of the uncrosslinked

particles offers little control over bulk mechanical properties or material behavior *in vivo* as the individual particles are bound only by space limitations and may migrate. Self-assembly techniques that result in crosslinking of the particles allow for augmented mechanical characteristics and control over scaffold architecture even as tissue remodeling commences. Ionically crosslinked networks of positively and negatively charged nano-[295] and microspheres[296] exhibit tunable mechanical properties and hold potential as both drug and cell delivery vehicles. Salem *et al.* crosslinked biotinylated PLA-PEG microparticles using avidin in the presence of cells to create injectable cell-containing matrices with mechanical strength suitable to support bone regeneration *in vivo* (Figure 2.5).[297]

2.6 Drug delivery via injectable scaffolds

Most of the materials and techniques used in the development of injectable scaffolds for tissue engineering were first or have concurrently been investigated as injectable drug delivery systems. Many of the requirements for injectable drug delivery systems and injectable scaffolds are the same as any injectable biomaterial in that they must be biocompatible, and precise control of drug release kinetics will be of great benefit in both areas. In tissue engineering, there are, particularly for applications such as bone and dental regeneration, more demands upon a material and scaffold to be mechanically similar to the tissue being replaced since at the time of delivery the material must not only support regeneration but also largely perform the structural function of the native tissue. Because of this, not all materials developed for drug delivery are suitable

for tissue engineering purposes. Detailed reviews of injectable materials for drug delivery[298] and drug delivery from injectable tissue engineering matrices[167] are available; the following sections will briefly examine delivery of antibiotics and growth factors, two agents critical to successful tissue regeneration within the CFC, within injectable tissue engineering scaffolds.

2.6.1 Antibiotic delivery

The presence of infection is an important parameter that must be considered for nearly any reconstructive technique, be it the currently used surgical techniques utilizing implants and flaps or proposed tissue engineering solutions. Infections following traumatic craniofacial injuries are a common occurrence, particularly when the injury involves wound contamination through either penetration of a foreign object or loss of skin.[299] Additonally, open communication with the oral cavity can lead to infection from oral flora, and in many cases latent infection that may not lead to clinical signs of infection but may hinder wound healing and tissue regeneration is present.[300-302] Antibiotic delivery may thus be an important aspect of tissue engineering strategies in the CFC, both for curing and preventing latent or active posttraumatic and postsurgical infections.

Although antibiotics can and have been incorporated into many commercially available bone cements, poor release kinetics and the sensitivity of many antibiotics to the high curing temperatures associated with cements such as PMMA make incorporation into the bulk material an inefficient and in some

cases ineffective strategy.[303-305] Many drug delivery systems for antibiotic and other bioactive factors utilize drug-loaded microspheres or microparticles. At small particle or sphere sizes, these systems are easily injectable, have well characterized and tunable release kinetics, and can be fabricated from biocompatible, biodegradable materials such as PLGA[306, 307] or gelatin.[308]

Tobramycin loaded PLGA-PEG blend microparticles have been shown to have well-controlled release profiles and can maintain tissue tobramycin concentrations over the minimum inhibitory concentration of *Staphyloccous aureus* for over one month,[309] resulting in more effective treatment of osteomyelitis when compared to tobramycin released from a bulk bone cement.[310] PLGA microspheres injected with chemically crosslinkable PPF exhibited continuous drug release over one month, and the degradation of the microspheres yielded scaffold porosity to facilitate tissue ingrowth without compromising the compressive strength of the scaffold.[311] In the absence of microspheres, greater control of release kinetics can be achieved by including a hydrogel component or coating along with a bulk CaP cement.[312, 313] Osteoblasts cultured in the presence of antibiotic-loaded microspheres made of nanohydroxyapatite attached to and proliferated well in the material;[314] however, there is some concern regarding stem cell proliferation and differentiation capacity in the presence of antibiotics,[315] meaning combined delivery of stem cells with antibiotics must be carefully considered and studied prior to implementation.

2.6.2 Growth factor delivery via injection for engineering multiple tissues

Growth factors are extracellular signal proteins that mediate the growth, proliferation and differentiation of cells. All these processes are crucial for tissue growth and repair *in vivo,* often determining the success of an engineered tissue. Growth factors act by binding to specific receptors on the same cell that has secreted the factors (autocrine signaling), neighboring cells (paracrine signaling), or distant cells (endocrine signaling). Upon binding, a cascade of cellular events is initiated, leading to cell proliferation, differentiation and maturation, as well as to the production of extracellular matrix and other growth factors.[316] Growth factors can act on multiple cell types and are generally not specific for one type of tissue, making them especially useful for complex tissue engineering. The following paragraphs aim to categorize the use of growth factors towards regeneration of certain tissues, and review the injectable carriers available for their delivery.

Angiogenic growth factors

The formation of blood vessels has been identified as a key factor towards tissue regeneration and growth. Angiogenesis is the formation of new blood vessels from existing ones and is driven by endothelial cell proliferation and migration. This is opposed to vasculogenesis which is the formation of blood vessels *de novo*.[317] The two main growth factor families that have been shown to directly stimulate angiogenesis are vascular endothelial growth factor (VEGF) and FGF. Moreover, the well-characterized transforming growth factor-β (TGF-β)

superfamily has an indirect effect on angiogenesis *in vivo*, as does the PDGF family[18]. Growth factors inducing angiogenesis contribute largely to the wound healing process, as for example the TGF-β superfamily.[318]

Osteogenic growth factors

Growth factors that encourage the formation of new bone have been identified and applied to heal bone defects around medical and dental implants and without implant placement.[319] Review articles on the properties and delivery of osteogenic growth factors are available.[320, 321] BMPs, which are part of the TGF-β superfamily, have osteo- and chondroinductive properties.[322] The BMP family consists of at least 20 different proteins, among which two (BMP-2 and BMP-7) are commercially available for clinical applications.[323] Other factors include the insulin-like growth factors (IGF), which have been shown to have an effect on tissue formation, especially bone, FGF, which are synthesized by skeletal cells,[316] and PDGF, which is known for enhancing protein synthesis in bone.[324]

Chondrogenic growth factors

Members of the growth factor families listed above have been also shown to stimulate the formation of new cartilage, including TGF-β, BMP and IGF proteins.[325-327] The regulatory effects of growth factors on articular chondrogenesis are summarized elsewhere.[328, 329]

2.6.3 Injectable growth factor delivery

Tissue engineering of complex craniofacial tissues, as has been stressed in previous sections, requires thorough understanding of these tissues' biology as well as their environment. In order to mimic physiological processes and regenerate tissue *in vivo*, growth factor delivery will be an important aspect to consider. The expression of different growth factors during the healing cascade within complex tissue defects has been the object of much research, and the challenge facing tissue engineers is to direct the release of multiple growth factors at various time intervals from a scaffold as to simulate and enhance the actual healing process.[159] Many studies so far have used growth factors at concentrations much higher than physiological concentration in order to increase their bioavailability, although improving efficiency in growth factor loading and delivery is the focus of some new delivery vehicles.[330] Delivery of higher concentrations of growth factor than physiologically encountered may not, however, have the desired effects and also increases costs tremendously. Controlled release of growth factors is therefore a crucial variable in achieving a safe and effective dosage, and the scaffold can play a role in achieving appropriate temporal and spatial delivery. The next paragraphs will review the recent advancements in growth factor delivery from injectable tissue engineering carriers.

Polymeric carrier materials for multiple tissue regeneration

Polymers are probably the most widely used class of injectable materials for achieving controlled growth factor release. The importance of controlled release kinetics was highlighted in a study conducted by Woo *et al.*[331] Using a carboxymethylcellulose hydrogel with PLGA microparticles loaded with recombinant human BMP-2, they showed that sustained release of the growth factor promoted bone healing significantly better than a burst release system. Similar to antibiotic delivery, many other systems incorporating microparticles for growth factor delivery have been developed. The encapsulation of growth-factor loaded gelatin microparticles in OPF hydrogels minimizes the burst release often associated with this type of material.[326] Growth factor loading on gelatin microparticles is achieved by polyionic complexation, and the *in vivo* release is governed by the enzymatic degradation of gelatin.[332] A design for multiple tissue regeneration was suggested with such a composite. A bilayered OPF hydrogel system with incorporated TGF-β1-loaded gelatin microparticles, consisting of a bone forming and a cartilage forming layer, was used with promising results for osteochondral repair (Figure 2.6).[333] The same scaffold was later used for dual delivery of TGF-β1 and IGF-1. It was designed to release TGF-β1, a chemoattractant and morphogen, rapidly, followed by release of IGF-1, a stimulator of extracellular matrix formation, in a more sustained manner.[334] The *in vivo* findings, however, did not suggest a synergy between these factors as expected from *in vitro* observations and did not result in significant improvement

of new tissue quality. Dual growth factor delivery has been also proposed for bone repair. Patel *et al.*[19] have investigated the effect of dual delivery of an angiogenic (VEGF) and an osteogenic (BMP-2) growth factor in a rat critical size cranial defect. The growth factors were incorporated in gelatin microparticles and were injected into porous PPF scaffolds. After four weeks, the dual release system resulted in much higher bone formation than either growth factor alone, indicating a synergistic effect in this time interval. At twelve weeks, BMP-2 and dual release groups showed increased bone formation over VEGF alone and control groups but were not significantly different from each other (Figure 2.7). In addition to growth factors released from polymer matrices to induce cellular differentiation, an alternate strategy utilizes growth factors to encourage cell migration into or throughout a hydrogel in a similar manner to the previously mentioned adhesion molecule-modified peptide amphiphiles and fibrin gels.[335]

Thermoresponsive hydrogels have been also used for growth factor delivery. These hydrogels are typically liquid at ambient temperature and solidify at close to physiological temperatures. A poly(NIPAAm-*co*-acrylic acid) hydrogel was blended with hyaluronic acid and used for TGF-β3, dexamethasone, and cell delivery.[336] Gao *et al.*[337] were able to conjugate rhBMP-2 to thermoreversible polymers while maintaining the osteoinductive properties of the growth factor. Thermoresponsive Tetronic® was copolymerized with ε-caprolactone and subsequently conjugated with heparin, resulting in polymeric micelles. Basic FGF, a heparin-binding growth factor, could be released from these micelles in a

controlled manner over two months.[338] Moreover, the amphiphilic nature of the micelles allows for the dual delivery of a hydrophilic molecule such as a growth factor together with a more hydrophobic compound.[339]

Heparin has been also used in combination with a modified chitosan hydrogel for sustained release of FGF-2. Significant angiogenesis and fibrous tissue formation was observed in animals following injection of the loaded hydrogel.[340] The angiogenic effects of VEGF alone[341] or in sequential release with PDGF-BB[342] were investigated using different molecular weight alginate polymers. Good spatiotemporal control of the release kinetics was achieved with these hydrogels, resulting in a promising vehicle for stimulating angiogenesis. Hosseinkhani *et al.* developed another interesting carrier applied towards the same goal. They synthesized an injectable, self-assembling peptide-amphiphile that allows for simple mixing of an aqueous solution with basic FGF suspension and can be injected and self-assemble *in vivo*. This system proved advantageous for angiogenesis as compared to basic FGF or amphiphile injection alone and holds promise as a carrier for therapeutic proteins.[343] Hiemstra *et al.* have also investigated a dextran-based system for FGF delivery that forms *in situ* via a Michael-type addition.[344]

2.6.4 Injectable ceramic materials and their composites for bone tissue regeneration

Calcium phosphate (CaP) cements have been used with good results in bone tissue engineering. Their advantages include easy handling and injectability

as well as osteoconductivity.[345] In order to further improve their potential for bone regeneration, these carriers have been delivered together with growth factors, such as recombinant human TGF-β1.[346] Using calcium phosphate cement as a delivery vehicle for recombinant human BMP-2, Kroese-Deutman *et al.* observed bone growth in an ectopic, subcutaneous, animal model after ten weeks of implantation.[174] This and other studies have revealed the potency of rhBMP-2 as an osteoinductive factor, and further attempts have been made towards achieving a more controlled release profile. The use of CaP with embedded PLGA microspheres resulted in an injectable delivery system that exhibited linear release profiles without an initial burst *in vivo*[347] and showed that the controlled release of a low BMP-2 dose was able to induce bone growth in an experimental animal model.[220]

2.7 Cell delivery for engineering complex tissues

The delivery of cells to a defect is a means to accelerate the healing process as the body would not have to rely on host cells being recruited to that site. Cellular delivery vehicles may also allow for regeneration of native tissues before fibrosis and scarring occur. The cell source and type is a topic of much discussion and research over the past decades, and approaches using xenogeneic, allogeneic, or autologous cells have been studied. There are advantages and disadvantages involved in all of these approaches, and the decision has to be made with careful consideration of the application and the necessary steps to translate from research to a final tissue engineered product.

The other big question facing researchers is the choice between differentiated cells and either embryonic or adult stem cells. Stem cells have the ability to proliferate in an undifferentiated state or, with the application of certain stimuli, to differentiate into one or more cell lineages. Investigators have recognized the tremendous potential of stem cells in regenerative medicine, and given their versatility, they can offer a valuable solution for engineering complex tissues. Embryonic stem cells are isolated from embryonic or fetal tissues, and are capable of giving rise to all types of tissues.[348] Adult stem cells can be mainly categorized into hematopoietic and mesenchymal stem cells. Hematopoietic stem cells (HSCs) are derived from the bone marrow and are blood cell progenitors. MSCs can be found in a variety of tissues, including bone marrow, periosteum, adipose, and possibly the umbilical cord matrix and can differentiate into bone, cartilage, muscle, fat, and other tissues.[349-352] Most craniofacial tissues derive from MSCs, and there is evidence that for some craniofacial structures such as the TMJ, MSCs are better suited for tissue regeneration than differentiated cells (Figure 2.8).[353] A recent review article by Mao *et al.*[162] outlines advances in the field of craniofacial tissue engineering using stem cells.

Once in the body, stem cells receive signals that govern their fate. These signals can be chemical or mechanical in nature, and are provided either by the physiologic environment or can be incorporated in the cell delivery vehicle. The mechanisms by which these signals affect stem cells are not yet fully understood. The field of tissue engineering is greatly advanced by stem cell biology findings,

and tissue engineering scaffolds have been used with promising results for stem cell delivery for various tissues. The nature of injectable materials, which allows for simultaneous cell and bioactive agent encapsulation, makes them particularly attractive for this application, as does the ability to control scaffold mechanical properties, which can provide the appropriate mechanobiological environment for cell proliferation and differentiation.

2.7.1 Cell delivery systems

Hydrogels, due to their high water content, are excellent ECM analogues, and are used extensively for cell delivery. Injectable hydrogel systems such as OPF, with or without the addition of growth factors, were shown to promote mesenchymal stem cell differentiation, with possible applications in bone and cartilage regeneration (Figure 2.9).[354, 355] By controlling the scaffold swelling and mechanical characteristics, appropriate signals were transduced to the cells. Also the addition of a functional group to the polymer, for example a group that will enhance biomineralization, has been shown to induce cell differentiation, helping MSCs turn into osteoblast-like cells.[356] The importance of growth factors in enhancing cell function for tissue engineering applications has been outlined in the previous section. Yamada *et al.* utilized the abundance of growth factors released by platelets by delivering MSCs in a platelet-rich plasma gel, observing bone formation and neovascularization *in vivo*.[357] Morphogenic factors are often co-injected with cells but can also be applied to the cells to pre-differentiate them *in vitro* prior to administration. An example for engineering complex tissues using

the latter strategy is the work of Alhadlaq *et al.*[358] Rat MSCs were treated for three to four days with either chondrogenic or osteogenic supplements and loaded in two hydrogel layers formed by photopolymerization. After four weeks *in vivo*, stratified layers of chondrogenesis and osteogenesis were observed. The authors concluded that this approach could offer a solution for tissue engineering complex tissues using a single adult mesenchymal stem cell population.

2.7.2 Co-culture models and future considerations

Another exciting option for stimulating cell differentiation and proliferation is the co-culture of multiple cell types. The signals exchanged between cells help augment tissue regeneration by guiding differentiation and matrix production down the desired pathway. Co-cultures essentially mimic the physiological environment, where different cells act cooperatively and bioactive factors secreted by one cell type provide cues for the action of another cell type. It is known, for example, that in endochondral bone formation, cartilage precedes bone development. Alsberg *et al.*[359] co-transplanted chondrocytes and osteoblasts embedded in hydrogels and observed formation of distinct tissue types. Gerstenfeld *et al.*[360] investigated the effect of chondrocytes on mesenchymal stem cell osteogenesis. They found that MSCs co-cultured with chondrocytes underwent osteogenic differentiation, but did not observe this when MSCs were cultured with fibroblasts or osteoblasts. In a parallel study, treatment of MSCs with BMP-7 induced both chondrogenesis and osteogenesis. Osteogenic differentiation alone was observed in the MSCs co-cultured with

chondrocytes.[360] Interestingly, co-culture of MSCs with cartilage, separated by a membrane and without any external growth factors, was found to increase markers of chondrogenic differentiation. Therefore, it seems that the secretion of soluble factors from the whole cartilaginous matrix controls chondrogenesis of mesenchymal stem cells, and that the MSCs in turn influence the already formed cartilage, possibly preventing its hypertrophy or ossification.[361]

One of the important hurdles to overcome in tissue engineering is the blood supply to the growing tissue. Cell co-cultures could potentially play a role in this area by delivering cell populations that would form new blood vessels and also initiate tissue development. Early studies by Sun *et al.* showed promise in bone regeneration and angiogenesis using a vascular endothelial cell / bone marrow MSC co-culture model.[362] Using a different approach, the formation of microvascular networks *in vivo* was demonstrated with neural progenitor and endothelial cells embedded in a macroporous hydrogel.[363]

Research in the area of co-culture systems is crucial to our understanding of cell communication with soluble signaling molecules. Models for establishing these relations exist; however, it must be noted that precautions should be taken until there is a clear understanding of the mechanisms that govern cellular interactions, especially involving stem cells. In a direct co-culture setup, there may be danger of cell fusion and endocytosis.[364] Therefore, many researchers use membrane-separated cell culture chambers where cells are not in direct contact, but soluble factors secreted by one population can freely float in the

culture medium and act on the other cell type. Once it is determined whether direct cell contact is necessary or paracrine mechanisms are involved, new directions for cell co-culture and possibly the delivery of multiple cell types together with stem cells will be developed. Facing the problem of complex tissue regeneration, the option of cell therapy with multiple populations seems appealing, particularly considering the multipotency of stem cells. We can anticipate great progress towards that goal in the years to come.

2.8 Injectable materials for engineering complex tissues

The last 15 years has seen a remarkable influx of ideas and technologies to the areas of biomaterials and tissue engineering. While this research has resulted in an expansion of knowledge and in select cases an impact on clinical medicine, regenerating complex tissues remains a largely unaddressed challenge. Advances specifically in injectable biomaterials are frequently presented; however, tissue regeneration in humans using injectable materials remains an unmet goal. As has been shown, regenerating complex tissues is a complicated endeavor that, particularly in the CFC where a number of structures reside in limited space, will require a synergistic approach drawing on knowledge from many areas of science and engineering.

2.8.1 Goals and future directions

Continued advances in biomaterials and tissue engineering will be required to realize the goal of regenerating complex craniofacial tissues using

injectable biomaterials. First, a more complete understanding of the function and utility of stem cells within the context of tissue engineering will be necessary for regenerating any complex tissue. Adult and embryonic stem cells are a powerful tool for regenerative medicine applications, but to tailor complex tissues, precise control over differentiation and subsequently morphogenesis must be achieved. Advances in these areas may result from better understanding of development and natural tissue regeneration, such as more precise knowledge of growth factor and cell signaling cascades.

At the materials level, new materials are continually introduced, and much current work focuses on promising materials tailored for engineering specific tissues. The integration of these materials with one another or the development of materials with multiple patterned, micro- and nanoscale domains for specific tissue and organ patterning will be critical to complex tissue engineering.[365, 366] The interaction of these domains with stem cells and the effect of bioactive factor release kinetics must be well characterized and utilized. The creation of surface[367, 368]and 3D[369] patterning or pore gradients and orientation,[370, 371] for example, and in particular mechanical gradients via any of the methods for solidification discussed can be of great benefit to tissue engineers, as such patterning can influence cell behavior including differentiation.[372] For complex tissue engineering, an injectable material that can encapsulate cells and bioactive factors and deliver them to a multi-tissue defect so that different regions of the defect regenerate into anatomically oriented and functionally capable

tissues is the end goal; however, many hurdles must be overcome in the path to developing such a system.

2.9 Conclusions

This chapter aims to examine recent advances in injectable biomaterials for tissue engineering within the challenging but illustrative context of complex tissue engineering within the craniofacial complex. A region with great need for better biomaterials and tissue engineering strategies, currently used techniques and biomaterials for craniofacial augmentation and repair were described to establish the current end-stage state of the art. The challenge of engineering complex tissues and advances in tissue engineering the broad scope of craniofacial tissues were described followed by an overview of injectable material technologies and drug and cellular delivery via injectable materials. Finally, the notable challenges and perceived future needs and directions in addressing the challenges described were mentioned. Many promising injectable biomaterials exist, and forays into *in vivo* testing using animal models have been largely successful. The goal, however, of regenerating complex tissues remains unmet in the clinic and will require continued commitment and advancement within the field.

2.10 Figures

Table 2.1. Materials and methods currently used for craniofacial reconstruction.

Tissue Type	Source	Clinically Available Methods & Materials
Hard tissue	Autologous	Non-vascularized bone grafts from iliac crest, tibia, skull, and mandible.
	Allogeneic	Mineralized allogeneic bone available from tissue banks. Demineralized bone matrix combined with various carriers: w/ hyaluronic acid (i.e. DBX®) w/ glycerol (i.e. Grafton®) w/ gelatin (i.e. Regenafil®) w/ poloxamer (i.e. Dynagraft®) w/ calcium sulfate (i.e. Allomatrix®)
	Xenogeneic	Crosslinked bovine collagen I coated in hydroxyapatite (i.e. Healos®). Deproteinized bovine bone (i.e. Bio-Oss®). Porcine collagen I and III resorbable membrane (i.e. Bio-Gide®). 60% hydroxyapatite + 40% tricalcium phosphate ceramics in bovine fibrillar collagen carrier (i.e. Collagraft®).
	Synthetic	Ceramics Hydroxyapatite of natural origin Coral sources (i.e. Pro Osteon® and Biocoral®). Bovine bone (i.e. Bio-Oss®). Synthetic hydroxyapatite. Synthetic unsintered calcium deficient apatite. Synthetic β-tricalcium phosphate. Synthetic biphasic calcium phosphate. Calcium phosphate cements (i.e. Norian®, BoneSource®,

		Mimix®). Polymers Poly(α-hydroxy esters) such as poly(lactic acid), poly(glycolic acid), and poly(lactic-*co*-glycolic acid). Applications include resorbable fixation plates and screws, and resorbable membranes. Porous high density polyethylene implants (i.e. MedPor®). Poly(methyl methacrylate) implants. Recombinant growth factors Bone morphogenetic protein-2 in an absorbable collagen sponge (i.e. Infuse®). Platelet-derived growth factor in a β-tricalcium phosphate carrier (i.e. GEM 21S®).
Soft Tissue	Autologous	Soft tissue grafts Full-thickness and partial-thickness skin grafts. Oral mucosa grafts (i.e from the free gingiva, buccal mucosa, palate, etc.). Microfat grafting. Dermal fibroblast harvest, *ex vivo* culture and re-implantation (i.e. Isolagen®). Soft tissue flaps Local flaps (i.e. buccal fat pad). Regional flaps (i.e. from pectoralis major, deltopectoral, temporalis). Vascularized free flaps (i.e. from the radial forearm, anterolateral thigh, etc.).
	Allogeneic	Short-term skin allografts. Long-term face transplants. Freeze-dried de-epithelialized acellular dermal graft (i.e. Alloderm®).
	Xenogeneic	Dermal fillers Fibrillar bovine collagen I and III (i.e. Zyderm®). Crosslinked fibrillar bovine collagen I and III (i.e. Zyplast®). Crosslinked hyaluronic acid derivatives (i.e. Hylaform®, Restylane®, Captique®).
	Synthetic	Dermal fillers

	Synthetic	Dermal fillers Liquid silicone. Poly(methyl methacrylate) microspheres in collagen solution (i.e. ArteFill®). Poly(L-lactic acid) microparticles in carboxymethylcellulose gel (i.e. Sculptra®).
Composite tissue	Autologous	Vascularized osseo-fascio-cutaneous free flaps (i.e. from the radial forearm, fibula, iliac crest, deltoid, and scapula). Non-vascularized osteochondral grafts (i.e. from the ribs).
	Synthetic	Polymeric prosthesis materials Poly(methyl methacrylate) Polyurethane elastomers Silicone elastomers (i.e. MDX 4-4210®) Tissue engineering approaches Titanium mesh scaffold filled with bone marrow and Bio-Oss® blocks coated with recombinant BMP-7. Construct placed in muscle for 7 weeks, then transplanted to

Figure 2.1. Craniofacial tissues needed for reconstruction. Reproduced from [161]. Copyright 2007 Springer.

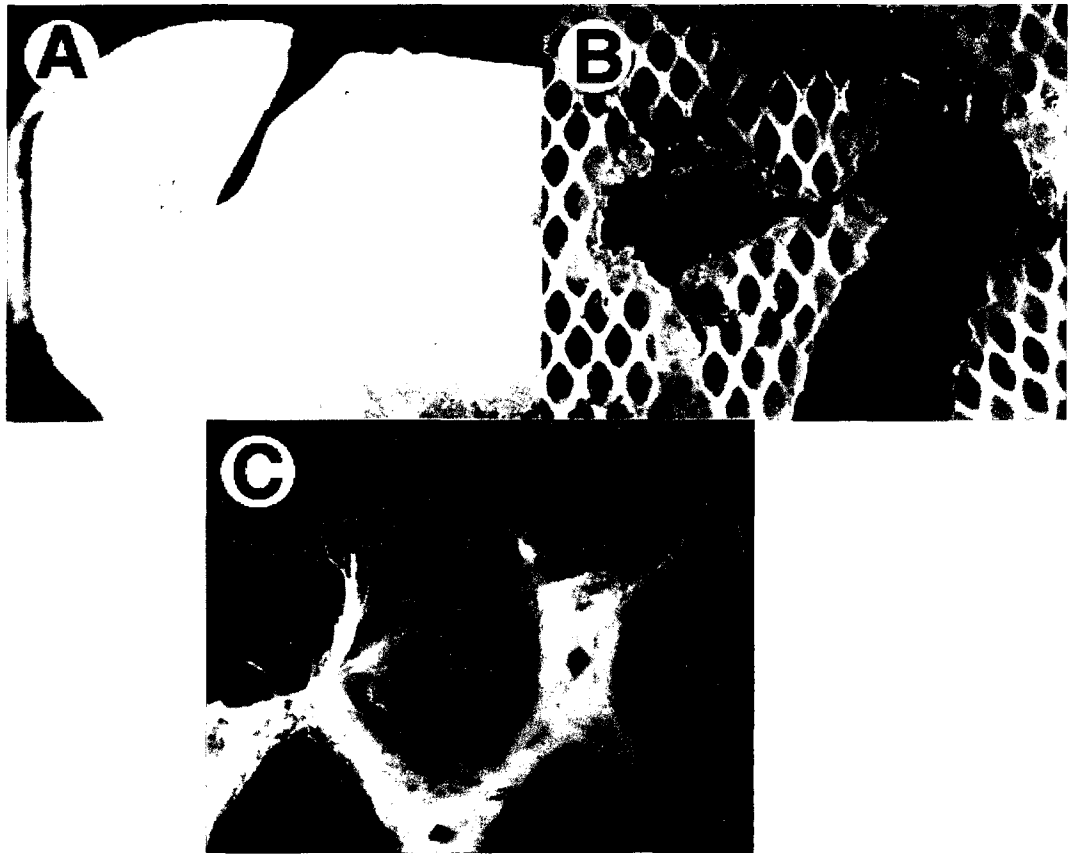

Figure 2.2. Silastic implant fragments surgically retrieved from patients. The primary reason for retrieval was patient pain, likely secondary to implant failure. A and B show fracture lines within the implant, while C shows fraying and exposure of Dacron fibers that are intended to reinforce the implant. Reproduced from [204]. Copyright 2008 Elsevier, Inc.

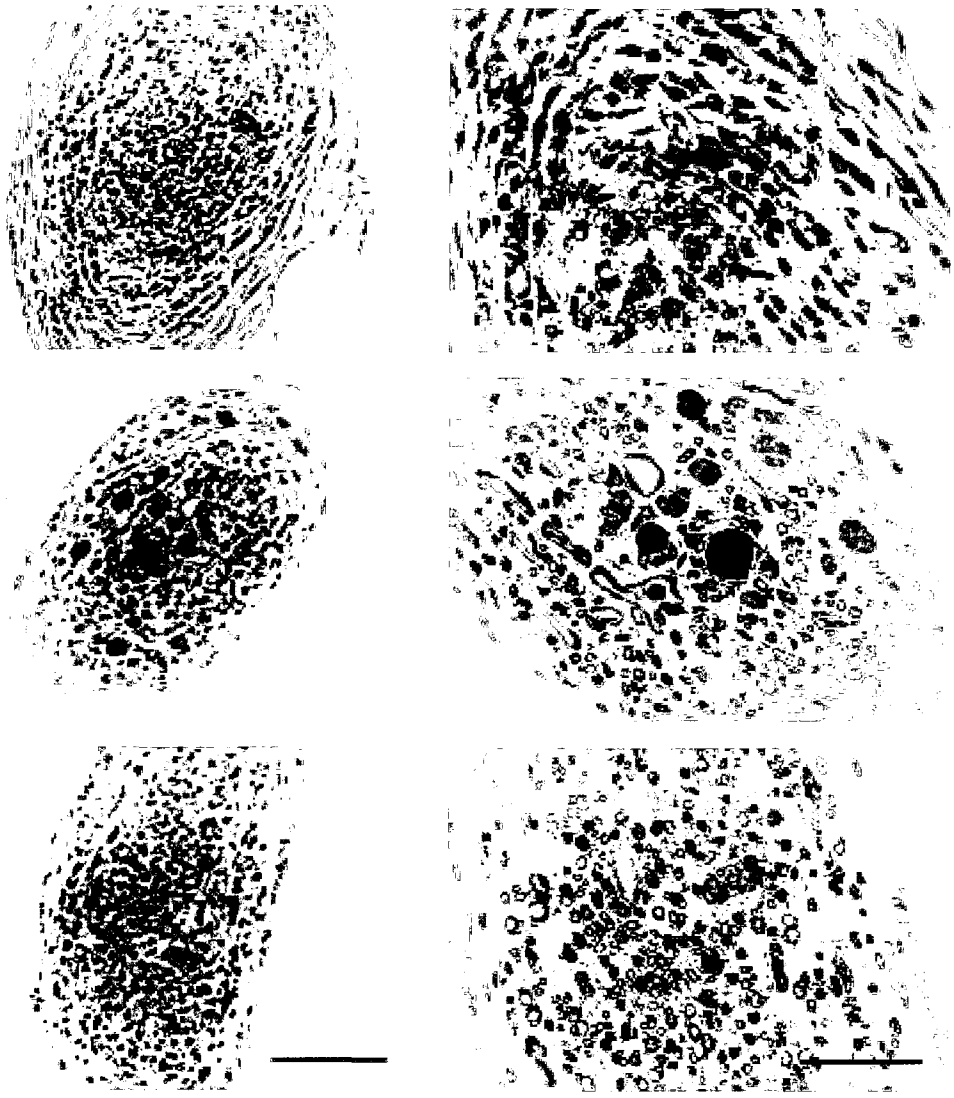

Figure 2.3. Cross sectional images of nerves regenerated in self assembling fibrin tubes. A 4 mm segmental defect was created in the dorsal root nerve of a rat and then bridged with a polymer tube implant. The gap was either left empty (A, B), filled with unmodified fibrin (C, D), or filled with fibrin modified with four peptides from the laminin family of adhesion molecules (E, F). The homogeneity of the nerve and alignment of the neuritis can be appreciated in the samples receiving peptide-modified fibrin bridges (A, C, E bar= 50 μm, B, D, F bar = 25 μm). Reproduced from [284]. Copyright 2000 Nature Publishing Group.

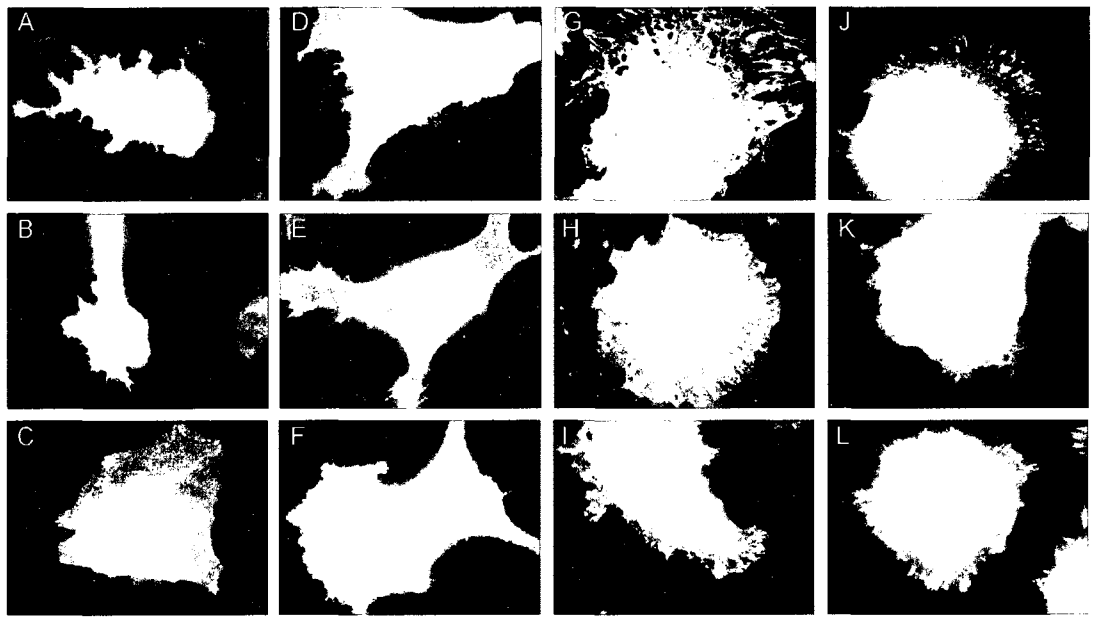

Figure 2.4. Focal adhesion formation of cells expressing green fluorescent protein labeled integrin (A-F) or yellow fluorescent protein labeled signal transduction protein (paxillin, G-L) in response to peptide amphiphiles expressing RGDS sequence(s). (A, G) branched peptide amphiphile with one cyclic RGDS, (B, H) branched peptide amphiphile with two RGDS, (C, I) branched peptide amphiphile with one RGDS, (D, J) branched peptide amphiphile with one d-RGDS, (E, K) linear peptide amphiphile with one RGDS, and (F, L) show cells on linear peptide amphiphile with one RGDS. Focal adhesions are seen as brightly fluorescent spots and demonstrate the presence of cellular organization during adhesion and migration in response to the presence of RGDS. This represents an example of how at the cellular level behavior can be regulated via substrate modification, a potentially powerful tool for regenerating of complex tissues. Reproduced from [287]. Copyright 2007 Elsevier B.V.

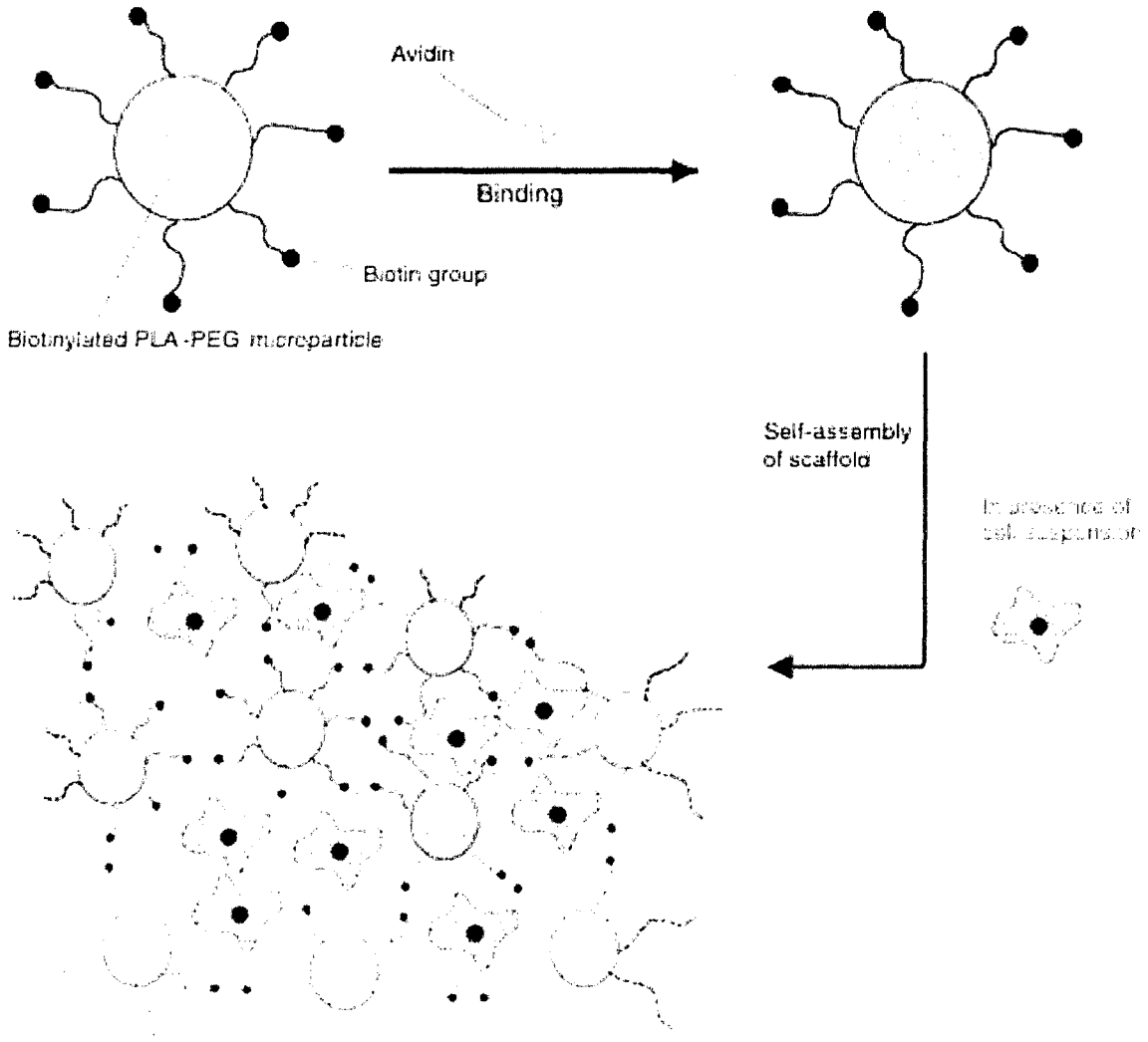

Figure 2.5. Schematic representation of avidin induced self assembly of biotinylated PEG-PLA microparticles. Reproduced from [297]. Copyright Wiley 2003 VCH.

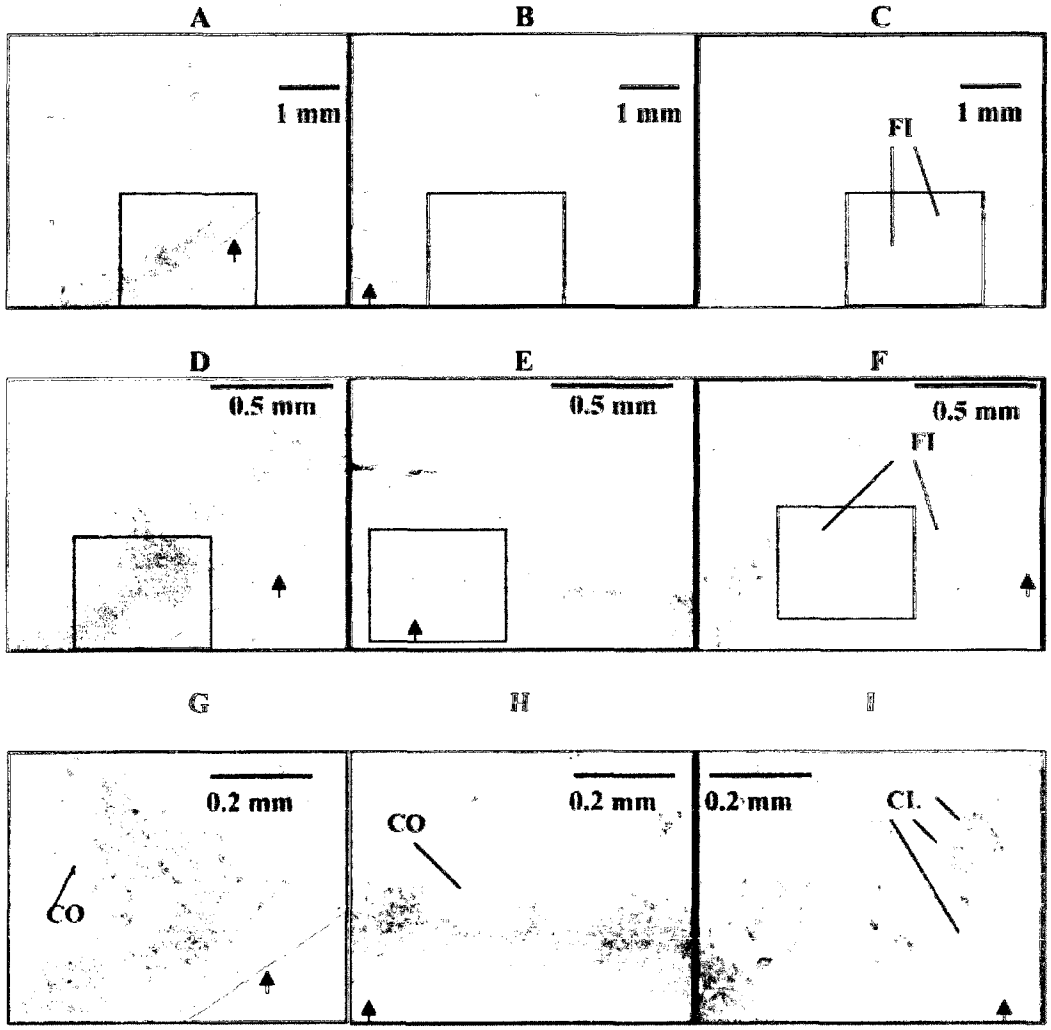

Figure 2.6. Osteochondral tissue repair in rabbit knees 14 weeks after implantation with a bilayered scaffold (A, D, G – TGF-β1 releasing porous chondral and porous subchondral layers; B, E, H - TGF-β1 releasing porous chondral and nonporous subchondral layers; C, F, I porous chondral layer and nonporous subchondral layer). The boxed regions in (A-C) (2.5× magnification) are shown at higher magnifications in (D-F) (10×), and (G-I) (20×). Arrows point towards the joint surface, while columnar arrangements of chondrocytes, cell clusters, and cartilage fissures are respectively indicated by CO, CL, and FI. The image demonstrate the ability of a bilayered scaffold along with regionally specific growth factor release to regenerate multiple tissues within the same construct. Reproduced from [333]. Copyright 2005 Wiley Interscience.

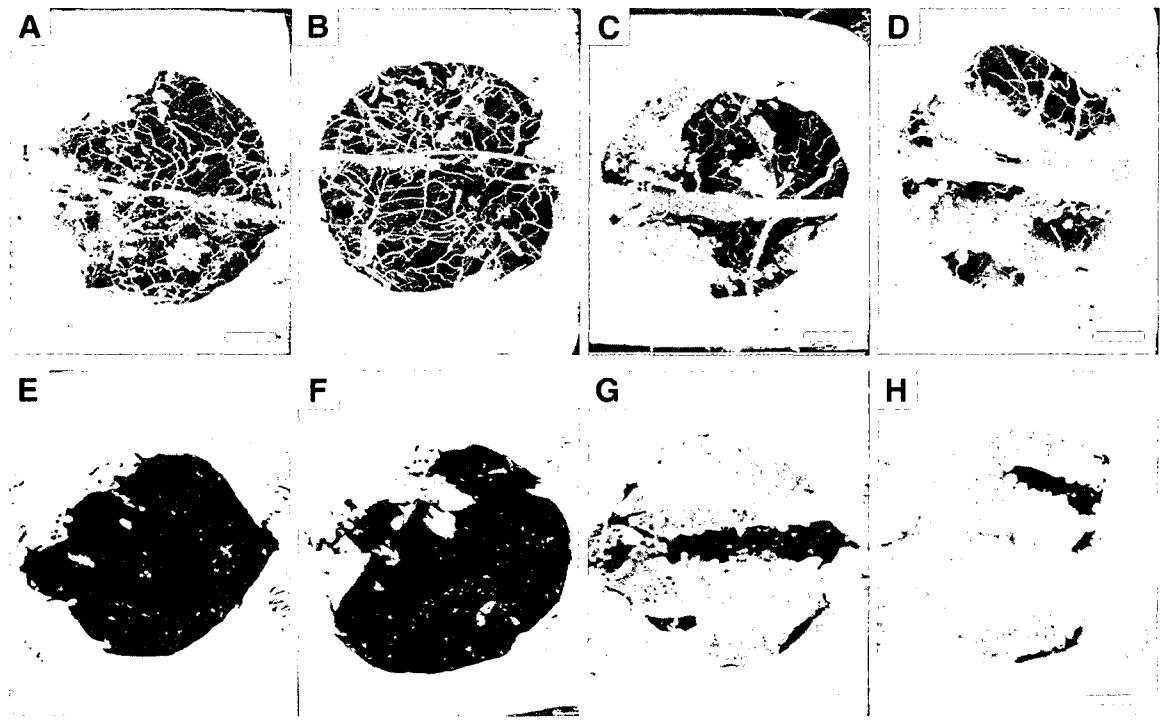

Figure 2.7. Microcomputed tomography images of rat cranial bone defects treated with angiogenic, osteogenic or both growth factors. Figures A-D represent an untreated control group, angiogenic VEGF-treated group, osteogenic BMP-2-treated group, and a dual delivery group at 4 weeks. Blood vessels and bone are visible. Figures E-H represent control, VEGF, BMP-2 and dual groups at 12 weeks. Blood vessel formation was not evaluated at this time point. Bar represents 200 μm. Reproduced from [19]. Copyright 2005 Elsevier B.V.

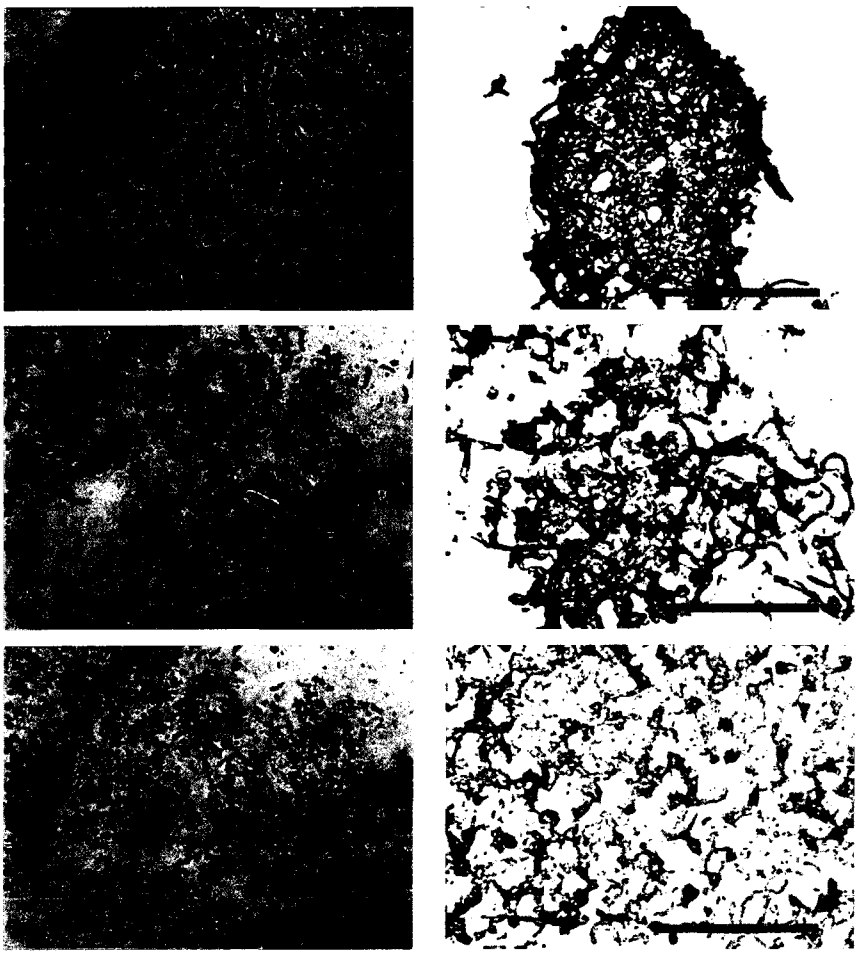

Figure 2.8. Safranin O/fast green stained (left) and chondroitin-4-sulfate immunohistochemically stained cultures of human umbilical cord matrix (HUCM) derived stem cells and TMJ cartilage cells. HUCM were cultured in control (top left) and chondrogenically supplemented (top right) media for 4 weeks following initial culture in chondrogenic media. HUMCs produced more glycosaminoglycans as shown by both staining modalities than already differentiated TMJ chondrocytes, indicating the utility of stem cells in craniofacial tissue engineering compared to differentiated cells. Reproduced from [353].

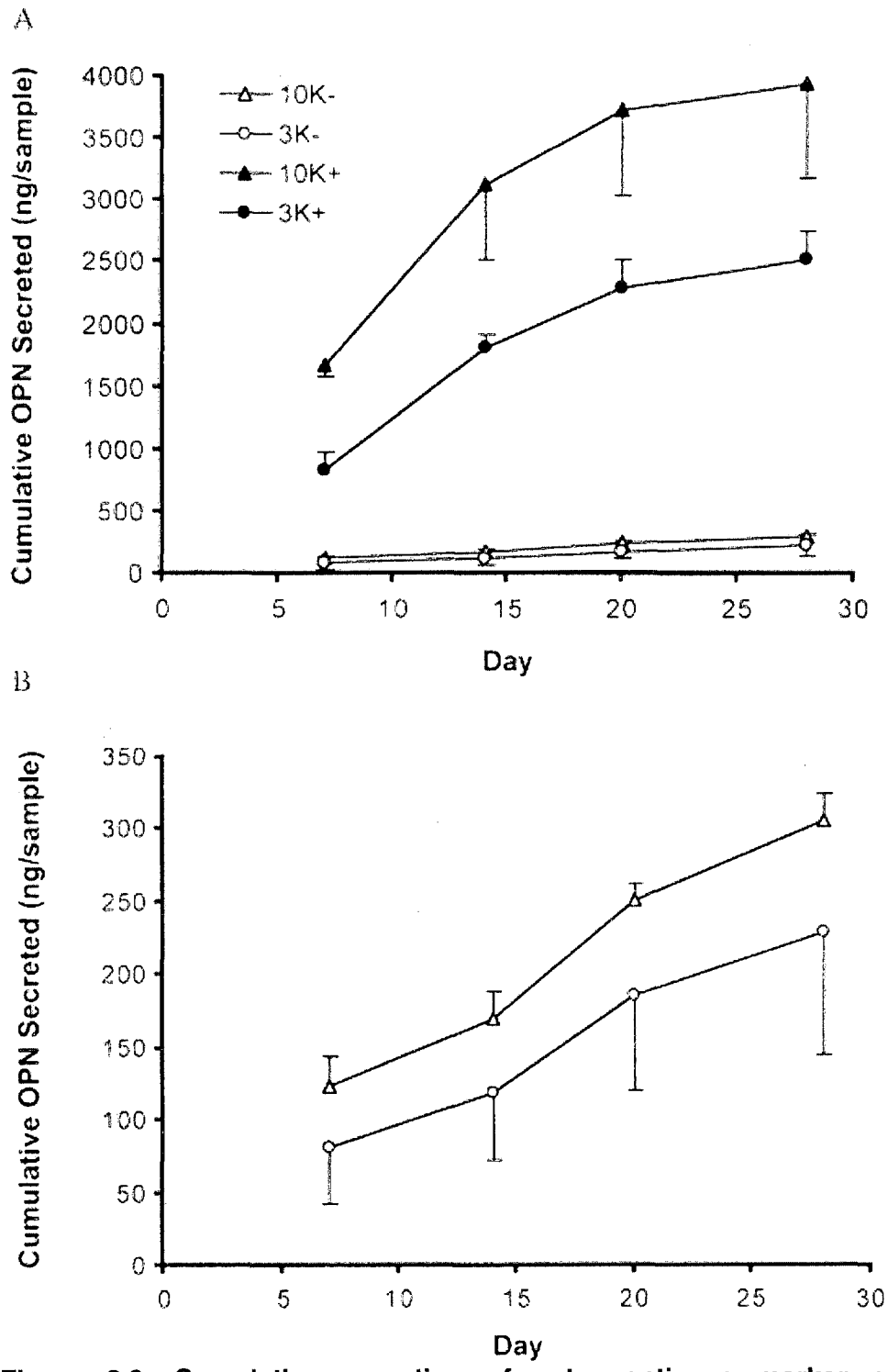

Figure 2.9. Cumulative secretion of osteopontin, a marker of osteogenic differentiation, from OPF hydrogel matrices with encapsulated MSCs. (A) MSCs encapsulated in OPF formulated from PEG with MW 10,000 Da and 3,000 Da were cultured in dexamethasone containing (+) and non-supplemented (-)culture media for 28 days. (B) Two types of OPF/MSC formulations maintained for 28 days in culture media without dexamethasone. The samples with higher molecular

weight PEG (10K) underwent greater swelling than the less hydrophilic samples (PEG MW 3K), which led to enhanced osteogenic differentiation of encapsulated MSCs. Reproduced from [355]. Copyright 2004 Wiley Interscience.

Chapter 3

Objectives

There are many promising techniques for bone tissue engineering in isolaton; that is, without regard to factors such as cost, translational potential, concomitant morbidities, or other factors that would affect the adoption of the technique for clinical use. Increasing consideration of these factors shaped the work presented here.

The original goal of this work was to develop a hydrogel cell carrier for bone tissue engineering applications. Such a cell carrier would need to not only support cell viability and ideally initiate osteodifferentiation of delivered progenitor cells, but would perhaps most importantly need the mechanical strength necessary to provide support within a bony defect.

As this project progressed, the focus shifted towards more translational approaches for cell delivery and tissue engineering. The effect of donor age and extended cell culture in the form of passages was investigated to determine whether *ex vivo* handling of cells had any deleterious effects and to investigate whether such effects were dependent on donor age. After determining that there were potentially negative effects associated with culture, delivery of uncultured bone marrow mononuclear cells to scaffolds using an existing FDA-approved fibrin glue was explored to determine if freshly harvested cells without *ex vivo* culture or expansion could regenerate bone within a critical size defect.

Finally, considerations of the types of injuries being treated led to the final objective of the project. Traumatic craniofacial injuries, particularly those resulting from military combat, often result in soft tissue loss and subsequent infection. Such comorbidities would likely render a tissue engineering approach, such as those explored in the first two objectives of this thesis, ineffective at worst. Delayed definitive treatment would thus be necessary, but without a bridge to prevent scarring and tissue contraction, delays in treatment might negatively effect long term results. Thus a space maintainer technology was investigated for use in these situations.

The specific objectives of the work presented within this thesis are:

1. Synthesize and characterize stimulus responsive polymers and hydrogels for cell delivery applications in bone tissue engineering, focusing on cytocompatible methods for gel formation and reinforcement.
2. Investigate the effect of cell culture on the differentiation capacity of mesenchymal stem cells from donors of different ages.
3. Investigate the use of gel-encapsulated, uncultured bone marrow mononuclear cells for bone tissue regeneration within a critical size defect.
4. Investigate methods to facilitate soft tissue healing and bony space maintenance within a critical size bone defect using an

animal model that more realistically simulates that encountered following traumatic craniofacial injury.

Chapter 4

Synthesis and characterization of dual stimuli responsive macromers based on poly(N-isopropylacrylamide) and poly(vinylphosphonic acid)[†]

Abstract

Stimulus responsive materials hold great promise in biological applications as they can react to changes in physiological stimuli to produce a desired effect. Stimulus responsive macromers designed to respond to temperature changes at or around 37 °C and the presence of divalent cations were synthesized from N-isopropylacrylamide, pentaerythritol diacrylate monostearate, 2-hydroxyethyl acrylate, and vinylphosphonic acid by free radical polymerization. Monomers were incorporated into the macromers in ratios approximating the molar feed ratios, and macromers underwent thermogelation around normal body temperature (36.2 – 40.5 °C) as determined by rheology and differential scanning calorimetry. Macromers containing vinylphosphonic acid interacted with calcium ions in solution, displaying decreased sol-gel transition temperatures (27.6 – 34.4 °C in 100 mM $CaCl_2$), with decreases of greater magnitude observed for macromers with higher relative vinylphosphonic acid content. Critical micellar

[†] This chapter will be published as the following: Kretlow JD, Hacker MC, Klouda L, Ma BB, Mikos AG. Synthesis and characterization of dual stimuli responsive macromers based on poly(N-isopropylacrylamide) and poly(vinylphosphonic acid). Biomacromolecules 2009: in press.

concentrations also decreased in a dose-dependent manner with increased vinylphosphonic acid incorporation in solutions with $CaCl_2$ but not in solutions with NaCl. These dually responsive macromers allow examination of the effect of increasing vinylphosphonic acid content in a macromer which holds promise in biological applications such as drug and cell delivery or tissue engineering due to the macromer responsiveness at physiological temperatures and concentrations of calcium.

Abbreviations

AAm	acrylamide
AIBN	2,2'-azobis(2-methylpropionitrile)
CMC	critical micellar concentration
DLS	dynamic light scattering
DSC	differential scanning calorimetry
HEA	2-hydroxyethyl acrylate
LCST	lower critical solution temperature
NIPAAm	N-isopropylacrylamide
pNIPAAm	poly(N-isopropylacrylamide)
TGA	thermogravimetric analysis
THF	tetrahydrofuran

4.1 Introduction

The development of injectable biomaterials and similarly the identification of methods through which materials may form *in situ* are popular topics in materials science, particularly in the area of biomaterials. Injectable materials are attractive for biological applications as they can potentially be delivered using minimally invasive techniques, precisely fill complex three-dimensional voids in regenerative medicine applications without the need for extensive imaging and custom fabrication, and controllably deliver bioactive molecules and/or cells for therapeutic purposes.

Most research and development in the area of injectable biomaterials focuses on *in situ* formation via self-assembly[297, 373], phase separation[374], or *in situ* polymerization and cross linking.[238, 375-378] Materials that undergo phase separation or self assemble in response to environmental cues or stimuli are promising for biological applications as the stimulus triggering the phase separation or assembly can be one normally encountered upon injection into living tissues, such as a temperature increase or pH change. Such methods for *in situ* formation may reduce or eliminate the need for radical initiators or crosslinking agents that may be cytotoxic at high concentrations,[243, 244] potentially making these materials ideal for cellular encapsulation and delivery as well as alleviating potential damage to existing host tissues.

Biomaterials have recently been developed that respond to a large number of internal or externally applied environmental stimuli, including

temperature,[379-381] pH,[382] ionic strength,[383] the presence of specific biological molecules,[384-386] and magnetic field presence.[387] Recent reviews are available describing the roles of these materials in scaffold fabrication,[388] drug delivery,[389] and as tunable bio-interfaces.[390]

In order to impart greater versatility or allow better control over the behavior of these "smart" biomaterials, materials have been developed that respond to multiple stimuli, such as both pH and temperature.[391-395] The response to each stimuli may be different[396] or additive.[397]

Materials that undergo tandem gelation via a stimulus responsive, physical mechanism, typically thermogelation, and an additional mechanism such as chemical crosslinking offer comparable versatility to dual stimuli responsive materials. Tandem gelling materials can offer the favorable, nearly instantaneous gelation kinetics of physical gelation coupled with the stability and irreversibility of chemical crosslinking.[272, 398] These materials may be particularly attractive alternatives for applications where the environmental stimuli that triggers physical gelation is subject to variability, such as pH within a healing wound or fracture, which can be both variable and unpredictable.[399]

We have previously synthesized and characterized a series of thermally and chemically gelable macromers based on poly(N-isopropylacrylamide) (pNIPAAm).[262] By copolymerizing N-isopropylacrylamide (NIPAAm) with other monomers to vary the amphiphilic structure of the resulting macromers, we were able to synthesize macromers with variable rheological properties and lower

critical solution temperatures (LCSTs) around 37 °C. These macromers displayed less syneresis at body temperature than macromers that thermogelled at lower temperatures; however, chemical modification and subsequent chemical crosslinking was still necessary to produce stable gels.

The goal of the present study is to examine the effect of ionic interactions on the rheological and micellar behavior of pNIPAAm-based macromers similar to those previously synthesized and characterized in our laboratory by incorporating phosphonic acid moieties through copolymerization of NIPAAm, vinylphosphonic acid (VPA), and other monomers to modulate the amphiphilic structure of the macromers. A hydrophobic chain was incorporated through copolymerization with pentaerythritol diacrylate monostearate (PEDAS), a bifunctional monomer incorporating a stearic acid chain and two acrylic acids esterified to the biocompatible alcohol pentaerythritol. Hydroxyethylacrylate (HEA) was incorporated to allow for possible chemical modifications of the accessible hydroxyl groups and also to further balance the hydrophobicity of the macromers. The synthesis and characterization of macromers that thermogel near normal physiological temperature, as well as the interactions of these macromers with divalent ions in solution towards gel and micelle formation, is described.

4.2 Materials and Methods

4.2.1 Materials

Pentaerythritol diacrylate monostearate (PEDAS), N-isopropylacrylamide (NIPAAm), acrylamide (AAm), 2-hydroxyethyl acrylate (HEA), vinylphosphonic acid (VPA), and 2,2'-azobis(2-methylpropionitrile) (azobisisobutyronitrile, AIBN) were purchased from Sigma-Aldrich (Sigma, St. Louis, MO) and used as received. Analytical grade tetrahydrofuran (THF), diethyl ether, isopropyl alcohol, and acetone were purchased from Fisher Scientific (Pittsburgh, PA) and used as received.

4.2.2 Methods

Macromer synthesis

Macromers were synthesized using free radical polymerization (Scheme 4.1) as previously described.[262] Briefly, 3 g of PEDAS and amounts corresponding to the desired molar ratios of comonomers (NIPAAm, VPA, HEA, AAm) were dissolved in 250 mL THF at 60 °C under nitrogen and initiated with 1.5 mol % AIBN. Reactions proceeded under nitrogen for 18 h at 60 °C followed by an additional 1 h of reflux. Products were isolated by rotoevaporation, precipitation in ice-cold diethyl ether followed by drying and a second dissolution in THF and precipitation in ice-cold diethyl ether. Products were then vacuum dried at ambient temperature for 7 days before being dissolved in 200 mL isopropanol and dialyzed against isopropanol for 4 days in a 1,000 MWCO

membrane (Spectra-Pore, Spectrum Laboratories, Rancho Dominguez, CA). Following dialysis, purified products were isolated through azeotropic distillation with acetone followed by precipitation in ice-cold diethyl ether and finally followed by filtration and vacuum drying at ambient temperature for 7 days. A summary of the synthesized macromers is provided in Table 4.1.

Nuclear magnetic resonance

^{1}H and ^{31}P NMR spectra were obtained using a 500 MHz spectrometer (Inova, Varian, Inc., Palo Alto, CA). Samples were dissolved at a concentration of 20 mg/mL in equal parts $CDCl_3$ and deuterated DMSO. Post-acquisition data analysis was performed using MestRe Nova software (Mestrelab Research S.L., Spain).

Osmometry

Freezing point osmometry was used to determine the number average molecular weight of the synthesized macromers. Macromers were dissolved at varying concentrations (0.5%-15% w/v) in ultrapure (Type I) water (Super Q, Millipore Corporation, Billerica, MA) and left overnight on an orbitally rotating platform. Samples were tested to determine which samples fell within the calibrated detection range of the osmometer (Osmette A, Precision Systems, Inc., Natick, MA), and osmometry measurements were performed on 1% w/v samples in triplicate.

Thermogravimetric analysis (TGA)

Thermal stability of the synthesized macromers was analyzed under a nitrogen atmosphere (80 mL/min) using a TA Instruments TGA Q50. Approximately 5 mg of vacuum dried sample was ground into a fine powder and evenly distributed over the surface of a platinum sampling pan (TA Instruments). Samples were heated to 100 °C and held at that temperature for 5 minutes to remove residual moisture, after which the samples were heated from 100 °C – 800 °C at a rate of 10 °C/min.

Rheology

For rheological characterization of the macromers, samples were dissolved in ultrapure water, and pH was adjusted to 7.4 using 0.5 N NaOH. $CaCl_2$, NaCl, $MgCl_2$, were added to samples at varying ($CaCl_2$ and $MgCl_2$: 2.5 mM, 100 mM, NaCl: 5 mM, 200 mM) concentrations. Sample concentration was finally adjusted to 7.5% w/v. All samples were left overnight on an orbitally rotating platform to ensure complete dissolution.

Measurements were performed using a thermostatted, oscillating rheometer (Rheolyst AR1000, TA Instruments, New Castle, DE) equipped with a 6 cm steel cone geometry (1°). Gelation properties and transition temperatures were determined as previously described.[262] Briefly, samples were loaded onto the rheometer and cooled to 5 °C, presheared for 1 min (rate 1 s^{-1}), and equilibrated for 15 minutes before a temperature sweep was performed from 5-60 °C at a rate of 1 °C/minute and a displacement of 1 $\times 10^{-4}$ rad. All formulations

were tested in triplicate, and analysis was performed using the manufacturer's supplied software (TA Data Analysis, TA Instruments).

Differential scanning calorimetry (DSC)

Transition temperatures were also determined by DSC. Samples were prepared in the same manner as performed for rheological characterization (7.5% w/v, pH 7.4), and 20 μL of each sample were pipetted into an aluminum sample pan (TA Instruments, Newcastle, DE) that was then hermetically sealed. Experiments were performed in triplicate on a TA Instruments DSC 2920 with a refrigerated cooling system. Samples were equilibrated at 5 °C for 10 minutes and then heated to 60 °C at a rate of 5 °C/minute.

Calcium-binding assay

Samples were prepared in triplicate in ultrapure water (7.5% w/v, pH 7.4) augmented with $CaCl_2$ at concentrations of 0.01 mM, 0.1 mM, 1 mM, 2.5 mM, 4.0 mM, 10 mM, 25 mM, 100 mM, and 1000 mM and stored for 24h at 37 °C on a shaker table. After 24 h, the supernatant was removed, cooled to room temperature, and analyzed for residual calcium ions using a colorimetric calcium assay (Arsenazo III, Genzyme Diagnostics, Framingham, MA). Samples were diluted to within the assay's linear range ($\leq$ 5.0 mM), and sample concentration was determined by comparison to a standard curve using an absorbance microplate reader (650 nm, FLx800, Bio-Tek Instruments, Winooski, VT).

Dynamic light scattering (DLS)

Dynamic light scattering (DLS) characterization of macromers in aqueous solution was performed using a 90PLUS particle size analyzer (Brookhaven Instruments Corp, Holtsville, NY)) operating at 659 nm wavelength. Dilute macromer samples (0.01%, 0.10%, 0.25%, 0.5%, 1.0%, 2.5% w/v) were prepared in freshly filtered (0.22 μm, Millipore Corporation) ultrapure water with 0, 100 μM, 500 μM, 2.5 mM, 4.0 mM, 10 mM, or 100 mM of $CaCl_2$ or control solutions with double the $CaCl_2$ concentration of NaCl (200 μM, 1 mM, 5 mM, etc.) to better elucidate effects due to calcium ions rather than chloride ions in solution. Prepared samples were left on an orbitally rotating platform overnight before sampling. DLS was performed on samples at 25 °C and 37 °C in triplicate; each sample was allowed to temperature equilibrate for 15 min prior to measurement. Intensity weighted size (R_h) distributions were determined from the autocorrelation function through the inverse Laplace transform non-negatively constrained least squares (CONTIN, regularized) algorithm.[400]

Statistical analyses

Statistical analysis was performed between groups for rheological and DSC characterization of transition temperature, TGA of residual sample weight percentages, and calcium binding assays. Analyses of variance were performed using Minitab® statistical software (Minitab, Inc., State College, PA) and an *a priori* significance level of 0.05. Pairwise comparisons were performed using

Tukey's HSD test. Where applicable, data are presented as mean ± standard deviation.

4.3 Results and Discussion

4.3.1 Macromer synthesis and structural characterization

Macromers were synthesized as shown in Table 4.1. Relative molar contents of the macromers were calculated from ^{1}H NMR spectra (Figure 4.1) and correlated well to the theoretical and actual comonomer feed ratios. The peak at 0.85 ppm was assigned to the methyl protons of PEDAS, peaks at 1.1 and 1.2 ppm were assigned to the methyl protons contributed by NIPAAm and 28 of the 32 methylene protons of the stearate chain of PEDAS, respectively, and the peak at 3.7 ppm was assigned to the backbone methine proton of VPA. A solvent ($CD_3(SO)$) peak is visible at 2.5 ppm in all spectra. ^{31}P NMR (Figure 4.1) also confirms the presence of the phosphorous in polymerized VPA at 30 ppm, close to previously reported values.[401] VPA monomer impurities, previously reported to appear between 16.0-18.6 ppm on ^{31}P NMR,[401, 402] were not observed after dialysis.

Number average molecular weights as determined by freezing point depression osmometry are reported in Table 4.1. Consistent decreases in Mn were observed with increasing VPA in the monomer feed and subsequently in the synthesized macromers; however, the comonomer ratios of the synthesized macromers approximated the feed ratios well despite the slight variability in Mn.

These values are within the range of molecular weights for similarly synthesized macromers containing PEDAS and NIPAAm as reported by Hacker *et al.*[262]

TGA curves (Figure 4.2) show 60-80% thermal decomposition of all macromers by 500 °C. Differential TGA curves (Figure 4.2) show a left shoulder followed by a peak at around 430 °C for the low and medium VPA containing macromers while the high VPA containing macromer shows two distinct peaks at 310 °C and 380 °C along with a broad right shoulder extending from 410 °C to 500 °C. Pure pNIPAAm has previously been shown to thermally decompose at 422 °C; however, when copolymerized at high molar ratios with other monomers, the decomposition temperature of pNIPAAm falls.[403] The TGA curve for the control macromer demonstrate this effect. The different character of the differential TGA curve for the high VPA containing macromer is likely due to a similar decrease in the decomposition temperature of pNIPAAm due to the relatively high NIPAAm composition of this formulation combined with cleavage of the more abundant carbon-phosphorus bond of polymerized VPA.[404]

Figure 4.3 shows the average residual weight percentages at 800 °C for all VPA-containing macromers and the control macromer. Poly(VPA) or copolymers containing VPA or other pendant phosphorous moieties typically leave a nonvolatile residue of approaching 40 wt% when degraded in nitrogen.[405, 406] The residual weight percentages for each synthesized macromer was significantly different from that of all the other synthesized macromers ($p < 0.05$) and the relative differences between the groups correlated well to the relative

differences in VPA molar ratios between the macromers, further verifying the incorporation of the VPA and its effect on macromer functional character despite the relatively low amounts of VPA present.

4.3.2 Functional characterization

Thermogelation by rheology and DSC

Rheology and DSC were used to characterize the transition temperatures of the synthesized macromers. For rheological characterization, the gelation temperature, denoted T_{δ}, was considered to be the inflection point of the phase angle (δ) curve. In general, below this inflection point the storage (G') and loss (G") moduli for each macromer remained below 1 Pa and then increased rapidly by at least 4 orders of magnitude at temperatures above T_{δ}. Figure 4.4 shows representative rheological traces of a 7.5% w/v aqueous macromer solution of VPA_H, as well as the effect of the presence of both divalent (Ca^{++}) and monovalent (Na^{+}) ions on the complex viscosity and phase angle during temperature sweeps.

Using DSC, the transition temperature (T_{DSC}) of the macromers was defined as the onset at inflection of the endothermic peak in the DSC thermogram. Transition temperatures for the synthesized macromers from both DSC (in water only) and rheological experiments are shown in Figure 4.5. Statistically significant differences ($p < 0.05$) were found for the T_{δ} of all three VPA-containing macromers in water. Furthermore, for the VPA_H macromer, increasing concentrations of $CaCl_2$ led to significant decreases in T_{δ} when

compared to the same macromer in water alone and also when compared to similar solutions of VPA_M. T_{DSC} values for the VPA_H macromer were significantly different from the low and medium VPA-containing macromers in water, and all three VPA-containing macromers had significantly lower T_{DSC} than the control macromer, which was synthesized using AAm instead of VPA. Significant differences for T_s, of the Control_AAm macromer were also found in the presence of $CaCl_2$ when compared to all of the VPA-containing macromers. At high concentrations (100 mM) of $CaCl_2$, there were significant differences in the T_s, of the Control_AAm compared to the same macromer at lower (2.5 mM) salt concentrations. There were significant differences in the T_s, of all VPA-containing macromers in 100 mM $CaCl_2$ when compared to the T_s, of the same macromers in 200 mM NaCl. There was, however, no significant difference between T_s, in the presence of 100 mM $CaCl_2$ or 200 mM NaCl for the control macromer. Changes due to the presence of $MgCl_2$ compared to equimolar concentrations to $CaCl_2$ were not significant (not shown). Additionally, no differences in T_{DSC} were found in the presence of any salt solutions when compared to the macromer T_{DSC} in water alone (not shown). It is important to note that due to the design of these macromers for biological and specifically cell delivery applications, all macromer solutions were characterized at pH 7.4. Adjustment of the pH with NaOH thus added slight variability in solution osmolarity between the VPA-containing macromers; however, the amount of salt contained in the tested solutions was greater than that used for pH adjustment.

Previous studies have shown that salts tend to decrease the LCST of pNIPAAm-based materials based on the concentration of the salt and following the trend of the Hofmeister series.[407, 408] While these and other studies have shown that the DSC-determined transition temperature of the materials does change due to a salting out phenomenon, the concentrations of salt used to elicit these changes are far higher than those used in the current study.[409] Furthermore, the changes in transition temperature observed with DSC often differ with those reported using other methods.[410, 411] In the present study, decreases in T_{DSC} were not found in the presence of relatively low concentrations of salt; however, similar concentrations of salts containing divalent cations resulted in changes in sol-gel transition temperature (T_s) when detected using rheology. Considered along with the lack of change in T_{DSC}, this more functional measurement of material gelation and the fact that equivalent salt concentrations with monovalent cations did not change the gelation temperature indicates that ionic crosslinking of macromer strands is likely responsible for this behavior rather than a salting out phenomenon. The transition is still primarily due to the hydrophobic collapse of the NIPAAm moieties, but ionic crosslinking likely gives the material the stability to meet the criteria for rheological gelation at a lower temperature than that which is detected calorimetrically. Fine-tuning of the LCST via the addition of salts or through the fabrication of materials that will interact with salts *in situ* could prove to be a useful technique for biomaterial applications. Gan *et al.* recently characterized microgel system of copolymerized NIPAAm and

2-hydroxyethyl methacrylate in a 7:3 ratio that required the presence of $CaCl_2$ or sufficiently high concentrations of NaCl for the formation of a gel with increasing temperatures.[412] This is likely due to the purely hydrophilic nature of the 2-hydroxyethyl methacrylate comonomer, which allows rearrangement of the colloidal dispersion at high temperatures such that the collapsed NIPAAm domains arrange in the core of microgel particles, minimizing cohesive interactions between particles that would lead to gel formation.

Previous work investigating the sol-gel transition of thermogelling copolymers of VPA and NIPAAm focused on copolymers synthesized from monomer feeds with a NIPAAm:VPA ratio of at least 9:1.[413, 414] Comparing the sol-gel transition temperatures reported in the present study to those previously reported, much greater amounts of calcium ions were needed to elicit similar changes in the sol-gel transition temperature than those found using the current formulations, which have a much lower ratio of NIPAAm to other monomers. Although the magnitude of the sol-gel transition, with respect to viscosity increase, may be diminished due to the lower relative amount of NIPAAm, the proportionally higher amount of VPA enables larger changes in the LCST to occur at physiologically relevant calcium concentrations that should not be toxic to encapsulated cells or cells present at a delivery site.

The pendant stearic acid chain of PEDAS likely contributes to this effect as well. Previous work has shown that for hydrogels with long pendant hydrophobic chains ($R > C_8$) binding and mixed micelle formation occurs with

surfactant molecules in a relatively concentration independent manner.[415] Additionally, cohesive associations between hydrophobic pendant groups has been shown to increase the mechanical toughness of hydrogels.[416] From a design standpoint, PEDAS was included in the macromers for this reason, as for potentially mineralizable hydrogels to have a role in hard tissue applications such as bone tissue engineering, they will need to have a greater mechanical toughness and compressive properties than typically achieved with hydrogels. Thus a combination of the presence of the stearic acid chain of PEDAS and the relatively high VPA content of the macromers may explain the observed rheological changes at low salt concentrations relative to previous studies. Furthermore, the presence of additional functional moieties such as the hydroxyl group of HEA potentially allow for these macromers to be acrylated or methacrylated and then chemically crosslinked with increasing temperature. Such reactions have been carried out on similar macromers while not compromising the cytocompatibility of the macromers.[417] Such covalent crosslinking could strengthen the gels at temperatures above the sol-gel transition temperature beyond what might be achieved by increasing the relative content of NIPAAm.

Calcium-binding assay

Macromer binding or complexation of free calcium ions in solution was measured by determining the concentration of free calcium ions in the supernatant of 7.5% w/v samples of each macromer after 24 h incubation. Data

are presented (Figure 4.6) as the absolute millimoles of calcium ion bound per 1 gram of macromer in solution. Statistically significant differences in calcium binding were present for all VPA-containing macromers at and above concentrations of 10 mM $CaCl_2$. Calcium binding for the Control_AAm macromer was significantly different from all macromers at concentrations of $CaCl_2$ greater than and equal to 1 mM, except for formulations in 100 mM $CaCl_2$ solutions, where the binding was not significantly different from the VPA_M group. Increases in the bound Ca^{++} were observed for the Control_AAm macromers with increasing $CaCl_2$ concentrations; however, given the rheological behavior of these macromers, these are thought to be nonspecific interactions such as entrapment in micelles or other salted out colloids.

The ability of these materials to bind or complex calcium as described in this assay could potentially prove useful in a number of biological applications. Surface induced mineralization of a number of substrates has been demonstrated previously through surface modification with nucleating proteins or moieties that mimic such proteins has been demonstrated as a way to potentially increase orthopaedic implant adhesion to bone or to create a synthetic bone analogue.[418-420] Many of these natural nucleators contain phosphoserines, and, when dephosphorylated or degraded lose their ability to interact with apatite mineral, leading to decreased calcification of the organic matrices to which they are associated and indicating the key role of these moieties in mineralization.[421] A number of strategies can be used to mineralize a synthetic matrix,[169] including

modification with phosphoserine itself.[422] Schneiders *et al.* modified hydroxyapatite/collagen composite bone cements with phosphoserine and after implanting the composites into a bone defect within a rat tibia found that new bone formation, particularly in the early phases of healing, was significantly greater in defects implanted with the phosphoserine modified composites compared to unmodified composites.[423]

Phosphonic acid, the structure of which is similar to that of the phosphoserines found in many nucleators, has previously been used in biomaterials applications to improve the adhesion of dental cements to the mineralized components of teeth.[401, 424, 425] Copolymers of VPA have been shown to mineralize *in vitro* over 1 month in a solution super saturated with calcium phosphate.[426] Copolymers of VPA and AAm have also been shown to increase attachment and proliferation of fibroblasts and osteoblast like cells.[427, 428] The interactions shown between the macromers synthesized in the present study and calcium ions similarly reflect the ability of phosphonic acid containing materials to interact with cations such as those found in the inorganic matrix of bone. In the present study, the presence of phosphonic acid along with calcium ions at concentrations similar to those found in plasma significantly affect the sol-gel transition of the material in a dose dependent manner, thereby facilitating additional control over the handling and delivery of such macromers in addition to the previously shown effect on mineralization and cell-material interactions.

Dynamic light scattering

DLS experiments were used to characterize the behavior of dilute concentrations of macromers in aqueous solutions. The approximate critical micellar concentration (CMC), reported in Table 4.1, was determined by analyzing the size distributions of macromers over a range of concentrations and identifying the concentration at which there was a consistent increase in the peak particle size. Additionally, the effect of calcium ions on macromer conformation was analyzed through the addition of $CaCl_2$. Representative size (R_h) distributions are shown in Figure 4.7. Control solutions containing NaCl were also examined at twice the molar concentration as the tested $CaCl_2$ solutions to clearly elucidate the effect of divalent ions versus monovalent (Na^+, Cl^-) ions.

In general, the CMC decreased with increasing VPA content. At 25 °C, the presence of calcium ions led to the disruption or prevented the formation of micelles for the experimental macromers at concentrations above the CMC but did not affect micelle formation of a control macromer that did not contain VPA (Figure 4.7). Increasing VPA content also led to decreased calcium sensitivity with respect to micelle formation, evidenced by lower concentrations of calcium eliciting a greater effect on the size distribution of macromers with low VPA content (not shown). For example, at 25 °C a 500 μM $CaCl_2$ solution consistently shifted the R_h peak intensity of the macromer containing the lowest relative VPA (VPA_L) content back to the radius observed at concentrations below the CMC, while for the macromer containing the highest relative amount of VPA (VPA_H),

similar changes were only observed in solutions containing greater than 500 μM $CaCl_2$. This is potentially due in part to the larger size of macromers containing lower VPA content, as intramolecular salt bridging may be more likely in these macromers than for smaller VPA_H chains. Additionally, in the VPA_H chains, interactions of hydrophilic charged moieties with surrounding water are not stabilized in the presence of $CaCl_2$ relative to VPA_L or VPA_M macromers, resulting in a greater propensity to form micelles to shield hydrophobic moieties from water, as reflected in the general trend for the CMC.

Similar changes in the presence of calcium salts were previously observed for dispersions of poly(1,3-butadiene-*co*-methacrylic acid).[429] In solutions with high enough pH that $RCOO^-$ groups were present, ionic crosslinking of with calcium ions prevented particle aggregation and swelling. In the present study, calcium ions were needed to prevent or disrupt micelle formation; however, NaCl did not have the same effect (not shown). NaCl decreased the CMC of all tested formulations, probably due to charge stabilization and reduced repulsion within or between macromers,[430] whereas calcium ions may have facilitated intramacromer or intermacromer ionic crosslinking or, as a divalent ion in excess, may not have resulted in charge stabilization in binding to single phosphonic acid moieties.

At 37 °C, all macromer formulations showed peak R_h greater than three times those observed above the CMC at 25 °C. This is likely due to micellar aggregation as the stearate chains of PEDAS probably still reside in the core of

the micelles, thus as NIPAAm undergoes hydrophobic collapse, stabilization of the hydrophobic moieties located on the shell of the micelles is likely achieved through aggregation in a manner similar to that observed in previously studied PNIPAAm-based polymers.[431-433] Below the CMC as determined at 25 °C, macromers tended to form micelles or aggregates upon temperature increases above 37 °C. The addition of NaCl and $CaCl_2$ did not have a noticeable effect on the peak R_h for macromers at 37 °C, as aggregation following hydrophobic collapse of the NIPAAm moieties likely drives micelle formation or chain aggregation rather than charge stabilization or ionic crosslinking, although when taken over a series of temperatures it is likely that the addition of salts would lead to a more discrete point at which micelles aggregate.[434] Similarly, it is important to note that while 37 °C is below the LCST reported for some of the macromer formulations and conditions tested, R_h representing micellar aggregates were uniformly seen as the dominant species; however, the intensity weighted CONTIN method used to analyze the DLS exaggerates the proportion of large particles, thus for these samples, micellar aggregates may not have been the dominant species.[435]

Polymeric micelles that can serve as nanocarriers for drug delivery are currently being investigated for a number of applications, including intracellular drug delivery.[436-438] Micelles that respond to environmental stimuli present within pathological cell populations, such as decreased pH within cancerous tissue, or within specific intracellular domains, have been proposed as potential delivery

agents whereby disruption or rearrangement of the micelle conformation could result in environmentally-cued drug release.[439] In the current study, VPA-containing thermosensitive macromers did not form micelles in the presence of calcium ions below the LCST of the materials. Modifications such that the materials gel above body temperature or do not gel could enhance the potential for use of these materials in drug delivery applications to specific sites with higher local calcium content than surrounding environments, such as the lysosome.[440]

4.4 Conclusions

In conclusion, thermosensitive macromers based on PNIPAAm and other functional monomers, including VPA, were synthesized and characterized with an end goal of creating functional, environmentally responsive materials for biological applications. Because of this, macromers were characterized over temperatures ranging from room temperature to body temperature at physiological pH. The synthesized macromers incorporated the monomers in ratios close to those of the molar feed ratios and underwent a sol-gel transition close to body temperature. Due to the addition of vinylphosphonic acid, the macromers interacted with calcium ions in solution and underwent ionic crosslinking and subsequent decreases in the sol-gel transition temperatures at physiologically relevant calcium ion concentrations. This effect was dependent on the relative amount of vinylphosphonic acid incorporated in the macromer. At temperatures below the transition temperature, calcium ions prevented or disrupted micelle formation while at temperatures above the transition

temperature, hydrophobic interactions promoted aggregation of macromer micelles. Based on previous efforts in this area and the results presented, these macromers hold potential in drug and cell delivery applications as well as bone tissue engineering applications.

Table 1. Compositions, Molecular Weights, and Characteristics of Synthesized Macromers

designation	theoretical composition	actual comonomer feed [mol] (based on 1 mol PEDAS)	^{1}H-NMR results (based on 1 mol PEDAS)	molecular weight	critical micellar concentration
	PEDAS/VPA/HEA/NIPAAm/AAm	VPA/HEA/NIPAAm/AAm	VPA/HEA/NIPAAm/AAm	Mn, [Da]	wt. %, $\log_{10}$
VPA_L	1/1.125/3.375/10.5/0	1.14/3.38/10.50/0	0.9/4.6/11.4/0	1810	-0.3
VPA_M	1/2.25/2.25/10.5/0	2.25/2.25/10.51/0	1.8/2.7/10.3/0	1790	-0.6
VPA_H	1/3.375/1.125/10.5/0	3.40/1.14/10.51	2.9/1.6/12.1/0	1340	-1
Control_Aam	1/0/3/14/3	0/3.07/14.03/3.01	0/3.2/15.3/1.9	2410	0

Table 4.1. Compositions, Molecular Weights, and Characteristics of Synthesized Macromers

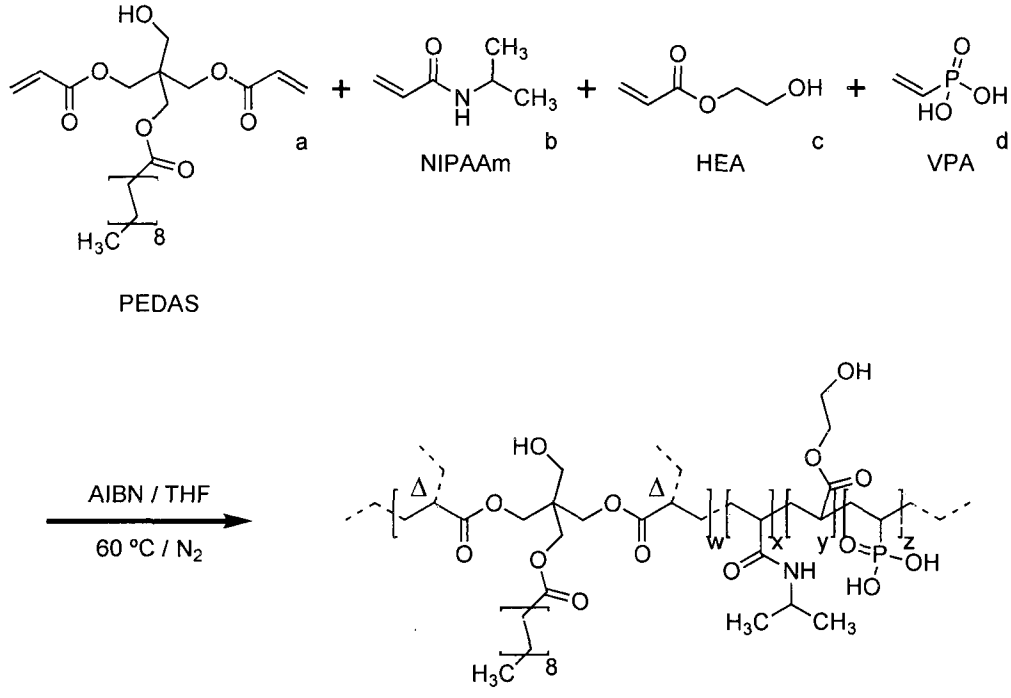

Scheme 4.1. Simplified schematic of the radical copolymerization of experimental macromers from pentaerthritol diacrylate monostearate (PEDAS), N-isopropylacrylamide (NIPAAm), 2-hydroxyethyl acrylate (HEA), and vinylphosphonic acid (VPA). Δ indicates possible branching sites in the highly simplified schematic of the branched statistical copolymer structure.

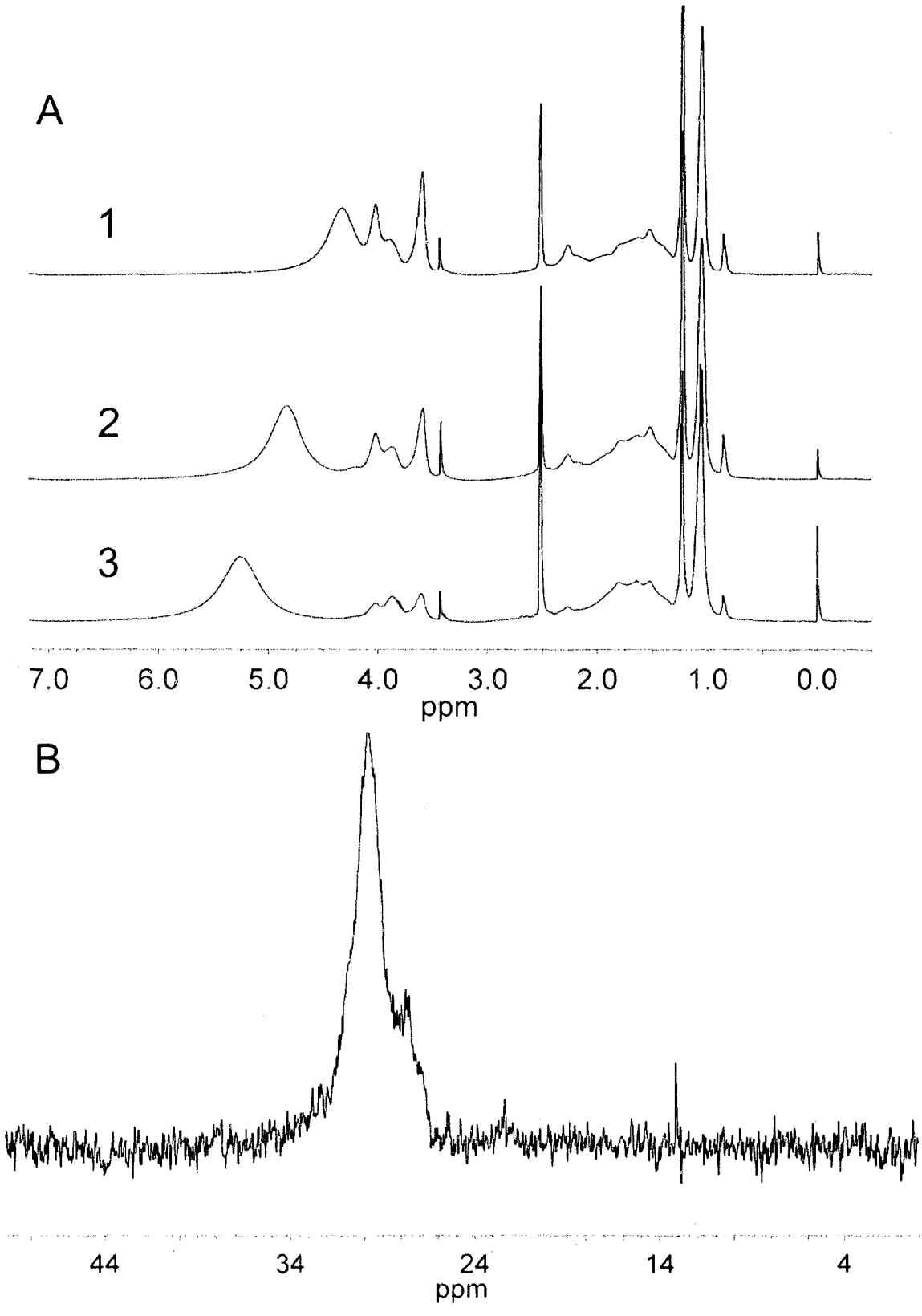
A
1
2
3
7.0
6.0
5.0
4.0
3.0
2.0
1.0
0.0
ppm
B
44
34
24
14
4
ppm

Figure 4.1. (A) ^{1}H-NMR of the three experimental macromers of the form poly(PEDAS$_{1}$-*stat*-VPA$_{n}$-*stat*-HEA$_{4.5-n}$-*stat*-NIPAAm$_{10.5}$) where the spectra represent: (1) VPA_H (n=3.375), (2) VPA_M (n=2.25), and (3) VPA_L (n=1.125).

(B) Representative ^{31}P-NMR of VPA_M verifying the presence of polymerized VPA in the macromer.

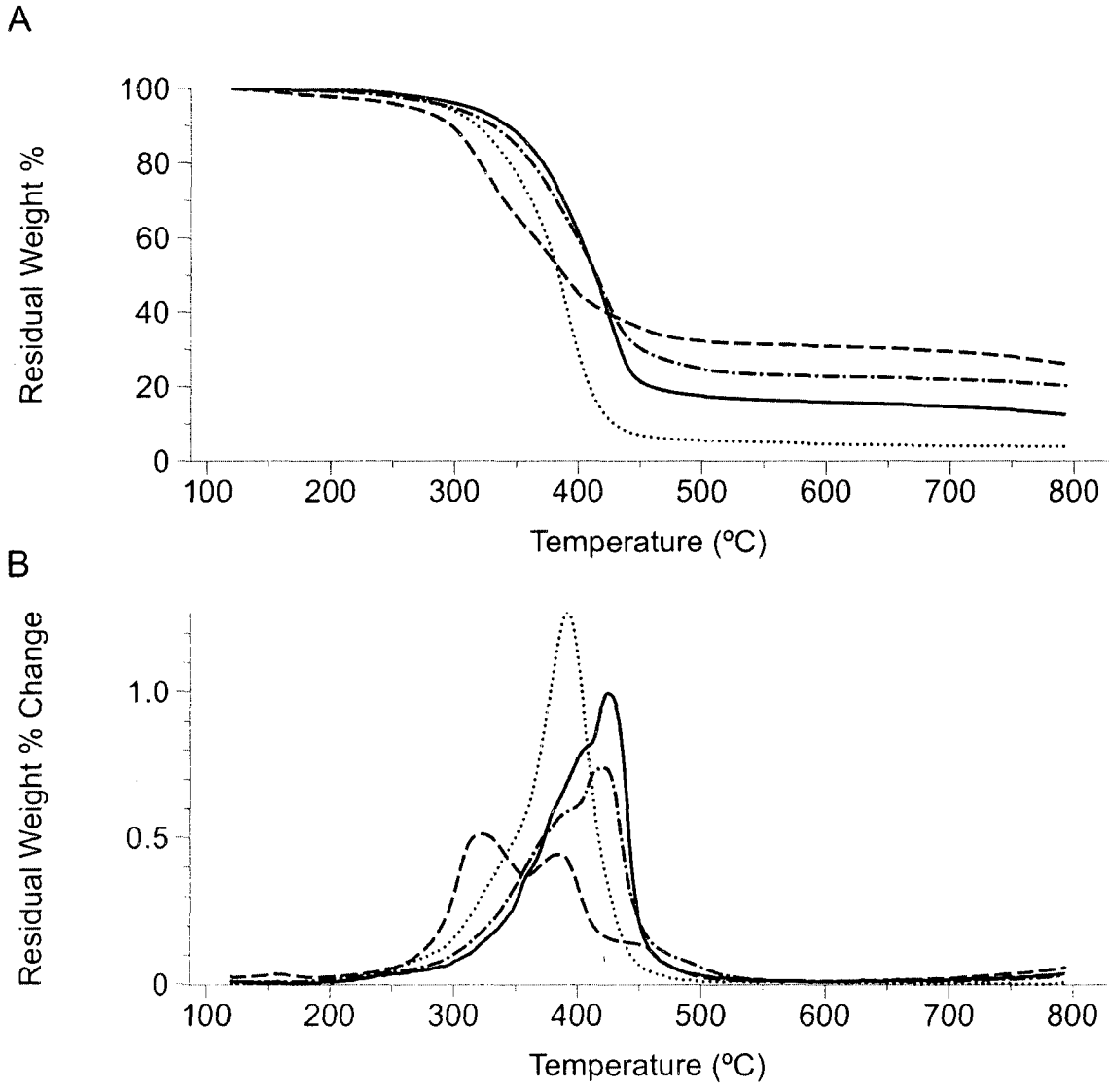

Figure 4.2. (A) TGA curve showing the degradation of the three experimental macromers (--- VPA_H, -·-· VPA_M, – VPA_L, ··· Control_AAm) thermally degraded at a rate of 10 °C/min in a nitrogen atmosphere. (B) Differential % weight loss as a function of increasing temperature.

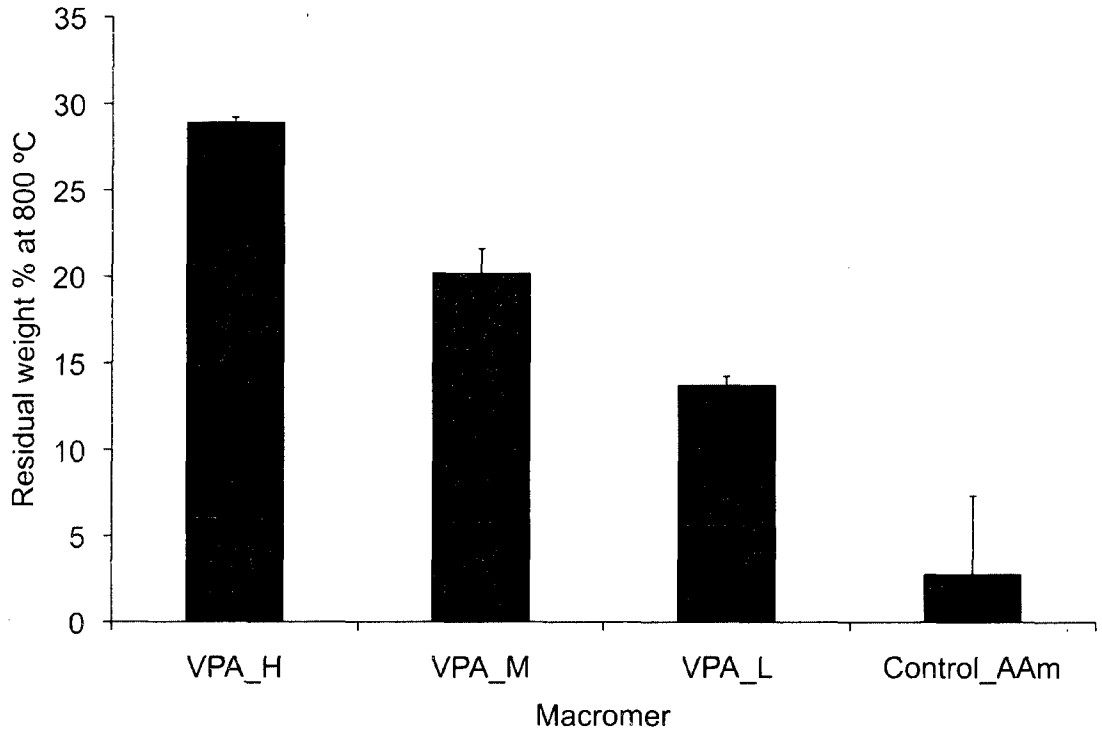

Figure 4.3. Residual weight % (n=3, means ± SD) remaining after thermal degradation of macromer samples from 100 °C – 800 °C.

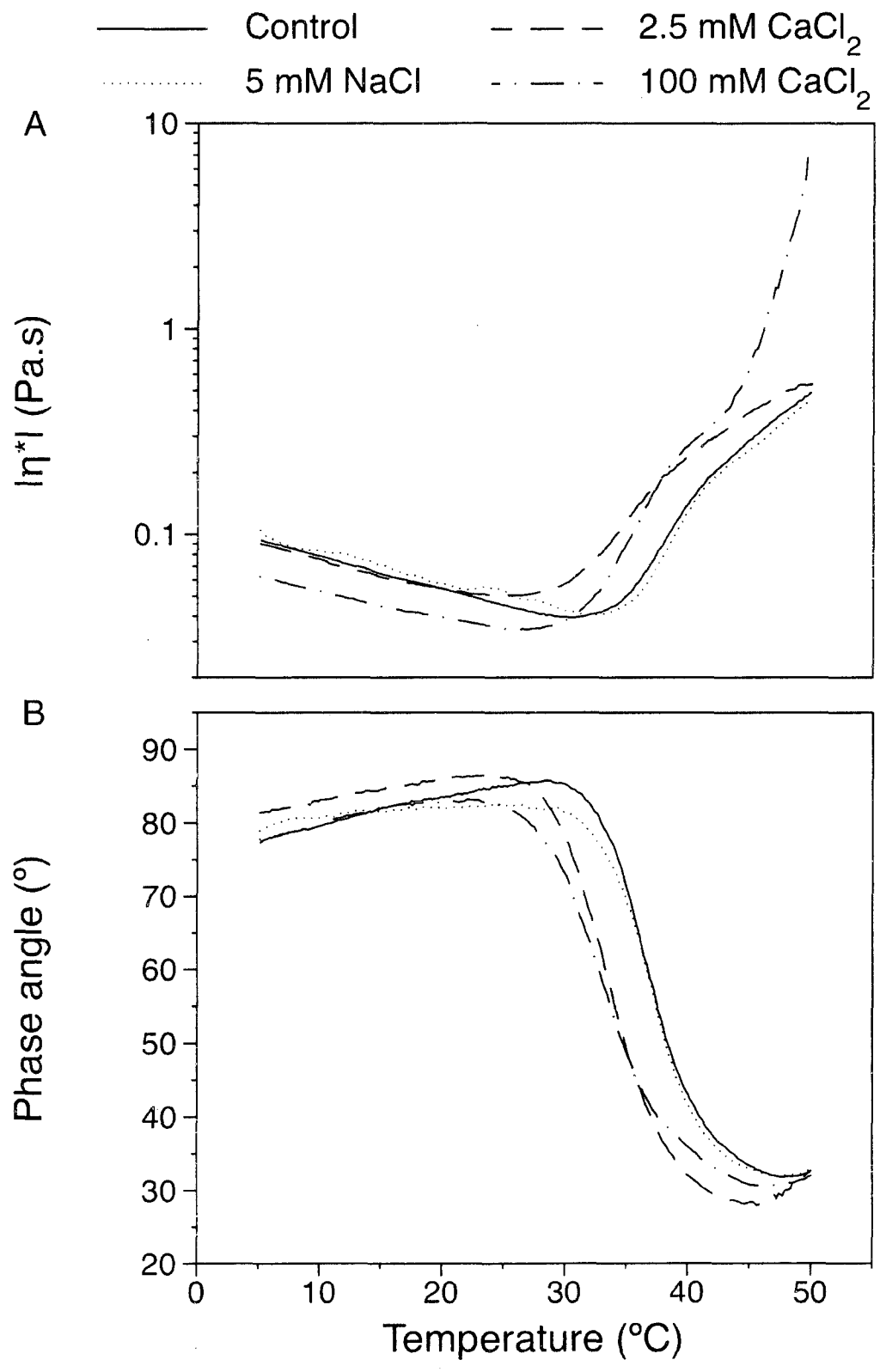
Control
2.5 mM CaCl2
5 mM NaCl
100 mM CaCl2
A
B
|η*| (Pa.s)
Phase angle (°)
Temperature (°C)
10
1
0.1
90
80
70
60
50
40
30
20
0
10
20
30
40
50

Figure 4.4. (A) Representative complex viscosity ($|\eta^*|$) rheograms of VPA_H. (B) Representative phase angle changes of VPA_H in aqueous solutions with and without added salts. Rheograms were obtained by increasing the temperature at a rate of 1 °C/minute and with a constant displacement of 1 $\times 10^{-4}$ rad.

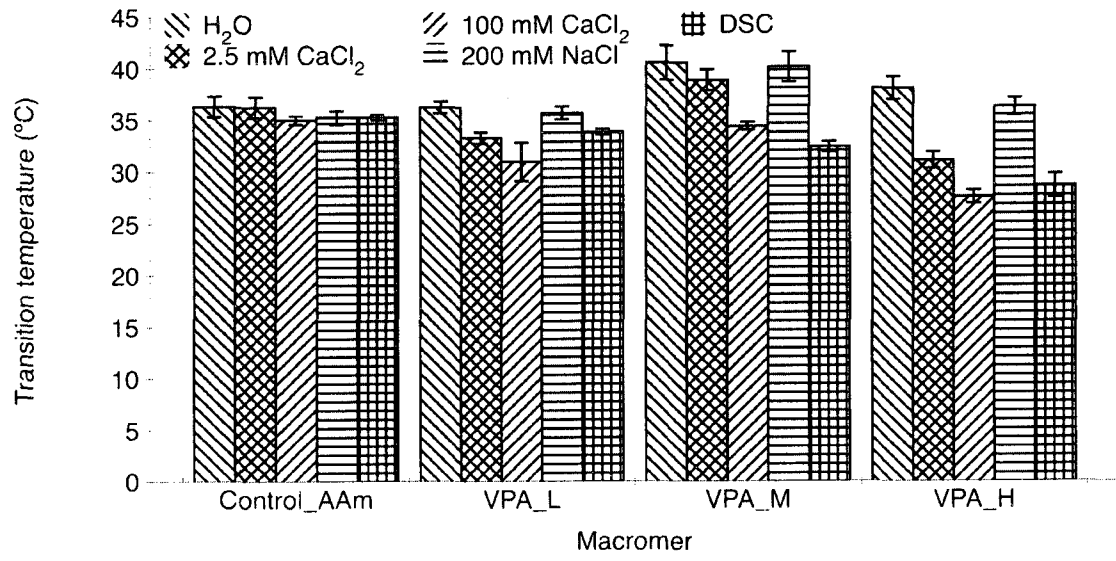

Figure 4.5. Gelation temperatures (n=3, means ± SD) or LCST as determined by rheology or DSC for all VPA-containing macromers and the control macromer.

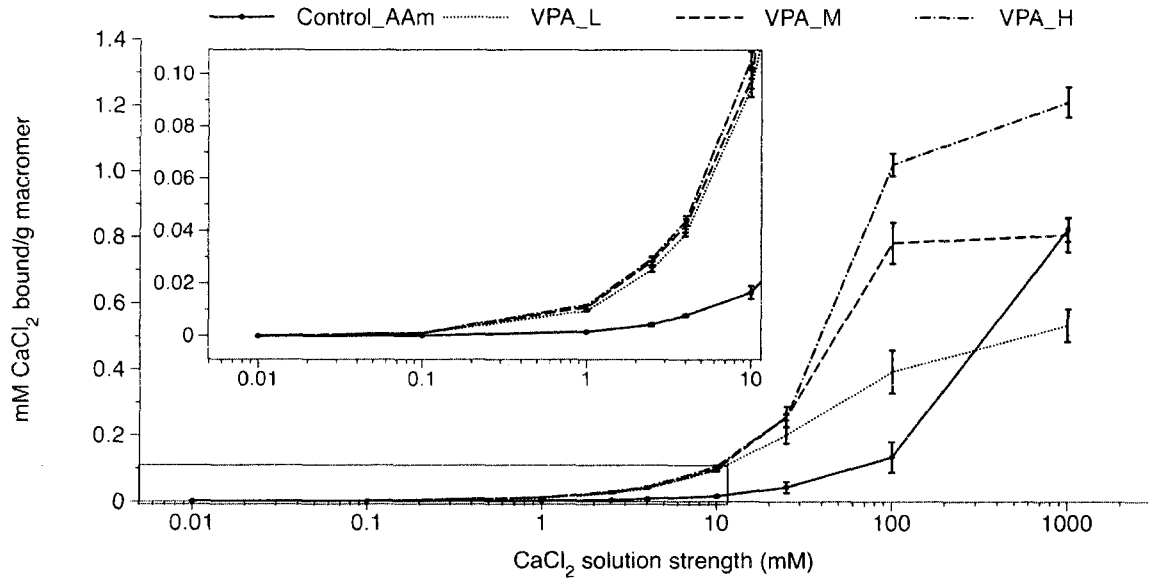

Figure 4.6. Calcium binding or complexation for macromers was measured spectrophotometrically using a colorimetric calcium assay. The millimoles Ca^{++} bound per gram of macromers (inset depicts binding at low $CaCl_2$ concentrations) is shown for macromers dissolved at 7.5 % w/v in H_2O. Data points and error bars represent means ± SD (n=3).

A

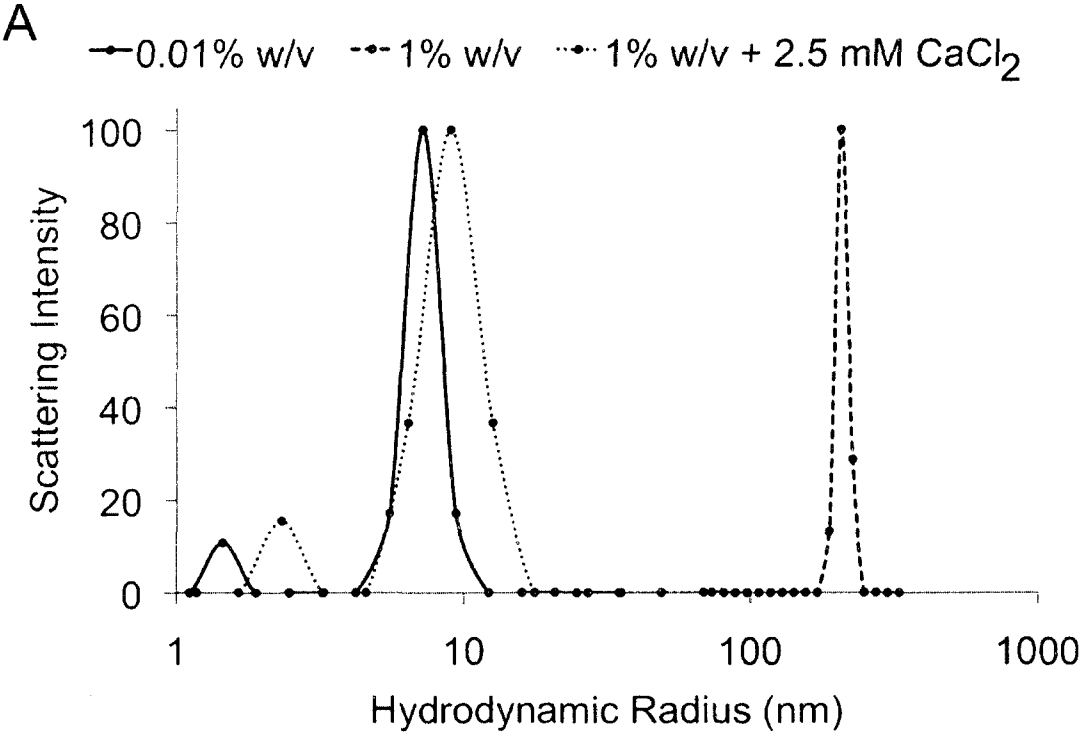
0.01% w/v
1% w/v
1% w/v + 2.5 mM CaCl2
Scattering Intensity
100
80
60
40
20
0
1
10
100
1000
Hydrodynamic Radius (nm)

B

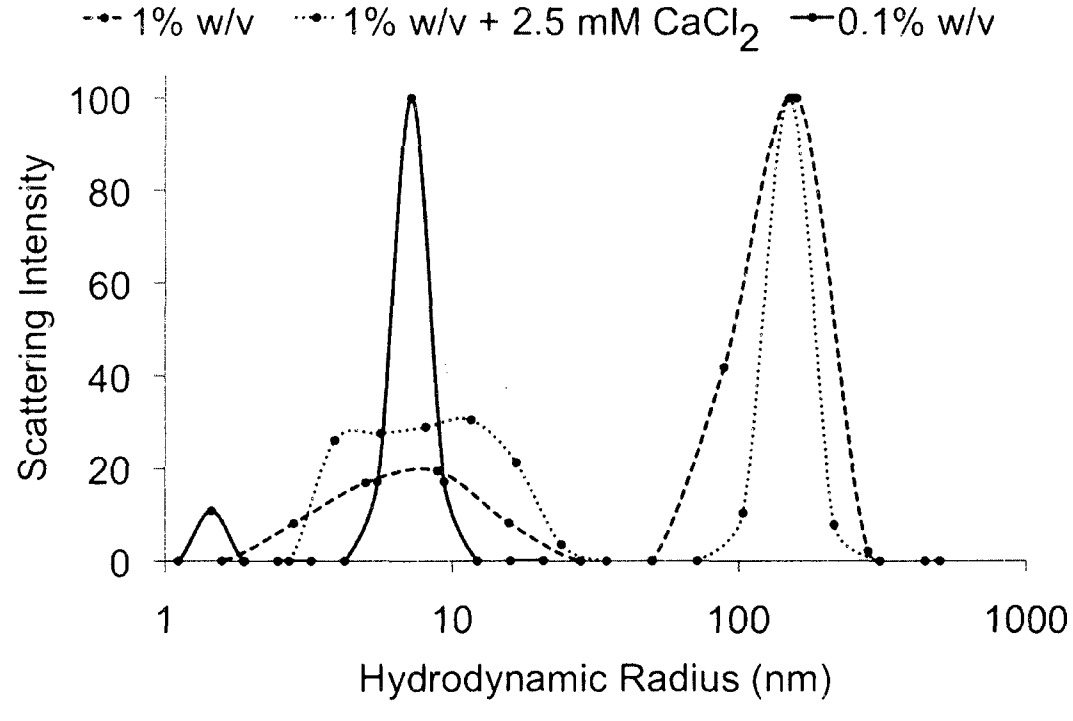
1% w/v
1% w/v + 2.5 mM CaCl2
0.1% w/v
Scattering Intensity
100
80
60
40
20
0
1
10
100
1000
Hydrodynamic Radius (nm)

Figure 4.7. Representative hydrodynamic radius plots of (A) VPA_M and (B) Control_AAm macromers at different concentrations in water and in aqueous solutions with 2.5 mM $CaCl_2$ at 25 °C.

Chapter 5

Donor age and cell passage affects differentiation potential of murine bone marrow-derived stem cells[†]

Abstract

Background: Bone marrow-derived mesenchymal stem cells (BMSCs) are a widely researched adult stem cell population capable of differentiation into various lineages. Because many promising applications of tissue engineering require cell expansion following harvest and involve the treatment of diseases and conditions found in an aging population, the effect of donor age and *ex vivo* handling must be understood in order to develop clinical techniques and therapeutics based on these cells. Furthermore, there currently exists little understanding as to how these two factors may be influenced by one another.

Results: Differences in the adipogenic, chondrogenic, and osteogenic differentiation capacity of murine MSCs harvested from donor animals of different age and number of passages of these cells were observed. Cells from younger donors adhered to tissue culture polystyrene better and proliferated in greater number than those from older animals. Chondrogenic and osteogenic potential

---

[†] This chapter was published as: Kretlow, J. D.; Jin, Y. Q.; Liu, W.; Zhang, W. J.; Hong, T. H.; Zhou, G.; Baggett, L. S.; Mikos, A. G.; Cao, Y., Donor age and cell passage affects differentiation potential of murine bone marrow-derived stem cells. *BMC Cell Biol* 2008, 9, 60.

decreased with age for each group, and adipogenic differentiation decreased only in cells from the oldest donors. Significant decreases in differentiation potentials due to passage were observed as well for osteogenesis of BMSCs from the youngest donors and chondrogenesis of the cells from the oldest donors.

Conclusions: Both increasing age and the number of passages have lineage dependent effects on BMSC differentiation potential. Furthermore, there is an obvious interplay between donor age and cell passage that in the future must be accounted for when developing cell-based therapies for clinical use.

Abbreviations

AdMSC(s)	adipose-derived mesenchymal stem cell(s)
BMSC(s)	bone marrow-derived mesenchymal stem cells(s)
eGFP	enhanced green fluorescent protein
FBS	fetal bovine serum
GAG	glycosaminoglycan
IGF	insulin-like growth factor
IHC	immunohistochemistry
MSC(s)	mesenchymal stem cell(s)
PPARγ	peroxisome proliferator-activated receptor γ
TGF-β1	transforming growth factor β1
TNFα	tumor necrosis factor α

5.1 Introduction

As the prospect of stem cell based therapeutics entering the clinic becomes more of a reality, researchers and clinicians must account for variability among stem cell populations used to evaluate therapeutic modalities in regenerative medicine and also among the patient populations that will potentially provide autogenous or allogeneic stem cells.[441-443] As hinted by the role of stem cell senescence and dysfunction in natural aging,[444-447] donor or patient age will be a critical factor that must be accounted for in clinical and laboratory evaluations of stem cell based technology.

There is currently little consensus and in many cases conflicting reports regarding the effect of donor age and cell processing on adult mesenchymal stem cell (MSC) function. A number of studies have previously shown no age related differences in differentiation using human BMSCs;[448-451] however, many studies demonstrating no change in differentiation have found changes in proliferation, attachment, senescence or self-renewal in mouse,[452] rat,[453, 454] and human[455, 456] BMSCs. Using mouse adipose derived MSCs (AdMSCs), Shi *et al.* found an age related decrease in adipogenic differentiation but no difference in osteogenic differentiation,[457] while Wall *et al.* found that with increasing passage, human AdMSCs tended towards osteogenic differentiation over adipogenic differentiation.[458] Similarly, work by Kirkland *et al.* found that advanced age in rats results in decreased levels of mRNA associated with adipogenic differentiation in preadipocytes,[459] a change that has since been linked to

decreased expression of CCAAT/enhancer binding protein (C/EBP)-α,[460] caused by overexpression of C/EBP homologous protein, and increased release of TNFα.[461] In contrast, studies have found an age related decrease in osteoblastic but not adipogenic differentiation in BMSCs from rats[462] and humans.[463, 464] Numerous other studies have found significantly decreased differentiation capability with increasing BMSC donor age, particularly for osteogenic,[465-467] chondrogenic,[468] and myogenic[469] differentiation.

Another important parameter that must be considered, particularly because of decreased proliferation and the propensity towards senescence observed in cells from aged donors, is the effect of cell passage on the differentiation capability of adult MSCs. BMSCs largely lose their *in vitro* differentiation capability at or around the 6th passage,[470, 471] but there is evidence of adverse changes as early as the first[472] or second passage.[467] *In vivo* benefits from MSC based therapies are also abated with increased passage.[473] Interestingly, however, while some reports indicate an age related decline in adipogenic differentiation capability for AdMSCs[457] and a similar passage related decline in osteogenic differentiation capability with a simultaneous enhancement in adipogenic differentiation,[471] previous results and hypotheses suggested that with increasing passage cells progressed through a lineage hierarchy, whereby bone marrow derived progenitors would retain a capacity towards osteogenic differentiation and adipose derived progenitors towards adipogenicity.[474] Recent comparisons of human BMSC and AdMSC differentiation[475] and

transcriptomes[476] supports this hierarchical model of preferential or retained differentiation.

In the only published study that examined the combined effects of increased *in vitro* passages and donor age on BMSC differentiation, Stenderup *et al.* examined osteogenic and adipogenic differentiation of human BMSCs.[456] They found decreased osteoblastic and adipogenic differentiation with increased number of passages for BMSCs from both young and old donors, but did not observe effects on differentiation when comparing across the two age groups.

To simultaneously evaluate the effects of both age and passage on BMSC differentiation, we utilized a full factorial study design investigating the adipogenic, chondrogenic, and osteogenic differentiation of mouse BMSCs from postnatal, adult, and aged mice at passage 1 and passage 6. The objective of such a study design was to provide a controlled analysis of two variables (age and passage) and possible interaction between these crucial factors in developing adult stem cell based therapeutics and for which no consensus exists regarding their role in MSC differentiation.

5.2 Methods

5.2.1 Experimental design

This study uses a factorial design to investigate the effects of donor age and cell passage on BMSC differentiation into 3 mesenchymal lineages. Murine bone marrow derived mesenchymal stem cells were harvested from donors aged

6 days (postnatal), 6 weeks (adult), and 1 year (aged) and cultured through either 1 or 6 passages before differentiation was induced. The harvested and cultured cells used were the adherent population of cells within the bone marrow and are often referred to as either marrow stromal cells or mesenchymal stem cells (a sub-population of marrow stromal cells). For this study, the adherent cell population examined will be referred to as bone marrow derived mesenchymal stem cells or BMSCs.

5.2.2 BMSC harvest and culture

All experiments followed protocols approved by the Animal Experiment and Care Committee of Shanghai Jiao Tong University School of Medicine. Postnatal (6-day old), adult (6-weeks old), and aged (1-year old) transgenic male eGFP C57Bl/6 mice were obtained from a local breeder colony. Mice were euthanized via cervical dislocation and bilateral thoracotomy and then immersed in 75% ethanol for 15 minutes. The bilateral femurs and tibias were aseptically excised, stripped of connective tissues, and the epiphyses and metaphyses were then removed. The remaining diaphyses were placed in a culture dish with 7.5 ml sterile PBS, and the bone marrow was flushed from the shafts via 3-5 minutes of vigorous pipetting of the PBS. The PBS/marrow suspension was then filtered through a 70-μm cell strainer (BD Biosciences, Mississauga, ON, Canada), collected and centrifuged for 5 minutes at 524×g. After removal of the supernatant, the resulting pellet was resuspended in α-MEM supplemented with 10% fetal bovine serum (FBS, HyClone, Logan, UT), 2mM L-glutamine and

plated at a density of 1.7-2.0×10^4 cells/cm^2. Media were changed every 3 days, and cells were passaged when confluent (~5×10^4 cells/cm^2) with 0.05% trypsin in 0.02% ethylenediaminetetraacetic acid (Gibco, Canada). Cells were replated at a density of 3×10^3 cells/cm^2. First and sixth passage cells were used as indicated for all experiments. Each experiment was performed with cells pooled from 2-7 mice for each age group. Experiments were repeated in triplicate using different batches of marrow isolates.

5.2.3 Cell attachment and proliferation

After harvesting and resuspension, cells from postnatal, adult, and aged mice were plated individually in wells of 6-well tissue culture plates at a density of 1×10^4 cells/cm^2. At ½, 1, 2, 4, 8, 16, and 24 hours after plating, media were gently aspirated and the remaining cells were fixed with 4% paraformaldehyde (Sigma, St. Louis, MO) in phosphate buffered saline (PBS) for 15 minutes. Cell adhesion was measured by counting the total cell number per well under fluorescence.

For proliferation, first passage cells from postnatal, adult, and aged mice were plated individually at 2×10^3 cells/cm^2 in wells of 6-well tissue culture plates. At days 1, 2, 4, 6, and 8 cells were trypsinized and counted using a hemacytometer.

Attachment and proliferation assays were performed in triplicate. Cell doublings were calculated as:[477] doublings = $\log_2$ (number of cells at passage/number of cells seeded).

5.2.4 Adipogenic differentiation and characterization

As previously described,[478] the first or the sixth passage cells were seeded in 2 wells each of a 6-well plate at a density of 3000 cells/cm^2. Cells were maintained for 24 hours in regular culture media, after which adipogenic differentiation was induced using Dulbecco's modified Eagle medium (DMEM) supplemented with 10% FBS, 0.5 mM isobutylmethylxanthine, 10 μM insulin, 1 μM dexamethasone, and 200 μM indomethacin (all from Sigma) for 3 weeks with full medium changes performed every 3 days. 2 control wells were maintained in DMEM with 10% FBS over the same time course. Each experiment was repeated in triplicate, resulting in 6 total wells for adipogenic differentiation and 6 control wells.

Differentiated and control wells were stained with Oil Red O. At 3 weeks post-induction, wells were gently rinsed with PBS and then fixed with cold 4% paraformaldehyde for 10 minutes. Wells were then washed with 60% isopropyl alcohol (Sigma), incubated for 5 minutes at room temperature in 2% (w/v) Oil Red O reagent (Sigma), and then washed once with isopropyl alcohol followed by repeated washes with distilled water.

For each well, 3 fields were randomly chosen and examined by light and fluorescence microscopy. The number of total cells per field was determined under fluorescence followed by determination of the number of cells containing Oil Red O stained inclusions. A cell containing a visibly stained vacuole was considered to be positively stained. Additionally, for each view the percent area

of positive staining was determined using ImageJ (NIH, Bethesda, MD). The area stained was determined by quantifying the actual area stained rather than the area covered by cells containing stained vacuoles. The average percentage was determined from total 3 views of each well and means plus standard deviation were derived from the average percentage of total six wells.

5.2.5 Chondrogenic differentiation and characterization

As previously described,[478] following monolayer culture until the first or the sixth passage, cells were trypsinized, counted, and centrifuged into pelletted micromass cultures (5×10^6 cells/pellet) in 15 ml conical tubes (BD Biosciences). After centrifugation and culture in regular culture media for 24 hours, chondrogenesis was induced using low glucose DMEM supplemented with 10% FBS, 10 ng/ml TGF-β1, 100 ng/ml IGF (Peprotech, Rocky Hill, NJ), and 10 nM dexamethasone (Sigma). Cells were cultured in induction or control media (low glucose DMEM with 10% FBS only) in incubators with the conical tube lids loosely fastened for 3 weeks and half media were changed every other day. Four pellets (2 for induction, 2 for control) per age/passage batch were cultured, and each batch was repeated in triplicate.

Following culture, 3 pellets from each group were analyzed for type II collagen expression and glycosaminoglycan (GAG) quantification. Immunohistochemical staining was performed as previously described.[479] Briefly, pellets were fixed with 4% paraformaldehyde for 2h and embedded in Tissue-Tek OCT (Fisher Scientific, Pittsburgh, PA) and sliced into 10 μm thick sections.

Samples were blocked and incubated overnight at 4°C in 1:100 diluted mouse anti-Collagen-II (Lab Vision, Fremont, CA) in 1% bovine serum albumin (Sigma) PBS solution. Samples were then incubated with horseradish peroxidase (HRP)-conjugated goat anti-mouse antibody (DAKO, Carpinteria, CA) diluted in phosphate buffered solution (PBS, 1:100) for 30 minutes at room temperature and developed with diaminobenzidine tetrachloride (DAB). Cells were counterstained with hematoxylin. Slides were also stained with Safranin O by being fixed for 10 minutes in 10% formalin in PBS, rinsed with distilled water, and then stained for 2 minutes with 6% Safranin O (Sigma) in distilled water.

Sulfated GAG production was measured from the remaining 3 pellets per group using an Alcian blue binding assay as previously described.[480]

5.2.6 Osteogenic differentiation and characterization

As previously described,[478] the first or the sixth passage cells were seeded in 2 wells each of a 6-well plate at a density of 3000 cells/cm^2 as similarly performed in 2.3. Cells were maintained for 24 hours in regular culture media, after which they were cultured in low glucose DMEM supplemented with 10% FBS, 0.1 μM dexamethasone, 50 μM ascorbate-2-phosphate, and 10 mM β-glycerophosphate (all from Sigma) to induce osteogenic differentiation. The induction culture was maintained for 3 weeks with full medium changes every 3 days, whereas the control cells were cultured for 3 weeks in low glucose DMEM with 10% FBS. Experiments were performed in triplicate.

Following culture, 3 wells per group were stained with Alizarin Red to visualize calcified deposits. Wells were gently rinsed with PBS and then fixed with 70% ice-cold ethanol for 1 hour. After washing with distilled water, Alizarin Red solution (40 mM Alizarin Red-Tris-HCl, pH 4.1; Sigma) was left at room temperature in wells for 10 minutes. Wells were then extensively washed with distilled water to remove any nonspecific staining, and the stained area was quantified using ImageJ as in 2.4. For the remaining 3 wells per group, calcium cation (Ca^{2+}) concentration was determined via a colorimetric assay (Diagnostic Chemicals, Charlottetown, PEI, Canada) as previously described.[481]

5.2.7 Statistical analyses

Analyses of variance (ANOVA) were performed using SAS software (SAS Institute Inc., Cary, NC), followed by Tukey's multiple comparison tests to determine pairwise statistical significance within 95% confidence intervals ($p<0.05$). All results are reported as means ± standard deviations. Due to quasi-complete separation, binary logistic regression was not performed on the data for collagen II staining of pellets.

5.3 Results

5.3.1 Postnatal BMSCs exhibit more rapid proliferation and greater attachment than BMSCs from aged donors

Following primary harvest, equal numbers of BMSCs were plated in 6-well plates and attachment was measured over 24 hours. Overall, donor age was

found to have a statistically significant effect on cell attachment ($p<0.0001$). As shown in Figure 5.1, at 8 hours and beyond there were significant differences ($p<0.05$) in attachment between cells harvested from both 6-day and 6-week-old donors and cells harvested from 1-year-old donors. Over 24 hours there were no significant differences in attachment between cells from 6 day and 6-week-old donors ($p>0.05$).

Proliferation was assessed for 8 days following primary harvest. After 2 days there was significantly greater proliferation among cultures harvested from 6-day-old donors compared to cultures from 6-week and 1-year-old donors ($p<0.05$, Figure 5.2). This significant difference persisted throughout the 8 days of culture. At 6 and 8 days, significant differences in proliferation were also observed between cultures from 6 week and 1-year-old donors ($p<0.05$). Overall, donor age was found to have a statistically significant effect on cell proliferation ($p<0.0001$). There was a 4.9 ± 0.2 fold increase in cell number in cultures of postnatal BMSCs after 8 days compared to cell number after 24 hours, and confluence in these cultures was reached by day 6. An increase of 3.9 ± 0.2 and 3.0 ± 0.1 fold was observed in cultures from adult and aged donors compared to cell numbers after 24 hours, respectively. For the differentiation experiments, passage 1 cells had undergone approximately 2.7 cell doublings, while passage 6 cells had undergone 11.4 doublings. Cells from 6-day-old donors doubled in approximately 2.3 days, with little variation between passage 1 and 6, while cells

from 6-week-old and 1-year-old donors had approximate cell doubling times of 3.1 and 3.5 days over the entire culture duration, respectively.

5.3.2 Adipogenic potential is diminished in BMSCs from aged donors

To assess the adipogenic potential of BMSCs, Oil Red O staining was quantified following 3 weeks of culture in standard adipogenic media. Quantification was performed in 2 ways, firstly by determining the percentage of cells that contained Oil Red O stained lipid laden vacuoles, and secondly by determining the overall area within a field of view that was stained by Oil Red O. Figure 5.3 shows results of both quantification methods along with representative histology from each group.

Based on the percentage of cells staining positive for lipid inclusions, there were no significant differences between cells from 6-day and 6-week-old donors, and within these groups there were no differences between cells at passage 1 or 6. A significantly lower percentage of cells stained positive with Oil Red O was found in 1-year-old donors comparing to passage matched numbers of 6-day and 6-week groups ($p<0.05$). Additionally, within 1-year old group there was also a statistically significant difference between passage 1 and passage 6 cells (52.9 ± 14.7 percent versus 37.7 ± 8.9 percent, $p < 0.05$). Based on the percentage of cells stained, all groups were significantly different from corresponding age and passage matched controls ($p<0.05$), and there were significant overall effects related to both donor age ($p<0.0001$) and cell passage ($p<0.05$). Additionally,

there was a significant statistical interaction effect ($p<0.05$) between donor age and cell passage for this method of quantifying adipogenic differentiation.

Quantifying the area stained with Oil Red O showed no statistically significant differences in adipogenic differentiation of BMSCs between 6-day and 6-week-old donors when compared at the same passage (passage 1: 17.7 ± 4.2 percent versus 17.7 ± 4.4 percent, passage 6: 13.4 ± 3.3 percent versus 11.0 ± 3.9 percent, 6-day and 6-week donors respectively). At the same passage, BMSCs from 1-year-old donors revealed statistically significantly less adipogenic staining area (passage 1: 8.1 ± 2.8 percent, passage 6: 5.2 ± 1.7 percent) than similarly passaged cells from younger donors ($p<0.05$). For cells from aged donors, there was also no significant effect of increased passages ($p>0.05$), whereas in the other two donor age groups, passage significantly decreased the area stained ($p<0.05$). In all groups BMSCs displayed significantly different stained areas than age and passage matched controls ($p<0.05$) except for passage 6 BMSCs from 1-year-old donors (5.2 ± 1.7 percent vs. 2.3 ± 1.6 percent stained, $p>0.05$). Significant overall effects were determined for donor age ($p<0.0001$) and cell passage ($p<0.0001$); however, there was no statistically significant interaction between donor age and passage based on the area stained ($p>0.05$).

5.3.3 Chondrogenic potential decreases with age and repeated passage abrogates chondrogenic differentiation in aged donors

Sulfated glycosaminoglycan content was quantified for pellets cultured for 3 weeks in chondrogenic media. As shown in Figure 5.4, compared across donor age groups at constant passage, sulfated GAG content per pellet significantly decreased with each progressive increase in donor age ($p<0.05$). Increased passage of cells yielded statistically significant differences within donor age matched groups only for BMSCs from 1-year-old donors (2.9 ± 1.2 μg per pellet versus 0.6 ± 0.6 μg per pellet, $p<0.05$). Additionally, passage 6 BMSCs from 1-year-old donors did not display significantly more sulfated GAG per pellet than passage and donor age matched controls (1-year, passage 6 control: 0.1 ± 0.1 μg per pellet, $p>0.05$). All other groups had significantly greater GAG content per pellet than passage and age matched controls ($p<0.05$). Overall, donor animal age ($p<0.005$) but not cell passage ($p>0.1$) was found to have a significant affect on the amount of sulfated GAG per pellet.

To further evaluate chondrogenesis, pelleted tissue was immunohistochemically stained for collagen II. As shown in Table 5.1, with the increase of donor age and cell passage, the number of collagen II-positive pellets decreased. In addition, a typical lacunar structure was observed in histology of collagen II-positive pellets as shown in Figure 5.4.

5.3.4 Osteogenic potential decreases with age and passage only affects postnatal -harvested BMSCs

Osteogenic potential was determined by quantifying the percent area stained with Alizarin Red, a dye that stains calcium deposition, and by determining the amount of extracellular calcium within a well. Both measures showed that within age groups, the only statistically significant difference based on passage was found in BMSC cultures from postnatal donors (Figure 5.5, $p<0.05$), where passage 1 cultures displayed 46.7 ± 9.0 percent area stained and 0.27 ± 0.06 mM Ca^{2+} versus 31.1 ± 10.1 percent area stained and 0.2 ± 0.04 mM Ca^{2+} for passage 6 cultures. BMSCs from 6-week-old and 1-year-old donors did not show significant differences in osteogenic potential for cultures at different passages. For both passage 1 and passage 6 cultures, an overall decreased osteogenic potential was found with increased donor age for all ages of donor in term of both area and calcium content ($p<0.05$). Tukey's multiple comparison tests revealed a significant difference of any two passage-matched groups comparisons in either stained area or calcium content ($p<0.05$), except for passage 6 stained area between 6-day-old and 6-week-old donors (31.1 ± 10.1 percent versus 27.2 ± 8.0 percent, $p>0.05$). Representative micrographs showing Alizarin Red stained samples are also displayed in Figure 5.5. The percent area stained using Alizarin Red was significantly different from age and passage matched controls ($p<0.05$); however, the calcium assay showed no significant difference between control and induced groups for both passage 1 and

6 BMSC cultures of 1 year old donors ($p>0.05$). Analysis of both stained area and calcium content showed a significant effect of donor age ($p<0.001$); however, analysis of stained area showed a significant overall effect for passage ($p<0.001$) while analysis of calcium content did not show an overall effect for passage ($p>0.05$). No statistically significant interaction was found between donor age and passage for either method of evaluation of osteogenic differentiation.

5.4 Discussion

In the present study, we investigated the effects of both donor age and passage on murine BMSC differentiation potentials towards adipogenic, chondrogenic, and osteogenic lineages. Murine BMSCs were used to facilitate future studies performed *in vivo*, where implantation of tissue engineering constructs containing fluorescently labeled progenitor cells allows histologic determination of the cell source for regenerated tissues.[482-485] Additionally, the availability of transgenic mice and mouse cell lines presents the opportunity for tissue engineers to investigate emerging strategies in more clinically appropriate disease models.[486] It is important, however, to note that transgenic animals do not uniformly express GFP, and this expression is variable between tissues with values for murine bone marrow reported at close to 90%[487] in some studies but significantly lower in others,[488] thus necessitating a careful comparison of light and fluorescence microscopy when cell numbers are quantified. Routine flow cytometric characterization of the breeder colony used in this study has

repeatedly shown over 90% of adherent marrow cells express GFP, even after multiple passages (unpublished data).

No standardized practice exists for the harvest, expansion, and *in vitro* differentiation of BMSCs. As noted in the Materials and Methods section, BMSCs in this study and many others refers to the adherent marrow stromal cells[456, 476, 489]. Within the adherent BMSC-containing population, our data suggest that a more rapid decline occurs in differentiation potential for osteoblastic and chondrogenic lineages relative to the decline in adipogenic differentiation.

We found that osteogenic and chondrogenic potentials are adversely affected by increased donor age across all three tested donor age groups, while adipogenic differentiation potential is maintained in all but the aged donors (1 year). These results are in agreement with previous work which found that donor age affected osteogenic differentiation of BMSCs more than it affected adipogenic differentiation.[464] Analysis of the transcriptomes of human BMSCs at passage 2 from young donors (average age = 13) suggested that BMSCs should preferentially form bone and cartilage over adipose tissue.[476] Peng *et al.* recently found similar results, noting that expression of osteogenesis-related genes peaked very early following induction in BMSCs.[490] Other studies addressed the hypothesis that age related decreases in bone regeneration were due to BMSC aging, resulting in a decreased osteogenic potential with a concurrent increase in adipogenic potential.[448] In this study BMSCs maintained their potential for

adipogenic differentiation in early aging but exhibited decreased potential for chondrogenic and osteogenic differentiation, and, although no absolute increase in adipogenic potential was observed with increasing age, the relative differences between differentiation potentials with age would thus favor adipogenesis over osteogenesis and chondrogenesis. Age related cellular dysfunction has been hypothesized to be the cause of multiple diseases of bone and cartilage associated almost exclusively with aging including osteoarthritis and osteoporosis, and loss of progenitor cell differentiation potential could contribute to these diseases.[491] The present study supports these hypotheses.

The effect of *in vitro* culture period prior to the induction of differentiation was also investigated by expanding cells through 6 passages and comparing differentiation to cells after a single passage. For chondrogenesis, increased passage only affected cells from 1-year-old donors, rendering them equal to control groups at the level of significance ($p>0.05$). For osteogenesis, the opposite effect was observed; a difference in osteogenesis due to passage alone was only observed in BMSC cultures from postnatal mice. Previous work using human BMSCs observed a greater passage related decrease in osteogenic differentiation in cells from young donors compared to cells from aged donors.[456] Early passage postnatal BMSCs may be preferentially inclined towards osteogenesis and this preference may be quickly eliminated with repeated passages and aging, leading to the observed differences between passage 1 postnatal BMSCs and all other groups with respect to osteogenic differentiation.

The effect of passage on adipogenesis was more obscure. Quantifying the percentage of cells stained with Oil Red O showed significant passage related differences only in cultures from aged donors, whereas quantifying the percentage area stained showed significant differences in cultures from postnatal and adult donors but not those from aged mice. A previous study investigating adipogenic differentiation with increasing BMSC passages found that the size of adipocytes decreased with increased passage.[456] Thus for postnatal and adult derived BMSCs, passage related changes in area might be largely due to decreased cell volume rather than a decrease in the number of differentiated cells. In cultures of BMSCs from aged donors, the relatively decreased number of cells undergoing adipogenic differentiation may render this effect statistically insignificant at the designated sample size (n=6). When characterizing adipogenic differentiation via quantification of the percentage of cells stained with Oil Red O, the statistically significant interaction effect of donor age and passage reflects that cultures from aged donors were the only group to be both significantly decreased from other age groups and to have a significant decrease in cells stained between passage 1 and passage 6 cultures. This may reflect a loss of adipogenic differentiation capacity only experienced by MSCs from aged donors that is not detected when quantifying the stained area due to passage-related decreases in adipocyte size experienced in cultures from all donors. It is also important to note that the selected adipogenic cocktail utilized indomethacin, a commonly used chemical for these applications that inhibits cyclooxygenase.

Indomethacin has been shown to both positively and negatively effect PPARγ in a concentration dependent manner.[492] Although adipogenic differentiation can be induced via PPARγ dependent and independent signaling,[493] PPARγ2 activation may be critical in BMSC differentiation as this pathway this pathway promotes terminal differentiation and suppresses *Osf2/Cbfa1*.[494] A PPARγ ligand such as *rosiglitazone* may therefore be a more ideal component for adipogenic induction media for BMSCs.

Working with human BMSCs, Banfi *et al.* found decreased adipogenic, chondrogenic, and osteogenic potentials when increasing from passage 1 to passage 5 and found adipogenic potential to be compromised prior to osteo- or chondrogenic potential.[472] In the present study, passage effects were variable when considered along with specific donor ages. For example, for 6-week-old donors, osteogenesis and chondrogenesis were unaffected by passage, but adipogenesis as measured by percent area stained was significantly decreased with increased passage. These results correlate well to published studies using human BMSCs;[472, 474] however, it should be noted that due to the use of biochemical characterization methods in addition to histology to characterize osteogenic and chondrogenic differentiation, the sample size for these methods was smaller (n=3) than for evaluation of adipogenic differentiation (n=6). Passage adversely affected osteogenic potential in BMSCs from postnatal donors, while chondrogenesis was only diminished by passage in BMSCs from 1-year-old donors, suggesting differences in passage effects for different differentiation

lineages at different ages. When evaluating changes associated with passage, it is important to note that the adherent marrow stroma is a heterogeneous cell population, therefore there is concern that changes attributed to altered MSC function could actually be due to the preferential proliferation of one or several type(s) of cell(s) over others. The observed variable effects of passage with age suggest that different or additional factors other than BMSC number and differences in attachment/proliferation contribute to differences in differentiation potential, as, in the case that heterogeneity and subsequent differential proliferation, one would expect effects due to frequency or proliferation to be exhibited across all lineages.

5.5 Conclusions

Based on the results of this study and many other previous studies, it appears that many variables must be considered when choosing an ideal or appropriate cell source for a specific application. Future studies should address tissue regeneration *in vivo*, as this will allow parameters such as aging and passage to be compared using criteria more closely related to the clinical goal of regenerating destroyed or dysfunctional tissues. As more is learned regarding aging and passage of adult stem cells, it may be determined that a certain population of cells is more appropriate for specific therapies based on patient age and the tissue of interest. While the present study offers little in the way of mechanistic explanations for the observed phenomena, it provides one of the first analyses of age in combination with passage in an animal model that will be

useful for developing future tissue engineering strategies. There is little doubt that aging of adult stem cells plays a role in the spectrum of changes during normal aging and that consideration of age and passage in combination will prove to be critical to the success of any strategy that seeks to regenerate tissue through the use of implanted progenitor cells.

5.6 Figures

Table 5.1 The ratio of collagen II positive pellets

	6 day	6 week	1 year
Passage 1	3/3	3/3	1/3
Passage 6	3/3	2/3	0/3

Table 5.1. The ratio of collagen II positive pellets to pellets cultured per group, denoted as x:3, where x is the number of pellets staining positively for collagen II.

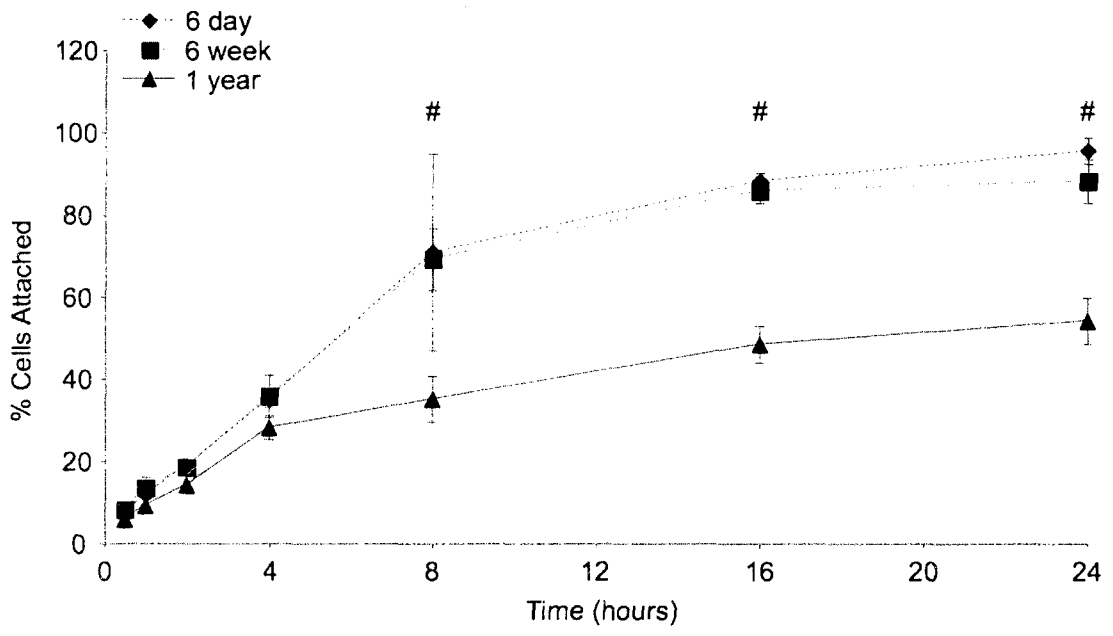

Figure 5.1. BMSC attachment. Results from the 24-hour assessment of BMSC attachment immediately following harvest. The '#' sign indicates significant differences between cells harvested from both 6-day and 6-week-old mice and those harvested from 1-year-old mice. Error bars designate means ± standard deviation (n=3, $p<0.05$).

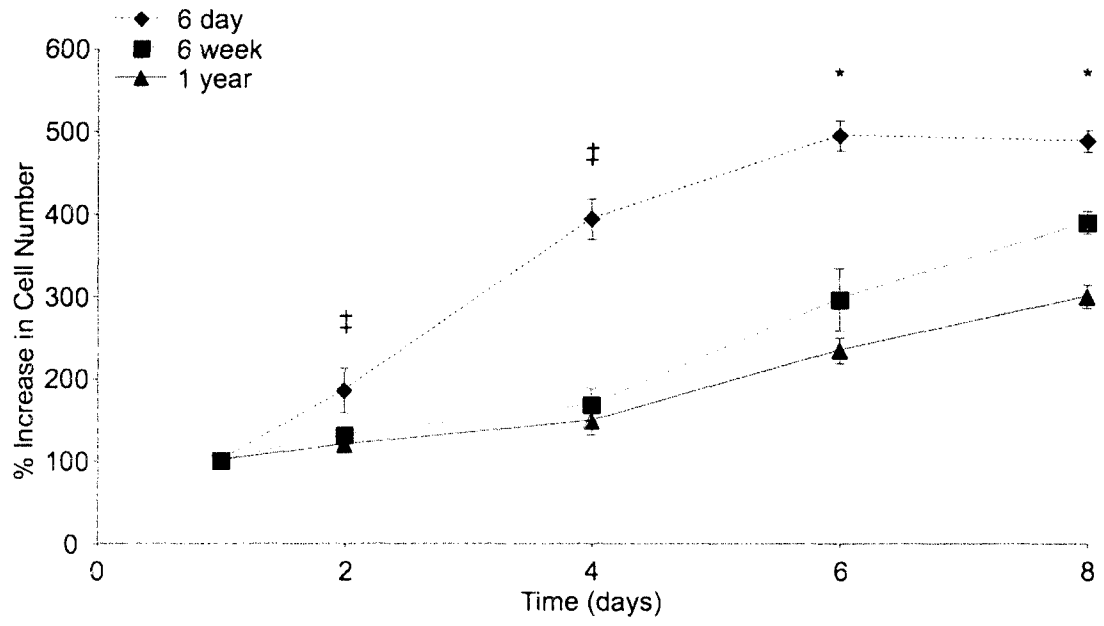

Figure 5.2. BMSC proliferation. Results from the 8-day assessment of BMSC proliferation during primary cell expansion. The '‡' symbol indicates significant differences between cells harvested from 6-day-old mice and all older donors. The '*' symbol indicates significant differences between groups from all donors. Error bars designate means ± standard deviation (n=3, $p<0.05$).

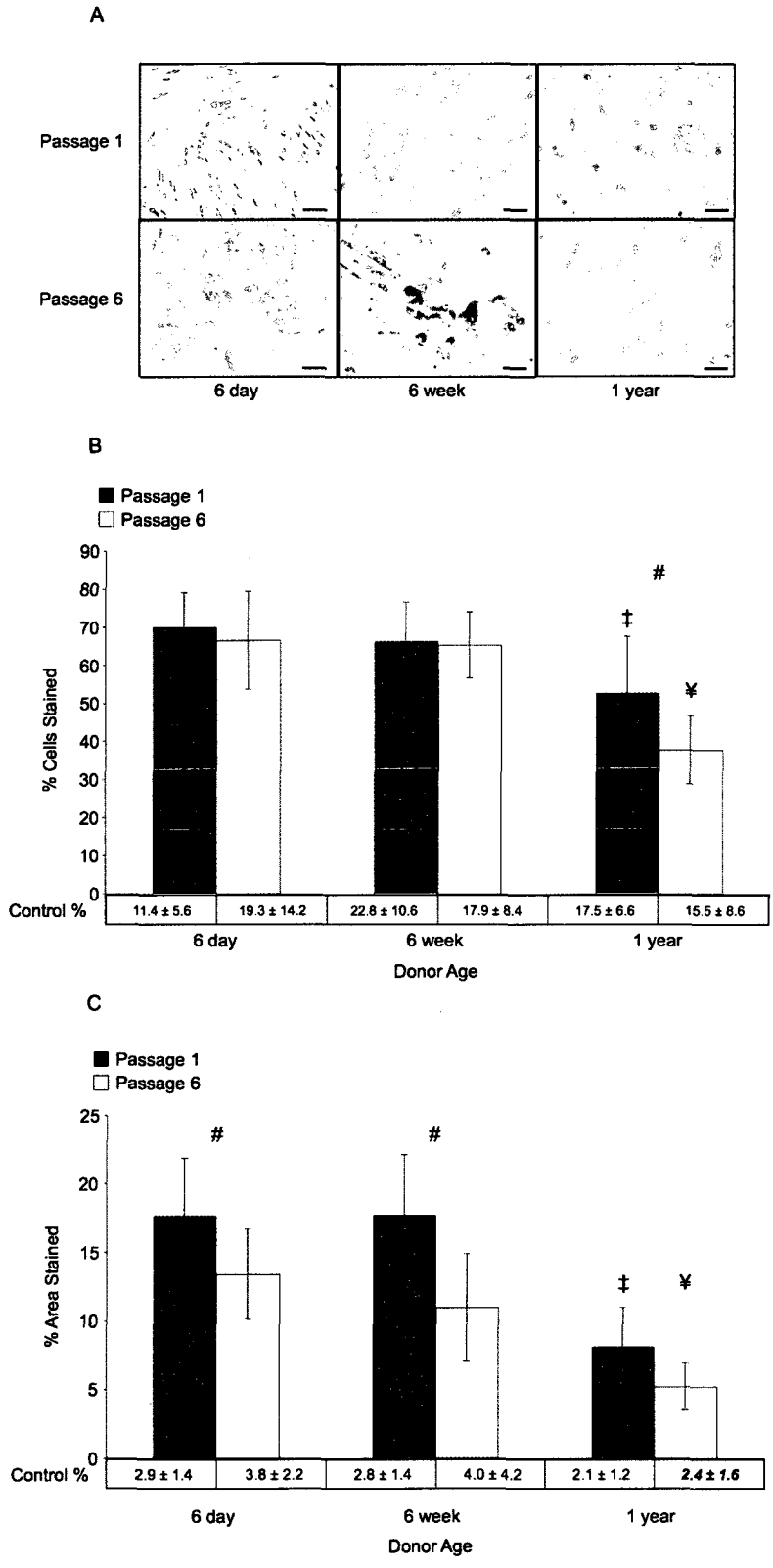
A
Passage 1
Passage 6
6 day
6 week
1 year
B
Passage 1
Passage 6
% Cells Stained
90
80
70
60
50
40
30
20
10
0
#
‡
¥
Control %
11.4 ± 5.6
19.3 ± 14.2
22.8 ± 10.6
17.9 ± 8.4
17.5 ± 6.6
15.5 ± 8.6
6 day
6 week
1 year
Donor Age
C
Passage 1
Passage 6
% Area Stained
25
20
15
10
5
0
#
#
‡
¥
Control %
2.9 ± 1.4
3.8 ± 2.2
2.8 ± 1.4
4.0 ± 4.2
2.1 ± 1.2
2.4 ± 1.6
6 day
6 week
1 year
Donor Age

Figure 5.3. Adipogenic differentiation. Results of adipogenic differentiation after 3 weeks. (*A*) Representative micrographs showing Oil Red O stained lipid inclusions in cultured BMSCs from each experimental group. Magnification bars represent 100 μm in all images. (*B*) Percentage of cells that had intracellular Oil Red O stained inclusions after 3 weeks. Passage related significant difference in staining was only observed in BMSC cultures from 1-year-old donors ($p<0.05$). (*C*) Percentage of total area that was positively stained with Oil Red O. Passage related significant differences were observed for BMSC cultures from 6-day and 6-week-old donors, and age related differences were only observed between 1-year-old donors and the other groups. The '#' sign indicates a significant difference between passage 1 and passage 6 cultures from similarly aged donors, '‡' indicates a significant difference between the indicated group and any passage 1 groups from younger donors, and '¥' indicates a significant difference between the indicated group and any passage 6 groups from younger donors ($p>0.05$). Error bars designate means ± standard deviation (n=6).

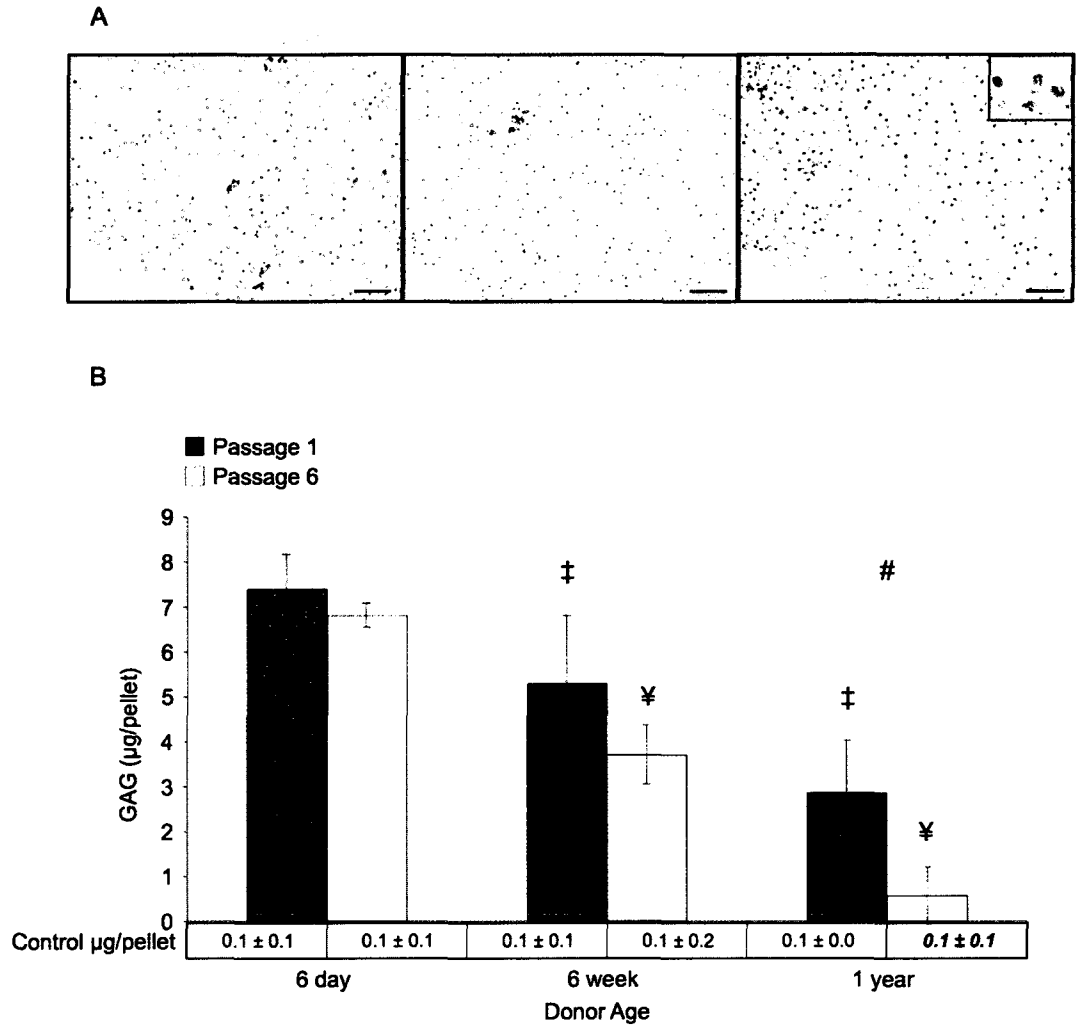

Figure 5.4. Chondrogenic differentiation. Results of chondrogenic differentiation of pelletted micromasses after 3 weeks. (*A*) Representative micrographs of differentiated micromasses from passage 1 cells of 6-day-old donors. Safranin O (*left*), hematoxylin and eosin (*middle*), and immunohistochemical staining for collagen II (*right*) staining were used to show the morphological structure and biochemical components of induced pellets. The inset demonstrates the lacunar morphology typically observed in cartilage. Magnification bars represent 100 µm in all images. (*B*) Micrograms of sulfated GAG per pellet. The '#' sign indicates a significant difference between passage 1 and passage 6 cultures from similarly aged donors, '‡' indicates a significant difference between the indicated group and any passage 1 groups from younger donors, and '¥' indicates a significant difference between the indicated group and any passage 6 groups from younger donors ($p<0.05$). At a constant number of passages, significant differences were found across all age groups. Passage related differences were only significant in BMSCs from 1-year-old donors. Error bars designate means ± standard deviation (n=3).

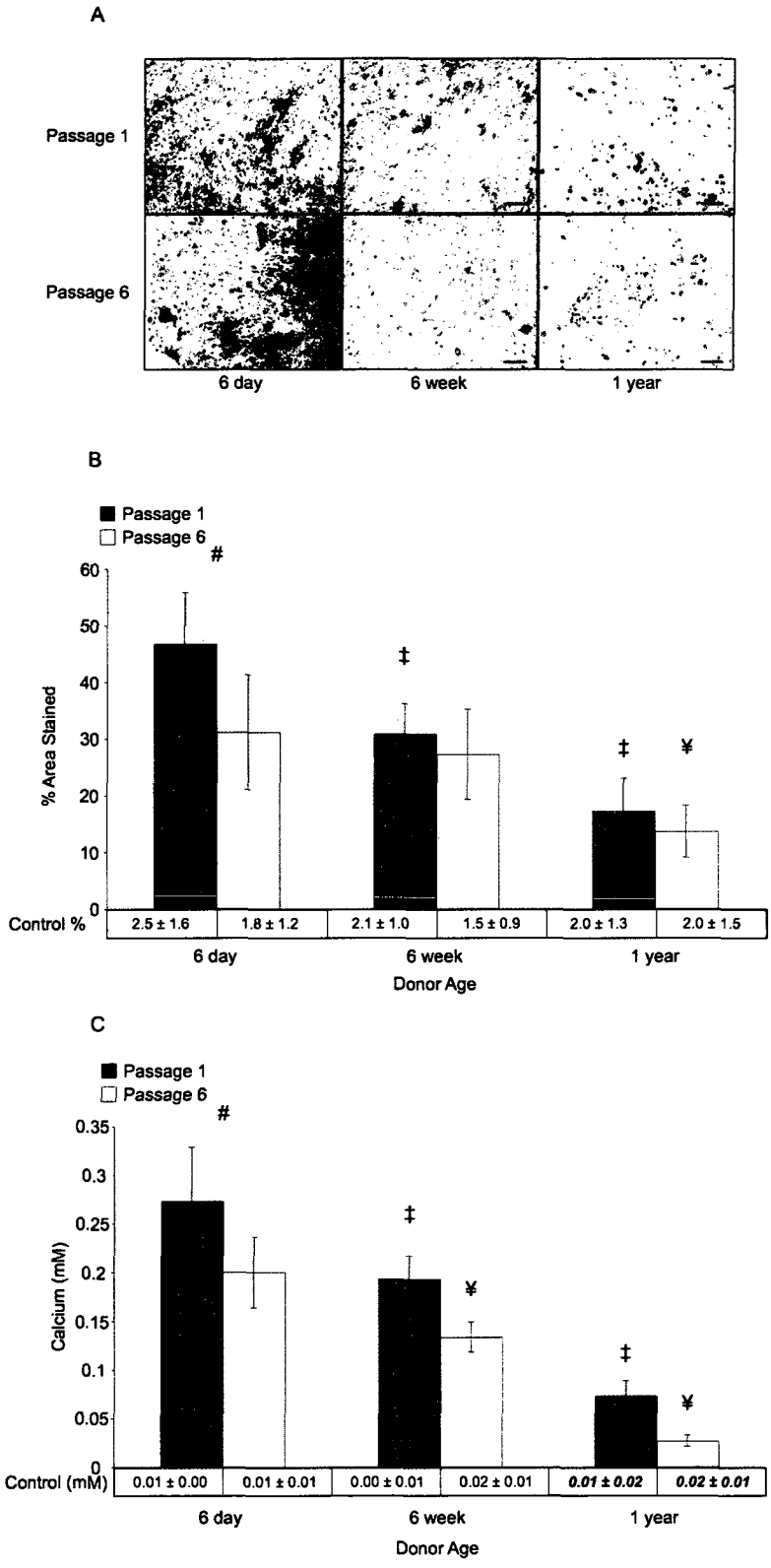
A
Passage 1
Passage 6
6 day
6 week
1 year
B
Passage 1
Passage 6
#
‡
‡
¥
% Area Stained
60
50
40
30
20
10
0
Control %
2.5 ± 1.6
1.8 ± 1.2
2.1 ± 1.0
1.5 ± 0.9
2.0 ± 1.3
2.0 ± 1.5
6 day
6 week
1 year
Donor Age
C
Passage 1
Passage 6
#
‡
¥
‡
¥
Calcium (mM)
0.35
0.3
0.25
0.2
0.15
0.1
0.05
0
Control (mM)
0.01 ± 0.00
0.01 ± 0.01
0.00 ± 0.01
0.02 ± 0.01
0.01 ± 0.02
0.02 ± 0.01
6 day
6 week
1 year
Donor Age

Figure 5.5. Osteogenic differentiation. Results of osteogenic differentiation after 3 weeks. (*A*) Representative micrographs showing Alizarin Red stained mineral deposits on cultured BMSCs from each experimental group. Magnification bars represent 100 μm in all images. (*B*) Percentage of total area viewed that was positively stained with Alizarin Red. (*C*) Quantified calcium cation (mM) determined using a colorimetric calcium assay. For B and C, The '#' sign indicates a significant difference between passage 1 and passage 6 cultures from similarly aged donors, '‡' indicates a significant difference between the indicated group and any passage 1 groups from younger donors, and '¥' indicates a significant difference between the indicated group and any passage 6 groups from younger donors ($p<0.05$). Age-related decreases in staining and calcium were significant across all age groups, and significant passage related decreases were only observed in BMSCs from 6-day-old donors. Error bars designate means ± standard deviation (n=3).

Chapter 6

Uncultured marrow mononuclear cells delivered within fibrin glue to porous scaffolds enhance bone regeneration within critical size rat cranial defects[†]

Abstract

For bone tissue engineering, the benefits of incorporating mesenchymal stem cells (MSCs) into porous scaffolds are well established. There is, however, little consensus on the effects of or need for MSC handling *ex vivo*. Culture and expansion of MSCs adds length, cost, and likely increases risk associated with treatment. We evaluated the effect of using uncultured bone marrow mononuclear cells (bmMNCs) seeded within porous scaffolds to regenerate bone over 12 weeks in an 8 mm diameter, critical size rat cranial defect. A full factorial experimental design was used to evaluate bone formation within poly(L-lactic acid) and corraline hydroxyapatite scaffolds with or without platelet rich plasma (PRP) and bmMNCs. Mechanical push-out testing, microcomputed tomographical (μCT) analyses, and histology were performed. PRP showed no benefit for bone formation. Cell-laden PLLA scaffolds without PRP required

[†] This chapter is in preparation as the following: Kretlow JD, Spicer PP, Picozza E, Kasper FK, Mikos AG. Uncultured marrow mononuclear cells delivered within fibrin glue to porous scaffolds enhance bone regeneration within critical size rat cranial defects. Tissue Engineering 2010.

significantly greater force to displace from surrounding tissues than control (cell-free) scaffolds, but no differences were observed during push out testing of coral scaffolds. For bone volume formation as analyzed by μCT, significant overall effects were observed with bmMNC incorporation. These data suggest that bmMNCs may provide therapeutic advantages in bone tissue engineering applications without the need for culture, expansion, and purification.

Abbreviations

ANOVA	analysis of variance
bmMNC	bone marrow mononuclear cells
BMP-2	bone morphogenetic protein-2
BMP-7	bone morphogenetic protein-7
FDA	Food and Drug Administration (U.S.A.)
H&E	hematoxylin & eosin
MIP	maximum intensity projection
MSC	mesenchymal stem cell
PBS	phosphate buffered saline
PLLA	poly(L-lactic acid)
PRP	platelet rich plasma
TGF-β1	transforming growth factor-β1
β-TCP	β-tricalcium phosphate
μCT	microcomputed tomography

6.1 Introduction

Tissue engineering approaches to regenerating lost or damaged tissues often focus on the use of adult stem cells. Among many available sources, mesenchymal stem cells (MSCs) derived from bone marrow or adipose tissue are commonly used as multipotent autologous cell sources and can be collected through relatively noninvasive methods.[495] A number of studies have demonstrated the advantages of using MSCs for the repair or regeneration of multiple tissue types,[69, 496-502] and multiple clinical trials are underway investigating the use of MSCs for the treatment of both acute and chronic conditions.[503]

Despite many studies establishing the benefits of MSCs, a number of factors remain unaddressed regarding their widespread use. First, there is little to no standardization of MSC harvest, expansion, and characterization,[504-507] and studies suggest that these factors may play a significant role in the success or failure of applications employing these cells.[508-514]

In addition to raising questions about the standardization and optimization of culture techniques, *ex vivo* expansion of autologous MSCs requires a delay between harvest and treatment, a likely increased cost of treatment to the patient, and introduces the risk for contamination or adverse cellular changes related to the expansion.[472, 515, 516] Limited long-term data is available to adequately understand the risks of using culture-expanded MSC in clinical

therapy, and, while early reports are promising,[517] a number of concerns, including those of genomic instability and resultant tumorigenesis, remain.[518-522] Additionally, it is unclear how patient-to-patient variability and changes in cellular function related to age or other demographic factors may impact the use and success of such cell-based therapies.[441, 443, 456, 457, 523-525]

One potential method to avoid many of the problems associated with harvest and subsequent culture of MSCs is to use uncultured cell sources that may contain MSCs. Such an approach greatly diminishes the number and purity of the available multipotent cell population and, in certain cases of cardiovascular repair and regeneration, has been shown to limit the efficacy of cell-based therapies.[526, 527] In contrast, Samdani *et al.* directly compared bone marrow mononuclear cells (bmMNCs) to culture expanded MSCs in a spinal cord injury model and found that bmMNCs offered a greater protective benefit and reduced scar formation relative to MSC treated injuries.[528]

Previous studies in bone and cartilage tissue engineering have shown significant therapeutic benefits associated with the use of uncultured whole bone marrow or bmMNCs.[529-532] The ability to perform the necessary cell harvest and any purification steps perioperatively and the relative ease of clinical translation for these one-step processes were cited as advantages to more commonly investigated techniques involving culture-expanded MSCs.[528, 533] Gan *et al.* found that marrow mononuclear cells enriched perioperatively using a cell processor performed as well as bone grafts in spinal fusion.[533] Muschler *et al.* found similar

results for spinal fusion using a matrix-enrichment procedure to increase bmMNC engraftment.[534] Further supplementing uncultured whole marrow with growth factors such as transforming growth factor-β1 (TGF-β1) has also been shown to have a beneficial effect on healing of critical sized bone defects.[535]

Due to the decreased number of multipotent cells available without *in vitro* expansion and purification and the decreased amount of time available for seeding cell-scaffold constructs during perioperative construct fabrication, cell delivery vehicles have been used to ensure MSC localization to a defect site or within a scaffold. The presence and properties of these delivery vehicles, which are primarily hydrogels such as fibrin glue,[536-538] alginate,[65] hydroxypropylmethylcellulose,[226] and platelet-rich gels,[539] can greatly influence cell survival and differentiation. Catelas *et al.* and Ho *et al.* previously demonstrated the balance between MSC proliferation and differentiation achieved by modulating the fibrinogen concentration within fibrin gels.[281, 282] Similar effects have also been seen in collagen gels.[540]

In the present study, we hypothesized that bone formation within a critical sized defect would be enhanced using uncultured bone marrow mononuclear cells encapsulated in fibrin gels for delivery of the cells within scaffolds made of poly(L-lactic acid) (PLLA) or coralline hydroxyapatite. Platelet rich plasma (PRP) was included for potential growth factor delivery to the encapsulated cells. All materials used were FDA-regulated, and an attempt to minimize processing procedures was made in order to simulate an entire harvest and construct

fabrication protocol that could be reasonably completed over the course of a single operation.

6.2 Materials and Methods

6.2.1 Experimental design

This study used a full factorial design with 3 factors tested at two levels each (scaffold material – coral or PLLA, platelet rich plasma – presence or absence, and uncultured marrow mononuclear cells – presence or absence), resulting in a total of 8 experimental groups. The groups are described in Table 6.1. For each group, a total sample size of 14 was used, with 6 samples per group randomly assigned for mechanical (push-out) testing and the remaining 8 used for microcomputed tomography (μCT) and histology.

6.2.2 Materials

Coralline hydroxyapatite scaffolds (Pro Osteon 200, Interpore Cross International, Irvine, CA) measuring 8 mm in diameter × 2 mm in height and sterilized by gamma irradiation were used as supplied by the manufacturer. Nonwoven PLLA fiber mesh scaffolds (Concordia Medical, Warwick, RI) measuring 8 mm in diameter × 1 mm in height with a volumetric porosity of 90%, 300-500 μm pore sizes, and a 40 μm fiber diameter were sterilized using ethylene oxide and placed in a sterile biosafety cabinet to ventilate for a minimum of 24 hours before use. Fibrin glue (Tisseel^{TM}, Baxter Healthcare Corp., Biosurgery, Bioscience, Westlake Village, CA) consisting of a human fibrinogen

complex (or sealer protein) and human thrombin was used as described below. The fibrinogen complex possibly contains osteogenic growth factors such as TGF-β1 and basic fibroblast growth factor.[282]

6.2.3 Animal use

All animal work was performed in accordance with protocols approved by the Rice University Institutional Animal Care and Use Committee. A total of 134 healthy, male syngeneic Fisher 344 rats (Harlon Bioproducts, Indianapolis, IN) aged 12 weeks old and weighing 225-249 grams were used in this study. Twenty-two rats were used as bone marrow and/or blood donors, and the remaining 112 rats were used in surgery.

6.2.4 PRP harvest and processing

PRP was freshly harvested the day of surgery from donor rats. Rats were euthanized under general anesthesia via CO_2 asphyxiation and upon confirmation of death, a cardiac puncture was performed to withdraw ~5 mL of blood into a sterile syringe containing 500 μL sterile filtered 3.8% sodium citrate (Sigma-Aldrich, St. Louis, MO). Blood from multiple donors was pooled into sterile 15 mL centrifuge tubes (BD Biosciences, Mississauga, ON, Canada) and placed on ice. PRP was isolated using a standard laboratory centrifuge (Precision Durafuge 100, Thermo Fisher Scientific, Waltham, MA) according to a previously established method.[541] Briefly, following centrifugation at 400 × g for 10 minutes with no brake applied, the supernatant was sterilely pipetted to a second sterile centrifuge tube, which was then centrifuged at 800 × g for 10

minutes with a brake applied at the end of the cycle. The supernatant of platelet poor plasma was then removed, and the remaining PRP was returned to ice. Platelet enrichment between peripheral blood and PRP from 8 donor rats was confirmed during a preliminary study using a veterinary hematology analyzer (scil Vet abc, scil animal care company, Gurnee, IL). Prior to use, PRP fibrinogen content was quantified using a spectrophotometric method.[542]

6.2.5 Bone marrow harvest and construct preparation

On the day of surgery, bone marrow was harvested from the long bones of the hind limbs of euthanized donor rats. Under sterile conditions, the femora and tibiae were isolated, stripped of soft tissue, and placed into sterile α-MEM (HyClone Laboratories Inc., Logan, UT). The epiphyses were then removed. Bone marrow was flushed by piercing the diaphyses with a 16-gauge syringe and delivering heparinized phosphate buffered saline (PBS, HyClone Laboratories Inc.). Marrow was disaggregated by serially passaging through 18 followed by 20 gauge syringes. A cell suspension was created by vacuum filtering the marrow through a 100-μm nylon filter (Millipore Corporation, Billerica, MA). Mononuclear cells were then isolated by Ficoll density gradient centrifugation (Accuspin™ System Histopaque®-1077, ρ=1.077 g/mL, Sigma-Aldrich) performed according to the manufacturer's instructions. Cells were washed 3 times and resuspended in sterile Tris-buffered saline (TBS, Sigma-Aldrich) or PRP to a final concentration of 6×10^7 cells/mL.

PLLA and coral scaffolds were prewet in gradient ethanol beginning 24 hours before seeding and/or implantation. Both the fibrinogen complex and thrombin components of the fibrin glue were freshly prepared each morning according to the manufacturer's instructions, and the fibrinogen concentration was verified using the Ellis method.[542] The fibrinogen concentration was diluted with TBS to 102 mg/mL, and the thrombin solution was diluted with 30 mM sterile $CaCl_2$ in TBS to a concentration of 200 IU/mL.

For all experimental groups, 50 μL each of fibrinogen complex and thrombin were delivered to the scaffold, resulting in 100 μL of fibrin glue with final concentrations of 17 mg fibrinogen/mL and 100 IU thrombin/mL. For scaffolds loaded with bmMNCs without PRP, volumes of cells suspended in TBS and fibrinogen complex were added in a 2:1 ratio to a sterile centrifuge tube and vortexed. For scaffolds loaded with PRP, the bmMNC/PRP suspension or PRP alone was added to an equal volume of fibrinogen complex diluted with TBS and vortexed such that the final fibrinogen concentration within the PRP/fibrinogen complex solution was 34 mg/mL. For all experimental groups, after vortexing, 50 μL of the fibrinogen complex solution were then pipetted onto each prewet scaffold within separate wells of an ultra-low attachment 24-well plate (Corning Inc., Corning, NY) that was then placed within a 37°C incubator for 5 minutes to allow the fibrinogen complex to soak the scaffold. After this, 50 μL of thrombin solution were pipetted onto the scaffolds, which were then returned to the incubator for 15 minutes. After 15 minutes, a thin layer of α-MEM was added to

the well to cover the scaffold. Scaffolds were returned to the incubator until implantation.

6.2.6 Animal surgery, euthanasia, and implant harvest

Critical sized, 8 mm diameter defects within the rat calvarium were created under general inhalational anesthesia, filled with freshly prepared implants, closed, and cared for postoperatively as previously described.[19] After 12 postoperative weeks, animals were euthanized according to established and approved methods,[19] and the implants and surrounding tissues were harvested with a high-speed surgical drill (TPS®, Stryker, Kalamazoo, MI) and 701 cutting bur. Prior to harvest, samples were randomly designated for mechanical testing or μCT/histology. After harvest, samples to be mechanically tested were stripped of any extraneous soft tissues superficial or deep to the implant, immediately placed in ice cold PBS, and mechanically tested within 20 minutes. Samples designated for μCT/histology were individually placed in 10% neutral buffered formalin and stored on a shaker table at 4 °C for 72h.

6.2.7 Mechanical push-out testing

Push-out testing was performed to determine the interfacial shear strength of the implanted constructs after 12 weeks. Test were performed on a mechanical testing bench (858 Mini Bionix II, MTS Systems Corp., Eden Prairie, MN) using a custom made push-out and support jigs allowing 1 mm of clearance between the construct and the support jig around the entire circumference of the construct to minimize the effect of the testing jig on the interfacial stress

distribution.[543] Tissue samples were oriented with the construct centered over the support jig, and the push-out jig was applied a vertical force on the constructs at a constant rate of 0.5 mm/min. Testing was stopped after a peak force was reached.

6.2.8 Microcomputed tomography imaging and analysis

Bone volume and extent of bridging within the explanted samples were analyzed by μCT (SkyScan 1172 high-resolution micro-CT, SkyScan, Aartselaar, Belgium) as previously described.[544] For PLLA constructs, lower and upper threshold indices were 70 and 255, respectively. For coral constructs, threshold indices of 90 and 255 were used. For PLLA samples, axial maximum intensity projections (MIPs) were generated, and bony bridging was evaluated by three observers (JDK, PPS, FKK) according to the scoring system described in Table 6.2.

6.2.9 Histological processing

Fixed samples were serially dehydrated in graded ethanol (70-100%). Samples with PLLA constructs were left undecalcified and embedded in methylmethacrylate. Samples with coral constructs were mildly decalcified with EDTA and embedded in methyl methacrylate. Serial 5-μm coronal sections through the center of the construct were then cut using a rotation microtome (Leica) and stained with hematoxylin and eosin (H&E), von Kossa/van Gieson (PLLA constructs only), or Goldner's trichrome according to established methods.

6.2.10 Light microscopy and histological scoring

Stained sections will be analyzed and imaged using a standard light microscope with attached digital camera (Eclipse E600, Nikon Instruments Inc., Melville, NY). Three observers (JDK, PPS, FKK) will evaluate each of the sections according to a previously used scoring system, shown in Table 6.3, for assessing the construct-bone interface and the bone growth within the construct pores.[544]

6.2.11 Statistical analyses

Continuous variable data are represented as means ± standard deviation. Ordinal variables are presented as frequencies. All analyses were performed using R version 2.10.0 (R Foundation for Statistical Computing, Vienna, Austria). The *a priori* defined significance level for all statistical tests was 0.05.

Peak loads obtained from push-out testing and percentage bone volumes were analyzed using two-way analyses of variance (ANOVA, bmMNC × PRP). Post hoc multiple comparisons were made using the step down Holm-Sidak test.[545]

MIP and histology scoring were analyzed using a nonparametric method for analyzing two way ordinal data from factorial experiments.[546, 547] Statistical significance for main effects and interaction were determined using ANOVA-type statistics, and multiple comparisons were made based on estimated 95% confidence intervals.

6.3 Results

6.3.1 PRP processing

Approximately 250 μL of PRP were obtained from 4.5 mL peripheral blood per donor rat. Preliminary studies showed an 8.6 ± 3.2 fold platelet enrichment in the PRP compared to peripheral blood. Fibrinogen concentrations in the PRP were 14.2 ± 4.5 mg/mL. In order to keep the fibrinogen concentration constant in the gel fraction of all constructs, the fibrinogen complex concentration in constructs with PRP was slightly lower than in those without.

6.3.2 Construct fabrication and animal surgeries

Constructs were successfully fabricated, with each construct containing 100 μL of gel with, where appropriate, 1.5×10^6 bmMNCs/scaffold, 17 mg/mL fibrinogen and 100 IU/mL thrombin within the gel, and 25 μL PRP. Gel was well formed within the pores of the scaffolds approximately 1 minute after the addition of thrombin.

One animal died intraoperatively and was replaced prior to the completion of the study. All other animals survived the surgery and postoperative period without complications. At the time of euthanasia and sample harvest, there were no signs of gross infection or adverse tissue response surrounding the implants.

6.3.3 Mechanical push-out testing

Push-out testing results in the form of peak loads are shown in Figure 6.1. Due to differences in the Young's moduli of the scaffold materials, direct

comparisons between coral and PLLA constructs cannot be made.[543] For the PLLA constructs, the group containing only bmMNCs (P-M) required significantly more force to displace the construct than the control (P--) constructs. Among the PLLA constructs, no other significant differences were found. Overall, the presence of bmMNCs had a significant effect on the push-out force ($p < 0.005$), while PRP and the interaction of PRP and bmMNCs were not significant.

No significant differences in push-out strength were found for the coral constructs. The overall effect of bmMNCs seeded onto the scaffolds, the presence of PRP, and any interaction between these factors were also insignificant.

6.3.4 Microcomputed tomography analysis

Results from μCT imaging were analyzed to determine the volume percentage of regenerated bone within the constructs (Figure 6.2). For PLLA constructs, significant differences in bone formation again existed only between the control constructs and the group containing only bmMNCs (P-M). For coral constructs, no significant differences were present in pairwise comparisons; however, for both PLLA and coral constructs, the addition of bmMNCs had a significant overall effect on bone formation. The effect of PRP and the interaction of PRP and bmMNCs were not significant for both types of constructs.

Bony bridging across defects filled with PLLA constructs was evaluated by scoring MIPs as shown in Figure 6.3. Again, the presence of bmMNCs had a significant effect on bony bridging, but the effect of PRP and the interaction of

PRP with bmMNCs were not significant. Pairwise comparisons found the observed bridging between both groups containing bmMNCs (P-M, PPM) to be significantly different from both groups without bmMNCs (P--, PP-). Complete bridging through the midline of the defect was only observed in one sample from group PPM.

6.3.5 Histology

Representative histological samples are shown in Figure 6.4.

6.4 Discussion

To facilitate the translation of many tissue engineering technologies for clinical use, standardization or simplification of the approaches taken is necessary.[486] In the present study, we hypothesized that a process which could be completely performed over the course of a single surgical intervention could be developed incorporating uncultured bmMNCs within FDA-regulated materials for enhanced bone formation within a critical sized rat cranial defect. For many of the analyses used, this was indeed the case. Uncultured bmMNCs encapsulated within a fibrin gel inside the pores of PLLA scaffolds regenerated significantly more bone within the defect, achieved greater bony bridging of the defect, and were better incorporated into the cranium as measured by mechanical testing than were cell-free controls.

When comparing cell-laden and cell-free coral constructs, the results were not as clear. The presence of bmMNCs did not significantly increase the bone

formation within the scaffolds as detected by μCT, and the peak force needed to display the cellular constructs was smaller than that needed to displace the cell-free scaffolds, although not significantly so. The presence of platelet rich plasma had no effect on bone formation regardless of scaffold material or whether bmMNCs were also present.

Scaffold material played an obvious role in bone formation, mechanical integrity of the implanted constructs, and the effect of bmMNC incorporation. PLLA was chosen as a polymeric scaffold due to its regulatory status, long-term maintenance of mechanical properties, and because MSCs have previously been demonstrated to differentiate well on PLLA fiber meshes.[548] Polymeric fiber meshes with similar fiber diameters and densities have previously been used to characterize the effect of MSC culture and differentiation in the rat cranial defect.[549]

Coralline HA bone grafts have long been used both in research and clinical applications.[549] In this study, bone formation in coral scaffolds was not significantly different across groups; however, for μCT analysis of bone formation there was an overall significant effect of bmMNC incorporation. This result was somewhat surprising, as previous work has demonstrated MSC osteogenic differentiation and ingrowth on similar scaffolds.[550-552] Although reports showing little to no osteogenesis on coralline HA scaffolds do exist,[553] bony ingrowth did occur in all of the tested formulations using coral.

The use of PRP did not significantly affect bone formation in this study. This result is similar to those reported elsewhere in rats,[554] although there are multiple reports in humans[555] and animals[556], including rats,[557, 558] enhancing bone formation. Still, evaluating the efficacy of PRP remains complicated. PRP in combination with uncultured bmMNCs has been found to increase bone regeneration in humans,[559] and rat PRP gels have similarly been shown to increase *in vitro* osteogenic differentiation of rat MSCs.[560, 561] Other studies have shown that PRP does not increase *in vitro* or *in vivo* differentiation of rat MSCs when compared with the effect of growth factors such as bone morphogenetic protein-7 (BMP-7)[562] and was found to inhibit MSC differentiation in a study comparing PRP and bone morphogenetic protein-2 (BMP-2).[563]

A number of considerations regarding the variability and evaluation of PRP must be factored in when analyzing the discordant results for PRP use found in the literature. First, processing techniques, donor factors, and overall platelet enrichment play a significant role in the determining the actual composition of any PRP.[564-569] Furthermore, there is an established interspecies variation in the growth factors contained in and osteogenic capability of PRP, with human PRP having higher growth factor concentrations and eliciting an increased osteogenic response compared to rat or goat PRP.[561, 570] Additionally, PRP effectiveness may in part be modulated by scaffold and cell differentiation state for applications involving cell-laden constructs.[571, 572] Kasten *et al.* found that PRP increased

alkaline phosphatase activity in undifferentiated MSCs but not in those precultured in osteogenic media.[571]

The present study had a number of strengths. First, it further establishes the utility of uncultured bmMNCs in bone formation, including demonstrating a mechanical benefit for cell-laden PLLA scaffolds. Additionally, the study uses only commercially available materials that have already been approved for clinical use, meaning other parameters, such as the explicit role of fibrin glue in cell delivery, the relative effect of culture and expansion of bmMNCs on bone formation, and optimal seeding densities can be explored with minimal variability in the substrate materials. This may also allow for more rapid clinical evaluation of the results. The effect of the scaffold on bone formation using PRP and bmMNCs was also demonstrated by the difference in results for PLLA and coral constructs. Finally, mechanical effects of substrate stiffness were carefully controlled by maintaining a constant fibrinogen concentration across samples, thus any effect seen for PRP addition would have likely been based on bioactive factor delivery.

The primary weaknesses of the present study lie primarily in scope, and thus future studies are necessary to draw more definitive conclusions from the current study. As mentioned in the previous paragraph, future studies are needed to determine whether the benefits of using a simplified process that can be performed over the course of a single operation outweigh any benefits that may exist with MSC expansion and culture. Similarly, future studies should

incorporate more time points to determine if there are any temporal effects of PRP addition. Finally, more sophisticated analyses should be done to determine the role of the delivered bmMNCs in bone formation, as the ability of a seeded cell population to recruit host osteoprogenitors may be more important for bone regeneration than the regenerative capability of the seeded cells.[573]

A number of interesting results were found in this study. First, bmMNCs increased bone formation and construct incorporation for PLLA scaffolds but the benefit in coral scaffolds was not clear. For mechanical testing of coral constructs, bmMNC incorporation within scaffolds did not provide a significant change in implant mechanical properties, although a significant overall effect was found for μCT analysis. In a similar study by Le Nihouannen *et al.*, fibrin glue and granules of 60/40 HA/β-tri-calcium phosphate (β-TCP) cement were mixed with and without freshly isolated bone marrow and placed within defects in rabbit femora.[574] After 12 weeks, there was no difference in bone formation within the defects as detected by μCT. Ueno *et al.* did, however, demonstrate bone regeneration in rat calvarial defects filled with β-TCP granules and whole marrow.[575] Similarly, Becker *et al.* compared bone marrow and concentrated bmMNC seeding on β-TCP scaffolds and found that constructs seeded with bone marrow induced significantly more bone regeneration than those with bmMNCs, which were not statistically different from controls.[576]

Based on these studies, whole marrow may be a better cell source for scaffolds where significant adsorption of potentially osteogenic proteins from the

acellular marrow fraction may occur. Additionally, bone formation within the coral scaffolds was similar to that of PLLA scaffolds, but not significant when analyzed by pairs, when the object volume of control (unimplanted) coral scaffolds was not considered (Figure 6.5). Since the coral scaffolds cannot be differentiated from newly regenerated bone by μCT, variability in scaffold volume may have masked any effect of differences between the experimental groups. Furthermore, we noticed bone resorption around some of the coral scaffolds during μCT imaging. Although the resorption did not vary between groups as determined by imaging and quantifying the bone around the border of the scaffolds (Figure 6.6), this resorption likely affected the relatively high variability of the mechanical testing results.

The use of fibrin glue may also have confounded the findings with respect to PRP use. Platelet enriched fibrin glue has been shown to be an effective substrate for bone-tissue engineering applications both in the presence and absence of encapsulated MSCs.[577, 578] Ito *et al.* showed an increase in bone regeneration in a canine mandibular defect using MSC/PRP/fibrin glue hybrid constructs compared to MSC/fibrin glue constructs alone after 4 and 8 weeks;[579] however, other studies have reported no benefit to similar hybrid constructs.[580] Fibrin glue encapsulation alone likely imparts a benefit in the delivery and retention and cells within the scaffold or defect.[536, 581, 582] In previous studies demonstrating a benefit for PRP and MSCs in combination but not in comparison with other delivery methods or encapsulation substrates,[357, 583] the benefit may

be due in large part to the role of the PRP as a delivery vehicle for the MSCs,[584] given the otherwise short term survival of seeded MSCs.[585]

The need for a cell delivery vehicle may be dependent on the type of scaffold used; in a study by Haasper *et al.*, no benefit of cellular delivery by fibrin glue to scaffolds to which cells adhere more efficiently, such as bone matrix, has been demonstrated.[586] Fibrin glue may still play an important role in applications where bioactive factor delivery is appropriate and controllable and easily tuned release kinetics are desired.[587-589]

Because previous experiments have explicitly established that the fibrinogen concentration within the fibrin glue affects MSC differentiation and proliferation,[281, 282] an intermediate fibrinogen concentration (17 mg/mL), close to reported optimal values,[280] was selected in order to allow cells to proliferate while still providing some substrate stiffness. In constructs with PRP, the amount of fibrinogen complex incorporated into the final glue was reduced in order to keep the fibrinogen concentration constant. Because the fibrinogen complex may also contain growth factors, this reduction in concentration may have offset any benefits of growth factor delivery by PRP.

6.5 Conclusions

The many emerging technologies in tissue engineering provide a number of options and important considerations for researchers and clinicians. Efficacy, cost, and risk must be assessed, and researchers focused on quickly translating technologies must weigh regulatory pathways as well. The present study

characterized scaffold, uncultured bmMNC, and PRP combinations to determine their relative effectiveness in regenerating bone within a critical sized rat cranial defect. PLLA scaffolds laden with bmMNCs delivered within fibrin glue regenerated significantly greater bone than control groups. Cells seeded on coral scaffolds had no significant effect on bone formation. PRP was not found to have a benefit in any formulation. Taken in the context of previous reports in the literature, these results provide further indication that a complex interplay occurs between scaffolds, cells, growth factors, and the host environment. A translational approach employing freshly harvested bmMNCs is likely beneficial compared to a strictly biomaterials-based approach in some cases; however, further work is needed to better understand when such an approach is warranted.

6.6 Figures

Table 6.1 Experimental groups tested

Designation	Scaffold material	PRP	bmMNC
P--	PLLA	-	-
PP-	PLLA	+	-
P-M	PLLA	-	+
PPM	PLLA	+	+
C--	Coral	-	-
CP-	Coral	+	-
C-M	Coral	-	+
CPM	Coral	+	+

Key: PRP=platelet rich plasma, bmMNC=bone marrow mononuclear cell, PLLA= poly(L-lactic acid)

Table 6.2. Scoring Guide for Bony Bridging and Union Using Maximum Intensity Projections from Microcomputed Tomography

Description	Score
Bony bridging over entire span of defect at longest point (8 mm)	4
Bony bridging over partial length of defect	3
Bony bridging only at defect borders	2
Few bony spicules dispersed throughout defect	1
No bone formation within defect	0

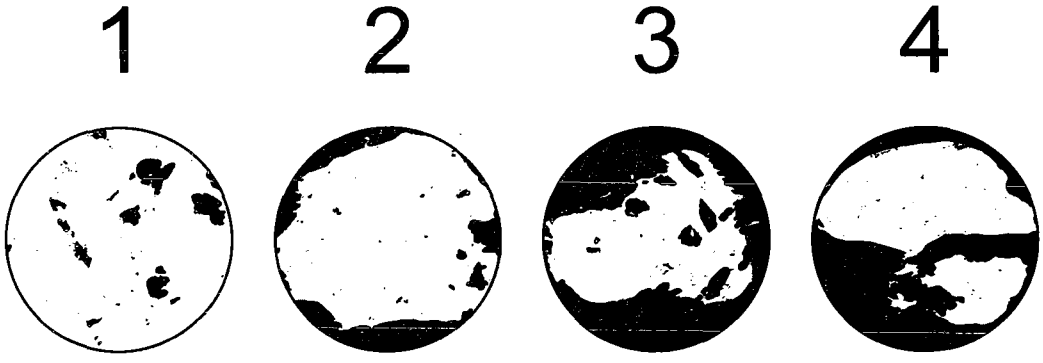

Table 6.3. Quantitative histological scoring parameters

Description	Score
Hard tissue response at scaffold–bone interface	
Direct bone to implant contact without soft interlayer	4
Remodeling lacuna with osteoblasts and/or osteoclasts at surface	3
Majority of implant is surrounded by fibrous tissue capsule	2
Unorganized fibrous tissue (majority of tissue is not arranged as capsule)	1
Inflammation marked by an abundance of inflammatory cells and poorly organized tissue	0
Hard tissue response within the pores of the scaffold	
Tissue in pores is mostly bone	4
Tissue in pores consists of some bone within mature, dense fibrous tissue and/or a few inflammatory response elements	3
Tissue in pores is mostly immature fibrous tissue (with or without bone) with blood vessels and young fibroblasts invading the space with few macrophages present	2
Tissue in pores consists mostly of inflammatory cells and connective tissue components in between (with or without bone) OR the majority of the pores are empty or filled with fluid	1
Tissue in pores is dense and exclusively of inflammatory type (no bone present)	0

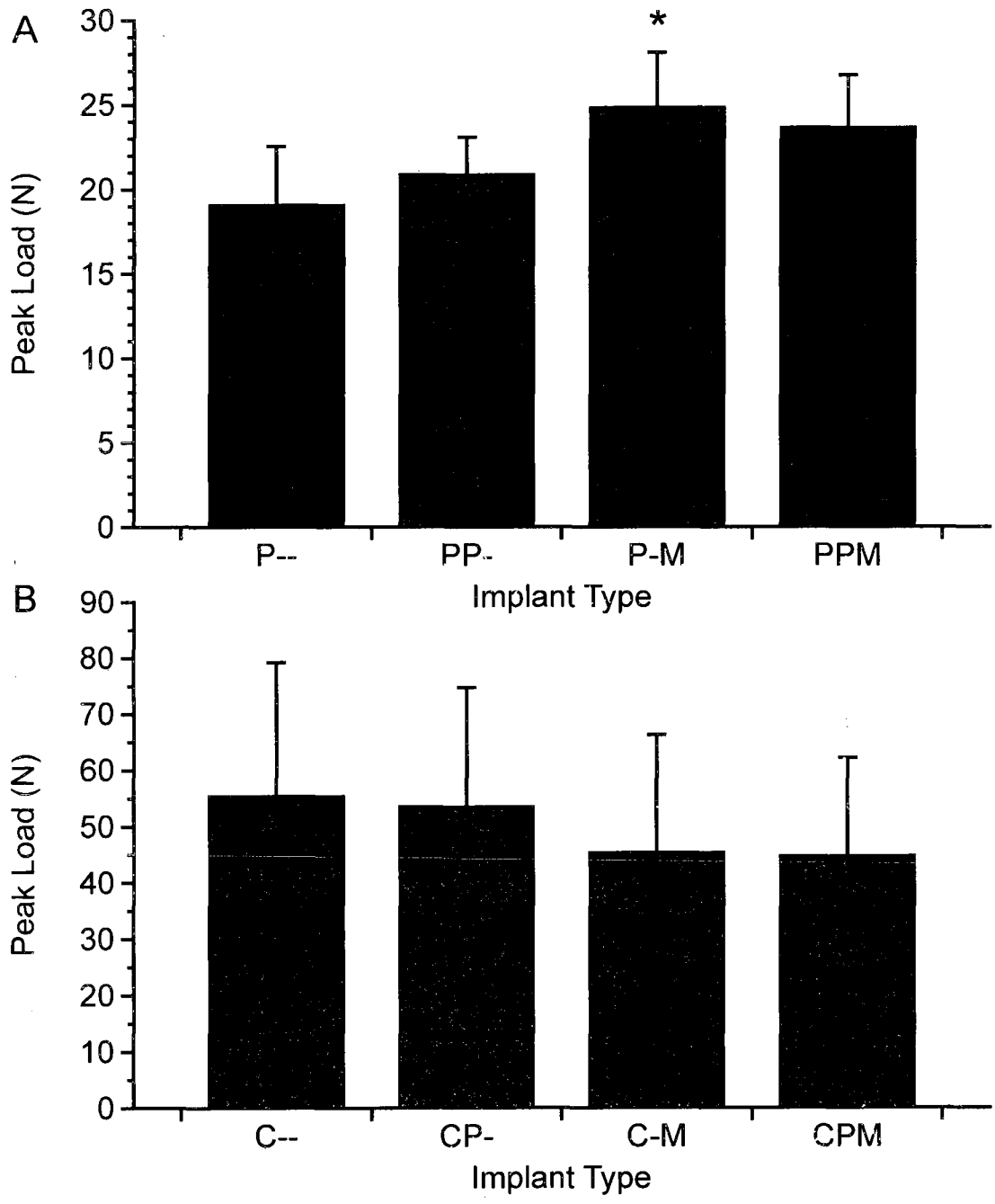

Figure 6.1. Results of mechanical push-out testing. Immediately after harvest, constructs were placed on a custom testing jig and a vertical force was applied. The peak load required to displace the implants from the surrounding tissues was recorded for both PLLA constructs (A) and coral constructs (B). Data are reported as mean ± standard deviation (n=6). Statistical significance between groups and the corresponding control is denoted by *.

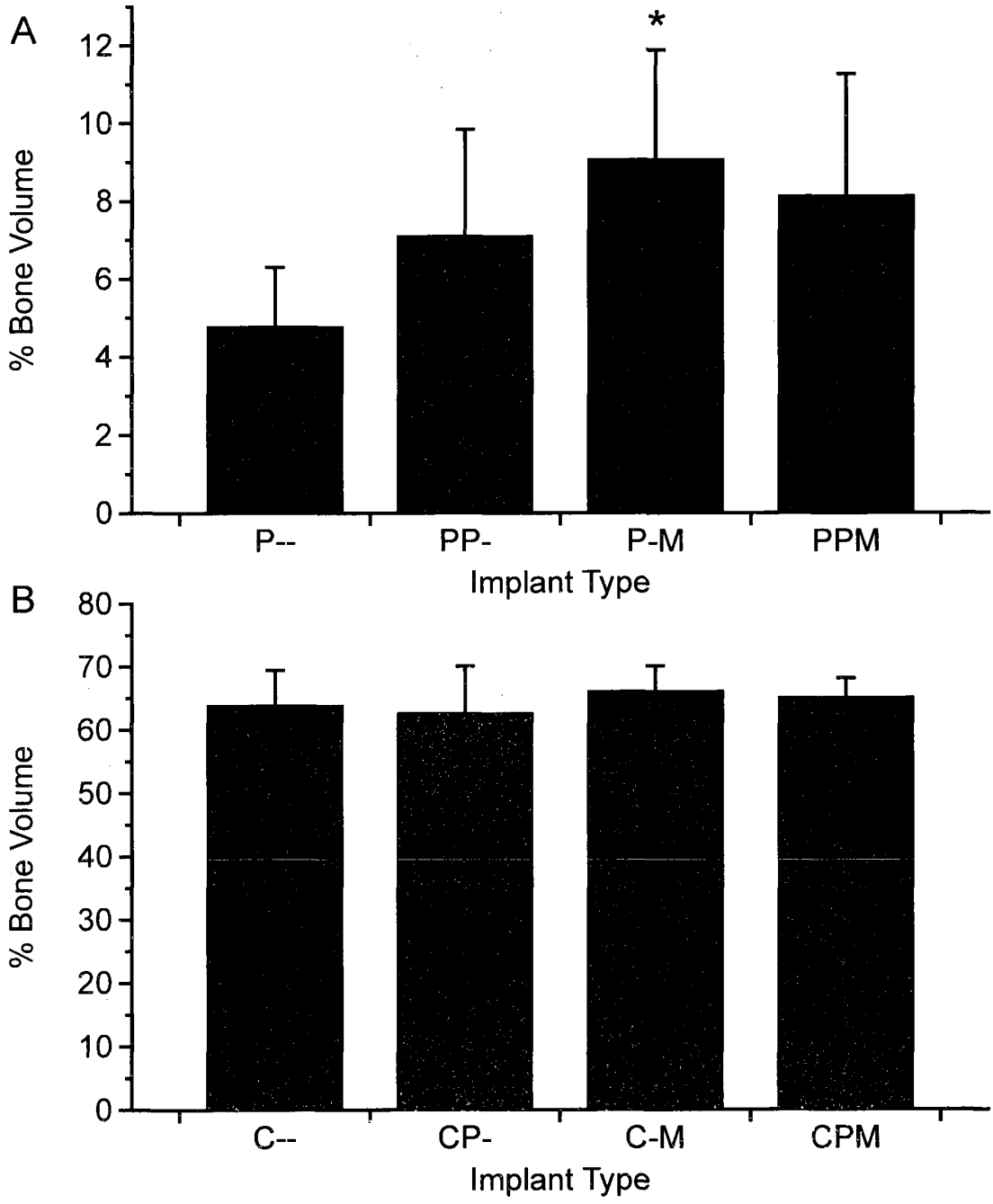

Figure 6.2. Percent object volume of bone formation within the cranial defect. Explanted constructs and surrounding tissues were scanned by μCT and analyzed to determine the percentage of volume within the defect space occupied by mineralized tissue for both PLLA constructs (A) and coral constructs (B). The reported values for the coral constructs include the volume of the scaffold. Data are reported as mean ± standard deviation (n=8). Statistical significance between groups and the corresponding control is denoted by *.

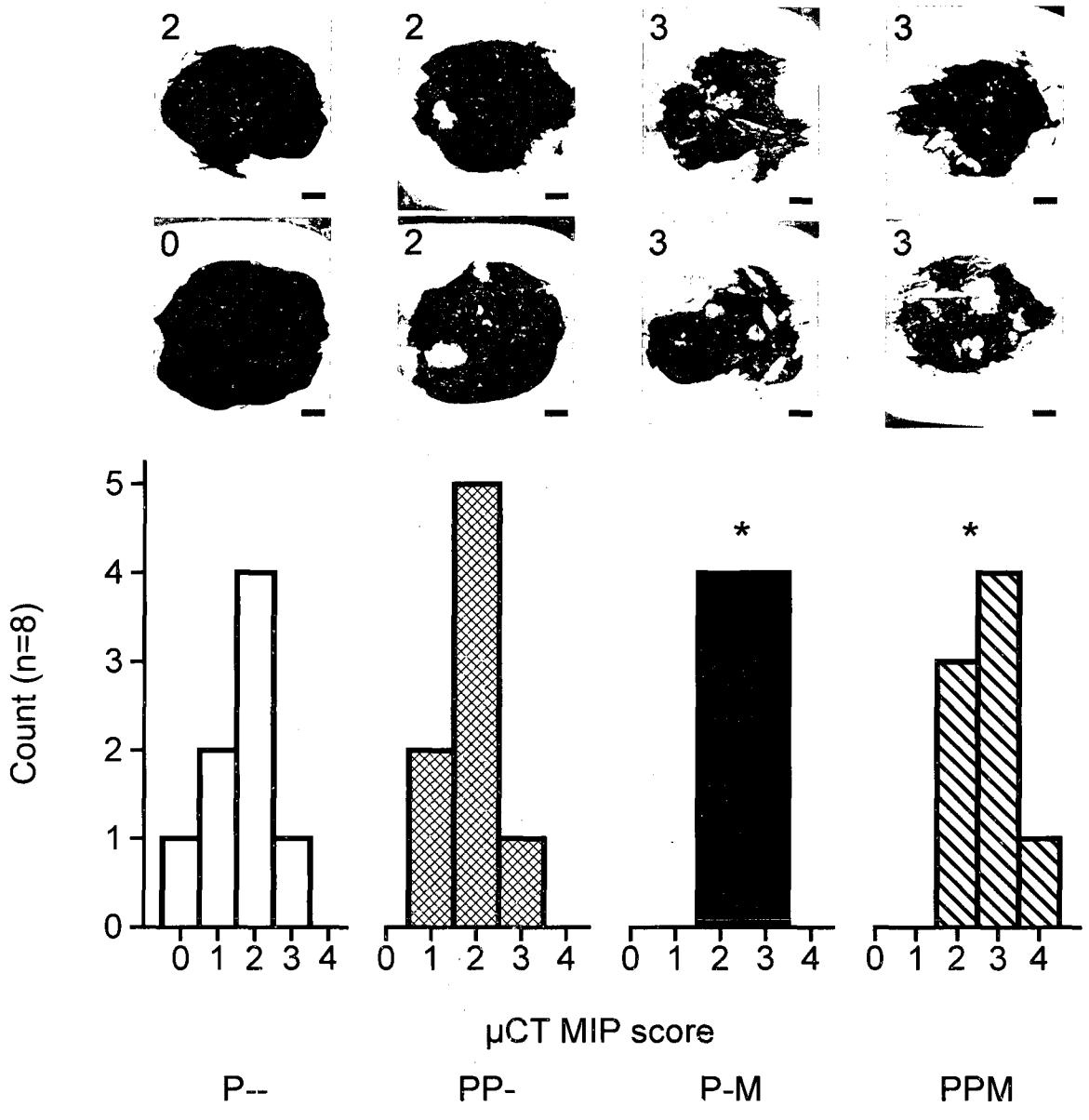

Figure 6.3. Scores of bony bridging across the cranial defects. Explanted PLLA constructs were scored by 3 observers for according to the criteria in Table 6.2. Histograms of the scores are reported for each type of construct, and significant differences between construct scores and the control (P--) score are denoted by *. Images depict representative MIPs along with the corresponding score assigned to these samples (upper left corner of each image). Scale bars (lower right corners) indicate 1 mm.

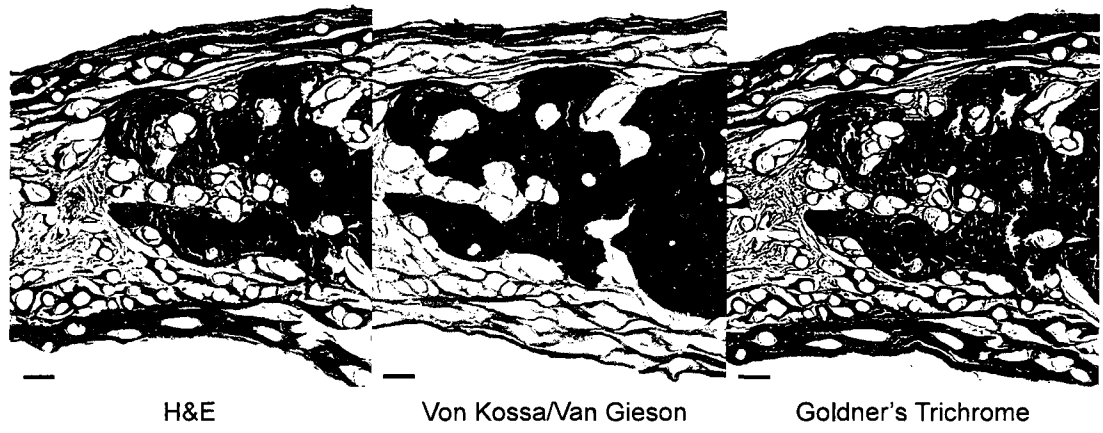

Figure 6.4. Representative histological sections demonstrating the three types of staining used. Scale bars represent 100 μm.

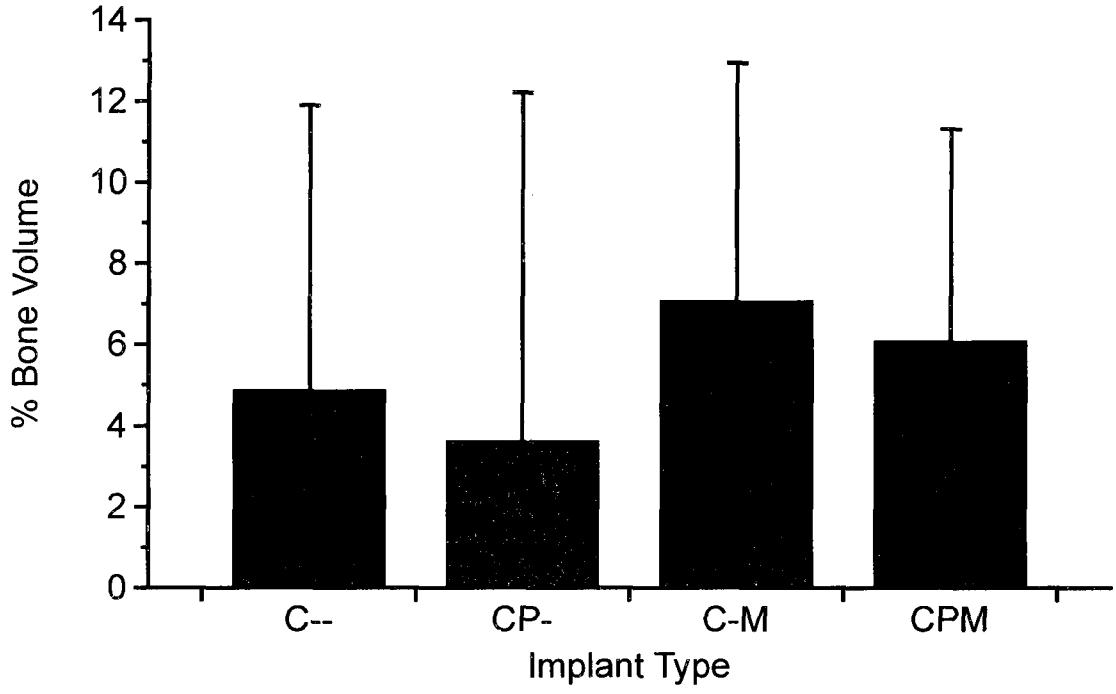

Figure 6.5. Average volume of regenerated bone within coral scaffolds. The average volume of unimplanted coral scaffolds (n=10, mean volume 70.89 ± 4.79 %) was subtracted from the volume of explanted samples (n=8), leaving an estimate of the bone regeneration within each coral construct. Data shown are means ± adjusted standard deviations.

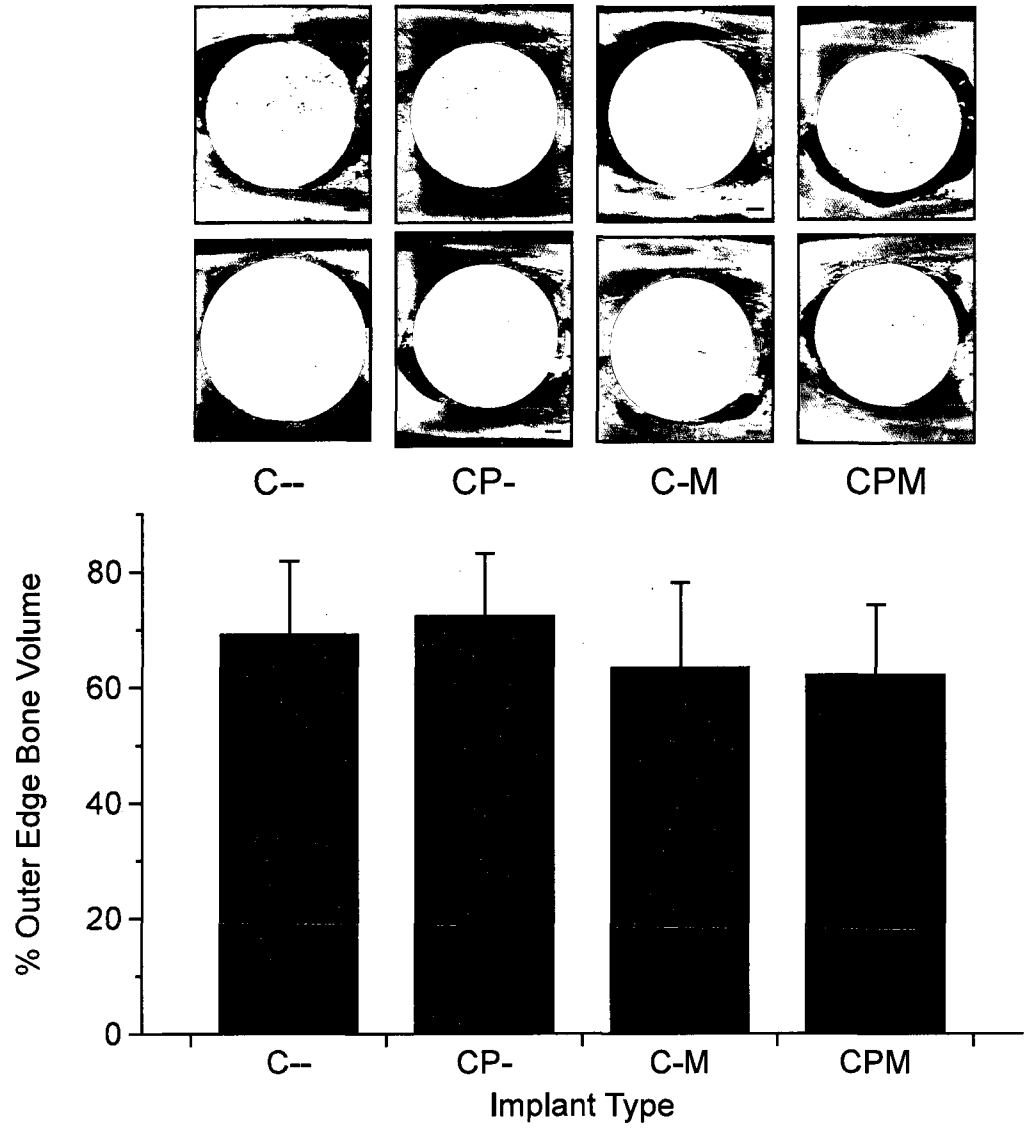

Figure 6.6. Bone growth or resorption around the outer volume of the coral constructs was quantified. Representative images (top) denote with false coloring the border where bone was quantified around the defect. Scale bars represent 1 mm. The figure (bottom) shows the average percent bone volume present in the outer ring (n=8, error bars = standard deviation). No significant differences were found.

Chapter 7

Porous Poly(methyl methacrylate) space maintainers promote soft tissue coverage of clean/contaminated alveolar bone defects[†]

Abstract

Current treatment of traumatic craniofacial injuries often involves early free tissue transfer, even if the recipient site is contaminated or lacks soft tissue coverage. There are no current tissue engineering strategies to definitively regenerate tissues in such an environment at an early time point. For a tissue engineering approach to be employed in the treatment of such injuries, a two-stage approach could potentially be used. The present study describes the fabrication, characterization and processing of porous polymethylmethacrylate (PMMA) space maintainers for temporary retention of space in bony craniofacial defects. Carboxymethylcellulose (CMC) hydrogels were used as a porogen. Implants with controlled porosity and pore interconnectivity were fabricated by varying the ratio of hydrogel:polymer and the amount of CMC within the hydrogel. The *in vivo* tissue response to the implants was observed 12 weeks after placement within a non-healing rabbit mandibular defect that included an oral

[†] This chapter has been submitted as the following: Kretlow JD, Shi M, Young S, Spicer PP, Demian N, Jansen JA, Wong ME, Kasper, FK Mikos AG. Evaluation of soft tissue coverage over porous poly(methyl methacrylate) space maintainers within non-healing alveolar bone defects. Tissue Engineering, Part C: Methods 2010.

mucosal defect to allow open communication between the oral cavity and the mandibular defect. Oral mucosal wound healing was complete at 12 weeks over 3/6 defects filled with solid PMMA implants and 5/6 defects filled with either a low or high porosity PMMA implant. The tissue response around and within the pores of the two formulations of porous implants tested *in vivo* was characterized, with the low porosity implants surrounded by a minimal but well formed fibrous capsule in contrast to the high porosity implants, which were surrounded and invaded by almost exclusively inflammatory tissue. Based on these results, PMMA implants with limited porosity hold promise for temporary implantation and space maintenance within clean/contaminated bone defects.

Abbreviations

ANOVA	analysis of variance
CMC	carboxymethylcellulose
FDA	United States Food & Drug Administration
MMA	methyl methacrylate
PMMA	poly(methyl methacrylate)
SEM	scanning electron microscopy
μCT	microcomputed tomography

7.1 Introduction

The incidence of traumatic facial injuries relative to injuries at other anatomic locations has risen sharply during combat operations in Iraq and Afghanistan compared to previous military conflicts.[590] The predominant cause of these wounds is improvised explosive devices, which often cause extensive damage to bone and soft tissues.[591] Similarly, combat related ballistic injuries often involve high velocity projectiles that cause significant and widespread damage to multiple types of tissue.[592]

Even in the civilian population, traumatic craniofacial bone injury is often accompanied by injury or loss of surrounding soft tissues.[593] One of the major difficulties reconstructive surgeons face when treating injuries involving significant bone loss is contracture and scarring of the overlying soft tissue envelope, which compromises facial projection and makes staged repair of bony structures difficult.[594, 595] Previously, definitive bone reconstruction was delayed until soft tissue coverage and a sterile wound environment were achieved.[596, 597] More recently, despite reports of local complications and wound infection rates as high as 100% in civilians suffering gunshot wounds to the face,[598, 599] early definitive repair of facial gunshot wounds via free tissue transfer has become common as the well vascularized tissues that are transferred survive well in hostile wound environments.[597, 600]

The field of regenerative medicine and the technologies borne from tissue engineering offer great hope towards providing an alternative and possibly better

approach to regenerating injured or destroyed tissues. Most proposed tissue engineering strategies, however, currently require planning in the form of material fabrication, autologous cell harvest and expansion, and/or *ex vivo* tissue generation. Additionally, little to no evaluation of tissue engineering approaches is currently performed in wound environments involving infection, significant vascular injury, and large-scale tissue devitalization such as that encountered in a battlefield wound. Therefore, the successful use of a tissue engineering approach to provide immediate, definitive regeneration of tissues injured during craniofacial trauma such as those encountered during military service is unlikely using current approaches.

In the absence of immediate reconstruction, clinical management of facial bone loss can involve the placement of an alloplastic space maintainer to provide a template for future definitive reconstruction and prevent wound contracture into the space normally occupied by bone.[601] Poly(methyl methacrylate) (PMMA), is commonly used in such space maintenance applications[601, 602] and others within the craniofacial complex.[603] Although PMMA has many desirable characteristics for such applications (moldable, FDA-regulated, familiar to surgeons), a number of problems exist with respect to wound healing around PMMA implants and other alloplastic craniofacial implants.[604-606]

For the purposes of facilitating a long-term tissue engineering approach to treating composite craniofacial defects, a temporary implant or space maintainer would allow time for a regenerative medicine approach to be used to definitively

regenerate the injured or absent tissue. In addition to providing space maintenance, such a temporary implant could be used to "prime" the defect site, enabling better long-term success of the definitive regenerated tissue construct. Previous work has shown that recipient site characteristics such as vascularity are important for the regeneration of new bone tissue and support of grafted tissue.[607, 608] For mandibular reconstruction, the defect site and surgical approach along with recipient site complications such as infection, intraoral exposure, and prolonged antibiotic use have been significantly linked to graft failure.[609, 610] An ideal temporary space maintainer will therefore not only maintain the osseous void and prevent soft tissue collapse or contracture into the space but also will allow or promote soft tissue coverage and healing without serving as a nidus for local infections.

Despite the aforementioned shortcomings associated with solid PMMA implants, we hypothesized that an implant made of modified PMMA could fulfill many of these criteria. Previously, a number of groups have explored different methods for making porous PMMA.[611-616] Based on this work, we hypothesized that porous PMMA implants with reproducibly tunable pore structure could be fabricated using a carboxymethylcellulose (CMC) hydrogel as an aqueous porogen. When tested in a clean/contaminated rabbit mandibular defect, we hypothesized these implants would be able to maintain the defect space while promoting soft tissue coverage of the implant.

7.2 Materials and Methods

7.2.1 Experimental design

For the first part of this study, porous PMMA implants were synthesized and characterized using a CMC hydrogel as an aqueous phase to impart porosity on the implants. The percent of CMC in the aqueous phase and the ratio of aqueous phase:polymer phase were varied in order to control the bulk and surface characteristics. Following characterization of the porous implants, two formulations, one with high bulk porosity and pore interconnectivity and one with lower porosity and less pore interconnectivity, were compared over 12 weeks *in vivo* to a solid PMMA implant within a modified rabbit mandibular defect.

7.2.2 Implant fabrication and characterization

Solid and porous PMMA implants were fabricated using a clinical grade PMMA bone cement (SmartSet High Viscosity, DePuy Orthopaedics, Warsaw, IN) consisting of a powder of methyl methacrylate / methyl acrylate copolymer, benzoyl peroxide, and zirconium dioxide and a liquid phase with methyl methacrylate (MMA), N,N-dimethyl-*p*-toluidine, and hydroquinone. For the solid implants, the solid and powder phases were mixed according the manufacturer's specifications for approximately 90 seconds and, once they reached a dough-like consistency, packed into 10 mm diameter × 6 mm height cylindrical Teflon® molds. The solid implants were then allowed to harden at room temperature for 30 minutes before being removed from the molds and vacuum-dried overnight.

For porous implants, 7 wt% and 9 wt% CMC hydrogels were prepared by dissolving the appropriate amount of United States Pharmacopeia grade low viscosity CMC (Spectrum Chemical Manufacturing Corp., Gardena, CA) in distilled water. The powder component of the PMMA cement was then mixed with the CMC hydrogel such that the powder was uniformly suspended within the aqueous phase. The liquid component of the PMMA cement was then added to the mixture of aqueous/powder phases. Aqueous phase weight percentages of 30, 40, and 50 wt% were used to fabricate the implants, resulting in 6 experimental groups. The aqueous and polymer phases were then stirred by hand for approximately 90 seconds and packed into Teflon® molds of the same size as the solid PMMA implants. The porous implants within molds were then allowed to harden for 30 minutes before being removed from the molds, placed within individual cassettes, and the aqueous phase was then leached from the implants in deionized, distilled water. The porous PMMA implants were then vacuum dried overnight.

Implant porosity and pore interconnectivity were analyzed using microcomputed tomography (μCT) as previously described.[544] Briefly, implants (n=3) from all experimental groups were scanned using a SkyScan 1172 μCT imaging system (SkyScan, Aartselaar, Belgium). High resolution 1280 × 1024 pixel images were created by scanning at an 8 μm/pixel resolution with no filter at voltage and current settings of 40 kV and 250 μA, respectively. Serial tomograms were reconstructed, resliced, and analyzed using NRecon and CTAn

software packages provided by SkyScan. For porosity and pore interconnectivity analyses, the scanned object volumes were binarized using a global threshold of 60-255. Porosity and interconnectivity were determined using a 9 mm diameter × 5 mm height cylindrical volume of interest to eliminate edge effects. Pore interconnectivity was determined by repeatedly applying a shrink wrap algorithm with minimum interconnection sizes ranging from 40-320 μm. Interconnectivity is reported as the percentage of pore volume accessible from outside the volume of interest with pores considered accessible only if the interconnection to that pore allowed a sphere with diameter of the user defined minimum interconnection size to pass through.

Scanning electron microscopy (SEM) was also used to examine the external surface of the implants. Implant surfaces were sputter-coated with gold for 40 s at 100 mA using a CrC-150 sputtering system (Torr International, New Windsor, NY) and observed at an accelerating voltage of 10 kV using a FEI Quanta 400 field emission scanning electron microscope (FEI company, Hillsboro, OR).

7.2.3 *In vivo* implant evaluation

Solid PMMA implants and porous implants (9 wt% CMC within the aqueous phase and both 30 and 40 wt% total aqueous phase in the implant) were evaluated *in vivo* using a modification of a nonhealing rabbit mandibular defect model.[617] All surgical procedures followed protocols approved by the Institutional Animal Care and Use Committees at both Rice University and the

University of Texas Health Science Center at Houston. Eighteen healthy male adult New Zealand White rabbits (n = 6 per group), at least 6 months old and weighing 3.5-4 kg were purchased from Myrtle's Rabbitry (Thompson Station, TN). Prior to implantation, all implants were sterilized using ethylene oxide.

Briefly, each animal was given preoperative intramuscular doses of buprenorphine hydrochloride (0.1 mg/kg body weight) for postoperative analgesia and 0.5 mL Durapen® (150,000 U/mL penicillin G benzathine and 150,000 U/mL penicillin G procaine) for perioperative antibiotic coverage. Prior to induction, ketamine hydrochloride (40 mg/kg body weight) and xylazine hydrochloride (7.5 mg/kg body weight) were given, after which rabbits were placed in a supine position, intubated and placed under general anesthesia using an isoflurane/O_2 mixture (2.5-3% isoflurance for induction, 2% for maintenance) with constant cardiac and respiratory monitoring. The animals were then surgically prepped and draped, after which a 7 cm midline incision through the skin and superficial fascia was made beginning 0.5 cm posterior to the mentum. Using blunt dissection and electrocauterization, the left masseter was exposed and the soft tissue along the inferior border of the body of the left hemimandible was mobilized such that the periosteum covering the body of the mandible could be incised and elevated, exposing a 4 cm × 1.5 cm area on the lateral surface of the mandible. A 10 mm titanium trephine (Ace Surgical Supply, Inc., Brockton, MA) attached to a Stryker TPS® surgical handpiece (Stryker, Kalamazoo, MI) operating at 15,000 rpm was used to create a bicortical defect through the

exposed body of the left mandible. A 701 bur in combination with the surgical drilling unit was used to cut a 2-3 mm window through the alveolar ridge in the middle of the defect to provide access for removal of the crowns of the associated teeth and provide intraoral exposure of the defect. The defect site was thoroughly washed with normal saline, after which an implant was placed within the defect. Prior to closure, a titanium supporting plate (1.5 mm 6-hole heavy gauge titanium; Synthes, West Chester, PA) was secured in place to prevent iatrogenic fracture during the course of the study. The incision was then closed in 3 layers (muscle, fascia, and skin) using degradable sutures (Vicryl polyglactin sutures, Ethicon, Somerville, NJ). Following wound closure, anesthesia was reversed, and the animals were extubated.

Postoperatively, the animals were given access to food and water *ad libitum*. Food was limited to a soft recovery diet (Critical Care for Herbivores, Oxbow Pet Products, Murdock, NE) and shredded or mashed fruits and vegetables to reduce stress on the mandible. All animals survived the 12-week post-operative period without complications.

7.2.4 Gross characterization

After 12 postoperative weeks, each rabbit was euthanized via intravenous injection of 1 mL Beuthanasia-D® (390 mg/mL pentobarbital sodium and 50 mg/mL phenytoin sodium). The left hemimandibles were then carefully dissected from the cranium with care taken to preserve the soft tissue surrounding the implant and within the oral cavity. The oral mucosa and dentition covering the

alveolus of each specimen was examined to detect any areas of implant or bone exposure. Specimens were individually placed in 10% neutral buffered formalin and stored on a shaker table at 4 °C for 72h.

7.2.5 Histology

After fixation, samples were dehydrated and stored in 70% of ethanol and then embedded in MMA. Following polymerization of the MMA, 3 coronally oriented 10 μM thick sections through the center of each implant were cut using a modified diamond saw technique[618] and subsequently stained using methylene blue/basic fuchsin.

Each of the stained sections was analyzed using light microscopy (Zeiss Axio Imager Z1 and AxioCam MRc 5, Carl Zeiss AG, Oberkochen, Germany) by two blinded observers (SY and FKK). A quantitative scoring system (Table 6.1) was used to score the tissue response at the implant interface and within the pores of the porous implants.

7.2.6 Statistical analyses

Implant porosity data were analyzed using single factor analyses of variance (ANOVA) with post hoc pairwise comparisons made using Tukey's HSD. Oral mucosal wound healing, as observed grossly and confirmed by microscopy, was analyzed using a Fisher-Freeman-Halton test. Histological scoring was analyzed using nonparametric statistics. The tissue response at the implant interface was analyzed using a Kruskal–Wallis one-way analysis of variance with subsequent pairwise analyses made using the Dwass-Steel-

Critchlow-Fligner test. A Mann-Whitney U test was used to analyze the tissue response within the pores of the two porous implant types. The a priori level of significance for all analyses was chosen as $\alpha = 0.05$. All analyses were performed using R version 2.10.0 (R Foundation for Statistical Computing, Vienna, Austria).

7.3 Results

7.3.1 Implant fabrication and characterization

Porous PMMA/CMC implants were reproducibly fabricated as described in the Materials and Methods section. MicroCT analyses showed that porosity increased as expected with increasing incorporation of the aqueous phase (Figure 7.1). Significant differences in implant porosity were observed between all groups as the aqueous phase incorporation increased. Varying the amount of CMC within the aqueous phase did not significantly alter the implant porosity.

Pore interconnectivity also increased with increasing aqueous phase incorporation (Figure 7.2). Interconnectivity appeared to be affected by the percentage of CMC in the aqueous phase; the more negative slope observed for implants with 9% CMC within the aqueous phase indicates that more of the interconnections in these implants were smaller than for those implants fabricated with 7% CMC in the aqueous phase.

SEM images and μCT reconstructions also showed differences in the porosity and surfaces of the fabricated implants (Figure 7.3). The porosity

increases with increasing aqueous phase incorporation quantitatively detected with μCT are seen in cross sections and surface images of the implants. Furthermore, the pore size appears more consistent within implants fabricated using 9% CMC in the aqueous phase, likely resulting in the relative abundance of smaller pore interconnections within these implants when compared to those fabricated using 7% CMC.

7.3.2 *In vivo* implant evaluation

Based on the implant characterization, solid PMMA implants, 9% CMC 30 wt% (16.9 ± 4.1% porosity, 39.7 ± 9.4% interconnectivity at a 40 μm minimum connection size) and 9% CMC 40 wt% (44.6 ± 2.1% porosity, 81.2 ± 1.0% interconnectivity at a 40 μm minimum connection size) implants were chosen for implantation in the *in vivo* phase of the study. All animals survived the surgery and post-operative period without complications. No changes in eating habits or activity were noted by the investigators, husbandry staff, or veterinary staff.

7.3.3 Gross characterization

At the time of animal euthanasia and implant/hemimandible harvest, no signs of mobility or infection were noted in any of the animals or visible tissues following harvest. Wound healing (closure) of the oral mucosa over the alveolar ridge at the site of the intraoral communication was assessed grossly (Figure 7.4) and correlated to histological results (Table 7.2) to confirm the gross observations. Wound healing was considered incomplete when any exposed bone or implant could be grossly observed and histology also indicated a failure

of soft tissue coverage over the implant or within the defect. The increase in oral mucosal wound healing observed in defects filled with both low and high porosity implants (83% of defects healed) versus non-porous PMMA implants (50% healed) was not statistically significant.

7.3.4 Histology

Histology and histological scoring were performed to assess the ability of the implants to maintain space within the surgically created osseous void and to view and quantify the soft tissue response around and within the implants. At low magnifications allowing coronal views of the entire implant and defect in cross section, all implants successfully maintained the defect space within the hemimandible, as confirmed by the lack of tissue collapse or contracture into the space occupied by the implants with the exception of tissue invading the pores of the porous implants (Figure 7.5).

At higher magnification, the tissue response at the implant-tissue interface and within the implant pores could be observed (Figure 7.6). At the implant-tissue interface, both the low porosity and solid implants were in many cases surrounded by a thin, well-organized fibrous capsule. The low porosity implants were also in direct contact in many areas with any newly formed bone observed at the implant interface. The high porosity implants were primarily surrounded by an abundance of inflammatory plasma cells at the implant interface, and a similar inflammatory cell population was observed within the pores of the highly porous implants. When a quantitative scoring system was applied, the interfacial tissue

response for the highly porous implants was statistically significantly different from the response observed around both the solid and low porosity implants (Figure 7.7). Similarly, the difference in tissue response within the pores of the low and high porosity implants was statistically significant (Figure 7.7).

7.4 Discussion

Temporary space maintainers have historically been used clinically to prevent soft tissue collapse into bony defects and provide a template for delayed bone healing or grafting.[601, 619] Recently, however, space maintenance has been used infrequently, particularly in the staged repair of traumatic injuries, as immediate free tissue transfer has eliminated the need for space maintenance and staged repair. Additionally, problems with existing biomaterials such as problems with healing of surrounding tissues, implant extrusion, or bacterial colonization have further limited the use of space maintainers, particularly in applications where soft tissue healing or infection may be a concern.[620, 621] Unfortunately, due to limitations in current tissue engineering technology, injuries involving lacking or devitalized soft tissues or the possibility of infection are precisely the type a staged repair using temporary space maintenance might allow a regenerative medicine approach to be undertaken.

The present study aimed to fabricate and characterize porous PMMA implants using a CMC porogen and test selected formulations in a non-healing bone defect that approximated a more toxic wound environment than most traditional animal models. In the first part of the study, porous PMMA implants

were fabricated in a one step process by incorporating a CMC hydrogel that could be leached away rapidly *in vitro* or *in vivo*. Varying both the amount of CMC within the aqueous phase and the relative amount of aqueous phase to polymer phase allowed for well controlled porosity and pore interconnectivity. As expected, higher percentages of porogen resulted in greater implant porosity, while increasing the viscosity of the aqueous phase porogen by incorporating of greater amounts of CMC within the hydrogel led to a more consistent pore size and higher pore interconnectivity when the minimum interconnection size was decreased.

In the second part of the study, two formulations of porous PMMA implants and solid PMMA implants were implanted into non-healing rabbit mandibular defects that had been contaminated through an open communication with the oral cavity. Porous PMMA formulations were selected such that both a highly porous, highly interconnected implant and an implant of lower porosity and lower interconnectivity could be compared. Healing of the communication into the oral cavity was assessed as well as the tissue response both around and within the implants. All formulations successfully maintained space within the defect. Soft tissue was only observed within the defect when it was penetrating the pore network in the two formulations of porous implant. The oral mucosal defects created to allow communication into the bone defect healed in more cases (5/6 healed for both low and high porosity implants) when the bony defects were filled

with porous implants than when filled with solid implants (3/6 healed), although the differences between groups was not statistically significant.

Although the gross mucosal defect closure over the high and low porosity implants was equivalent, microscopically, the tissue response around and within the pores of the low porosity implants was more favorable. At the implant – tissue interface, a small, well formed capsule or direct tissue – implant contact was typically observed around the low porosity implants. Immature fibrous tissue with few inflammatory elements was generally seen within the filled pores of the low porosity implants. Contrastingly, the tissue surrounding and within the pores of the highly porous implants was almost exclusively inflammatory, consisting mostly of plasma cells. A well-formed fibrous capsule was only observed surrounding one of the six high porosity implants implanted within the mandibular defect. Thus while all the implants tested *in vivo* successfully maintained the defect space, the low porosity and solid implants elicited a more favorable soft tissue response than the highly porous implants, while the porous implants may have provided a template for improved wound healing in comparison to the solid implants.

The current study has a number of strengths. First, although porous PMMA has been well studied,[612, 615, 622-625] including porous PMMA fabricated using an aqueous phase consisting of a CMC hydrogel as a porogen,[613, 626] the present study is one of the first systematic studies to quantitatively examine the effect of both the ratio of aqueous phase to polymer phase but also the effect of

the aqueous phase viscosity as done by varying the amount of CMC within the aqueous phase. Increasing the viscosity of the aqueous phase by using a 9 wt% CMC hydrogel, as opposed to a 7 wt% CMC gel as has been previously used,[627] resulted in a more consistent pore architecture with smaller, more consistently sized pore interconnections. Because of this, both porous implant formulations chosen for the *in vivo* study were fabricated with 9 wt% CMC hydrogels. An additional benefit of the chosen materials is that both PMMA and CMC are FDA regulated for craniofacial applications, and the fabrication of the implants can be done in a standard operating room with only minor alterations in the manufacturer recommended preparation of PMMA.

A strength of the *in vivo* portion of the study was the use of a more clinically relevant animal model that may better simulate the type of clinical situation in which the technology investigated may be used. The animal model was based on a previously developed rabbit mandibular defect[617] that was modified to allow contamination of the wound through an opening into the oral cavity. This conferred several advantages. First, mucosal wound healing within the rabbit oral cavity is a well established method for evaluating wound healing,[628-632] particularly when evaluating biomaterial-guided wound healing.[633-638] Second, in the clinical setting, the presence of intraoral communication is significantly correlated to decreased bone graft survival time,[610] and thus an implant evaluation strategy that focuses on the closure of these communications is relevant for a situation where definitive repair will be performed using a

standard or tissue engineered bone graft. With relation to the presence of these intraoral communications, infection is a major concern when dealing with any implantable biomaterial,[639] particularly PMMA,[640, 641] and thus evaluating the tissue response to the implant in an environment where it will most likely be exposed to bacteria strengthens any conclusions drawn with respect to optimal material formulations. Finally, although the observed differences in oral mucosal wound healing does not allow one to draw any definitive conclusions about how the presence of porosity affected the oral mucosal wound healing, this study establishes the statistical parameters necessary to determine the statistical power needed to achieve significance in future studies using this model. While a difference in healing clearly existed between both the high and low porosity implants and the solid PMMA implants, the difference was not significant. Somewhat surprisingly, the difference in tissue response to the porous implants based on histological scoring was significantly different and may be an important parameter not only for initial wound healing but also for subsequent bone regeneration.[642-644]

This study is not, however, without weaknesses. First, an ideal tissue engineering solution to the problem of complicated craniofacial bone defects would not involve multiple interventions and delayed reconstruction. An ideal solution would use a degradable material[645] that could address the issues of soft tissue coverage, infection, and bone regeneration concurrently, thus eliminating the need for and risks associated with repeated operations. At present, such a

solution does not exist nor does there appear to be any such solution developed for use in the near future. While the animal model chosen is viewed by the authors as one of the strengths of the study, the complexity of the model may also be viewed as a weakness. Not only is the tooth bearing segment of the mandible more complicated in structure than many craniofacial bones, it also is exposed to very different mechanical stresses than other bones.[646] Furthermore, the method of wound contamination was poorly controlled. Oral flora of the rabbits and the amount of flora that passed through the communication was likely variable between animals. Additionally, rabbits produce and eat caecotrophes, and it is not known whether this reingestion further complicates the model by exposing the implant to gut or colonic flora.

Limited research is available investigating PMMA strictly for use as a space maintainer; however, PMMA has a long track record of use in craniofacial applications. In an early study using PMMA to repair canine mandibular defects, Worley reported that repair failed in 7 of 11 dogs due to wound dehiscence over solid PMMA implants.[647] Kangur *et al.* reported similar problems with mucosal dehiscence over solid PMMA used to fix canine mandibular fractures and attributed the presence of an acute inflammatory tissue response to the PMMA to this oral communication.[648] Despite these findings, a number of studies exist that report no complications with solid PMMA use in craniofacial applications.[601, 621, 649, 650]

Porous PMMA, as previously mentioned has also been investigated in animal studies and limited clinical use. In a long term study in guinea pigs comparing porous and solid PMMA implanted in the hypodermis, van Mullem *et al.* reported implant extrusion occurred in 4/36 solid implants and none of the porous implants.[614] Similar to the present study, the same study noted that foci of inflammatory cells were found more frequently around and within the porous PMMA implants (1:1 aqueous phase:polymer phase) than the solid implants. Clinically, the porous PMMA seems to have been used successfully with little note of complications,[651] and, while reports of long-term results are rarely found, it should be noted that the current study differs from those previously published as the intent is for the porous implants to only be used as temporary implants.

In the present study, the porous PMMA implants appeared to promote or allow wound healing of the oral mucosa better than the solid implants, although not significantly so. Significant differences in the tissue response to the two formulations of porous implants were also observed. A number of possible explanations exist for these two findings. The trend of improved wound healing with use of the porous implants may best be explained by increased tissue integration within the pores of the implants. This may have limited implant micromovement and improved the rate at which new tissue formed across the implant to close the communication. Similar improvements in wound healing and implant retention have been found when using porous polyethylene for the fixation of bone-anchored hearing aids.[652, 653]

The inflammatory tissue response around and within the highly porous implants was likely caused by increased bacterial seeding of these implants. The increased porosity and interconnectivity of these implants compared to those of the low porosity and lower interconnectivity group likely led to bacterial accumulation deeper within the implant in areas where the bacteria could not effectively be cleared. Kiechel *et al.* compared infection control within porous and nonporous PMMA seeded with *Staphylococcus aureus* and implanted in the paravertebral fascia of rabbits and found increased infections occurred in animals implanted with porous PMMA implants.[654] Sclafani *et al.* found that increased porosity increased the resistance to infection in implants inoculated 14 days after implantation but not if the implants were inoculated at the time of implantation.[655] Thus in applications and models where contamination or infection exists at the time of implant placement, an appropriate balance with respect to porosity is needed to allow tissue ingrowth and implant integration but not bacterial seeding deep within the implant. If contamination is not present at the time of implantation, fibrovascular ingrowth has been shown to occur rapidly and thus a more porous implant may be acceptable.[656] Additionally, studies of induced membranes or capsules around PMMA implants suggest that the formation of well-formed capsule around the implants, as seen more frequently around the low porosity implants in this study, may facilitate greater success of later efforts aimed at definitive bone regeneration, provided the capsule is not destroyed during implant removal and any necessary debridement.[642-644] Finally, it is

important to note that the method of fabrication of the porous PMMA implants may lead to particulate PMMA release,[657] which could account for the inflammatory response elicited by the highly porous implants.[658]

Based on the results of the present study, the low porosity space maintainers appear to be a promising alternative to solid PMMA for temporary implantation as part of a regenerative medicine approach to treating traumatic craniofacial injuries. Future work in this area should focus on tissue regeneration within the maintained space as well as release of any bioactive factors from the space maintainer such as antibiotics or growth factors that may better ensure success of later stage tissue engineering efforts. The characterized implants may provide a critical step in allowing the use of regenerative medicine approaches as an alternative to traditional approaches in treating contaminated or open traumatic defects.

7.5 Conclusions

Porous PMMA space maintainers can be reproducibly fabricated using a CMC hydrogel as an aqueous phase porogen. Porosity and pore interconnectivity can be controlled by varying the ratio of the aqueous phase to polymer phase and the concentration of CMC within the hydrogel, respectively. *In vivo*, porous space maintainers potentially improve oral mucosal healing over a clean/contaminated bone defect created in the rabbit mandible. The tissue response to a porous implant of low porosity and pore interconnectivity was more favorable than the response to a more porous and interconnected implant. This

low porosity implant may be ideal for temporary space maintenance within craniofacial defects.

Table 7.1. Quantitative histological scoring parameters

Description	Score
Hard tissue response at scaffold–bone interface	
Direct bone to implant contact without soft interlayer	4
Remodeling lacuna with osteoblasts and/or osteoclasts at surface	3
Majority of implant is surrounded by fibrous tissue capsule	2
Unorganized fibrous tissue (majority of tissue is not arranged as capsule)	1
Inflammation marked by an abundance of inflammatory cells and poorly organized tissue	0
Hard tissue response within the pores of the scaffold	
Tissue in pores is mostly bone	4
Tissue in pores consists of some bone within mature, dense fibrous tissue and/or a few inflammatory response elements	3
Tissue in pores is mostly immature fibrous tissue (with or without bone) with blood vessels and young fibroblasts invading the space with few macrophages present	2
Tissue in pores consists mostly of inflammatory cells and connective tissue components in between (with or without bone) OR the majority of the pores are empty or filled with fluid	1
Tissue in pores is dense and exclusively of inflammatory type (no bone present)	0

Table 7.2. Oral mucosal coverage over implant by implant type

Implant type	Healed/Non-healed
Solid	3/3
Low porosity	5/1
High porosity	5/1

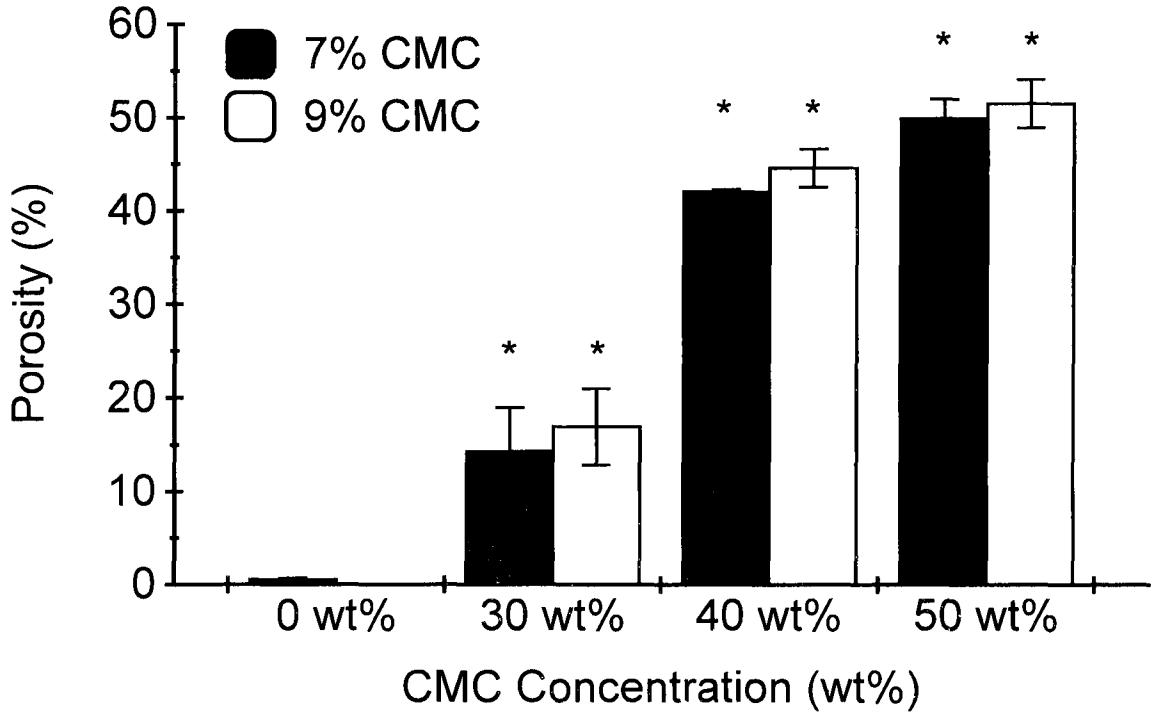

Figure 7.1. Porosity values as calculated by μCT. Samples were scanned and the resultant scans were reconstructed, reoriented, and binarized. Implant porosity was determined using a cylindrical (9 mm diameter × 5 mm height) volume of interest slightly smaller than the implant dimensions to eliminate edge effects. Data are reported as means ± standard deviation (n=3). The * over a bar denotes a statistically significant difference ($p < 0.05$) as detected using ANOVA and Tukey's post hoc tests between the group marked and the group with the same %CMC but lower aqueous phase in relation to polymer phase. No statistically significant differences in porosity were found as a result of changing the %CMC from 7% to 9%.

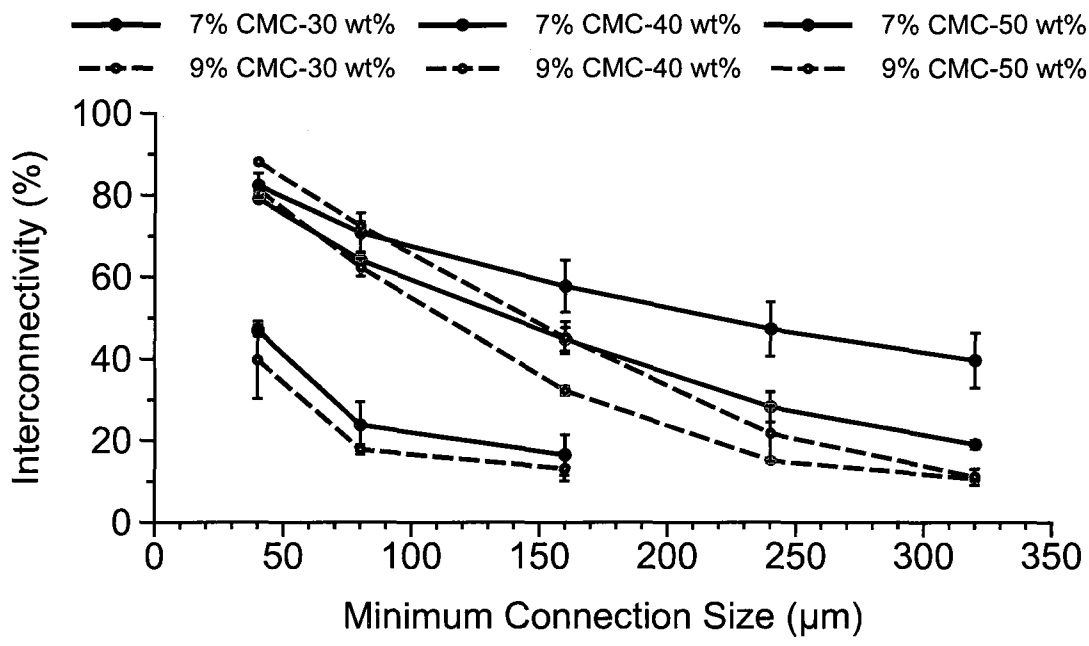

Figure 7.2. Implant interconnectivity percentages as a function of the minimum interconnection size. Samples were scanned and processed as reported in the methods section, and a built in software package was used to determine the percentage of the implant porosity that was accessible from outside the volume of interest. Data are reported as means ± standard deviation (n=3).

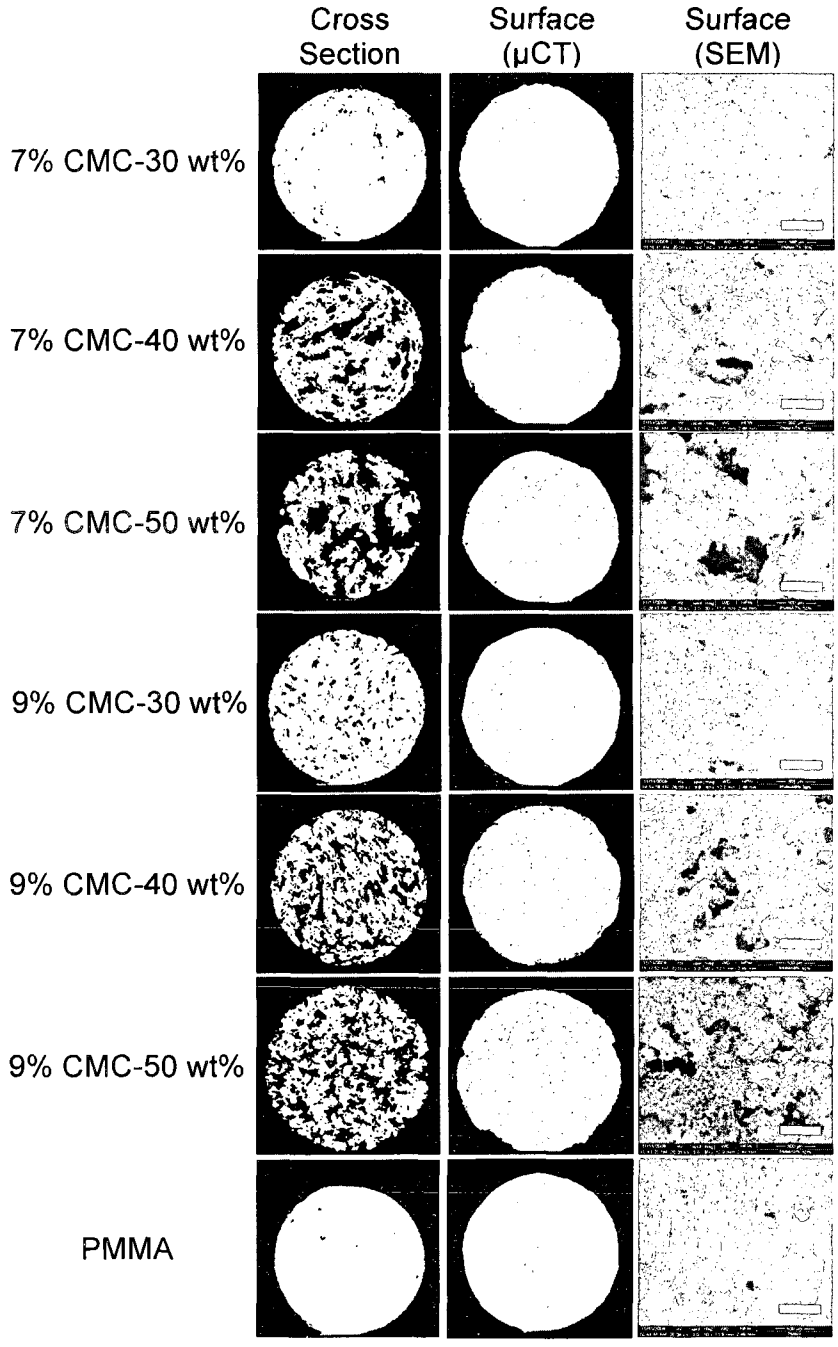

Figure 7.3. Representative images of implant cross sections and surfaces. Cylindrical implants (10 mm diameter × 6 mm height) from each experimental group were scanned by μCT or SEM. Virtual μCT cross sections of the implants were made by slicing through the center of the axially oriented implant. For electron micrographs, the scale bar represents 500 μm.

Figure 7.4. Representative gross views of harvested tissue covering the alveolus and implant. (A) Failure of wound healing over a solid PMMA implant is shown. The exposed implant is denoted by white arrows. (B, C) Well healed soft tissue covering the intraoral exposure is seen where dentition is missing over low porosity (B) and high porosity (C) implants.

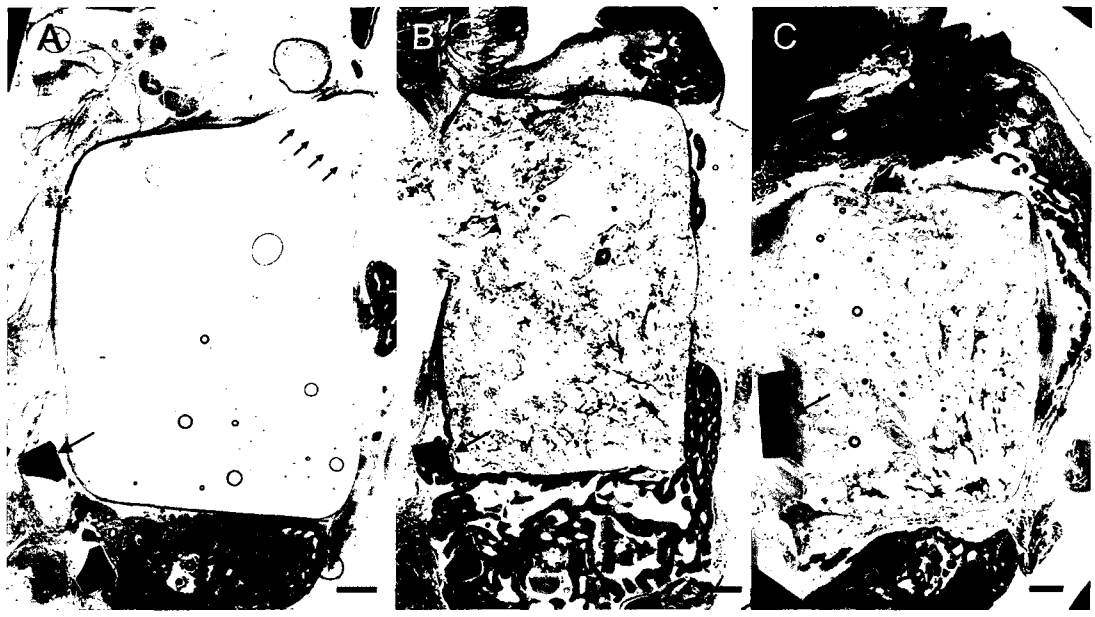

Figure 7.5. Representative light micrographs (25× magnification) of coronally sectioned tissue samples through the center of the A) Solid PMMA, (B) Low porosity, (C) High porosity space maintainers. The intraoral exposure of the solid implant (A) is shown with black arrows. Blue arrows denote the titanium plate used to stabilize the mandible. Tissue ingrowth is seen within both porous implants, and, for all implants, the original defect space appears well maintained with minimal tissue collapse or contracture. In B and C, soft tissue discontinuities at the left (buccal) side of the implant capsule are due to embedding and processing artifacts. Scale bars represent 1 mm.

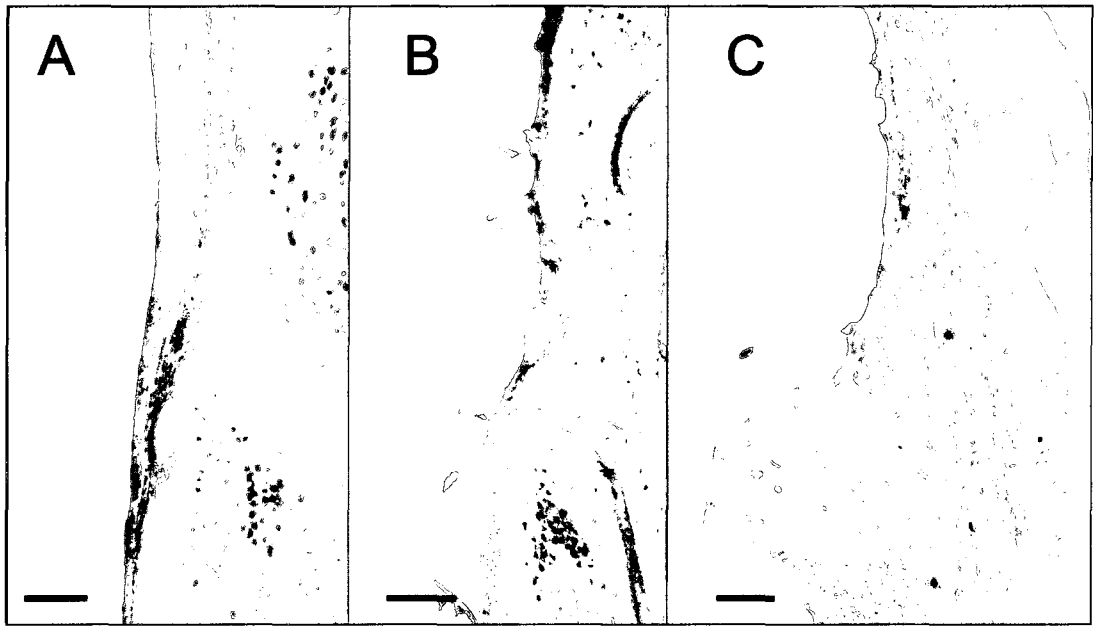

Figure 7.6. Representative light micrographs (200× magnification) of the lingual surface of coronally sectioned tissue samples through the center of the implanted A) Solid PMMA, (B) Low porosity, (C) High porosity space maintainers. Regenerated bone is seen near the surface of all implants. A well-formed capsule is seen in (A), while only a thin layer of loosely organized fibrous is seen at the surface of the low porosity space maintainer (B). An abundance of plasma cells is seen at the surface and penetrating the surface porosity of the highly porous space maintainer (C). Scale bars represent 100 μm.

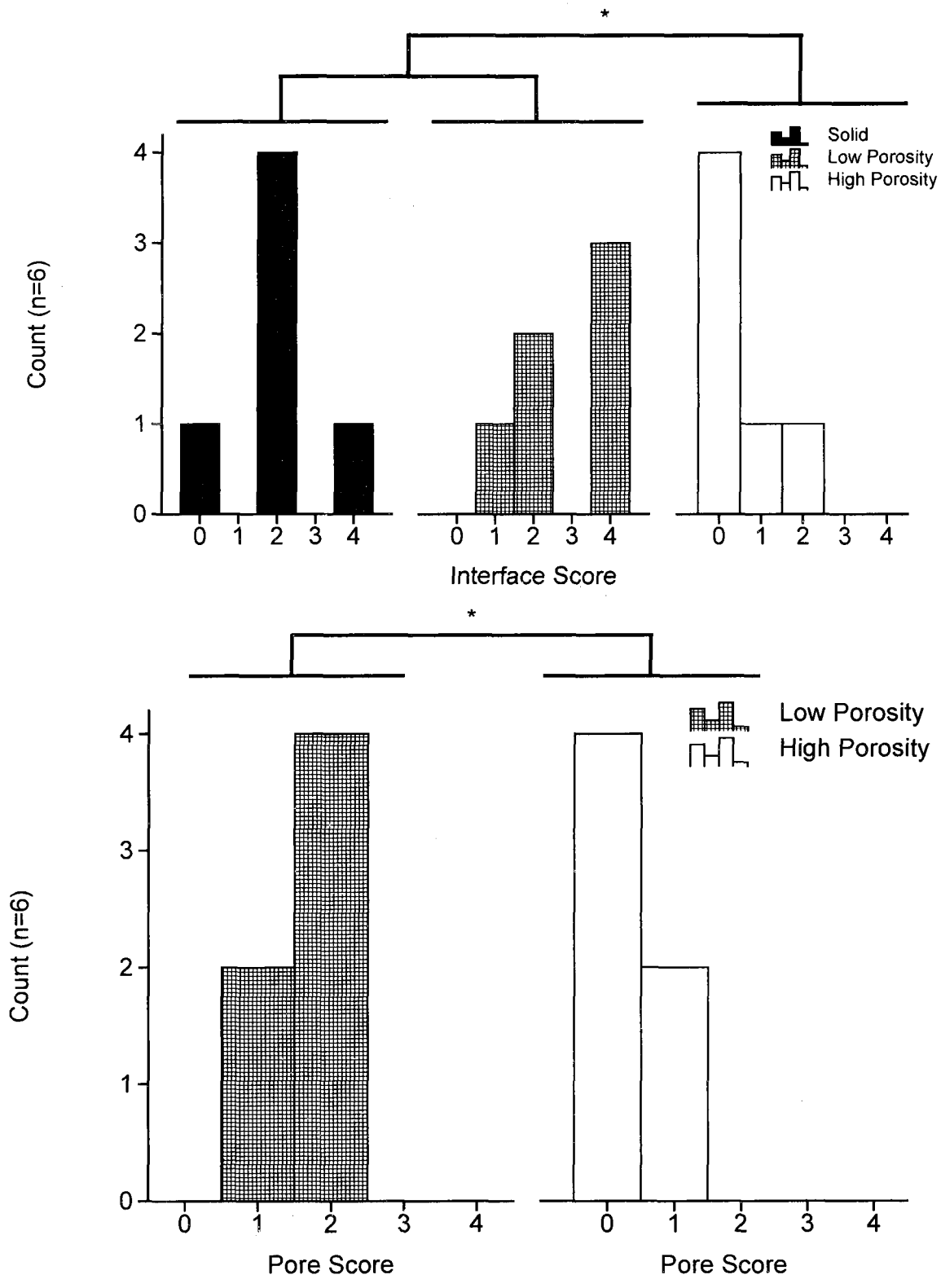

Figure 7.7. Score distributions for the graded (top) implant interface for all formulations tested *in vivo* and (bottom) tissue response within pores for the two porous implant formulations. Scoring criteria are defined in Table 7.1.

Statistically significant differences ($p < 0.05$) between groups, denoted by *, were determined using pairwise Dwass-Steel-Critchlow-Fligner tests for the implant interface scoring (top) and a Mann-Whitney U test for the tissue response within pores (bottom).

Chapter 8

Summary

The goals of this work were to investigate biomaterial-based strategies for tissue engineering in the craniofacial complex. A novel biomaterial with potential applications in cell delivery was investigated in the first objective, detailed in Chapter 4 and in two of the appendices, and a combination of physical gelation with increasing temperatures and ionic crosslinking in the presence of divalent ions was explored to increase gel mechanical stability. Increasing amount of vinylphosphonic acid incorporated into the synthesized macromers influenced macromer behavior in the presence of calcium ions, and the macromers underwent a reversible sol-gel transition around normal body temperature.

In exploring the second objective of the study as described in Chapter 5, we found that donor age and extended cell passages in combination had a significant effect on the *in vitro* differentiation potential of mesenchymal stem cells taken from the bone marrow of donor mice. These results point to potential problems that may be associated with *ex vivo* cell culture for the purpose of expanding and isolating certain populations of progenitor cells.

To explore the third and fourth objectives, described in Chapters 6 and 7, we limited our use of materials to novel formulations of FDA-approved products in order to potentially improve the rate at which these technologies could be translated. In Chapter 6, we determined that the use of uncultured bone marrow

mononuclear cells within a biomaterial scaffold can significantly improve bone regeneration when compared to the biomaterial scaffold alone. In the third objective, temporary space maintainers were fabricated and tested within a contaminated bone defect. We found that low porosity space maintainers allowed wound healing over the bone defect, maintained space effectively, and elicited a largely fibrous tissue response.

These approaches demonstrate that biomaterial-encapsulated cell delivery to bony defects is beneficial for bone healing, and that cells can be used immediately after harvest, thus foregoing any lengthy *ex vivo* processing. Additionally, for injuries where immediate placement of a cell-scaffold construct for definitive bone repair is not possible, a porous space maintainer may be placed to retain bony volume, support surrounding tissues, and potentially aid soft tissue healing around the defect.

Overall this project provides motivation for simplified biomaterial and stem cell based approaches in tissue engineering. Tailored biomaterials, such as those investigated in the first objective and in Chapter 4 hold promise and may alleviate some of the problems described in the subsequent chapters; however, the regulatory process is such that this promise may not be realized for some time. In fulfilling the subsequent aims, a strong case was made for simplified approaches utilizing currently regulated materials. Additionally, Chapter 7 described work that may be translated in order to facilitate the use of

regenerative medicine approaches for traumatic injuries that involve non-ideal wound conditions.

Finally, the work presented provides compelling evidence of the need for further investigation in these areas. First, a number of different animal models were utilized. Ideally, much of the work would be repeated within large animals and with human cells when possible, to further explore the validity of the conclusions drawn for clinical translation. Additionally, as more materials and methods for cell harvesting and processing become available for clinical use, the results presented here must be reevaluated, as better materials and methods may alleviate some of the problems which this study aimed to explore and address.

RICE UNIVERSITY

Biomaterial-Based Strategies for Craniofacial Tissue Engineering

by

James D. Kretlow

A THESIS SUBMITTED
IN PARTIAL FULFILLMENT OF THE
REQUIREMENTS FOR THE DEGREE

Doctor of Philosophy

Volume II

References and Appendices

HOUSTON, TX
JANUARY, 2010

Chapter 9

Literature Cited

1. Langer, R.; Vacanti, J. P., Tissue engineering. *Science* **1993,** 260, (5110), 920-926.

2. Mikos, A. G.; Johnson, P. C., Redefining Tissue Engineering... and Our New Rapid Publication Policy. *Tissue Eng* **2006,** 12, (6), 1379-1380.

3. Vacanti, C. A., History of tissue engineering and a glimpse into its future. *Tissue Eng* **2006,** 12, (5), 1137-42.

4. Santoni-Rugiu, P.; Sykes, P. J., *A History of Plastic Surgery.* Springer-Verlag: Berlin, 2007; p 395.

5. Aarabi, S.; Bhatt, K. A.; Shi, Y.; Paterno, J.; Chang, E. I.; Loh, S. A.; Holmes, J. W.; Longaker, M. T.; Yee, H.; Gurtner, G. C., Mechanical load initiates hypertrophic scar formation through decreased cellular apoptosis. *FASEB J* **2007,** 21, (12), 3250-61.

6. Derderian, C. A.; Bastidas, N.; Lerman, O. Z.; Bhatt, K. A.; Lin, S. E.; Voss, J.; Holmes, J. W.; Levine, J. P.; Gurtner, G. C., Mechanical strain alters gene expression in an in vitro model of hypertrophic scarring. *Ann Plast Surg* **2005,** 55, (1), 69-75; discussion 75.

7. Aarabi, S.; Longaker, M. T.; Gurtner, G. C., Hypertrophic scar formation following burns and trauma: new approaches to treatment. *PLoS Medicine* **2007,** 4, (9), e234.

8. Fu, X.; Li, H., Mesenchymal stem cells and skin wound repair and regeneration: possibilities and questions. *Cell Tissue Res* **2009,** 335, (2), 317-21.

9. Sushruta, The Sushruta Samhita. In *An English Translation of the Sushruta Samhita,* Bhishagratna, K. K., Ed. Kaviraj Kunjalal Bhishagratna: Calcutta, 1911; Vol. 2.

10. Eisenberg, I., A history of rhinoplasty. *S Afr Med J* **1982,** 62, (9), 286-92.

11. Myers, M. B.; Cherry, G., Augmentation of tissue survival by delay: an experimental study in rabbits. *Plast Reconstr Surg* **1967,** 39, (4), 397-401.

12. Gurunluoglu, R.; Gurunluoglu, A., Giulio Cesare Arantius (1530-1589): a surgeon and anatomist: his role in nasal reconstruction and influence on Gaspare Tagliacozzi. *Ann Plast Surg* **2008,** 60, (6), 717-22.

13. Zimbler, M. S., Gaspare Tagliacozzi (1545-1599): renaissance surgeon. *Arch Facial Plast Surg* **2001,** 3, (4), 283-4.

14. Ghali, S.; Butler, P. E.; Tepper, O. M.; Gurtner, G. C., Vascular delay revisited. *Plast Reconstr Surg* **2007,** 119, (6), 1735-44.

15. Ribuffo, D.; Atzeni, M.; Corrias, F.; Guerra, M.; Saba, L.; Sias, A.; Balestrieri, A.; Mallarini, G., Preoperative Angio-CT preliminary study of the TRAM flap after selective vascular delay. *Ann Plast Surg* **2007,** 59, (6), 611-6.

16. Kajikawa, A.; Ueda, K.; Tateshita, T.; Katsuragi, Y., Breast reconstruction using tissue expander and TRAM flap with vascular enhancement procedures. *J Plast Reconstr Aesthet Surg* **2009,** 62, (9), 1148-53.

17. Johnson, P. C.; Mikos, A. G.; Fisher, J. P.; Jansen, J. A., Strategic Directions in Tissue Engineering. *Tissue Eng* **2007,** 13, (12), 2827-2837.

18. Patel, Z. S.; Mikos, A. G., Angiogenesis with biomaterial-based drug- and cell-delivery systems. *J Biomater Sci Polym Ed* **2004,** 15, (6), 701-26.

19. Patel, Z. S.; Young, S.; Tabata, Y.; Jansen, J. A.; Wong, M.; Mikos, A. G., Dual delivery of an angiogenic and an osteogenic growth factor for bone regeneration in a critical size defect model. *Bone* **2008,** 43, (5), 931-40.

20. Dobson, J., *John Hunter.* E. & S. Livingstone Ltd.: Edinburgh, 1969.

21. Churchhill, W., *My Early Life.* Butterworth: London, 1930.

22. Gibson, T.; Medawar, P. B., The fate of skin homografts in man. *J Anat* **1943,** 77, (Pt 4), 299-310 4.

23. George, A. J.; Larkin, D. F., Corneal transplantation: the forgotten graft. *Am J Transplant* **2004,** 4, (5), 678-85.

24. Senn, N., On the healing of aseptic bone cavities by implantation of antiseptic decalcified bone. *Am J Med Sci* **1889,** 98, 219-240.

25. Zirm, E. K., Eine erfolgreiche totale Keratoplastik (A successful total keratoplasty). 1906. *Refract Corneal Surg* **1989,** 5, (4), 258-61.

26. Carrel, A.; Guthrie, C. C., Functions of a Transplanted Kidney. *Science* **1905,** 22, (563), 473.

27. Carrel, A.; Lindbergh, C. A., The Culture of Whole Organs. *Science* **1935,** 81, (2112), 621-623.

28. Saltzman, W. M., *Tissue Engineering.* Oxford University Press: New York, 2004.

29. Voorhees, A. B., Jr.; Jaretzki, A., 3rd; Blakemore, A. H., The use of tubes constructed from vinyon "N" cloth in bridging arterial defects. *Ann Surg* **1952,** 135, (3), 332-6.

30. Urist, M. R.; Mc, L. F., Osteogenetic potency and new-bone formation by induction in transplants to the anterior chamber of the eye. *J Bone Joint Surg Am* **1952,** 34-A, (2), 443-76.

31. Urist, M. R.; McLean, F. C., The local physiology of bone repair with particular reference to the process of new bone formation by induction. *Am J Surg* **1953,** 85, (3), 444-9.

32. Urist, M. R., Bone: Formation by Autoinduction. *Science* **1965,** 150, (3698), 893-899.

33. Urist, M. R.; Mikulski, A.; Lietze, A., Solubilized and Insolubilized Bone Morphogenetic Protein. *Proc Natl Acad Sci U S A* **1979,** 76, (4), 1828-1832.

34. Lacroix, P., Recent Investigations of the Growth of Bone. *Nature* **1945,** 156, 576.

35. Sampath, T. K.; Reddi, A. H., Dissociative extraction and reconstitution of extracellular matrix components involved in local bone differentiation. *Proc Natl Acad Sci U S A* **1981,** 78, (12), 7599-603.

36. Govender, S.; Csimma, C.; Genant, H. K.; Valentin-Opran, A.; Amit, Y.; Arbel, R.; Aro, H.; Atar, D.; Bishay, M.; Borner, M. G.; Chiron, P.; Choong, P.; Cinats, J.; Courtenay, B.; Feibel, R.; Geulette, B.; Gravel, C.; Haas, N.; Raschke, M.; Hammacher, E.; van der Velde, D.; Hardy, P.; Holt, M.; Josten, C.; Ketterl, R. L.; Lindeque, B.; Lob, G.; Mathevon, H.; McCoy, G.; Marsh, D.; Miller, R.; Munting, E.; Oevre, S.; Nordsletten, L.; Patel, A.; Pohl, A.; Rennie, W.; Reynders, P.; Rommens, P. M.; Rondia, J.; Rossouw, W. C.; Daneel, P. J.; Ruff, S.; Ruter, A.; Santavirta, S.; Schildhauer, T. A.; Gekle, C.; Schnettler, R.; Segal, D.; Seiler, H.; Snowdowne, R. B.; Stapert, J.; Taglang, G.; Verdonk, R.; Vogels, L.; Weckbach, A.; Wentzensen, A.; Wisniewski, T., Recombinant Human Bone Morphogenetic Protein-2 for Treatment of Open Tibial Fractures: A Prospective, Controlled, Randomized Study of Four Hundred and Fifty Patients. *J Bone Joint Surg Am* **2002,** 84, (12), 2123-2134.

37. Lutolf, M. P.; Weber, F. E.; Schmoekel, H. G.; Schense, J. C.; Kohler, T.; Muller, R.; Hubbell, J. A., Repair of bone defects using synthetic mimetics of collagenous extracellular matrices. *Nat Biotechnol* **2003,** 21, (5), 513-518.

38. Ruhe, P. Q.; Hedberg, E. L.; Padron, N. T.; Spauwen, P. H.; Jansen, J. A.; Mikos, A. G., rhBMP-2 release from injectable poly(DL-lactic-co-glycolic acid)/calcium-phosphate cement composites. *J Bone Joint Surg Am* **2003,** 85-A Suppl 3, 75-81.

39. Altman, J., Are new neurons formed in the brains of adult mammals? *Science* **1962,** 135, 1127-8.

40. Altman, J.; Das, G. D., Post-natal origin of microneurones in the rat brain. *Nature* **1965,** 207, (5000), 953-6.

41. Till, J. E.; Mc, C. E., Early repair processes in marrow cells irradiated and proliferating in vivo. *Radiat Res* **1963,** 18, 96-105.

42. Friedenstein, A. J.; Deriglasova, U. F.; Kulagina, N. N.; Panasuk, A. F.; Rudakowa, S. F.; Luria, E. A.; Ruadkow, I. A., Precursors for fibroblasts in different populations of hematopoietic cells as detected by the in vitro colony assay method. *Exp Hematol* **1974,** 2, (2), 83-92.

43. Kleinsmith, L. J.; Pierce, G. B., Jr., Multipotentiality of Single Embryonal Carcinoma Cells. *Cancer Res* **1964,** 24, 1544-51.

44. Martin, G. R., Isolation of a pluripotent cell line from early mouse embryos cultured in medium conditioned by teratocarcinoma stem cells. *Proc Natl Acad Sci U S A* **1981,** 78, (12), 7634-8.

45. Evans, M. J.; Kaufman, M. H., Establishment in culture of pluripotential cells from mouse embryos. *Nature* **1981,** 292, (5819), 154-6.

46. Chick, W. L.; Like, A. A.; Lauris, V.; Galletti, P. M.; Richardson, P. D.; Panol, G.; Mix, T. W.; Colton, C. K., A hybrid artifical pancreas. *Trans Am Soc Artif Intern Organs* **1975,** 21, 8-15.

47. Whittemore, A. D.; Chick, W. L.; Galletti, P. M.; Mannick, J. A., Function of hybrid artificial pancreas in diabetic rats. *Surg Forum* **1977,** 28, 93-7.

48. Maki, T.; Ubhi, C. S.; Sanchez-Farpon, H.; Sullivan, S. J.; Borland, K.; Muller, T. E.; Solomon, B. A.; Chick, W. L.; Monaco, A. P., Successful treatment of diabetes with the biohybrid artificial pancreas in dogs. *Transplantation* **1991,** 51, (1), 43-51.

49. Green, W. T., Jr.; Ferguson, R. J., Histochemical and electron microscopic comparison of tissue produced by rabbit articular chondrocytes in vivo and in vitro. *Arthritis Rheum* **1975,** 18, (3), 273-80.

50. Viola, J.; Lal, B.; Grad, O. *The Emergence of Tissue Engineering as a Research Field*; The National Science Foundation: Arlington, VA, 2003.

51. Bell, E.; Ehrlich, H. P.; Buttle, D. J.; Nakatsuji, T., Living tissue formed in vitro and accepted as skin-equivalent tissue of full thickness. *Science* **1981,** 211, (4486), 1052-4.

52. Yannas, I. V.; Burke, J. F.; Warpehoski, M.; Stasikelis, P.; Skrabut, E. M.; Orgill, D.; Giard, D. J., Prompt, long-term functional replacement of skin. *Trans Am Soc Artif Intern Organs* **1981,** 27, 19-23.

53. Wolter, J. R.; Meyer, R. F., Sessile macrophages forming clear endothelium-like membrane on inside of successful keratoprosthesis. *Trans Am Ophthalmol Soc* **1984,** 82, 187-202.

54. Vacanti, J. P.; Morse, M. A.; Saltzman, W. M.; Domb, A. J.; Perez-Atayde, A.; Langer, R., Selective cell transplantation using bioabsorbable artificial polymers as matrices. *J Pediatr Surg* **1988,** 23, (1 Pt 2), 3-9.

55. Cima, L. G.; Ingber, D. E.; Vacanti, J. P.; Langer, R., Hepatocyte culture on biodegradable polymeric substrates. *Biotechnol Bioeng* **1991,** 38, (2), 145-58.

56. Vacanti, C. A.; Langer, R.; Schloo, B.; Vacanti, J. P., Synthetic polymers seeded with chondrocytes provide a template for new cartilage formation. *Plast Reconstr Surg* **1991,** 88, (5), 753-9.

57. Cohen, S.; Bano, M. C.; Cima, L. G.; Allcock, H. R.; Vacanti, J. P.; Vacanti, C. A.; Langer, R., Design of synthetic polymeric structures for cell transplantation and tissue engineering. *Clin Mater* **1993,** 13, (1-4), 3-10.

58. Mikos, A. G.; Sarakinos, G.; Lyman, M. D.; Ingber, D. E.; Vacanti, J. P.; Langer, R., Prevascularization of porous biodegradable polymers. *Biotechnol Bioeng* **1993,** 42, (6), 716-723.

59. Vacanti, C. A., The history of tissue engineering. *J Cell Mol Med* **2006,** 10, (3), 569-76.

60. Gronthos, S.; Graves, S. E.; Ohta, S.; Simmons, P. J., The STRO-1+ fraction of adult human bone marrow contains the osteogenic precursors. *Blood* **1994,** 84, (12), 4164-73.

61. Pittenger, M. F.; Mackay, A. M.; Beck, S. C.; Jaiswal, R. K.; Douglas, R.; Mosca, J. D.; Moorman, M. A.; Simonetti, D. W.; Craig, S.; Marshak, D. R., Multilineage potential of adult human mesenchymal stem cells. *Science* **1999,** 284, (5411), 143-7.

62. Cao, Y.; Vacanti, J. P.; Paige, K. T.; Upton, J.; Vacanti, C. A., Transplantation of chondrocytes utilizing a polymer-cell construct to produce tissue-engineered cartilage in the shape of a human ear. *Plast Reconstr Surg* **1997,** 100, (2), 297-302; discussion 303-4.

63. Shinoka, T.; Shum-Tim, D.; Ma, P. X.; Tanel, R. E.; Isogai, N.; Langer, R.; Vacanti, J. P.; Mayer, J. E., Jr., Creation of viable pulmonary artery autografts through tissue engineering. *J Thorac Cardiovasc Surg* **1998,** 115, (3), 536-45; discussion 545-6.

64. Shin'oka, T.; Imai, Y.; Ikada, Y., Transplantation of a tissue-engineered pulmonary artery. *N Engl J Med* **2001,** 344, (7), 532-3.

65. Vacanti, C. A.; Bonassar, L. J.; Vacanti, M. P.; Shufflebarger, J., Replacement of an avulsed phalanx with tissue-engineered bone. *N Engl J Med* **2001,** 344, (20), 1511-4.

66. Miller, M. J.; Goldberg, D. P.; Yasko, A. W.; Lemon, J. C.; Satterfield, W. C.; Wake, M. C.; Mikos, A. G., Guided Bone Growth in Sheep: A Model for Tissue-Engineered Bone Flaps. *Tissue Eng* **1996,** 2, (1), 51-59.

67. Cheng, M. H.; Brey, E. M.; Ulusal, B. G.; Wei, F. C., Mandible augmentation for osseointegrated implants using tissue engineering strategies. *Plast Reconstr Surg* **2006,** 118, (1), 1e-4e.

68. Atala, A.; Bauer, S. B.; Soker, S.; Yoo, J. J.; Retik, A. B., Tissue-engineered autologous bladders for patients needing cystoplasty. *Lancet* **2006,** 367, (9518), 1241(6).

69. Macchiarini, P.; Jungebluth, P.; Go, T.; Asnaghi, M. A.; Rees, L. E.; Cogan, T. A.; Dodson, A.; Martorell, J.; Bellini, S.; Parnigotto, P. P.; Dickinson, S. C.; Hollander, A. P.; Mantero, S.; Conconi, M. T.; Birchall, M. A., Clinical transplantation of a tissue-engineered airway. *Lancet* **2008,** 372, (9655), 2023-30.

70. Quaini, F.; Urbanek, K.; Beltrami, A. P.; Finato, N.; Beltrami, C. A.; Nadal-Ginard, B.; Kajstura, J.; Leri, A.; Anversa, P., Chimerism of the transplanted heart. *N Engl J Med* **2002,** 346, (1), 5-15.

71. Meng, Y.; Qin, Y. X.; Dimasi, E.; Ba, X.; Rafailovich, M.; Pernodet, N., Biomineralization of a Self-Assembled Extracellular Matrix for Bone Tissue Engineering. *Tissue Eng Part A* **2009,** 15, (2), 355-66.

72. Woodrow, K. A.; Wood, M. J.; Saucier-Sawyer, J. K.; Solbrig, C.; Saltzman, W. M., Biodegradable Meshes Printed with Extracellular Matrix Proteins Support Micropatterned Hepatocyte Cultures. *Tissue Eng Part A* **2009,** 15, (5), 1169-79.

73. Datta, N.; Holtorf, H. L.; Sikavitsas, V. I.; Jansen, J. A.; Mikos, A. G., Effect of bone extracellular matrix synthesized in vitro on the osteoblastic differentiation of marrow stromal cells. *Biomaterials* **2005,** 26, (9), 971-7.

74. Pham, Q. P.; Kasper, F. K.; Scott Baggett, L.; Raphael, R. M.; Jansen, J. A.; Mikos, A. G., The influence of an in vitro generated bone-like extracellular matrix on osteoblastic gene expression of marrow stromal cells. *Biomaterials* **2008,** 29, (18), 2729-39.

75. Axhausen, W., The osteogenetic phases of regeneration of bone; a historical and experimental study. *J Bone Joint Surg Am* **1956,** 38-A, (3), 593-600.

76. Gutta, R.; Waite, P. D., Cranial bone grafting and simultaneous implants: A submental technique to reconstruct the atrophic mandible. *Br J Oral Maxillofac Surg* **2007**.

77. Louis, P. J.; Gutta, R.; Said-Al-Naief, N.; Bartolucci, A. A., Reconstruction of the maxilla and mandible with particulate bone graft and titanium mesh for implant placement. *J Oral Maxillofac Surg* **2008,** 66, (2), 235-45.

78. Sen, M. K.; Miclau, T., Autologous iliac crest bone graft: should it still be the gold standard for treating nonunions? *Injury* **2007,** 38 Suppl 1, S75-80.

79. Smolka, W.; Iizuka, T., Surgical reconstruction of maxilla and midface: clinical outcome and factors relating to postoperative complications. *J Craniomaxillofac Surg* **2005,** 33, (1), 1-7.

80. Ito, H.; Koefoed, M.; Tiyapatanaputi, P.; Gromov, K.; Goater, J. J.; Carmouche, J.; Zhang, X.; Rubery, P. T.; Rabinowitz, J.; Samulski, R. J.; Nakamura, T.; Soballe, K.; O'Keefe, R. J.; Boyce, B. F.; Schwarz, E. M., Remodeling of cortical bone allografts mediated by adherent rAAV-RANKL and VEGF gene therapy. *Nat Med* **2005,** 11, (3), 291-7.

81. Tomford, W. W.; Mankin, H. J., Bone banking. Update on methods and materials. *Orthop Clin North Am* **1999,** 30, (4), 565-70.

82. Nguyen, H.; Morgan, D. A.; Forwood, M. R., Sterilization of allograft bone: effects of gamma irradiation on allograft biology and biomechanics. *Cell Tissue Bank* **2007,** 8, (2), 93-105.

83. Buck, B. E.; Malinin, T. I., Human bone and tissue allografts. Preparation and safety. *Clin Orthop Relat Res* **1994**, (303), 8-17.

84. Boyce, T.; Edwards, J.; Scarborough, N., Allograft bone. The influence of processing on safety and performance. *Orthop Clin North Am* **1999,** 30, (4), 571-81.

85. Peleg, M., Using allogenic block grafts to augment the alveolar ridge. *Dent Implantol Update* **2004,** 15, (12), 89-94.

86. Sandhu, H. S.; Khan, S. N.; Suh, D. Y.; Boden, S. D., Demineralized bone matrix, bone morphogenetic proteins, and animal models of spine fusion: an overview. *Eur Spine J* **2001,** 10 Suppl 2, S122-31.

87. Wildemann, B.; Kadow-Romacker, A.; Haas, N. P.; Schmidmaier, G., Quantification of various growth factors in different demineralized bone matrix preparations. *J Biomed Mater Res A* **2007,** 81, (2), 437-42.

88. Peterson, B.; Whang, P. G.; Iglesias, R.; Wang, J. C.; Lieberman, J. R., Osteoinductivity of Commercially Available Demineralized Bone Matrix.

Preparations in a Spine Fusion Model. *J Bone Joint Surg Am* **2004,** 86, (10), 2243-2250.

89. Acarturk, T. O.; Hollinger, J. O., Commercially available demineralized bone matrix compositions to regenerate calvarial critical-sized bone defects. *Plast Reconstr Surg* **2006,** 118, (4), 862-73.

90. Laurencin, C. T.; El-Amin, S. F., Xenotransplantation in orthopaedic surgery. *J Am Acad Orthop Surg* **2008,** 16, (1), 4-8.

91. Dormont, D., How to limit the spread of Creutzfeldt-Jakob disease. *Infect Control Hosp Epidemiol* **1996,** 17, (8), 521-8.

92. Wenz, B.; Oesch, B.; Horst, M., Analysis of the risk of transmitting bovine spongiform encephalopathy through bone grafts derived from bovine bone. *Biomaterials* **2001,** 22, (12), 1599-606.

93. Mannai, C., Early implant loading in severely resorbed maxilla using xenograft, autograft, and platelet-rich plasma in 97 patients. *J Oral Maxillofac Surg* **2006,** 64, (9), 1420-6.

94. Garofalo, G. S., Autogenous, allogenetic and xenogenetic grafts for maxillary sinus elevation: literature review, current status and prospects. *Minerva Stomatol* **2007,** 56, (7-8), 373-92.

95. Vance, G. S.; Greenwell, H.; Miller, R. L.; Hill, M.; Johnston, H.; Scheetz, J. P., Comparison of an allograft in an experimental putty carrier and a bovine-derived xenograft used in ridge preservation: a clinical and histologic study in humans. *Int J Oral Maxillofac Implants* **2004,** 19, (4), 491-7.

96. Scheyer, E. T.; Velasquez-Plata, D.; Brunsvold, M. A.; Lasho, D. J.; Mellonig, J. T., A clinical comparison of a bovine-derived xenograft used alone and in combination with enamel matrix derivative for the treatment of periodontal osseous defects in humans. *J Periodontol* **2002,** 73, (4), 423-32.

97. Bernhardt, A.; Lode, A.; Boxberger, S.; Pompe, W.; Gelinsky, M., Mineralised collagen--an artificial, extracellular bone matrix--improves osteogenic

differentiation of bone marrow stromal cells. *J Mater Sci Mater Med* **2008,** 19, (1), 269-75.

98. LeGeros, R. Z., Properties of Osteoconductive Biomaterials: Calcium Phosphates. *Clin Orthop* **2002,** 395, 81-98.

99. Shors, E. C., Coralline bone graft substitutes. *Orthop Clin North Am* **1999,** 30, (4), 599-613.

100. Friedman, C. D., Future directions in alloplastic materials for facial skeletal augmentation. *Facial Plast Surg Clin North Am* **2002,** 10, (2), 175-80.

101. Cunningham, L. L., The use of calcium phosphate cements in the maxillofacial region. *J Long Term Eff Med Implants* **2005,** 15, (6), 609-15.

102. Spivak, J. M.; Hasharoni, A., Use of hydroxyapatite in spine surgery. *Eur Spine J* **2001,** 10 Suppl 2, S197-204.

103. Daculsi, G.; Laboux, O.; Malard, O.; Weiss, P., Current state of the art of biphasic calcium phosphate bioceramics. *J Mater Sci Mater Med* **2003,** 14, (3), 195-200.

104. Oner, F. C.; Dhert, W. J.; Verlaan, J. J., Less invasive anterior column reconstruction in thoracolumbar fractures. *Injury* **2005,** 36 Suppl 2, B82-9.

105. Friedman, C. D.; Costantino, P. D.; Takagi, S.; Chow, L. C., BoneSource™ hydroxyapatite cement: A novel biomaterial for craniofacial skeletal tissue engineering and reconstruction. *J Biomed Mater Res* **1998,** 43, (4), 428-432.

106. Dunne, M.; Corrigan, I.; Ramtoola, Z., Influence of particle size and dissolution conditions on the degradation properties of polylactide-co-glycolide particles. *Biomaterials* **2000,** 21, (16), 1659-68.

107. Sanger, C.; Soto, A.; Mussa, F.; Sanzo, M.; Sardo, L.; Donati, P. A.; Di Pietro, G.; Spacca, B.; Giordano, F.; Genitori, L., Maximizing results in craniofacial surgery with bioresorbable fixation devices. *J Craniofac Surg* **2007,** 18, (4), 926-30.

108. Fedorowicz, Z.; Nasser, M.; Newton, J. T.; Oliver, R. J., Resorbable versus titanium plates for orthognathic surgery. *Cochrane Database Syst Rev* **2007**, (2), CD006204.

109. Bell, R. B.; Kindsfater, C. S., The use of biodegradable plates and screws to stabilize facial fractures. *J Oral Maxillofac Surg* **2006,** 64, (1), 31-9.

110. Laughlin, R. M.; Block, M. S.; Wilk, R.; Malloy, R. B.; Kent, J. N., Resorbable plates for the fixation of mandibular fractures: a prospective study. *J Oral Maxillofac Surg* **2007,** 65, (1), 89-96.

111. Christgau, M.; Bader, N.; Schmalz, G.; Hiller, K. A.; Wenzel, A., GTR therapy of intrabony defects using 2 different bioresorbable membranes: 12-month results. *J Clin Periodontol* **1998,** 25, (6), 499-509.

112. Quatela, V. C.; Chow, J., Synthetic facial implants. *Facial Plast Surg Clin North Am* **2008,** 16, (1), 1-10, v.

113. Yaremchuk, M. J., Facial skeletal reconstruction using porous polyethylene implants. *Plast Reconstr Surg* **2003,** 111, (6), 1818-27.

114. Moreira-Gonzalez, A.; Jackson, I. T.; Miyawaki, T.; Barakat, K.; DiNick, V., Clinical outcome in cranioplasty: critical review in long-term follow-up. *J Craniofac Surg* **2003,** 14, (2), 144-53.

115. Santin, M.; Motta, A.; Borzachiello, A.; Nicolais, L.; Ambrosio, L., Effect of PMMA cement radical polymerisation on the inflammatory response. *J Mater Sci Mater Med* **2004,** 15, (11), 1175-80.

116. Groth, M.; Bhatnagar, A.; Clearihue, W.; Goldberg, R.; Douglas, R., Long-term efficacy of biomodeled polymethyl methacrylate implants for orbitofacial defects. *Arch Facial Plast Surg* **2006,** 8, (6), 381.

117. Lara, W. C.; Schweitzer, J.; Lewis, R. P.; Odum, B. C.; Edlich, R. F.; Gampper, T. J., Technical considerations in the use of polymethylmethacrylate in cranioplasty. *J Long Term Eff Med Implants* **1998,** 8, (1), 43-53.

118. Vaandrager, J. M.; Vanmullem, P. J.; Dewijn, J. R., Craniofacial Contouring and Porous Acrylic Cement. *Ann Plast Surg* **1988,** 21, (6), 583-593.

119. Herford, A. S.; Boyne, P. J.; Williams, R. P., Clinical applications of rhBMP-2 in maxillofacial surgery. *J Calif Dent Assoc* **2007,** 35, (5), 335-41.

120. Closmann, J. J.; Pogrel, M. A.; Schmidt, B. L., Reconstruction of perioral defects following resection for oral squamous cell carcinoma. *J Oral Maxillofac Surg* **2006,** 64, (3), 367-74.

121. Rapidis, A. D.; Alexandridis, C. A.; Eleftheriadis, E.; Angelopoulos, A. P., The use of the buccal fat pad for reconstruction of oral defects: review of the literature and report of 15 cases. *J Oral Maxillofac Surg* **2000,** 58, (2), 158-63.

122. Marx, R. E.; Smith, B. R., An improved technique for development of the pectoralis major myocutaneous flap. *J Oral Maxillofac Surg* **1990,** 48, (11), 1168-80.

123. Wong, T. Y.; Chung, C. H.; Huang, J. S.; Chen, H. A., The inverted temporalis muscle flap for intraoral reconstruction: its rationale and the results of its application. *J Oral Maxillofac Surg* **2004,** 62, (6), 667-75.

124. Gonzalez-Garcia, R.; Rodriguez-Campo, F. J.; Naval-Gias, L.; Sastre-Perez, J.; Munoz-Guerra, M. F.; Usandizaga, J. L.; Diaz-Gonzalez, F. J., Radial forearm free flap for reconstruction of the oral cavity: clinical experience in 55 cases. *Oral Surg Oral Med Oral Pathol Oral Radiol Endod* **2007,** 104, (1), 29-37.

125. Wolff, K. D.; Kesting, M.; Loffelbein, D.; Holzle, F., Perforator-based anterolateral thigh adipofascial or dermal fat flaps for facial contour augmentation. *J Reconstr Microsurg* **2007,** 23, (8), 497-503.

126. Ramirez, O. M., Buccal fat pad pedicle flap for midface augmentation. *Ann Plast Surg* **1999,** 43, (2), 109-18.

127. Locke, M. B.; de Chalain, T. M., Current practice in autologous fat transplantation: suggested clinical guidelines based on a review of recent literature. *Ann Plast Surg* **2008,** 60, (1), 98-102.

128. Ward, B. B.; Feinberg, S. E.; Friedman, C. D., Tissue matrices for soft tissue and mucosal augmentation and replacement. *Facial Plast Surg* **2002,** 18, (1), 3-11.

129. Bajnrauh, R.; Nguyen, E. V.; Reifler, D. M.; Wilcox, R. M., Dressing ignition and facial burns following orbital exenteration. *Ophthal Plast Reconstr Surg* **2007,** 23, (5), 409-11.

130. Banks, N. D.; Milner, S., Persistence of human skin allograft in a burn patient without exogenous immunosuppression. *Plast Reconstr Surg* **2008,** 121, (4), 230e-1e.

131. Wendt, J. R.; Ulich, T.; Rao, P. N., Long-term survival of human skin allografts in patients with immunosuppression. *Plast Reconstr Surg* **2004,** 113, (5), 1347-54.

132. Devauchelle, B.; Badet, L.; Lengele, B.; Morelon, E.; Testelin, S.; Michallet, M.; D'Hauthuille, C.; Dubernard, J. M., First human face allograft: early report. *Lancet* **2006,** 368, (9531), 203-9.

133. Pomahac, B.; Aflaki, P.; Chandraker, A.; Pribaz, J. J., Facial Transplantation and Immunosuppressed Patients: A New Frontier in Reconstructive Surgery. *Transplantation* **2008,** 85, (12), 1693-1697.

134. Dubernard, J. M.; Lengele, B.; Morelon, E.; Testelin, S.; Badet, L.; Moure, C.; Beziat, J. L.; Dakpe, S.; Kanitakis, J.; D'Hauthuille, C.; El Jaafari, A.; Petruzzo, P.; Lefrancois, N.; Taha, F.; Sirigu, A.; Di Marco, G.; Carmi, E.; Bachmann, D.; Cremades, S.; Giraux, P.; Burloux, G.; Hequet, O.; Parquet, N.; Frances, C.; Michallet, M.; Martin, X.; Devauchelle, B., Outcomes 18 months after the first human partial face transplantation. *N Engl J Med* **2007,** 357, (24), 2451-60.

135. Sclafani, A. P.; Romo, T., 3rd; Jacono, A. A.; McCormick, S.; Cocker, R.; Parker, A., Evaluation of acellular dermal graft in sheet (AlloDerm) and injectable (micronized AlloDerm) forms for soft tissue augmentation. Clinical observations and histological analysis. *Arch Facial Plast Surg* **2000,** 2, (2), 130-6.

136. Sclafani, A. P.; Romo, T., 3rd; Jacono, A. A.; McCormick, S. A.; Cocker, R.; Parker, A., Evaluation of acellular dermal graft (AlloDerm) sheet for soft tissue

augmentation: a 1-year follow-up of clinical observations and histological findings. *Arch Facial Plast Surg* **2001,** 3, (2), 101-3.

137. Callcut, R. A.; Schurr, M. J.; Sloan, M.; Faucher, L. D., Clinical experience with Alloderm: a one-staged composite dermal/epidermal replacement utilizing processed cadaver dermis and thin autografts. *Burns* **2006,** 32, (5), 583-8.

138. Taban, M.; Douglas, R.; Li, T.; Goldberg, R. A.; Shorr, N., Efficacy of "thick" acellular human dermis (AlloDerm) for lower eyelid reconstruction: comparison with hard palate and thin AlloDerm grafts. *Arch Facial Plast Surg* **2005,** 7, (1), 38-44.

139. Kellner, D. S.; Fracchia, J. A.; Voigt, E.; Armenakas, N. A., Preliminary report on use of AlloDerm for closure of intraoral defects after buccal mucosal harvest. *Urology* **2007,** 69, (2), 372-4.

140. Sclafani, A. P.; Romo, T., 3rd; Jacono, A. A., Rejuvenation of the aging lip with an injectable acellular dermal graft (Cymetra). *Arch Facial Plast Surg* **2002,** 4, (4), 252-7.

141. Douglas, R. S.; Donsoff, I.; Cook, T.; Shorr, N., Collagen fillers in facial aesthetic surgery. *Facial Plast Surg* **2004,** 20, (2), 117-23.

142. Monheit, G. D., Hylaform: a new hyaluronic acid filler. *Facial Plast Surg* **2004,** 20, (2), 153-5.

143. Rohrich, R. J.; Ghavami, A.; Crosby, M. A., The role of hyaluronic acid fillers (Restylane) in facial cosmetic surgery: review and technical considerations. *Plast Reconstr Surg* **2007,** 120, (6 Suppl), 41S-54S.

144. Homicz, M. R.; Watson, D., Review of injectable materials for soft tissue augmentation. *Facial Plast Surg* **2004,** 20, (1), 21-9.

145. Humble, G.; Mest, D., Soft tissue augmentation using silicone: an historical review. *Facial Plast Surg* **2004,** 20, (2), 181-4.

146. Rullan, P. P., Soft tissue augmentation using artecoll: a personal experience. *Facial Plast Surg* **2004,** 20, (2), 111-6.

147. Hoffmann, C.; Schuller-Petrovic, S.; Soyer, H. P.; Kerl, H., Adverse reactions after cosmetic lip augmentation with permanent biologically inert implant materials. *J Am Acad Dermatol* **1999,** 40, (1), 100-2.

148. Lam, S. M.; Azizzadeh, B.; Graivier, M., Injectable poly-L-lactic acid (Sculptra): technical considerations in soft-tissue contouring. *Plast Reconstr Surg* **2006,** 118, (3 Suppl), 55S-63S.

149. Lontz, J. F., State-of-the-art materials used for maxillofacial prosthetic reconstruction. *Dent Clin North Am* **1990,** 34, (2), 307-25.

150. Beumer, J.; Curtis, T. A.; Marunick, M. T., *Maxillofacial Rehabilitation: Prosthodontic and Surgical Considerations.* Ishiyaku EuroAmerica Inc.: St. Louis, 1996.

151. Chalian, V. A., Maxillofacial Prosthetic Materials. In *Biocompatibility of Dental Materials*, Smith, D. C.; Williams, D. F., Eds. CRC Press: Boca Raton, 1981; Vol. 4, pp 247-63.

152. Gonzalez, J. B., Polyurethane elastomers for facial prostheses. *J Prosthet Dent* **1978,** 39, (2), 179-87.

153. Andres, C. J.; Haug, S. P.; Brown, D. T.; Bernal, G., Effects of environmental factors on maxillofacial elastomers: Part II--Report of survey. *J Prosthet Dent* **1992,** 68, (3), 519-22.

154. Moore, D. J.; Glaser, Z. R.; Tabacco, M. J.; Linebaugh, M. G., Evaluation of polymeric materials for maxillofacial prosthetics. *J Prosthet Dent* **1977,** 38, (3), 319-26.

155. Aziz, T.; Waters, M.; Jagger, R., Development of a new poly(dimethylsiloxane) maxillofacial prosthetic material. *J Biomed Mater Res B Appl Biomater* **2003,** 65, (2), 252-61.

156. Aziz, T.; Waters, M.; Jagger, R., Surface modification of an experimental silicone rubber maxillofacial material to improve wettability. *J Dent* **2003,** 31, (3), 213-6.

157. Warnke, P. H.; Springer, I. N.; Wiltfang, J.; Acil, Y.; Eufinger, H.; Wehmoller, M.; Russo, P. A.; Bolte, H.; Sherry, E.; Behrens, E.; Terheyden, H., Growth and transplantation of a custom vascularised bone graft in a man. *Lancet* **2004,** 364, (9436), 766-70.

158. Warnke, P. H.; Wiltfang, J.; Springer, I.; Acil, Y.; Bolte, H.; Kosmahl, M.; Russo, P. A.; Sherry, E.; Lutzen, U.; Wolfart, S.; Terheyden, H., Man as living bioreactor: fate of an exogenously prepared customized tissue-engineered mandible. *Biomaterials* **2006,** 27, (17), 3163-7.

159. Mikos, A. G.; Herring, S. W.; Ochareon, P.; Elisseeff, J.; Lu, H. H.; Kandel, R.; Schoen, F. J.; Toner, M.; Mooney, D.; Atala, A.; Van Dyke, M. E.; Kaplan, D.; Vunjak-Novakovic, G., Engineering complex tissues. *Tissue Eng* **2006,** 12, (12), 3307-39.

160. Warren, S. M.; Fong, K. D.; Chen, C. M.; Loboa, E. G.; Cowan, C. M.; Lorenz, H. P.; Longaker, M. T., Tools and techniques for craniofacial tissue engineering. *Tissue Eng* **2003,** 9, (2), 187-200.

161. Goessler, U.; Stern-Straeter, J.; Riedel, K.; Bran, G.; Hörmann, K.; Riedel, F., Tissue engineering in head and neck reconstructive surgery: what type of tissue do we need? *Eur Arch Otorhinolaryngol* **2007,** 264, (11), 1343-1356.

162. Mao, J. J.; Giannobile, W. V.; Helms, J. A.; Hollister, S. J.; Krebsbach, P. H.; Longaker, M. T.; Shi, S., Craniofacial tissue engineering by stem cells. *J Dent Res* **2006,** 85, (11), 966-79.

163. Downey, P. A.; Siegel, M. I., Bone biology and the clinical implications for osteoporosis. *Phys Ther* **2006,** 86, (1), 77-91.

164. Habibovic, P.; de Groot, K., Osteoinductive biomaterials--properties and relevance in bone repair. *J Tissue Eng Regen Med* **2007,** 1, (1), 25-32.

165. Holland, T. A.; Mikos, A. G., Biodegradable polymeric scaffolds. Improvements in bone tissue engineering through controlled drug delivery. *Adv Biochem Eng Biotechnol* **2006,** 102, 161-85.

166. Khan, Y.; Yaszemski, M. J.; Mikos, A. G.; Laurencin, C. T., Tissue engineering of bone: material and matrix considerations. *J Bone Joint Surg Am* **2008,** 90 Suppl 1, 36-42.

167. Kretlow, J. D.; Klouda, L.; Mikos, A. G., Injectable matrices and scaffolds for drug delivery in tissue engineering. *Adv Drug Deliv Rev* **2007,** 59, (4-5), 263-73.

168. Salgado, A. J.; Oliveira, J. T.; Pedro, A. J.; Reis, R. L., Adult stem cells in bone and cartilage tissue engineering. *Curr Stem Cell Res Ther* **2006,** 1, (3), 345-64.

169. Kretlow, J. D.; Mikos, A. G., Review: mineralization of synthetic polymer scaffolds for bone tissue engineering. *Tissue Eng* **2007,** 13, (5), 927-38.

170. Villanueva, J. E.; Nimni, M. E., Promotion of calvarial cell osteogenesis by endothelial cells. *J Bone Miner Res* **1990,** 5, (7), 733-9.

171. Huang, Y. C.; Kaigler, D.; Rice, K. G.; Krebsbach, P. H.; Mooney, D. J., Combined angiogenic and osteogenic factor delivery enhances bone marrow stromal cell-driven bone regeneration. *J Bone Miner Res* **2005,** 20, (5), 848-57.

172. Leach, J. K.; Kaigler, D.; Wang, Z.; Krebsbach, P. H.; Mooney, D. J., Coating of VEGF-releasing scaffolds with bioactive glass for angiogenesis and bone regeneration. *Biomaterials* **2006,** 27, (17), 3249-55.

173. Jeon, O.; Song, S. J.; Kang, S. W.; Putnam, A. J.; Kim, B. S., Enhancement of ectopic bone formation by bone morphogenetic protein-2 released from a heparin-conjugated poly(L-lactic-co-glycolic acid) scaffold. *Biomaterials* **2007,** 28, (17), 2763-71.

174. Kroese-Deutman, H. C.; Ruhe, P. Q.; Spauwen, P. H.; Jansen, J. A., Bone inductive properties of rhBMP-2 loaded porous calcium phosphate cement implants inserted at an ectopic site in rabbits. *Biomaterials* **2005,** 26, (10), 1131-8.

175. Castano-Izquierdo, H.; ¡lvarez-Barreto, J.; Dolder, J. v. d.; Jansen, J. A.; Mikos, A. G.; Sikavitsas, V. I., Pre-culture period of mesenchymal stem cells in

osteogenic media influences their *in vivo* bone forming potential. *J Biomed Mater Res A* **2007,** 82A, (1), 129-138.

176. Dadsetan, M.; Hefferan, T. E.; Szatkowski, J. P.; Mishra, P. K.; Macura, S. I.; Lu, L.; Yaszemski, M. J., Effect of hydrogel porosity on marrow stromal cell phenotypic expression. *Biomaterials* **2008,** 29, (14), 2193-202.

177. Na, K.; Kim, S. W.; Sun, B. K.; Woo, D. G.; Yang, H. N.; Chung, H. M.; Park, K. H., Osteogenic differentiation of rabbit mesenchymal stem cells in thermo-reversible hydrogel constructs containing hydroxyapatite and bone morphogenic protein-2 (BMP-2). *Biomaterials* **2007,** 28, (16), 2631-7.

178. Sumanasinghe, R. D.; Osborne, J. A.; Loboa, E. G., Mesenchymal stem cell-seeded collagen matrices for bone repair: Effects of cyclic tensile strain, cell density, and media conditions on matrix contraction in vitro. *J Biomed Mater Res A* **2008**.

179. Burke, J. F.; Yannas, I. V.; Quinby, W. C., Jr.; Bondoc, C. C.; Jung, W. K., Successful use of a physiologically acceptable artificial skin in the treatment of extensive burn injury. *Ann Surg* **1981,** 194, (4), 413-28.

180. Tremblay, P. L.; Hudon, V.; Berthod, F.; Germain, L.; Auger, F. A., Inosculation of tissue-engineered capillaries with the host's vasculature in a reconstructed skin transplanted on mice. *Am J Transplant* **2005,** 5, (5), 1002-10.

181. Metcalfe, A. D.; Ferguson, M. W., Tissue engineering of replacement skin: the crossroads of biomaterials, wound healing, embryonic development, stem cells and regeneration. *J R Soc Interface* **2007,** 4, (14), 413-37.

182. Black, A. F.; Berthod, F.; L'Heureux, N.; Germain, L.; Auger, F. A., In vitro reconstruction of a human capillary-like network in a tissue-engineered skin equivalent. *FASEB J* **1998,** 12, (13), 1331-40.

183. Farhadi, J.; Fulco, I.; Miot, S.; Wirz, D.; Haug, M.; Dickinson, S. C.; Hollander, A. P.; Daniels, A. U.; Pierer, G.; Heberer, M.; Martin, I., Precultivation of engineered human nasal cartilage enhances the mechanical properties relevant for use in facial reconstructive surgery. *Ann Surg* **2006,** 244, (6), 978-85; discussion 985.

184. Isogai, N.; Kusuhara, H.; Ikada, Y.; Ohtani, H.; Jacquet, R.; Hillyer, J.; Lowder, E.; Landis, W. J., Comparison of different chondrocytes for use in tissue engineering of cartilage model structures. *Tissue Eng* **2006,** 12, (4), 691-703.

185. Kamil, S. H.; Kojima, K.; Vacanti, M. P.; Bonassar, L. J.; Vacanti, C. A.; Eavey, R. D., In vitro tissue engineering to generate a human-sized auricle and nasal tip. *Laryngoscope* **2003,** 113, (1), 90-4.

186. Allen, K. D.; Athanasiou, K. A., Tissue Engineering of the TMJ disc: a review. *Tissue Eng* **2006,** 12, (5), 1183-96.

187. Detamore, M. S.; Athanasiou, K. A., Motivation, characterization, and strategy for tissue engineering the temporomandibular joint disc. *Tissue Eng* **2003,** 9, (6), 1065-87.

188. Johns, D. E.; Athanasiou, K. A., Design characteristics for temporomandibular joint disc tissue engineering: learning from tendon and articular cartilage. *Proc Inst Mech Eng [H]* **2007,** 221, (5), 509-26.

189. Alhadlaq, A.; Mao, J. J., Tissue-engineered neogenesis of human-shaped mandibular condyle from rat mesenchymal stem cells. *J Dent Res* **2003,** 82, (12), 951-6.

190. Moioli, E. K.; Clark, P. A.; Xin, X.; Lal, S.; Mao, J. J., Matrices and scaffolds for drug delivery in dental, oral and craniofacial tissue engineering. *Adv Drug Deliv Rev* **2007,** 59, (4-5), 308-324.

191. Shah, R.; Sinanan, A. C. M.; Knowles, J. C.; Hunt, N. P.; Lewis, M. P., Craniofacial muscle engineering using a 3-dimensional phosphate glass fibre construct. *Biomaterials* **2005,** 26, (13), 1497-1505.

192. Kaar, J. L.; Li, Y.; Blair, H. C.; Asche, G.; Koepsel, R. R.; Huard, J.; Russell, A. J., Matrix metalloproteinase-1 treatment of muscle fibrosis. *Acta Biomater* **2008,** 4, (5), 1411-20.

193. Lewis, M. P.; Machell, J. R.; Hunt, N. P.; Sinanan, A. C.; Tippett, H. L., The extracellular matrix of muscle--implications for manipulation of the craniofacial musculature. *Eur J Oral Sci* **2001,** 109, (4), 209-21.

194. Tippett, H. L.; Dodgson, L. K.; Hunt, N. P.; Lewis, M. P., Indices of extracellular matrix turnover in human masseter muscles as markers of craniofacial form--a preliminary study. *Eur J Orthod* **2008,** 30, (2), 217-25.

195. Gawlitta, D.; Boonen, K. J.; Oomens, C. W.; Baaijens, F. P.; Bouten, C. V., The influence of serum-free culture conditions on skeletal muscle differentiation in a tissue-engineered model. *Tissue Eng Part A* **2008,** 14, (1), 161-71.

196. Stern-Straeter, J.; Bran, G.; Riedel, F.; Sauter, A.; Hormann, K.; Goessler, U. R., Characterization of human myoblast cultures for tissue engineering. *Int J Mol Med* **2008,** 21, (1), 49-56.

197. Powers, M. P.; Bosker, H., Functional and cosmetic reconstruction of the facial lower third associated with placement of the transmandibular implant system. *J Oral Maxillofac Surg* **1996,** 54, (8), 934-42.

198. Tzikas, T. L., Lipografting: autologous fat grafting for total facial rejuvenation. *Facial Plast Surg* **2004,** 20, (2), 135-43.

199. Alhadlaq, A.; Tang, M.; Mao, J. J., Engineered adipose tissue from human mesenchymal stem cells maintains predefined shape and dimension: implications in soft tissue augmentation and reconstruction. *Tissue Eng* **2005,** 11, (3-4), 556-66.

200. Mauney, J. R.; Nguyen, T.; Gillen, K.; Kirker-Head, C.; Gimble, J. M.; Kaplan, D. L., Engineering adipose-like tissue in vitro and in vivo utilizing human bone marrow and adipose-derived mesenchymal stem cells with silk fibroin 3D scaffolds. *Biomaterials* **2007,** 28, (35), 5280-90.

201. Neubauer, M.; Hacker, M.; Bauer-Kreisel, P.; Weiser, B.; Fischbach, C.; Schulz, M. B.; Goepferich, A.; Blunk, T., Adipose tissue engineering based on mesenchymal stem cells and basic fibroblast growth factor in vitro. *Tissue Eng* **2005,** 11, (11-12), 1840-51.

202. Hong, L.; Peptan, I. A.; Colpan, A.; Daw, J. L., Adipose tissue engineering by human adipose-derived stromal cells. *Cells Tissues Organs* **2006,** 183, (3), 133-40.

203. Marra, K. G.; Defail, A. J.; Clavijo-Alvarez, J. A.; Badylak, S. F.; Taieb, A.; Schipper, B.; Bennett, J.; Rubin, J. P., FGF-2 enhances vascularization for adipose tissue engineering. *Plast Reconstr Surg* **2008,** 121, (4), 1153-64.

204. Ferreira, J. N. A. R.; Ko, C.-C.; Myers, S.; Swift, J.; Fricton, J. R., Evaluation of Surgically Retrieved Temporomandibular Joint Alloplastic Implants: Pilot Study. *J Oral Maxillofac Surg* **2008,** 66, (6), 1112-1124.

205. Hollister, S. J.; Lin, C. Y.; Saito, E.; Lin, C. Y.; Schek, R. D.; Taboas, J. M.; Williams, J. M.; Partee, B.; Flanagan, C. L.; Diggs, A.; Wilke, E. N.; Van Lenthe, G. H.; Muller, R.; Wirtz, T.; Das, S.; Feinberg, S. E.; Krebsbach, P. H., Engineering craniofacial scaffolds. *Orthod Craniofac Res* **2005,** 8, (3), 162-73.

206. Schwartz-Dabney, C. L.; Dechow, P. C., Edentulation Alters Material Properties of Cortical Bone in the Human Mandible. *J Dent Res* **2002,** 81, (9), 613-617.

207. Schwartz-Dabney, C. L.; Dechow, P. C., Variations in cortical material properties throughout the human dentate mandible. *Am J Phys Anthropol* **2003,** 120, (3), 252-277.

208. Peterson, J.; Dechow, P. C., Material properties of the human cranial vault and zygoma. *Anat Rec A Discov Mol Cell Evol Biol* **2003,** 274A, (1), 785-797.

209. Hannam, A. G.; Stavness, I.; Lloyd, J. E.; Fels, S., A dynamic model of jaw and hyoid biomechanics during chewing. *J Biomech* **2008,** 41, (5), 1069-1076.

210. Friedman, C. D.; Costantino, P. D.; Takagi, S.; Chow, L. C., BoneSource hydroxyapatite cement: a novel biomaterial for craniofacial skeletal tissue engineering and reconstruction. *J Biomed Mater Res* **1998,** 43, (4), 428-32.

211. Sipp, J. A.; Ashland, J.; Hartnick, C. J., Injection Pharyngoplasty With Calcium Hydroxyapatite for Treatment of Velopalatal Insufficiency. *Arch Otolaryngol Head Neck Surg* **2008,** 134, (3), 268-271.

212. Real, R. P. d.; Ooms, E.; Wolke, J. G. C.; Vallet-Regí, M.; Jansen, J. A., *In vivo* bone response to porous calcium phosphate cement. *J Biomed Mater Res A* **2003,** 65A, (1), 30-36.

213. Ruhe, P. Q.; Hedberg, E. L.; Padron, N. T.; Spauwen, P. H.; Jansen, J. A.; Mikos, A. G., Biocompatibility and degradation of poly(DL-lactic-co-glycolic acid)/calcium phosphate cement composites. *J Biomed Mater Res A* **2005,** 74, (4), 533-44.

214. Habraken, W. J. E. M.; Wolfe, J. G. C.; Mikos, A. G.; Jansen, J. A., Injectable PLGA microsphere/calcium phosphate cements: physical properties and degradation characteristics. *J Biomater Sci Polym Ed* **2006,** 17, (9), 1057-1074.

215. Ruhe, P. Q.; Hedberg-Dirk, E. L.; Padron, N. T.; Spauwen, P. H. M.; Jansen, J. A.; Mikos, A. G., Porous poly(DL-lactic-co-glycolic acid)/calcium phosphate cement composite for reconstruction of bone defects. *Tissue Eng* **2006,** 12, (4), 789-800.

216. Link, D. P.; van den Dolder, J.; van den Beucken, J. J.; Cuijpers, V. M.; Wolke, J. G.; Mikos, A. G.; Jansen, J. A., Evaluation of the biocompatibility of calcium phosphate cement/PLGA microparticle composites. *J Biomed Mater Res A* **2008,** 87, (3), 760-9.

217. Habraken, W. J.; Zhang, Z.; Wolke, J. G.; Grijpma, D. W.; Mikos, A. G.; Feijen, J.; Jansen, J. A., Introduction of enzymatically degradable poly(trimethylene carbonate) microspheres into an injectable calcium phosphate cement. *Biomaterials* **2008,** 29, (16), 2464-76.

218. Habraken, W. J.; de Jonge, L. T.; Wolke, J. G.; Yubao, L.; Mikos, A. G.; Jansen, J. A., Introduction of gelatin microspheres into an injectable calcium phosphate cement. *J Biomed Mater Res A* **2008,** 87, (3), 643-55.

219. Ruhe, P. Q.; Boerman, O. C.; Russel, F. G.; Mikos, A. G.; Spauwen, P. H.; Jansen, J. A., In vivo release of rhBMP-2 loaded porous calcium phosphate cement pretreated with albumin. *J Mater Sci Mater Med* **2006,** 17, (10), 919-27.

220. Bodde, E. W.; Boerman, O. C.; Russel, F. G.; Mikos, A. G.; Spauwen, P. H.; Jansen, J. A., The kinetic and biological activity of different loaded rhBMP-2 calcium phosphate cement implants in rats. *J Biomed Mater Res A* **2008,** 87, (3), 780-91.

221. DiCicco, M.; Goldfinger, A.; Guirand, F.; Abdullah, A.; Jansen, S. A., In vitro tobramycin elution analysis from a novel beta-tricalcium phosphate-silicate-xerogel biodegradable drug-delivery system. *J Biomed Mater Res B Appl Biomater* **2004,** 70, (1), 1-20.

222. Xu, H. H. K.; Weir, M. D.; Burguera, E. F.; Fraser, A. M., Injectable and macroporous calcium phosphate cement scaffold. *Biomaterials* **2006,** 27, (24), 4279-4287.

223. Xu, H. H. K.; Quinn, J. B.; Takagi, S.; Chow, L. C., Synergistic reinforcement of in situ hardening calcium phosphate composite scaffold for bone tissue engineering. *Biomaterials* **2004,** 25, (6), 1029-1037.

224. Xu, H. H. K.; Carl G. Simon, J., Self-hardening calcium phosphate composite scaffold for bone tissue engineering. *J Orthop Res* **2004,** 22, (3), 535-543.

225. Fellah, B. H.; Weiss, P.; Gauthier, O.; Rouillon, T.; Pilet, P.; Daculsi, G.; Layrolle, P., Bone repair using a new injectable self-crosslinkable bone substitute. *J Orthop Res* **2006,** 24, (4), 628-635.

226. Trojani, C.; Boukhechba, F.; Scimeca, J. C.; Vandenbos, F.; Michiels, J. F.; Daculsi, G.; Boileau, P.; Weiss, P.; Carle, G. F.; Rochet, N., Ectopic bone formation using an injectable biphasic calcium phosphate/Si-HPMC hydrogel composite loaded with undifferentiated bone marrow stromal cells. *Biomaterials* **2006,** 27, (17), 3256-64.

227. Gauthier, O.; Goyenvalle, E.; Bouler, J. M.; Guicheux, J.; Pilet, P.; Weiss, P.; Daculsi, G., Macroporous biphasic calcium phosphate ceramics versus injectable bone substitute: A comparative study 3 and 8 weeks after implantation in rabbit bone. *J Mater Sci Mater Med* **2001,** 12, (5), 385-390.

228. Gauthier, O.; Khairoun, I.; Bosco, J.; Obadia, L.; Bourges, X.; Rau, C.; Magne, D.; Bouler, J. M.; Aguado, E.; Daculsi, G.; Weiss, P., Noninvasive bone replacement with a new injectable calcium phosphate biomaterial. *J Biomed Mater Res A* **2003,** 66, (1), 47-54.

229. Gauthier, O.; Muller, R.; Stechow, D.; Lamy, B.; Weiss, P.; Bouler, J. M.; Aguado, E.; Daculsi, G., In vivo bone regeneration with injectable calcium

phosphate biomaterial: A three-dimensional micro-computed tomographic, biomechanical and SEM study. *Biomaterials* **2005,** 26, (27), 5444-53.

230. Leeuwenburgh, S. C.; Jansen, J. A.; Mikos, A. G., Functionalization of oligo(poly(ethylene glycol)fumarate) hydrogels with finely dispersed calcium phosphate nanocrystals for bone-substituting purposes. *J Biomater Sci Polym Ed* **2007,** 18, (12), 1547-64.

231. Gonzalez-McQuire, R.; Green, D. W.; Partridge, K. A.; Oreffo, R. O. C.; Mann, S.; Davis, S. A., Coating of human mesenchymal cells in 3D culture with bioinorganic nanoparticles promotes osteoblastic differentiation and gene transfection. *Adv Mater* **2007,** 19, (17), 2236-2240.

232. Fisher, J. P.; Holland, T. A.; Dean, D.; Engel, P. S.; Mikos, A. G., Synthesis and properties of photocross-linked poly(propylene fumarate) scaffolds. *J Biomater Sci Polym Ed* **2001,** 12, (6), 673-87.

233. Fisher, J. P.; Dean, D.; Mikos, A. G., Photocrosslinking characteristics and mechanical properties of diethyl fumarate/poly(propylene fumarate) biomaterials. *Biomaterials* **2002,** 23, (22), 4333-43.

234. Buxton, A. N.; Zhu, J.; Marchant, R.; West, J. L.; Yoo, J. U.; Johnstone, B., Design and Characterization of Poly(Ethylene Glycol) Photopolymerizable Semi-Interpenetrating Networks for Chondrogenesis of Human Mesenchymal Stem Cells. *Tissue Eng* **2007,** 13, (10), 2549-2560.

235. Hahn, M. S.; Taite, L. J.; Moon, J. J.; Rowland, M. C.; Ruffino, K. A.; West, J. L., Photolithographic patterning of polyethylene glycol hydrogels. *Biomaterials* **2006,** 27, (12), 2519-2524.

236. Declercq, H. A.; Gorski, T. L.; Tielens, S. P.; Schacht, E. H.; Cornelissen, M. J., Encapsulation of osteoblast seeded microcarriers into injectable, photopolymerizable three-dimensional scaffolds based on D,L-lactide and epsilon-caprolactone. *Biomacromolecules* **2005,** 6, (3), 1608-1614.

237. Declercq, H. A.; Cornelissen, M. J.; Gorskiy, T. L.; Schacht, E. H., Osteoblast behaviour on in situ photopolymerizable three-dimensional scaffolds based on D, L-lactide, epsilon-caprolactone and trimethylene carbonate. *J Mater Sci Mater Med* **2006,** 17, (2), 113-22.

238. Elisseeff, J.; Anseth, K.; Sims, D.; McIntosh, W.; Randolph, M.; Langer, R., Transdermal photopolymerization for minimally invasive implantation. *Proc Natl Acad Sci U S A* **1999,** 96, (6), 3104-7.

239. Elisseeff, J.; Anseth, K.; Sims, D.; McIntosh, W.; Randolph, M.; Yaremchuk, M.; Langer, R., Transdermal photopolymerization of poly(ethylene oxide)-based injectable hydrogels for tissue-engineered cartilage. *Plast Reconstr Surg* **1999,** 104, (4), 1014-22.

240. Hahn, M. S.; Miller, J. S.; West, J. L., Three-dimensional biochemical and biomechanical patterning of hydrogels for guiding cell behavior. *Adv Mater* **2006,** 18, (20), 2679-2684.

241. Sun, Z. B.; Dong, X. Z.; Chen, W. Q.; Nakanishi, S.; Duan, X. M.; Kawata, S., Multicolor polymer nanocomposites: In situ synthesis and fabrication of 3D microstructures. *Adv Mater* **2008,** 20, (5), 914-919.

242. Burdick, J. A.; Khademhosseini, A.; Langer, R., Fabrication of gradient hydrogels using a microfluidics/photopolymerization process. *Langmuir* **2004,** 20, (13), 5153-5156.

243. Temenoff, J. S.; Shin, H.; Conway, D. E.; Engel, P. S.; Mikos, A. G., In vitro cytotoxicity of redox radical initiators for cross-linking of oligo(poly(ethylene glycol) fumarate) macromers. *Biomacromolecules* **2003,** 4, (6), 1605-13.

244. Shin, H.; Temenoff, J. S.; Mikos, A. G., In vitro cytotoxicity of unsaturated oligo[poly(ethylene glycol) fumarate] macromers and their cross-linked hydrogels. *Biomacromolecules* **2003,** 4, (3), 552-60.

245. Vernon, B.; Tirelli, N.; Bachi, T.; Haldimann, D.; Hubbell, J. A., Water-borne, in situ crosslinked biomaterials from phase-segregated precursors. *J Biomed Mater Res A* **2003,** 64, (3), 447-456.

246. Gray, D. H.; Hu, S. L.; Juang, E.; Gin, D. L., Highly ordered polymer-inorganic nanocomposites via monomer self-assembly: In situ condensation approach. *Adv Mater* **1997,** 9, (9), 731-736.

247. Wang, J.; Liu, C.; Chi, P., In situ preparation of glycoconjugate hollow microspheres mimics the extracellular matrix via interfacial polymerization. *Int J Biol Macromol* **2008,** 42, (5), 450-4.

248. Ehrbar, M.; Rizzi, S. C.; Hlushchuk, R.; Djonov, V.; Zisch, A. H.; Hubbell, J. A.; Weber, F. E.; Lutolf, M. P., Enzymatic formation of modular cell-instructive fibrin analogs for tissue engineering. *Biomaterials* **2007,** 28, (26), 3856-3866.

249. Sanborn, T. J.; Messersmith, P. B.; Barron, A. E., In situ crosslinking of a biomimetic peptide-PEG hydrogel via thermally triggered activation of factor XIII. *Biomaterials* **2002,** 23, (13), 2703-2710.

250. Jin, R.; Hiemstra, C.; Zhong, Z.; Feijen, J., Enzyme-mediated fast in situ formation of hydrogels from dextran-tyramine conjugates. *Biomaterials* **2007,** 28, (18), 2791-2800.

251. Halloran, D. O.; Grad, S.; Stoddart, M.; Dockery, P.; Alini, M.; Pandit, A. S., An injectable cross-linked scaffold for nucleus pulposus regeneration. *Biomaterials* **2008,** 29, (4), 438-47.

252. O Halloran, D. M.; Collighan, R. J.; Griffin, M.; Pandit, A. S., Characterization of a Microbial Transglutaminase Cross-linked Type II Collagen Scaffold. *Tissue Eng* **2006,** 12, (6), 1467-1474.

253. Griffin, M.; Casadio, R.; Bergamini, C. M., Transglutaminases: nature's biological glues. *Biochem J* **2002,** 368, (Pt 2), 377-96.

254. Heath, D. J.; Christian, P.; Griffin, M., Involvement of tissue transglutaminase in the stabilisation of biomaterial/tissue interfaces important in medical devices. *Biomaterials* **2002,** 23, (6), 1519-26.

255. Galaev, I. Y.; Mattiasson, B., 'Smart' polymers and what they could do in biotechnology and medicine. *Trends Biotechnol* **1999,** 17, (8), 335-40.

256. Qiu, Y.; Park, K., Environment-sensitive hydrogels for drug delivery. *Adv Drug Deliv Rev* **2001,** 53, (3), 321-39.

257. Jayawarna, V.; Ali, M.; Jowitt, T. A.; Miller, A. F.; Saiani, A.; Gough, J. E.; Ulijn, R. V., Nanostructured Hydrogels for Three-Dimensional Cell Culture Through Self-Assembly of Fluorenylmethoxycarbony-Dipeptides. *Adv Mater* **2006,** 18, 611-614.

258. Klouda, L.; Mikos, A. G., Thermoresponsive hydrogels in biomedical applications. *Eur J Pharm Biopharm* **2008,** 68, (1), 34-45.

259. Lin, H.-H.; Cheng, Y.-L., In-situ thermoreversible gelation of block and star copolymers of poly(ethylene glycol) and poly(n-isopropylacrylamide) of varying architectures. *Macromolecules* **2001,** 34, (11), 3710-3715.

260. Ohya, S.; Nakayama, Y.; Matsuda, T., Thermoresponsive artificial extracellular matrix for tissue engineering: hyaluronic acid bioconjugated with poly(N-isopropylacrylamide) grafts. *Biomacromolecules* **2001,** 2, (3), 856-63.

261. Ohya, S.; Nakayama, Y.; Matsuda, T., In vivo evaluation of poly(N-isopropylacrylamide) (PNIPAM)-grafted gelatin as an in situ-formable scaffold. *J Artif Organs* **2004,** 7, (4), 181-6.

262. Hacker, M. C.; Klouda, L.; Ma, B. B.; Kretlow, J. D.; Mikos, A. G., Synthesis and Characterization of Injectable, Thermally and Chemically Gelable, Amphiphilic Poly(N-isopropylacrylamide)-Based Macromers. *Biomacromolecules* **2008,** 9, (3), 1558-1570.

263. Sosnik, A.; Cohn, D., Ethoxysilane-capped PEO-PPO-PEO triblocks: A new family of reverse thermo-responsive polymers. *Biomaterials* **2004,** 25, (14), 2851-2858.

264. Sosnik, A.; Cohn, D., Reverse thermo-responsive poly(ethylene oxide) and poly(propylene oxide) multiblock copolymers. *Biomaterials* **2005,** 26, (4), 349-357.

265. Cohn, D.; Sosnik, A.; Garty, S., Smart hydrogels for in situ generated implants. *Biomacromolecules* **2005,** 6, (3), 1168-1175.

266. Fisher, J. P.; Jo, S.; Mikos, A. G.; Reddi, A. H., Thermoreversible hydrogel scaffolds for articular cartilage engineering. *J Biomed Mater Res A* **2004,** 71, (2), 268-274.

267. Seong, J.-Y.; Jun, Y. J.; Jeong, B.; Sohn, Y. S., New thermogelling poly(organophosphazenes) with methoxypoly(ethylene glycol) and oligopeptide as side groups. *Polymer* **2005,** 46, (14), 5075-81.

268. Jeong, B.; Lee, K. M.; Gutowska, A.; An, Y. H., Thermogelling Biodegradable Copolymer Aqueous Solutions for Injectable Protein Delivery and Tissue Engineering. *Biomacromolecules* **2002,** 3, (4), 865-868.

269. Nair, L. S.; Starnes, T.; Ko, J.-W. K.; Laurencin, C. T., Development of Injectable Thermogelling Chitosan - Inorganic Phosphate Solutions for Biomedical Applications. *Biomacromolecules* **2007,** 8, (12), 3779-3785.

270. Bhattarai, N.; Ramay, H. R.; Gunn, J.; Matsen, F. A.; Zhang, M., PEG-grafted chitosan as an injectable thermosensitive hydrogel for sustained protein release. *J Control Release* **2005,** 103, (3), 609-624.

271. Zan, J.; Chen, H.; Jiang, G.; Lin, Y.; Ding, F., Preparation and properties of crosslinked chitosan thermosensitive hydrogel for injectable drug delivery systems. *J Appl Polym Sci* **2006,** 101, (3), 1892-1898.

272. Cellesi, F.; Tirelli, N.; Hubbell, J. A., Materials for cell encapsulation via a new tandem approach combining reverse thermal gelation and covalent crosslinking. *Macromol Chem Phys* **2002,** 203, (10-11), 1466-1472.

273. Cellesi, F.; Tirelli, N.; Hubbell, J. A., Towards a fully-synthetic substitute of alginate: Development of a new process using thermal gelation and chemical cross-linking. *Biomaterials* **2004,** 25, (21), 5115-5124.

274. Lee, B. H.; West, B.; McLemore, R.; Pauken, C.; Vernon, B. L., In-situ injectable physically and chemically gelling NIPAAm-based copolymer system for embolization. *Biomacromolecules* **2006,** 7, (6), 2059-64.

275. Robb, S. A.; Lee, B. H.; McLemore, R.; Vernon, B. L., Simultaneously physically and chemically gelling polymer system utilizing a poly(NIPAAm-co-cysteamine)-based copolymer. *Biomacromolecules* **2007,** 8, (7), 2294-300.

276. Dunn, R.; English, J.; Cowsar, D.; Venderbelt, D. Biodegradable in-situ forming implants and methods of producing the same. 4 938 763 3 July 1990, 1990.

277. Bakhshi, R.; Vasheghani-Farahani, E.; Mobedi, H.; Jamshidi, A.; Khakpour, M., The effect of additives on naltrexone hydrochloride release and solvent removal rate from an injectable in situ forming PLGA implant. *Polym Adv Technol* **2006,** 17, (5), 354-9.

278. Tae, G.; Kornfield, J. A.; Hubbell, J. A., Sustained release of human growth hormone from in situ forming hydrogels using self-assembly of fluoroalkyl-ended poly(ethylene glycol). *Biomaterials* **2005,** 26, (25), 5259-66.

279. Brittberg, M.; Sjögren-Jansson, E.; Lindahl, A.; Peterson, L., Influence of fibrin sealant (Tisseel®) on osteochondral defect repair in the rabbit knee. *Biomaterials* **1997,** 18, (3), 235-242.

280. Bensaid, W.; Triffitt, J. T.; Blanchat, C.; Oudina, K.; Sedel, L.; Petite, H., A biodegradable fibrin scaffold for mesenchymal stem cell transplantation. *Biomaterials* **2003,** 24, (14), 2497-2502.

281. Ho, W.; Tawil, B.; Dunn, J. C. Y.; Wu, B. M., The Behavior of Human Mesenchymal Stem Cells in 3D Fibrin Clots: Dependence on Fibrinogen Concentration and Clot Structure. *Tissue Eng* **2006,** 12, (6), 1587-1595.

282. Catelas, I.; Sese, N.; Wu, B. M.; Dunn, J. C. Y.; Helgerson, S.; Tawil, B., Human Mesenchymal Stem Cell Proliferation and Osteogenic Differentiation in Fibrin Gels in Vitro. *Tissue Eng* **2006,** 12, (8), 2385-2396.

283. Schmoekel, H. G.; Weber, F. E.; Schense, J. C.; Grätz, K. W.; Schawalder, P.; Hubbell, J. A., Bone repair with a form of BMP-2 engineered for incorporation into fibrin cell ingrowth matrices. *Biotechnol Bioeng* **2005,** 89, (3), 253-262.

284. Schense, J. C.; Bloch, J.; Aebischer, P.; Hubbell, J. A., Enzymatic incorporation of bioactive peptides into fibrin matrices enhances neurite extension. *Nat Biotechnol* **2000,** 18, (4), 415-419.

285. Haines-Butterick, L.; Rajagopal, K.; Branco, M.; Salick, D.; Rughani, R.; Pilarz, M.; Lamm, M. S.; Pochan, D. J.; Schneider, J. P., Controlling hydrogelation kinetics by peptide design for three-dimensional encapsulation and injectable delivery of cells. *Proc Natl Acad Sci U S A* **2007,** 104, (19), 7791-7796.

286. Guler, M. O.; Hsu, L.; Soukasene, S.; Harrington, D. A.; Hulvat, J. F.; Stupp, S. I., Presentation of RGDS epitopes on self-assembled nanofibers of branched peptide amphiphiles. *Biomacromolecules* **2006,** 7, (6), 1855-1863.

287. Storrie, H.; Guler, M. O.; Abu-Amara, S. N.; Volberg, T.; Rao, M.; Geiger, B.; Stupp, S. I., Supramolecular crafting of cell adhesion. *Biomaterials* **2007,** 28, (31), 4608-4618.

288. Tysseling-Mattiace, V. M.; Sahni, V.; Niece, K. L.; Birch, D.; Czeisler, C.; Fehlings, M. G.; Stupp, S. I.; Kessler, J. A., Self-Assembling Nanofibers Inhibit Glial Scar Formation and Promote Axon Elongation after Spinal Cord Injury. *J Neurosci* **2008,** 28, (14), 3814-3823.

289. Kirkham, J.; Firth, A.; Vernals, D.; Boden, N.; Robinson, C.; Shore, R. C.; Brookes, S. J.; Aggeli, A., Self-assembling Peptide Scaffolds Promote Enamel Remineralization. *J Dent Res* **2007,** 86, (5), 426-430.

290. Firth, A.; Aggeli, A.; Burke, J. L.; Yang, X.; Kirkham, J., Biomimetic self-assembling peptides as injectable scaffolds for hard tissue engineering. *Nanomedicine* **2006,** 1, (2), 189-199.

291. Rajangam, K.; Behanna, H. A.; Hui, M. J.; Han, X.; Hulvat, J. F.; Lomasney, J. W.; Stupp, S. I., Heparin Binding Nanostructures to Promote Growth of Blood Vessels. *Nano Letters* **2006,** 6, (9), 2086-2090.

292. Sargeant, T. D.; Guler, M. O.; Oppenheimer, S. M.; Mata, A.; Satcher, R. L.; Dunand, D. C.; Stupp, S. I., Hybrid bone implants: self-assembly of peptide amphiphile nanofibers within porous titanium. *Biomaterials* **2008,** 29, (2), 161-71.

293. Kang, S.-W.; Jeon, O.; Kim, B.-S., Poly(lactic-co-glycolic acid) microspheres as an injectable scaffold, for cartilage tissue engineering. *Tissue Eng* **2005,** 11, (3-4), 438-447.

294. Rothenfluh, D. A.; Bermudez, H.; O'Neil, C. P.; Hubbell, J. A., Biofunctional polymer nanoparticles for intra-articular targeting and retention in cartilage. *Nat Mater* **2008,** 7, (3), 248-54.

295. Wang, Q.; Wang, L. M.; Detamore, M. S.; Berkland, C., Biodegradable colloidal gels as moldable tissue engineering scaffolds. *Adv Mater* **2008,** 20, (2), 236-239.

296. Van Tomme, S. R.; Van Steenbergen, M. J.; De Smedt, S. C.; Van Nostrum, C. F.; Hennink, W. E., Self-gelling hydrogels based on oppositely charged dextran microspheres. *Biomaterials* **2005,** 26, (14), 2129-2135.

297. Salem, A. K.; Rose, F. R. A. J.; Oreffo, R. O. C.; Yang, X.; Davies, M. C.; Mitchell, J. R.; Roberts, C. J.; Stolnik-Trenkic, S.; Tendler, S. J. B.; Williams, P. M.; Shakesheff, K. M., Porous polymer and cell composites that self-assemble in situ. *Adv Mater* **2003,** 15, (3), 210-213.

298. Hatefi, A.; Amsden, B., Biodegradable injectable in situ forming drug delivery systems. *J Control Release* **2002,** 80, (1-3), 9-28.

299. Malanchuk, V. O.; Kopchak, A. V., Risk factors for development of infection in patients with mandibular fractures located in the tooth-bearing area. *J Craniomaxillofac Surg* **2007,** 35, (1), 57-62.

300. Will, M. J.; Goksel, T.; Stone, C. G.; Doherty, M. J., Oral and Maxillofacial Injuries Experienced in Support of Operation Iraqi Freedom I and II. *Oral Maxillofacial Surg Clin N Am* **2005,** 17, (3), 331-339.

301. Petersen, K.; Hayes, D. K.; Blice, J. P.; Hale, R. G., Prevention and Management of Infections Associated With Combat-Related Head and Neck Injuries. *J Trauma* **2008,** 64, S265-S276.

302. Wade, A. L.; Dye, J. L.; Mohrle, C.; Galarneau, M. R., Head, Face, and Neck Injuries During Operation Iraqi Freedom II: Results From the US Navy-Marine Corps Combat Trauma Registry. *J Trauma* **2007,** 63, 836-840.

303. Penner, M. J.; Duncan, C. P.; Masri, B. A., The in vitro elution characteristics of antibiotic-loaded CMW and Palacos-R bone cements. *J Arthroplasty* **1999,** 14, (2), 209-14.

304. Penner, M. J.; Masri, B. A.; Duncan, C. P., Elution characteristics of vancomycin and tobramycin combined in acrylic bone-cement. *J Arthroplasty* **1996,** 11, (8), 939-44.

305. Bayston, R.; Rodgers, J., Production of extra-cellular slime by Staphylococcus epidermidis during stationary phase of growth: its association with adherence to implantable devices. *J Clin Pathol* **1990,** 43, (10), 866-70.

306. Jain, R. A., Manufacturing techniques of various drug loaded biodegradable poly(lactide-co-glycolide) (PLGA) devices. *Biomaterials* **2000,** 21, (23), 2475-2490.

307. Virto, M. R.; Elorza, B.; Torrado, S.; Elorza, M. d. L. A.; Frutos, G., Improvement of gentamicin poly(d,l-lactic-co-glycolic acid) microspheres for treatment of osteomyelitis induced by orthopedic procedures. *Biomaterials* **2007,** 28, (5), 877-885.

308. Young, S.; Wong, M.; Tabata, Y.; Mikos, A. G., Gelatin as a delivery vehicle for the controlled release of bioactive molecules. *J Control Release* **2005,** 109, (1-3), 256-74.

309. Ambrose, C. G.; Gogola, G. R.; Clyburn, T. A.; Raymond, A. K.; Peng, A. S.; Mikos, A. G., Antibiotic microspheres: preliminary testing for potential treatment of osteomyelitis. *Clin Orthop* **2003**, (415), 279-85.

310. Ambrose, C. G.; Clyburn, T. A.; Louden, K.; Joseph, J.; Wright, J.; Gulati, P.; Gogola, G. R.; Mikos, A. G., Effective treatment of osteomyelitis with biodegradable microspheres in a rabbit model. *Clin Orthop* **2004**, (421), 293-9.

311. Kempen, D. H. R.; Kim, C. W.; Lu, L.; Dhert, W. J. A.; Currier, B. L.; Yaszemski, M. J. In *Controlled release from poly(lactic-co-glycolic acid) microspheres embedded in an injectable, biodegradable scaffold for bone tissue engineering*, Leganes, Madrid, Spain, 2003; Trans Tech Publications: Leganes, Madrid, Spain, 2003; pp 3151-6.

312. Roman, J.; Cabanas, M. V.; Pena, J.; Doadrio, J. C.; Vallet-Regi, M., An optimized beta-tricalcium phosphate and agarose scaffold fabrication technique. *J Biomed Mater Res A* **2008,** 84, (1), 99-107.

313. Kim, H.-W.; Knowles, J. C.; Kim, H.-E., Hydroxyapatite porous scaffold engineered with biological polymer hybrid coating for antibiotic Vancomycin release. *J Mater Sci Mater Med* **2005,** 16, (3), 189-195.

314. Ferraz, M. P.; Mateus, A. Y.; Sousa, J. C.; Monteiro, F. J., Nanohydroxyapatite microspheres as delivery system for antibiotics: Release kinetics, antimicrobial activity, and interaction with osteoblasts. *J Biomed Mater Res A* **2007,** 81A, (4), 994-1004.

315. Cohen, S.; Samadikuchaksaraei, A.; Polak, J. M.; Bishop, A. E., Antibiotics reduce the growth rate and differentiation of embryonic stem cell cultures. *Tissue Eng* **2006,** 12, (7), 2025-2030.

316. J.M. Taboas, C. K. K., G. T-J. Huang, R.S. Tuan, Growth factors in adult stem-cell based skeletal tissue engineering. In *Translational Approaches in Tissue Engineering and Regenerative Medicine*, J.J. Mao, G. V.-N., A.G. Mikos, A. Atala, Ed. Artech House, Inc.: Boston, 2008; pp 83-124.

317. Drake, C. J., Embryonic and adult vasculogenesis. *Birth Defects Res C Embryo Today* **2003,** 69, (1), 73-82.

318. Lawrence, W. T.; Diegelmann, R. F., Growth factors in wound healing. *Clin Dermatol* **1994,** 12, (1), 157-69.

319. Jansen, J. A.; Vehof, J. W.; Ruhe, P. Q.; Kroeze-Deutman, H.; Kuboki, Y.; Takita, H.; Hedberg, E. L.; Mikos, A. G., Growth factor-loaded scaffolds for bone engineering. *J Control Release* **2005,** 101, (1-3), 127-36.

320. Luginbuehl, V.; Meinel, L.; Merkle, H. P.; Gander, B., Localized delivery of growth factors for bone repair. *Eur J Pharm Biopharm* **2004,** 58, (2), 197-208.

321. Varkey, M.; Gittens, S. A.; Uludag, H., Growth factor delivery for bone tissue repair: an update. *Expert Opin Drug Deliv* **2004,** 1, (1), 19-36.

322. Wozney, J. M.; Rosen, V.; Celeste, A. J.; Mitsock, L. M.; Whitters, M. J.; Kriz, R. W.; Hewick, R. M.; Wang, E. A., Novel regulators of bone formation: molecular clones and activities. *Science* **1988,** 242, (4885), 1528-34.

323. Schmidmaier, G.; Schwabe, P.; Wildemann, B.; Haas, N. P., Use of bone morphogenetic proteins for treatment of non-unions and future perspectives. *Injury* **2007,** 38 Suppl 4, S35-41.

324. Ross, R.; Raines, E. W.; Bowen-Pope, D. F., The biology of platelet-derived growth factor. *Cell* **1986,** 46, (2), 155-69.

325. Fan, H.; Zhang, C.; Li, J.; Bi, L.; Qin, L.; Wu, H.; Hu, Y., Gelatin microspheres containing TGF-beta3 enhance the chondrogenesis of mesenchymal stem cells in modified pellet culture. *Biomacromolecules* **2008,** 9, (3), 927-34.

326. Holland, T. A.; Tabata, Y.; Mikos, A. G., In vitro release of transforming growth factor-beta 1 from gelatin microparticles encapsulated in biodegradable, injectable oligo(poly(ethylene glycol) fumarate) hydrogels. *J Control Release* **2003,** 91, (3), 299-313.

327. Indrawattana, N.; Chen, G.; Tadokoro, M.; Shann, L. H.; Ohgushi, H.; Tateishi, T.; Tanaka, J.; Bunyaratvej, A., Growth factor combination for chondrogenic induction from human mesenchymal stem cell. *Biochem Biophys Res Commun* **2004,** 320, (3), 914-9.

328. Darling, E. M.; Athanasiou, K. A., Biomechanical strategies for articular cartilage regeneration. *Ann Biomed Eng* **2003,** 31, (9), 1114-24.

329. Holland, T. A.; Mikos, A. G., Advances in drug delivery for articular cartilage. *J Control Release* **2003,** 86, (1), 1-14.

330. Jay, S. M.; Shepherd, B. R.; Bertram, J. P.; Pober, J. S.; Saltzman, W. M., Engineering of multifunctional gels integrating highly efficient growth factor delivery with endothelial cell transplantation. *FASEB J* **2008,** 22, (8), 2949-56.

331. Woo, B. H.; Fink, B. F.; Page, R.; Schrier, J. A.; Jo, Y. W.; Jiang, G.; DeLuca, M.; Vasconez, H. C.; DeLuca, P. P., Enhancement of bone growth by sustained delivery of recombinant human bone morphogenetic protein-2 in a polymeric matrix. *Pharm Res* **2001,** 18, (12), 1747-53.

332. Tabata, Y.; Nagano, A.; Ikada, Y., Biodegradation of hydrogel carrier incorporating fibroblast growth factor. *Tissue Eng* **1999,** 5, (2), 127-38.

333. Holland, T. A.; Bodde, E. W.; Baggett, L. S.; Tabata, Y.; Mikos, A. G.; Jansen, J. A., Osteochondral repair in the rabbit model utilizing bilayered, degradable oligo(poly(ethylene glycol) fumarate) hydrogel scaffolds. *J Biomed Mater Res A* **2005,** 75, (1), 156-67.

334. Holland, T. A.; Bodde, E. W.; Cuijpers, V. M.; Baggett, L. S.; Tabata, Y.; Mikos, A. G.; Jansen, J. A., Degradable hydrogel scaffolds for in vivo delivery of single and dual growth factors in cartilage repair. *Osteoarthr Cartil* **2007,** 15, (2), 187-97.

335. Gobin, A. S.; West, J. L., Effects of Epidermal Growth Factor on Fibroblast Migration through Biomimetic Hydrogels. *Biotechnol Prog* **2003,** 19, (6), 1781-1785.

336. Na, K.; Kim, S.; Woo, D. G.; Sun, B. K.; Yang, H. N.; Chung, H. M.; Park, K. H., Combination material delivery of dexamethasone and growth factor in hydrogel blended with hyaluronic acid constructs for neocartilage formation. *J Biomed Mater Res A* **2007,** 83, (3), 779-86.

337. Gao, T. J.; Kousinioris, N. A.; Wozney, J. M.; Winn, S.; Uludag, H., Synthetic thermoreversible polymers are compatible with osteoinductive activity of recombinant human bone morphogenetic protein 2. *Tissue Eng* **2002,** 8, (3), 429-40.

338. Lee, J. S.; Go, D. H.; Bae, J. W.; Lee, S. J.; Park, K. D., Heparin conjugated polymeric micelle for long-term delivery of basic fibroblast growth factor. *J Control Release* **2007,** 117, (2), 204-9.

339. Lee, J. S.; Bae, J. W.; Joung, Y. K.; Lee, S. J.; Han, D. K.; Park, K. D., Controlled dual release of basic fibroblast growth factor and indomethacin from heparin-conjugated polymeric micelle. *Int J Pharm* **2008,** 346, (1-2), 57-63.

340. Fujita, M.; Ishihara, M.; Simizu, M.; Obara, K.; Ishizuka, T.; Saito, Y.; Yura, H.; Morimoto, Y.; Takase, B.; Matsui, T.; Kikuchi, M.; Maehara, T., Vascularization in vivo caused by the controlled release of fibroblast growth factor-2 from an injectable chitosan/non-anticoagulant heparin hydrogel. *Biomaterials* **2004,** 25, (4), 699-706.

341. Silva, E. A.; Mooney, D. J., Spatiotemporal control of vascular endothelial growth factor delivery from injectable hydrogels enhances angiogenesis. *J Thromb Haemost* **2007,** 5, (3), 590-8.

342. Hao, X.; Silva, E. A.; Mansson-Broberg, A.; Grinnemo, K. H.; Siddiqui, A. J.; Dellgren, G.; Wardell, E.; Brodin, L. A.; Mooney, D. J.; Sylven, C., Angiogenic effects of sequential release of VEGF-A165 and PDGF-BB with alginate hydrogels after myocardial infarction. *Cardiovasc Res* **2007,** 75, (1), 178-85.

343. Hosseinkhani, H.; Hosseinkhani, M.; Khademhosseini, A.; Kobayashi, H.; Tabata, Y., Enhanced angiogenesis through controlled release of basic fibroblast growth factor from peptide amphiphile for tissue regeneration. *Biomaterials* **2006,** 27, (34), 5836-44.

344. Hiemstra, C.; Zhong, Z.; van Steenbergen, M. J.; Hennink, W. E.; Feijen, J., Release of model proteins and basic fibroblast growth factor from in situ forming degradable dextran hydrogels. *J Control Release* **2007,** 122, (1), 71-78.

345. Jupiter, J. B.; Winters, S.; Sigman, S.; Lowe, C.; Pappas, C.; Ladd, A. L.; Van Wagoner, M.; Smith, S. T., Repair of five distal radius fractures with an investigational cancellous bone cement: a preliminary report. *J Orthop Trauma* **1997,** 11, (2), 110-6.

346. Blom, E. J.; Klein-Nulend, J.; Wolke, J. G.; van Waas, M. A.; Driessens, F. C.; Burger, E. H., Transforming growth factor-beta1 incorporation in a calcium phosphate bone cement: material properties and release characteristics. *J Biomed Mater Res* **2002,** 59, (2), 265-72.

347. Ruhe, P. Q.; Boerman, O. C.; Russel, F. G.; Spauwen, P. H.; Mikos, A. G.; Jansen, J. A., Controlled release of rhBMP-2 loaded poly(dl-lactic-co-glycolic acid)/calcium phosphate cement composites in vivo. *J Control Release* **2005,** 106, (1-2), 162-71.

348. Vogel, G., Harnessing the power of stem cells. *Science* **1999,** 283, (5407), 1432-4.

349. Caplan, A. I., Mesenchymal stem cells. *J Orthop Res* **1991,** 9, (5), 641-50.

350. Caplan, A. I., Review: mesenchymal stem cells: cell-based reconstructive therapy in orthopedics. *Tissue Eng* **2005,** 11, (7-8), 1198-211.

351. Romanov, Y. A.; Svintsitskaya, V. A.; Smirnov, V. N., Searching for alternative sources of postnatal human mesenchymal stem cells: candidate MSC-like cells from umbilical cord. *Stem Cells* **2003,** 21, (1), 105-10.

352. Wang, H. S.; Hung, S. C.; Peng, S. T.; Huang, C. C.; Wei, H. M.; Guo, Y. J.; Fu, Y. S.; Lai, M. C.; Chen, C. C., Mesenchymal stem cells in the Wharton's jelly of the human umbilical cord. *Stem Cells* **2004,** 22, (7), 1330-7.

353. Bailey, M. M.; Wang, L.; Bode, C. J.; Mitchell, K. E.; Detamore, M. S., A Comparison of Human Umbilical Cord Matrix Stem Cells and Temporomandibular Joint Condylar Chondrocytes for Tissue Engineering Temporomandibular Joint Condylar Cartilage. *Tissue Eng* **2007,** 13, (8), 2003-2010.

354. Park, H.; Temenoff, J. S.; Tabata, Y.; Caplan, A. I.; Mikos, A. G., Injectable biodegradable hydrogel composites for rabbit marrow mesenchymal stem cell and growth factor delivery for cartilage tissue engineering. *Biomaterials* **2007,** 28, (21), 3217-27.

355. Temenoff, J. S.; Park, H.; Jabbari, E.; Sheffield, T. L.; LeBaron, R. G.; Ambrose, C. G.; Mikos, A. G., In vitro osteogenic differentiation of marrow stromal cells encapsulated in biodegradable hydrogels. *J Biomed Mater Res A* **2004,** 70, (2), 235-44.

356. Wang, D.-A.; Williams, C. G.; Yang, F.; Cher, N.; Lee, H.; Elisseeff, J. H., Bioresponsive phosphoester hydrogels for bone tissue engineering. *Tissue Eng* **2005,** 11, (1-2), 201-213.

357. Yamada, Y.; Ueda, M.; Naiki, T.; Takahashi, M.; Hata, K.; Nagasaka, T., Autogenous injectable bone for regeneration with mesenchymal stem cells and platelet-rich plasma: tissue-engineered bone regeneration. *Tissue Eng* **2004,** 10, (5-6), 955-64.

358. Alhadlaq, A.; Elisseeff, J. H.; Hong, L.; Williams, C. G.; Caplan, A. I.; Sharma, B.; Kopher, R. A.; Tomkoria, S.; Lennon, D. P.; Lopez, A.; Mao, J. J., Adult stem cell driven genesis of human-shaped articular condyle. *Ann Biomed Eng* **2004,** 32, (7), 911-23.

359. Alsberg, E.; Anderson, K. W.; Albeiruti, A.; Rowley, J. A.; Mooney, D. J., Engineering growing tissues. *Proc Natl Acad Sci U S A* **2002,** 99, (19), 12025-30.

360. Gerstenfeld, L. C.; Cruceta, J.; Shea, C. M.; Sampath, K.; Barnes, G. L.; Einhorn, T. A., Chondrocytes provide morphogenic signals that selectively induce osteogenic differentiation of mesenchymal stem cells. *J Bone Miner Res* **2002,** 17, (2), 221-30.

361. Ahmed, N.; Dreier, R.; Gopferich, A.; Grifka, J.; Grassel, S., Soluble signalling factors derived from differentiated cartilage tissue affect chondrogenic differentiation of rat adult marrow stromal cells. *Cell Physiol Biochem* **2007,** 20, (5), 665-78.

362. Sun, H.; Qu, Z.; Guo, Y.; Zang, G.; Yang, B., In vitro and in vivo effects of rat kidney vascular endothelial cells on osteogenesis of rat bone marrow mesenchymal stem cells growing on polylactide-glycoli acid (PLGA) scaffolds. *Biomed Eng Online* **2007,** 6, 41.

363. Ford, M. C.; Bertram, J. P.; Hynes, S. R.; Michaud, M.; Li, Q.; Young, M.; Segal, S. S.; Madri, J. A.; Lavik, E. B., A macroporous hydrogel for the coculture of neural progenitor and endothelial cells to form functional vascular networks in vivo. *Proc Natl Acad Sci U S A* **2006,** 103, (8), 2512-7.

364. Popov, B. V.; Serikov, V. B.; Petrov, N. S.; Izusova, T. V.; Gupta, N.; Matthay, M. A., Lung epithelial cells induce endodermal differentiation in mouse

mesenchymal bone marrow stem cells by paracrine mechanism. *Tissue Eng* **2007,** 13, (10), 2441-50.

365. Dalby, M. J.; Gadegaard, N.; Tare, R.; Andar, A.; Riehle, M. O.; Herzyk, P.; Wilkinson, C. D. W.; Oreffo, R. O. C., The control of human mesenchymal cell differentiation using nanoscale symmetry and disorder. *Nat Mater* **2007,** 6, (12), 997-1003.

366. Sun, W.; Puzas, E.; Sheu, T.-J.; Liu, X.; Fauchetl, P. M., Nano- to Microscale Porous Silicon as a Cell Interface for Bone-Tissue Engineering. *Adv Mater* **2007,** 19, 921-924.

367. Isenberg, B. C.; Tsuda, Y.; Williams, C.; Shimizu, T.; Yamato, M.; Okano, T.; Wong, J. Y., A thermoresponsive, microtextured substrate for cell sheet engineering with defined structural organization. *Biomaterials* **2008,** 29, (17), 2565-2572.

368. Czarnecki, J. S.; Lafdi, K.; Tsonis, P. A., A Novel Approach to Control Growth, Orientation, and Shape of Human Osteoblasts. *Tissue Eng* **2008,** 14, (2), 255-65.

369. Albrecht, D. R.; Underbill, G. H.; Mendelson, A.; Bhatia, S. N., Multiphase electropatterning of cells and biomaterials. *Lab on a Chip* **2007,** 4, (6), 702-9.

370. Woodfield, T. B. F.; Van Blitterswijk, C. A.; De Wijn, J.; Sims, T. J.; Hollander, A. P.; Riesle, J., Polymer scaffolds fabricated with pore-size gradients as a model for studying the zonal organization within tissue-engineered cartilage constructs. *Tissue Eng* **2005,** 11, (9-10), 1297-1311.

371. Lavik, E. B.; Klassen, H.; Warfvinge, K.; Langer, R.; Young, M. J., Fabrication of degradable polymer scaffolds to direct the integration and differentiation of retinal progenitors. *Biomaterials* **2005,** 26, (16), 3187-96.

372. Engler, A. J.; Sen, S.; Sweeney, H. L.; Discher, D. E., Matrix Elasticity Directs Stem Cell Lineage Specification. *Cell* **2006,** 126, (4), 677-689.

373. Manjooran, N. J.; Pickrell, G. R., Biologically self-assembled porous polymers. *Journal of Materials Processing Technology* **2005,** 168, (2), 225-229.

374. Liu, Q.; Hedberg, E. L.; Liu, Z.; Bahulekar, R.; Meszlenyi, R. K.; Mikos, A. G., Preparation of macroporous poly(2-hydroxyethyl methacrylate) hydrogels by enhanced phase separation. *Biomaterials* **2000,** 21, (21), 2163-9.

375. Jabbari, E.; Wang, S.; Lu, L.; Gruetzmacher, J. A.; Ameenuddin, S.; Hefferan, T. E.; Currier, B. L.; Windebank, A. J.; Yaszemski, M. J., Synthesis, material properties, and biocompatibility of a novel self-cross-linkable poly(caprolactone fumarate) as an injectable tissue engineering scaffold. *Biomacromolecules* **2005,** 6, (5), 2503-11.

376. Declercq, H. A.; Gorski, T. L.; Tielens, S. P.; Schacht, E. H.; Cornelissen, M. J., Encapsulation of osteoblast seeded microcarriers into injectable, photopolymerizable three-dimensional scaffolds based on d,l-lactide and epsilon-caprolactone. *Biomacromolecules* **2005,** 6, (3), 1608-14.

377. Behravesh, E.; Jo, S.; Zygourakis, K.; Mikos, A. G., Synthesis of in situ cross-linkable macroporous biodegradable poly(propylene fumarate-co-ethylene glycol) hydrogels. *Biomacromolecules* **2002,** 3, (2), 374-381.

378. Anseth, K. S.; Metters, A. T.; Bryant, S. J.; Martens, P. J.; Elisseeff, J. H.; Bowman, C. N., In situ forming degradable networks and their application in tissue engineering and drug delivery. *J Control Release* **2002,** 78, (1-3), 199-209.

379. Yuan, Q.; Venkatasubramanian, R.; Hein, S.; Misra, R. D., A stimulus-responsive magnetic nanoparticle drug carrier: magnetite encapsulated by chitosan-grafted-copolymer. *Acta Biomater* **2008,** 4, (4), 1024-37.

380. Betre, H.; Liu, W.; Zalutsky, M. R.; Chilkoti, A.; Kraus, V. B.; Setton, L. A., A thermally responsive biopolymer for intra-articular drug delivery. *J Control Release* **2006,** 115, (2), 175-182.

381. Liu, X.-M.; Pramoda, K. P.; Yang, Y.-Y.; Chow, S. Y.; He, C., Cholesteryl-grafted functional amphiphilic poly(N-isopropylacrylamide-*co*-N-hydroxylmethylacrylamide): Synthesis, temperature-sensitivity, self-assembly and encapsulation of a hydrophobic agent. *Biomaterials* **2004,** 25, (13), 2619-2628.

382. Brock Thomas, J.; Tingsanchali, J. H.; Rosales, A. M.; Creecy, C. M.; McGinity, J. W.; Peppas, N. A., Dynamics of Poly(ethylene glycol)-Tethered, pH Responsive Networks. *Polymer* **2007,** 48, (17), 5042-5048.

383. Kostanski, L. K.; Huang, R.; Ghosh, R.; Filipe, C. D., Biocompatible poly(N-vinyllactam)-based materials with environmentally-responsive permeability. *J Biomater Sci Polym Ed* **2008,** 19, (3), 275-90.

384. Goessl, A.; Tirelli, N.; Hubbell, J. A., A hydrogel system for stimulus-responsive, oxygen-sensitive in situ gelation. *J Biomater Sci Polym Ed* **2004,** 15, (7), 895-904.

385. Guan, J.; Fujimoto, K. L.; Wagner, W. R., Elastase-sensitive elastomeric scaffolds with variable anisotropy for soft tissue engineering. *Pharm Res* **2008,** 25, (10), 2400-12.

386. Luo, R.; Li, H.; Lam, K. Y., Modeling the effect of environmental solution pH on the mechanical characteristics of glucose-sensitive hydrogels. *Biomaterials* **2009,** 30, (4), 690-700.

387. Satarkar, N. S.; Hilt, J. Z., Magnetic hydrogel nanocomposites for remote controlled pulsatile drug release. *J Control Release* **2008,** 130, (3), 246-51.

388. Moroni, L.; de Wijn, J. R.; van Blitterswijk, C. A., Integrating novel technologies to fabricate smart scaffolds. *J Biomater Sci Polym Ed* **2008,** 19, (5), 543-72.

389. Meng, F.; Zhong, Z.; Feijen, J., Stimuli-Responsive Polymersomes for Programmed Drug Delivery. *Biomacromolecules* **2009**.

390. Cole, M. A.; Voelcker, N. H.; Thissen, H.; Griesser, H. J., Stimuli-responsive interfaces and systems for the control of protein-surface and cell-surface interactions. *Biomaterials* **2009,** 30, (9), 1827-50.

391. Zhang, C.; Zhao, K.; Hu, T.; Cui, X.; Brown, N.; Boland, T., Loading dependent swelling and release properties of novel biodegradable, elastic and environmental stimuli-sensitive polyurethanes. *J Control Release* **2008,** 131, (2), 128-36.

392. Gonzalez, N.; Elvira, C.; Roman, J. S., Novel dual-stimuli-responsive polymers derived from ethylpyrrolidine. *Macromolecules* **2005,** 38, (22), 9298-9303.

393. Liu, F.; Urban, M. W., Dual temperature and pH responsiveness of poly(2-(N,N-dimethylamino)ethyl methacrylate-co-n-butyl acrylate) colloidal dispersions and their films. *Macromolecules* **2008,** 41, (17), 6531-6539.

394. Zhang, J.; Chu, L. Y.; Cheng, C. J.; Mi, D. F.; Zhou, M. Y.; Ju, X. J., Graft-type poly(N-isopropylacrylamide-co-acrylic acid) microgels exhibiting rapid thermo- and pH-responsive properties. *Polymer* **2008,** 49, (10), 2595-2603.

395. Yin, X.; Hoffman, A. S.; Stayton, P. S., Poly(N-isopropylacrylamide-co-propylacrylic acid) copolymers that respond sharply to temperature and pH. *Biomacromolecules* **2006,** 7, (5), 1381-1385.

396. You, Y. Z.; Hong, C. Y.; Pan, C. Y., Preparation of smart polymer/carbon nanotube conjugates via stimuli-responsive linkages. *Adv Func Mater* **2007,** 17, (14), 2470-2477.

397. Zhang, H.; Chu, L. Y.; Li, Y. K.; Lee, Y. M., Dual thermo- and pH-sensitive poly(N-isopropylacrylamide-co-acrylic acid) hydrogels with rapid response behaviors. *Polymer* **2007,** 48, (6), 1718-1728.

398. Cellesi, F.; Tirelli, N., A new process for cell microencapsulation and other biomaterial applications: Thermal gelation and chemical cross-linking in 'tandem'. *J Mater Sci Mater Med* **2005,** 16, (6), 559-565.

399. Penttinen, R., Metabolism of fracture callus of rat in vitro. I. Oxygen consumption and lactic acid production. *Acta Physiol Scand* **1973,** 87, (1), 133-7.

400. Provencher, S. W., A Constrained Regularization Method for Inverting Data Represented by Linear Algebraic or Integral-Equations. *Comput Phys Commun* **1982,** 27, (3), 213-227.

401. Greish, Y. E.; Brown, P. W., Chemically formed HAp-Ca poly(vinyl phosphonate) composites. *Biomaterials* **2001,** 22, (8), 807-816.

402. Braybrook, J. H.; Nicholson, J. W., Incorporation of Cross-Linking Agents into Poly(Vinyl Phosphonic Acid) as a Route to Glass Polyalkenoate Cements of Improved Compressive Strength. *J Mater Chem* **1993,** 3, (4), 361-365.

403. Fares, M. M.; Othman, A. A., Lower Critical Solution Temperature Determination of Smart, Thermosensitive N-Isopropylacrylamide-alt-2-Hydroxyethyl Methacrylate Copolymers: Kinetics and Physical Properties. *J Appl Polym Sci* **2008,** 110, (5), 2815-2825.

404. Erdemi, H.; Bozkurt, A., Synthesis and characterization of poly(vinylpyrrolidone-co-vinylphosphonic acid) copolymers. *Eur Polym J* **2004,** 40, (8), 1925-1929.

405. Jiang, D. D.; Yao, Q.; McKinney, M. A.; Wilkie, C. A., TGA/FTIR studies on the thermal degradation of some polymeric sulfonic and phosphonic acids and their sodium salts. *Polym Degrad Stab* **1999,** 63, (3), 423-434.

406. Wang, T. L.; Cho, Y. L.; Kuo, P. L., Flame-retarding materials. II. Synthesis and flame-retarding properties of phosphorus-on-pendent and phosphorus-on-skeleton polyols and the corresponding polyurethanes. *J Appl Polym Sci* **2001,** 82, (2), 343-357.

407. Schild, H. G.; Tirrell, D. A., Microcalorimetric detection of lower critical solution temperatures in aqueous polymer solutions. *J Phys Chem* **1990,** 94, (10), 4352-4356.

408. Zhang, Y. J.; Furyk, S.; Bergbreiter, D. E.; Cremer, P. S., Specific ion effects on the water solubility of macromolecules: PNIPAM and the Hofmeister series. *J Am Chem Soc* **2005,** 127, (41), 14505-14510.

409. Park, T. G.; Hoffman, A. S., Sodium Chloride-Induced Phase-Transition in Nonionic Poly(N-Isopropylacrylamide) Gel. *Macromolecules* **1993,** 26, (19), 5045-5048.

410. Otake, K.; Inomata, H.; Konno, M.; Saito, S., Thermal-Analysis of the Volume Phase-Transition with N-Isopropylacrylamide Gels. *Macromolecules* **1990,** 23, (1), 283-289.

411. Inomata, H.; Goto, S.; Otake, K.; Saito, S., Effect of Additives on Phase-Transition of N-Isopropylacrylamide Gels. *Langmuir* **1992,** 8, (2), 687-690.

412. Gan, T. T.; Zhang, Y. J.; Guan, Y., In Situ Gelation of P(NIPAM-HEMA) Microgel Dispersion and Its Applications as Injectable 3D Cell Scaffold. *Biomacromolecules* **2009,** 10, (6), 1410-1415.

413. Eom, G. T.; Oh, S. Y.; Park, T. G., In situ thermal gelation of water-soluble poly(N-isopropylacrylamide-co-vinylphosphonic acid). *J Appl Polym Sci* **1998,** 70, (10), 1947-1953.

414. Kim, S. Y.; Lee, S. C., Thermo-Responsive Injectable Hydrogel System Based on Poly(N-isopropylacrylamide-co-vinylphosphonic acid). I. Biomineralization and Protein Delivery. *J Appl Polym Sci* **2009,** 113, 3460-3469.

415. Nichifor, M.; Zhu, X. X.; Cristea, D.; Carpov, A., Interaction of hydrophobically modified cationic dextran hydrogels with biological surfactants. *J Phys Chem B* **2001,** 105, (12), 2314-2321.

416. Abdurrahmanoglu, S.; Can, V.; Okay, O., Design of high-toughness polyacrylamide hydrogels by hydrophobic modification. *Polymer* **2009,** 50, (23), 5449-5455.

417. Klouda, L.; Hacker, M. C.; Kretlow, J. D.; Mikos, A. G., Cytocompatibility evaluation of amphiphilic, thermally responsive and chemically crosslinkable macromers for in situ forming hydrogels. *Biomaterials* **2009,** 30, (27), 4558-66.

418. Campbell, A. A.; Fryxell, G. E.; Linehan, J. C.; Graff, G. L., Surface-induced mineralization: a new method for producing calcium phosphate coatings. *J Biomed Mater Res* **1996,** 32, (1), 111-8.

419. Saito, T.; Arsenault, A. L.; Yamauchi, M.; Kuboki, Y.; Crenshaw, M. A., Mineral induction by immobilized phosphoproteins. *Bone* **1997,** 21, (4), 305-311.

420. Song, J.; Malathong, V.; Bertozzi, C. R., Mineralization of synthetic polymer scaffolds: A bottom-up approach for the development of artificial bone. *J Am Chem Soc* **2005,** 127, (10), 3366-3372.

421. Boskey, A. L., Biomineralization: An Overview. *Connect Tissue Res* **2003,** 44, (Suppl. 1), 5-9.

422. Reinstorf, A.; Ruhnow, M.; Gelinsky, M.; Pompe, W.; Hempel, U.; Wenzel, K. W.; Simon, P., Phosphoserine – a convenient compound for modification of calcium phosphate bone cement collagen composites. *J Mater Sci Mater Med* **2004,** 15, (4), 451-455.

423. Schneiders, W.; Reinstorf, A.; Pompe, W.; Grass, R.; Biewener, A.; Holch, M.; Zwipp, H.; Rammelt, S., Effect of modification of hydroxyapatite/collagen composites with sodium citrate, phosphoserine, phosphoserine/RGD-peptide and calcium carbonate on bone remodelling. *Bone* **2007,** 40, (4), 1048-1059.

424. Nicholson, J. W.; Singh, G., The use of organic compounds of phosphorus in clinical dentistry. *Biomaterials* **1996,** 17, (21), 2023-2030.

425. Greish, Y. E.; Brown, P. W., Preparation and characterization of calcium phosphate-poly(vinyl phosphonic acid) composites. *J Mater Sci Mater Med* **2001,** 12, (5), 407-411.

426. Dogan, O.; Oner, M., Biomimetic Mineralization of Hydroxyapatite Crystals on the Copolymers of Vinylphosphonic Acid and 4-Vinilyimidazole. *Langmuir* **2006,** 22, (23), 9671-9675.

427. Tan, J.; Gemeinhart, R. A.; Ma, M.; Mark Saltzman, W., Improved cell adhesion and proliferation on synthetic phosphonic acid-containing hydrogels. *Biomaterials* **2005,** 26, (17), 3663-3671.

428. Gemeinhart, R. A.; Bare, C. M.; Haasch, R. T.; Gemeinhart, E. J., Osteoblast-like cell attachment to and calcification of novel phosphonate-containing polymeric substrates. *J Biomed Mater Res A* **2006,** 78, (3), 433-440.

429. Pinprayoon, O.; Groves, R.; Saunders, B. R., A study of poly (butadiene/methacrylic acid) dispersions: From pH-responsive behaviour to the effects of added Ca2+. *J Colloid Interface Sci* **2008,** 321, (2), 315-322.

430. Chattopadhyay, A.; Harikumar, K. G., Dependence of critical micelle concentration of a zwitterionic detergent on ionic strength: Implications in receptor solubilization. *FEBS Lett* **1996,** 391, (1-2), 199-202.

431. Cammas, S.; Suzuki, K.; Sone, C.; Sakurai, Y.; Kataoka, K.; Okano, T., Thermo-responsive polymer nanoparticles with a core-shell micelle structure as site-specific drug carriers. *J Control Release* **1997,** 48, (2-3), 157-164.

432. Kohori, F.; Sakai, K.; Aoyagi, T.; Yokoyama, M.; Sakurai, Y.; Okano, T., Preparation and characterization of thermally responsive block copolymer micelles comprising poly(N-isopropylacrylamide-b-DL-lactide). *J Control Release* **1998,** 55, (1), 87-98.

433. Teng, D. Y.; Hou, J. L.; Zhang, X. G.; Wang, X.; Wang, Z.; Li, C. X., Glucosamine-carrying temperature- and pH-sensitive microgels: Preparation, characterization, and in vitro drug release studies. *J Colloid Interface Sci* **2008,** 322, (1), 333-341.

434. Liu, X. M.; Wang, L. S.; Wang, L.; Huang, J. C.; He, C. B., The effect of salt and pH on the phase-transition behaviors of temperature-sensitive copolymers based on N-isopropylacrylamide. *Biomaterials* **2004,** 25, (25), 5659-5666.

435. Schilli, C. M.; Zhang, M. F.; Rizzardo, E.; Thang, S. H.; Chong, Y. K.; Edwards, K.; Karlsson, G.; Muller, A. H. E., A new double-responsive block copolymer synthesized via RAFT polymerization: Poly(N-isopropylacrylamide)-block-poly(acrylic acid). *Macromolecules* **2004,** 37, (21), 7861-7866.

436. Discher, D. E.; Eisenberg, A., Polymer vesicles. *Science* **2002,** 297, (5583), 967-73.

437. Nishiyama, N.; Kataoka, K., Current state, achievements, and future prospects of polymeric micelles as nanocarriers for drug and gene delivery. *Pharmacol Ther* **2006,** 112, (3), 630-48.

438. Cabral, H.; Nishiyama, N.; Kataoka, K., Optimization of (1,2-diamino-cyclohexane)platinum(II)-loaded polymeric micelles directed to improved tumor targeting and enhanced antitumor activity. *J Control Release* **2007,** 121, (3), 146-55.

439. Jiang, J. Q.; Tong, X.; Zhao, Y., A new design for light-breakable polymer micelles. *J Am Chem Soc* **2005,** 127, (23), 8290-8291.

440. Christensen, K. A.; Myers, J. T.; Swanson, J. A., pH-dependent regulation of lysosomal calcium in macrophages. *J Cell Sci* **2002,** 115, (Pt 3), 599-607.

441. Siddappa, R.; Licht, R.; Blitterswijk, C. v.; Boer, J. d., Donor variation and loss of multipotency during in vitro expansion of human mesenchymal stem cells for bone tissue engineering. *J Orthop Res* **2007,** 25, (8), 1029-1041.

442. Corsi, K. A.; Pollett, J. B.; Phillippi, J. A.; Usas, A.; Li, G.; Huard, J., Osteogenic Potential of Postnatal Skeletal Muscle Derived Stem Cells Is Influenced by Donor Sex. *J Bone Miner Res* **2007,** 22, (10), 1592-1602.

443. Crisostomo, P. R.; Markel, T. A.; Wang, M.; Lahm, T.; Lillemoe, K. D.; Meldrum, D. R., In the adult mesenchymal stem cell population, source gender is a biologically relevant aspect of protective power. *Surgery* **2007,** 142, (2), 215-221.

444. Van Zant, G.; Liang, Y., The role of stem cells in aging. *Exp Hematol* **2003,** 31, (8), 659-672.

445. Rando, T. A., Stem cells, ageing and the quest for immortality. *Nature* **2006,** 441, (7097), 1080-1086.

446. Ruzankina, Y.; Brown, E. J., Relationships between stem cell exhaustion, tumour suppression and ageing. *Br J Cancer* **2007,** 97, (9), 1189-93.

447. Wodarz, D., Effect of stem cell turnover rates on protection against cancer and aging. *J Theor Biol* **2007,** 245, (3), 449-458.

448. Justesen, J.; Stenderup, K.; Eriksen, E. F.; Kassem, M., Maintenance of Osteoblastic and Adipocytic Differentiation Potential with Age and Osteoporosis in Human Marrow Stromal Cell Cultures. *Calcif Tissue Int* **2002,** 71, (1), 36-44.

449. Leskela, H.-V.; Risteli, J.; Niskanen, S.; Koivunen, J.; Ivaska, K. K.; Lehenkari, P., Osteoblast recruitment from stem cells does not decrease by age at late adulthood. *Biochem Biophys Res Commun* **2003,** 311, (4), 1008-1013.

450. Stenderup, K.; Justesen, J.; Eriksen, E. F.; Rattan, S. I. S.; Kassem, M., Number and Proliferative Capacity of Osteogenic Stem Cells Are Maintained

During Aging and in Patients with Osteoporosis. *J Bone Miner Res* **2001,** 16, (6), 1120-1129.

451. Scharstuhl, A.; Schewe, B.; Benz, K.; Gaissmaier, C.; Buhring, H.-J.; Stoop, R., Chondrogenic Potential of Human Adult Mesenchymal Stem Cells Is Independent of Age or Osteoarthritis Etiology. *Stem Cells* **2007,** 25, (12), 3244-3251.

452. Bergman, R. J.; Gazit, D.; Kahn, A. J.; Gruber, H.; McDougall, S.; Hahn, T. J., Age-related changes in osteogenic stem cells in mice. *J Bone Miner Res* **1996,** 11, (5), 568-77.

453. Bellows, C. G.; Pei, W.; Jia, Y.; Heersche, J. N. M., Proliferation, differentiation and self-renewal of osteoprogenitors in vertebral cell populations from aged and young female rats. *Mech Ageing Dev* **2003,** 124, (6), 747-757.

454. Tokalov, S. V.; Gruner, S.; Schindler, S.; Wolf, G.; Baumann, M.; Abolmaali, N., Age-Related Changes in the Frequency of Mesenchymal Stem Cells in the Bone Marrow of Rats. *Stem Cells Dev* **2007,** 16, (3), 439-446.

455. Mareschi, K.; Ferrero, I.; Rustichelli, D.; Aschero, S.; Gammaitoni, L.; Aglietta, M.; Madon, E.; Fagioli, F., Expansion of mesenchymal stem cells isolated from pediatric and adult donor bone marrow. *J Cell Biochem* **2006,** 97, (4), 744-754.

456. Stenderup, K.; Justesen, J.; Clausen, C.; Kassem, M., Aging is associated with decreased maximal life span and accelerated senescence of bone marrow stromal cells. *Bone* **2003,** 33, (6), 919-926.

457. Shi, Y. Y.; Nacamuli, R. P.; Salim, A.; Longaker, M. T., The osteogenic potential of adipose-derived mesenchymal cells is maintained with aging. *Plast Reconstr Surg* **2005,** 116, (6), 1686-96.

458. Wall, M. E.; Bernacki, S. H.; Loboa, E. G., Effects of serial passaging on the adipogenic and osteogenic differentiation potential of adipose-derived human mesenchymal stem cells. *Tissue Eng* **2007,** 13, (6), 1291-8.

459. Kirkland, J. L.; Hollenberg, C. H.; Gillon, W. S., Ageing, differentiation, and gene expression in rat epididymal preadipocytes. *Biochem Cell Biol* **1993,** 71, (11-12), 556-61.

460. Karagiannides, I.; Tchkonia, T.; Dobson, D. E.; Steppan, C. M.; Cummins, P.; Chan, G.; Salvatori, K.; Hadzopoulou-Cladaras, M.; Kirkland, J. L., Altered expression of C/EBP family members results in decreased adipogenesis with aging. *Am J Physiol Regul Integr Comp Physiol* **2001,** 280, (6), R1772-80.

461. Tchkonia, T.; Pirtskhalava, T.; Thomou, T.; Cartwright, M. J.; Wise, B.; Karagiannides, I.; Shpilman, A.; Lash, T. L.; Becherer, J. D.; Kirkland, J. L., Increased TNF-alpha and CCAAT/enhancer-binding protein homologous protein with aging predispose preadipocytes to resist adipogenesis. *Am J Physiol Endocrinol Meta* **2007,** 293, (6), E1810-9.

462. Stolzing, A.; Scutt, A., Age-related impairment of mesenchymal progenitor cell function. *Aging Cell* **2006,** 5, (3), 213-24.

463. Stolzing, A.; Jones, E.; McGonagle, D.; Scutt, A., Age-related changes in human bone marrow-derived mesenchymal stem cells: Consequences for cell therapies. *Mech Ageing Dev* **2008,** 129, (3), 163-173.

464. Roura, S.; Farre, J.; Soler-Botija, C.; Llach, A.; Hove-Madsen, L.; Cairo, J. J.; Godia, F.; Cinca, J.; Bayes-Genis, A., Effect of aging on the pluripotential capacity of human CD105+ mesenchymal stem cells. *Eur J Heart Fail* **2006,** 8, (6), 555-63.

465. D'Ippolito, G.; Schiller, P.; Ricordi, C.; Roos, B.; Howard, G., Age-Related Osteogenic Potential of Mesenchymal Stromal Stem Cells from Human Vertebral Bone Marrow. *J Bone Miner Res* **1999,** 14, (7), 1115-1122.

466. Mendes, S. C.; Tibbe, J. M.; Veenhof, M.; Bakker, K.; Both, S.; Platenburg, P. P.; Oner, F. C.; de Bruijn, J. D.; van Blitterswijk, C. A., Bone Tissue-Engineered Implants Using Human Bone Marrow Stromal Cells: Effect of Culture Conditions and Donor Age. *Tissue Eng* **2002,** 8, (6), 911-920.

467. Chen, J.; Sotome, S.; Wang, J.; Orii, H.; Uemura, T.; Shinomiya, K., Correlation of in vivo bone formation capability and in vitro differentiation of human bone marrow stromal cells. *J Med Dent Sci* **2005,** 52, (1), 27-34.

468. Zheng, H.; Martin, J. A.; Duwayri, Y.; Falcon, G.; Buckwalter, J. A., Impact of aging on rat bone marrow-derived stem cell chondrogenesis. *J Gerontol A Biol Sci Med Sci* **2007,** 62, (2), 136-48.

469. Zhang, H.; Fazel, S.; Tian, H.; Mickle, D. A. G.; Weisel, R. D.; Fujii, T.; Li, R.-K., Increasing donor age adversely impacts beneficial effects of bone marrow but not smooth muscle myocardial cell therapy. *Am J Physiol Heart Circ Physiol* **2005,** 289, (5), H2089-2096.

470. Bonab, M.; Alimoghaddam, K.; Talebian, F.; Ghaffari, S.; Ghavamzadeh, A.; Nikbin, B., Aging of mesenchymal stem cell in vitro. *BMC Cell Biol* **2006,** 7, (1), 14.

471. Vacanti, V.; Kong, E.; Suzuki, G.; Sato, K.; Canty, J. M.; Lee, T., Phenotypic changes of adult porcine mesenchymal stem cells induced by prolonged passaging in culture. *J Cell Physiol* **2005,** 205, (2), 194-201.

472. Banfi, A.; Muraglia, A.; Dozin, B.; Mastrogiacomo, M.; Cancedda, R.; Quarto, R., Proliferation kinetics and differentiation potential of ex vivo expanded human bone marrow stromal cells: Implications for their use in cell therapy. *Exp Hematol* **2000,** 28, (6), 707-715.

473. Crisostomo, P. R.; Wang, M.; Wairiuko, G. M.; Morrell, E. D.; Terrell, A. M.; Seshadri, P.; Nam, U. H.; Meldrum, D. R., High passage number of stem cells adversely affects stem cell activation and myocardial protection. *Shock* **2006,** 26, (6), 575-80.

474. Muraglia, A.; Cancedda, R.; Quarto, R., Clonal mesenchymal progenitors from human bone marrow differentiate in vitro according to a hierarchical model. *J Cell Sci* **2000,** 113, (7), 1161-1166.

475. Im, G., Il; Shin, Y.-W.; Lee, K.-B., Do adipose tissue-derived mesenchymal stem cells have the same osteogenic and chondrogenic potential as bone marrow-derived cells? *Osteoarthr Cartil* **2005,** 13, (10), 845-853.

476. Liu, T. M.; Martina, M.; Hutmacher, D. W.; Hui, J. H. P.; Lee, E. H.; Lim, B., Identification of Common Pathways Mediating Differentiation of Bone Marrow- and Adipose Tissue-Derived Human Mesenchymal Stem Cells into Three Mesenchymal Lineages. *Stem Cells* **2007,** 25, (3), 750-760.

477. Jahoda, C. A.; Whitehouse, J.; Reynolds, A. J.; Hole, N., Hair follicle dermal cells differentiate into adipogenic and osteogenic lineages. *Exp Dermatol* **2003,** 12, (6), 849-59.

478. Chen, F. G.; Zhang, W. J.; Bi, D.; Liu, W.; Wei, X.; Chen, F. F.; Zhu, L.; Cui, L.; Cao, Y., Clonal analysis of nestin vimentin+ multipotent fibroblasts isolated from human dermis. *J Cell Sci* **2007,** 120, (16), 2875-2883.

479. Grigolo, B.; Roseti, L.; Neri, S.; Gobbi, P.; Jensen, P.; Major, E. O.; Facchini, A., Human articular chondrocytes immortalized by HPV-16 E6 and E7 genes: Maintenance of differentiated phenotype under defined culture conditions. *Osteoarthr Cartil* **2002,** 10, (11), 879-89.

480. Bjornsson, S., Simultaneous preparation and quantitation of proteoglycans by precipitation with alcian blue. *Anal Biochem* **1993,** 210, (2), 282-91.

481. Holtorf, H. L.; Jansen, J. A.; Mikos, A. G., Flow perfusion culture induces the osteoblastic differentiation of marrow stroma cell-scaffold constructs in the absence of dexamethasone. *J Biomed Mater Res A* **2005,** 72, (3), 326-34.

482. Iwata, Y.; Morihara, T.; Tachiiri, H.; Kajikawa, Y.; Yoshida, A.; Arai, Y.; Tokunaga, D.; Sakamoto, H.; Matsuda, K.; Kurokawa, M.; Kawata, M.; Kubo, T., Behavior of host and graft cells in the early remodeling process of rotator cuff defects in a transgenic animal model. *J Shoulder Elbow Surg* **2008,** 17, (1 Suppl), 101S-107S.

483. Kajikawa, Y.; Morihara, T.; Watanabe, N.; Sakamoto, H.; Matsuda, K.; Kobayashi, M.; Oshima, Y.; Yoshida, A.; Kawata, M.; Kubo, T., GFP chimeric models exhibited a biphasic pattern of mesenchymal cell invasion in tendon healing. *J Cell Physiol* **2007,** 210, (3), 684-91.

484. Oshima, Y.; Watanabe, N.; Matsuda, K.; Takai, S.; Kawata, M.; Kubo, T., Fate of transplanted bone-marrow-derived mesenchymal cells during osteochondral repair using transgenic rats to simulate autologous transplantation. *Osteoarthr Cartil* **2004,** 12, (10), 811-7.

485. Oshima, Y.; Watanabe, N.; Matsuda, K.; Takai, S.; Kawata, M.; Kubo, T., Behavior of transplanted bone marrow-derived GFP mesenchymal cells in

osteochondral defect as a simulation of autologous transplantation. *J Histochem Cytochem* **2005,** 53, (2), 207-16.

486. Klouda, L.; Kretlow, J. D.; Mikos, A., Tailored Biomaterials for Tissue Engineering Needs and Their Clinical Translation. In *Translational Approaches in Tissue Engineering and Regenerative Medicine*, 1 ed.; Mao, J. J.; Vunjak-Novakovic, G.; Mikos, A. G.; Atala, A., Eds. Artech House: Boston, MA, 2008; Vol. 1, pp 325-337.

487. Hasegawa, Y.; Ogihara, T.; Yamada, T.; Ishigaki, Y.; Imai, J.; Uno, K.; Gao, J.; Kaneko, K.; Ishihara, H.; Sasano, H.; Nakauchi, H.; Oka, Y.; Katagiri, H., Bone marrow (BM) transplantation promotes beta-cell regeneration after acute injury through BM cell mobilization. *Endocrinology* **2007,** 148, (5), 2006-15.

488. Biankin, S. A.; Collector, M. I.; Biankin, A. V.; Brown, L. J.; Kleeberger, W.; Devereux, W. L.; Zahnow, C. A.; Baylin, S. B.; Watkins, D. N.; Sharkis, S. J.; Leach, S. D., A histological survey of green fluorescent protein expression in 'green' mice: implications for stem cell research. *Pathology (Phila)* **2007,** 39, (2), 247-51.

489. Shimko, D. A.; Burks, C. A.; Dee, K. C.; Nauman, E. A., Comparison of in vitro mineralization by murine embryonic and adult stem cells cultured in an osteogenic medium. *Tissue Eng* **2004,** 10, (9-10), 1386-1398.

490. Peng, L.; Jia, Z.; Yin, X.; Zhang, X.; Liu, Y.; Chen, P.; Ma, K.; Zhou, C., Comparative Analysis of Mesenchymal Stem Cells from Bone Marrow, Cartilage and Adipose Tissue. *Stem Cells Dev* **2008,** In press.

491. Carrington, J. L., Aging bone and cartilage: cross-cutting issues. *Biochem Biophys Res Commun* **2005,** 328, (3), 700-708.

492. Bishop-Bailey, D.; Warner, T. D., PPARgamma ligands induce prostaglandin production in vascular smooth muscle cells: indomethacin acts as a peroxisome proliferator-activated receptor-gamma antagonist. *FASEB J* **2003,** 17, (13), 1925-7.

493. Torii, I.; Morikawa, S.; Nakano, A.; Morikawa, K., Establishment of a human preadipose cell line, HPB-AML-I: refractory to PPARgamma-mediated adipogenic stimulation. *J Cell Physiol* **2003,** 197, (1), 42-52.

494. Lecka-Czernik, B.; Gubrij, I.; Moerman, E. J.; Kajkenova, O.; Lipschitz, D. A.; Manolagas, S. C.; Jilka, R. L., Inhibition of Osf2/Cbfa1 expression and terminal osteoblast differentiation by PPARgamma2. *J Cell Biochem* **1999,** 74, (3), 357-71.

495. Porada, C. D.; Zanjani, E. D.; Almeida-Porad, G., Adult mesenchymal stem cells: a pluripotent population with multiple applications. *Curr Stem Cell Res Ther* **2006,** 1, (3), 365-9.

496. Liu, G.; Li, Y.; Sun, J.; Zhou, H.; Zhang, W.; Cui, L.; Cao, Y., In vitro and in vivo evaluation of osteogenesis of human umbilical cord blood derived mesenchymal stem cells on partially demineralized bone matrix. *Tissue Eng Part A* **2009**.

497. Guo, X.; Park, H.; Young, S.; Kretlow, J. D.; van den Beucken, J. J.; Baggett, L. S.; Tabata, Y.; Kasper, F. K.; Mikos, A. G.; Jansen, J. A., Repair of osteochondral defects with biodegradable hydrogel composites encapsulating marrow mesenchymal stem cells in a rabbit model. *Acta Biomater* **2010,** 6, (1), 39-47.

498. Hare, J. M.; Traverse, J. H.; Henry, T. D.; Dib, N.; Strumpf, R. K.; Schulman, S. P.; Gerstenblith, G.; DeMaria, A. N.; Denktas, A. E.; Gammon, R. S.; Hermiller, J. B., Jr.; Reisman, M. A.; Schaer, G. L.; Sherman, W., A randomized, double-blind, placebo-controlled, dose-escalation study of intravenous adult human mesenchymal stem cells (prochymal) after acute myocardial infarction. *J Am Coll Cardiol* **2009,** 54, (24), 2277-86.

499. Satar, B.; Karahatay, S.; Kurt, B.; Ural, A. U.; Safali, M.; Avcu, F.; Oztas, E.; Kucuktag, Z., Repair of transected facial nerve with mesenchymal stromal cells: histopathologic evidence of superior outcome. *Laryngoscope* **2009,** 119, (11), 2221-5.

500. Oh, J. Y.; Kim, M. K.; Shin, M. S.; Lee, H. J.; Ko, J. H.; Wee, W. R.; Lee, J. H., The anti-inflammatory and anti-angiogenic role of mesenchymal stem cells in corneal wound healing following chemical injury. *Stem Cells* **2008,** 26, (4), 1047-55.

501. Ringden, O.; Uzunel, M.; Sundberg, B.; Lonnies, L.; Nava, S.; Gustafsson, J.; Henningsohn, L.; Le Blanc, K., Tissue repair using allogeneic mesenchymal

stem cells for hemorrhagic cystitis, pneumomediastinum and perforated colon. *Leukemia* **2007,** 21, (11), 2271-6.

502. Kuo, Y. R.; Goto, S.; Shih, H. S.; Wang, F. S.; Lin, C. C.; Wang, C. T.; Huang, E. Y.; Chen, C. L.; Wei, F. C.; Zheng, X. X.; Lee, W. P., Mesenchymal stem cells prolong composite tissue allotransplant survival in a swine model. *Transplantation* **2009,** 87, (12), 1769-77.

503. Giordano, A.; Galderisi, U.; Marino, I. R., From the laboratory bench to the patient's bedside: an update on clinical trials with mesenchymal stem cells. *J Cell Physiol* **2007,** 211, (1), 27-35.

504. Sensebe, L., Clinical grade production of mesenchymal stem cells. *Biomed Mater Eng* **2008,** 18, (1 Suppl), S3-10.

505. Frohlich, M.; Grayson, W. L.; Wan, L. Q.; Marolt, D.; Drobnic, M.; Vunjak-Novakovic, G., Tissue engineered bone grafts: biological requirements, tissue culture and clinical relevance. *Curr Stem Cell Res Ther* **2008,** 3, (4), 254-64.

506. Sensebe, L.; Bourin, P., Producing MSC according GMP: process and controls. *Biomed Mater Eng* **2008,** 18, (4-5), 173-7.

507. Brinchmann, J. E., Expanding autologous multipotent mesenchymal bone marrow stromal cells. *J Neurol Sci* **2008,** 265, (1-2), 127-30.

508. Pountos, I.; Corscadden, D.; Emery, P.; Giannoudis, P. V., Mesenchymal stem cell tissue engineering: techniques for isolation, expansion and application. *Injury* **2007,** 38 Suppl 4, S23-33.

509. Lange, C.; Cakiroglu, F.; Spiess, A. N.; Cappallo-Obermann, H.; Dierlamm, J.; Zander, A. R., Accelerated and safe expansion of human mesenchymal stromal cells in animal serum-free medium for transplantation and regenerative medicine. *J Cell Physiol* **2007,** 213, (1), 18-26.

510. Schuh, E. M.; Friedman, M. S.; Carrade, D. D.; Li, J.; Heeke, D.; Oyserman, S. M.; Galuppo, L. D.; Lara, D. J.; Walker, N. J.; Ferraro, G. L.; Owens, S. D.; Borjesson, D. L., Identification of variables that optimize isolation

and culture of multipotent mesenchymal stem cells from equine umbilical-cord blood. *Am J Vet Res* **2009,** 70, (12), 1526-35.

511. Frith, J. E.; Thomson, B.; Genever, P., Dynamic three-dimensional culture methods enhance mesenchymal stem cell properties and increase therapeutic potential. *Tissue Eng Part C Methods* **2009**.

512. Oedayrajsingh-Varma, M. J.; van Ham, S. M.; Knippenberg, M.; Helder, M. N.; Klein-Nulend, J.; Schouten, T. E.; Ritt, M. J.; van Milligen, F. J., Adipose tissue-derived mesenchymal stem cell yield and growth characteristics are affected by the tissue-harvesting procedure. *Cytotherapy* **2006,** 8, (2), 166-77.

513. Seeger, F. H.; Tonn, T.; Krzossok, N.; Zeiher, A. M.; Dimmeler, S., Cell isolation procedures matter: a comparison of different isolation protocols of bone marrow mononuclear cells used for cell therapy in patients with acute myocardial infarction. *Eur Heart J* **2007,** 28, (6), 766-72.

514. Agata, H.; Asahina, I.; Watanabe, N.; Ishii, Y.; Kubo, N.; Ohshima, S.; Yamazaki, M.; Tojo, A.; Kagami, H., Characteristic change and loss of in vivo osteogenic abilities of human bone marrow stromal cells during passage. *Tissue Eng Part A* **2009**.

515. Lepperdinger, G.; Brunauer, R.; Jamnig, A.; Laschober, G.; Kassem, M., Controversial issue: is it safe to employ mesenchymal stem cells in cell-based therapies? *Exp Gerontol* **2008,** 43, (11), 1018-23.

516. Boquest, A. C.; Shahdadfar, A.; Fronsdal, K.; Sigurjonsson, O.; Tunheim, S. H.; Collas, P.; Brinchmann, J. E., Isolation and transcription profiling of purified uncultured human stromal stem cells: alteration of gene expression after in vitro cell culture. *Mol Biol Cell* **2005,** 16, (3), 1131-41.

517. Centeno, C. J.; Schultz, J. R.; Cheever, M.; Robinson, B.; Freeman, M.; Marasco, W., Safety and Complications Reporting on the Re-implantation of Culture-Expanded Mesenchymal Stem Cells using Autologous Platelet Lysate Technique. *Curr Stem Cell Res Ther* **2009**.

518. Foudah, D.; Redaelli, S.; Donzelli, E.; Bentivegna, A.; Miloso, M.; Dalpra, L.; Tredici, G., Monitoring the genomic stability of in vitro cultured rat bone-marrow-derived mesenchymal stem cells. *Chromosome Res* **2009**.

519. Duggal, S.; Fronsdal, K. B.; Szoke, K.; Shahdadfar, A.; Melvik, J. E.; Brinchmann, J. E., Phenotype and gene expression of human mesenchymal stem cells in alginate scaffolds. *Tissue Eng Part A* **2009,** 15, (7), 1763-73.

520. Kuhn, N. Z.; Tuan, R. S., Regulation of stemness and stem cell niche of mesenchymal stem cells: implications in tumorigenesis and metastasis. *J Cell Physiol* 222, (2), 268-77.

521. Zhou, Y. F.; Bosch-Marce, M.; Okuyama, H.; Krishnamachary, B.; Kimura, H.; Zhang, L.; Huso, D. L.; Semenza, G. L., Spontaneous transformation of cultured mouse bone marrow-derived stromal cells. *Cancer Res* **2006,** 66, (22), 10849-54.

522. Dahl, J. A.; Duggal, S.; Coulston, N.; Millar, D.; Melki, J.; Shahdadfar, A.; Brinchmann, J. E.; Collas, P., Genetic and epigenetic instability of human bone marrow mesenchymal stem cells expanded in autologous serum or fetal bovine serum. *Int J Dev Biol* **2008,** 52, (8), 1033-42.

523. Aalami, O. O.; Nacamuli, R. P.; Lenton, K. A.; Cowan, C. M.; Fang, T. D.; Fong, K. D.; Shi, Y. Y.; Song, H. M.; Sahar, D. E.; Longaker, M. T., Applications of a mouse model of calvarial healing: differences in regenerative abilities of juveniles and adults. *Plast Reconstr Surg* **2004,** 114, (3), 713-20.

524. Kretlow, J. D.; Jin, Y. Q.; Liu, W.; Zhang, W. J.; Hong, T. H.; Zhou, G.; Baggett, L. S.; Mikos, A. G.; Cao, Y., Donor age and cell passage affects differentiation potential of murine bone marrow-derived stem cells. *BMC Cell Biol* **2008,** 9, 60.

525. McCann, R. M.; Marsh, D. R.; Horner, A.; Clarke, S., Body Mass Index is more predictive of progenitor number in bone marrow stromal cell population than age in males- expanding the predictors of the progenitor compartment. *Tissue Eng Part A* **2009**.

526. Iwase, T.; Nagaya, N.; Fujii, T.; Itoh, T.; Murakami, S.; Matsumoto, T.; Kangawa, K.; Kitamura, S., Comparison of angiogenic potency between mesenchymal stem cells and mononuclear cells in a rat model of hindlimb ischemia. *Cardiovasc Res* **2005,** 66, (3), 543-51.

527. Mazo, M.; Gavira, J. J.; Abizanda, G.; Moreno, C.; Ecay, M.; Soriano, M.; Aranda, P.; Collantes, M.; Alegria, E.; Merino, J.; Penuelas, I. N.; Verdugo, J. M.; Pelacho, B.; Prosper, F., Transplantation of Mesenchymal Stem Cells exerts a greater long-term effect than Bone Marrow Mononuclear Cells in a chronic myocardial infarction model in rat. *Cell Transplant* **2009**.

528. Samdani, A. F.; Paul, C.; Betz, R. R.; Fischer, I.; Neuhuber, B., Transplantation of human marrow stromal cells and mono-nuclear bone marrow cells into the injured spinal cord: a comparative study. *Spine (Phila Pa 1976)* **2009,** 34, (24), 2605-12.

529. Okumura, M.; Ohgushi, H.; Tamai, S., Bonding osteogenesis in coralline hydroxyapatite combined with bone marrow cells. *Biomaterials* **1991,** 12, (4), 411-6.

530. Ohgushi, H.; Okumura, M.; Tamai, S.; Shors, E. C.; Caplan, A. I., Marrow cell induced osteogenesis in porous hydroxyapatite and tricalcium phosphate: a comparative histomorphometric study of ectopic bone formation. *J Biomed Mater Res* **1990,** 24, (12), 1563-70.

531. Ohgushi, H.; Goldberg, V. M.; Caplan, A. I., Heterotopic osteogenesis in porous ceramics induced by marrow cells. *J Orthop Res* **1989,** 7, (4), 568-78.

532. Chang, F.; Ishii, T.; Yanai, T.; Mishima, H.; Akaogi, H.; Ogawa, T.; Ochiai, N., Repair of large full-thickness articular cartilage defects by transplantation of autologous uncultured bone-marrow-derived mononuclear cells. *J Orthop Res* **2008,** 26, (1), 18-26.

533. Gan, Y.; Dai, K.; Zhang, P.; Tang, T.; Zhu, Z.; Lu, J., The clinical use of enriched bone marrow stem cells combined with porous beta-tricalcium phosphate in posterior spinal fusion. *Biomaterials* **2008,** 29, (29), 3973-82.

534. Muschler, G. F.; Matsukura, Y.; Nitto, H.; Boehm, C. A.; Valdevit, A. D.; Kambic, H. E.; Davros, W. J.; Easley, K. A.; Powell, K. A., Selective retention of bone marrow-derived cells to enhance spinal fusion. *Clin Orthop* **2005**, (432), 242-51.

535. Dean, D.; Wolfe, M. S.; Ahmad, Y.; Totonchi, A.; Chen, J. E.; Fisher, J. P.; Cooke, M. N.; Rimnac, C. M.; Lennon, D. P.; Caplan, A. I.; Topham, N. S.; Mikos,

A. G., Effect of transforming growth factor beta 2 on marrow-infused foam poly(propylene fumarate) tissue-engineered constructs for the repair of critical-size cranial defects in rabbits. *Tissue Eng* **2005,** 11, (5-6), 923-39.

536. Ryu, J. H.; Kim, I. K.; Cho, S. W.; Cho, M. C.; Hwang, K. K.; Piao, H.; Piao, S.; Lim, S. H.; Hong, Y. S.; Choi, C. Y.; Yoo, K. J.; Kim, B. S., Implantation of bone marrow mononuclear cells using injectable fibrin matrix enhances neovascularization in infarcted myocardium. *Biomaterials* **2005,** 26, (3), 319-26.

537. Falanga, V.; Iwamoto, S.; Chartier, M.; Yufit, T.; Butmarc, J.; Kouttab, N.; Shrayer, D.; Carson, P., Autologous bone marrow-derived cultured mesenchymal stem cells delivered in a fibrin spray accelerate healing in murine and human cutaneous wounds. *Tissue Eng* **2007,** 13, (6), 1299-312.

538. Kalbermatten, D. F.; Kingham, P. J.; Mahay, D.; Mantovani, C.; Pettersson, J.; Raffoul, W.; Balcin, H.; Pierer, G.; Terenghi, G., Fibrin matrix for suspension of regenerative cells in an artificial nerve conduit. *J Plast Reconstr Aesthet Surg* **2008,** 61, (6), 669-75.

539. Vadala, G.; Di Martino, A.; Tirindelli, M. C.; Denaro, L.; Denaro, V., Use of autologous bone marrow cells concentrate enriched with platelet-rich fibrin on corticocancellous bone allograft for posterolateral multilevel cervical fusion. *J Tissue Eng Regen Med* **2008,** 2, (8), 515-20.

540. Fernandes, H.; Dechering, K.; Van Someren, E.; Steeghs, I.; Apotheker, M.; Leusink, A.; Bank, R.; Janeczek, K.; Van Blitterswijk, C.; de Boer, J., The role of collagen crosslinking in differentiation of human mesenchymal stem cells and MC3T3-E1 cells. *Tissue Eng Part A* **2009,** 15, (12), 3857-67.

541. Elgazzar, R. F.; Mutabagani, M. A.; Abdelaal, S. E.; Sadakah, A. A., Platelet rich plasma may enhance peripheral nerve regeneration after cyanoacrylate reanastomosis: a controlled blind study on rats. *Int J Oral Maxillofac Surg* **2008,** 37, (8), 748-55.

542. Ellis, B. C.; Stransky, A., A quick and accurate method for the determination of fibronogen in plasma. *J Lab Clin Med* **1961,** 58, 477-88.

543. Dhert, W. J.; Verheyen, C. C.; Braak, L. H.; de Wijn, J. R.; Klein, C. P.; de Groot, K.; Rozing, P. M., A finite element analysis of the push-out test: influence of test conditions. *J Biomed Mater Res* **1992,** 26, (1), 119-30.

544. Young, S.; Patel, Z. S.; Kretlow, J. D.; Murphy, M. B.; Mountziaris, P. M.; Baggett, L. S.; Ueda, H.; Tabata, Y.; Jansen, J. A.; Wong, M.; Mikos, A. G., Dose effect of dual delivery of vascular endothelial growth factor and bone morphogenetic protein-2 on bone regeneration in a rat critical-size defect model. *Tissue Eng Part A* **2009,** 15, (9), 2347-62.

545. Glantz, S. A., *Primer of biostatistics*. 6 ed.; McGraw-Hill Medical: New York, 2005; p 500.

546. Shah, D. A.; Madden, L. V., Nonparametric analysis of ordinal data in designed factorial experiments. *Phytopathology* **2004,** 94, (1), 33-43.

547. Brunner, E.; Dette, H.; Munk, A., Box-Type Approximations in Nonparametric Factorial Designs. *J Am Stat Assoc* **1997,** 92, (440), 1494-1502.

548. Li, W. J.; Cooper, J. A., Jr.; Mauck, R. L.; Tuan, R. S., Fabrication and characterization of six electrospun poly(alpha-hydroxy ester)-based fibrous scaffolds for tissue engineering applications. *Acta Biomater* **2006,** 2, (4), 377-85.

549. Yoon, E.; Dhar, S.; Chun, D. E.; Gharibjanian, N. A.; Evans, G. R., In vivo osteogenic potential of human adipose-derived stem cells/poly lactide-co-glycolic acid constructs for bone regeneration in a rat critical-sized calvarial defect model. *Tissue Eng* **2007,** 13, (3), 619-27.

550. Abramovitch-Gottlib, L.; Geresh, S.; Vago, R., Biofabricated marine hydrozoan: a bioactive crystalline material promoting ossification of mesenchymal stem cells. *Tissue Eng* **2006,** 12, (4), 729-39.

551. Mygind, T.; Stiehler, M.; Baatrup, A.; Li, H.; Zou, X.; Flyvbjerg, A.; Kassem, M.; Bunger, C., Mesenchymal stem cell ingrowth and differentiation on coralline hydroxyapatite scaffolds. *Biomaterials* **2007,** 28, (6), 1036-47.

552. Flautre, B.; Descamps, M.; Delecourt, C.; Blary, M. C.; Hardouin, P., Porous HA ceramic for bone replacement: role of the pores and interconnections - experimental study in the rabbit. *J Mater Sci Mater Med* **2001,** 12, (8), 679-82.

553. Harris, C. T.; Cooper, L. F., Comparison of bone graft matrices for human mesenchymal stem cell-directed osteogenesis. *J Biomed Mater Res A* **2004,** 68, (4), 747-55.

554. Plachokova, A. S.; van den Dolder, J.; Stoelinga, P. J.; Jansen, J. A., The bone regenerative effect of platelet-rich plasma in combination with an osteoconductive material in rat cranial defects. *Clin Oral Implants Res* **2006,** 17, (3), 305-311.

555. Marx, R. E.; Carlson, E. R.; Eichstaedt, R. M.; Schimmele, S. R.; Strauss, J. E.; Georgeff, K. R., Platelet-rich plasma: Growth factor enhancement for bone grafts. *Oral Surg Oral Med Oral Pathol Oral Radiol Endod* **1998,** 85, (6), 638-46.

556. Kroese-Deutman, H. C.; Vehof, J. W. M.; Spauwen, P. H. M.; Stoelinga, P. J. W.; Jansen, J. A., Orthotopic bone formation in titanium fiber mesh loaded with platelet-rich plasma and placed in segmental defects. *Int J Oral Maxillofac Surg* **2008,** 37, (6), 542-549.

557. Messora, M. R.; Nagata, M. J.; Mariano, R. C.; Dornelles, R. C.; Bomfim, S. R.; Fucini, S. E.; Garcia, V. G.; Bosco, A. F., Bone healing in critical-size defects treated with platelet-rich plasma: a histologic and histometric study in rat calvaria. *J Periodontal Res* **2008,** 43, (2), 217-23.

558. Fontana, S.; Olmedo, D. G.; Linares, J. A.; Guglielmotti, M. B.; Crosa, M. E., Effect of platelet-rich plasma on the peri-implant bone response: an experimental study. *Implant Dent* **2004,** 13, (1), 73-8.

559. Filho Cerruti, H.; Kerkis, I.; Kerkis, A.; Tatsui, N. H.; da Costa Neves, A.; Bueno, D. F.; da Silva, M. C., Allogenous bone grafts improved by bone marrow stem cells and platelet growth factors: clinical case reports. *Artif Organs* **2007,** 31, (4), 268-73.

560. Hu, Z. M.; Peel, S. A.; Ho, S. K.; Sandor, G. K.; Clokie, C. M., Comparison of platelet-rich plasma, bovine BMP, and rhBMP-4 on bone matrix protein expression in vitro. *Growth Factors* **2009,** 27, (5), 280-8.

561. van den Dolder, J.; Mooren, R.; Vloon, A. P.; Stoelinga, P. J.; Jansen, J. A., Platelet-rich plasma: quantification of growth factor levels and the effect on growth and differentiation of rat bone marrow cells. *Tissue Eng* **2006,** 12, (11), 3067-73.

562. Roldan, J. C.; Jepsen, S.; Miller, J.; Freitag, S.; Rueger, D. C.; Acil, Y.; Terheyden, H., Bone formation in the presence of platelet-rich plasma vs. bone morphogenetic protein-7. *Bone* **2004,** 34, (1), 80-90.

563. Arpornmaeklong, P.; Kochel, M.; Depprich, R.; Kubler, N. R.; Wurzler, K. K., Influence of platelet-rich plasma (PRP) on osteogenic differentiation of rat bone marrow stromal cells. An in vitro study. *Int J Oral Maxillofac Surg* **2004,** 33, (1), 60-70.

564. Leitner, G. C.; Gruber, R.; Neumuller, J.; Wagner, A.; Kloimstein, P.; Hocker, P.; Kormoczi, G. F.; Buchta, C., Platelet content and growth factor release in platelet-rich plasma: a comparison of four different systems. *Vox Sang* **2006,** 91, (2), 135-9.

565. Kevy, S. V.; Jacobson, M. S., Comparison of methods for point of care preparation of autologous platelet gel. *J Extra Corpor Technol* **2004,** 36, (1), 28-35.

566. Weibrich, G.; Kleis, W. K.; Hitzler, W. E.; Hafner, G., Comparison of the platelet concentrate collection system with the plasma-rich-in-growth-factors kit to produce platelet-rich plasma: a technical report. *Int J Oral Maxillofac Implants* **2005,** 20, (1), 118-23.

567. Kim, E. S.; Park, E. J.; Choung, P. H., Platelet concentration and its effect on bone formation in calvarial defects: an experimental study in rabbits. *J Prosthet Dent* **2001,** 86, (4), 428-33.

568. Weibrich, G.; Kleis, W. K.; Kunz-Kostomanolakis, M.; Loos, A. H.; Wagner, W., Correlation of platelet concentration in platelet-rich plasma to the extraction method, age, sex, and platelet count of the donor. *Int J Oral Maxillofac Implants* **2001,** 16, (5), 693-9.

569. Weibrich, G.; Hansen, T.; Kleis, W.; Buch, R.; Hitzler, W. E., Effect of platelet concentration in platelet-rich plasma on peri-implant bone regeneration. *Bone* **2004,** 34, (4), 665-71.

570. Plachokova, A. S.; van den Dolder, J.; van den Beucken, J. J.; Jansen, J. A., Bone regenerative properties of rat, goat and human platelet-rich plasma. *Int J Oral Maxillofac Surg* **2009,** 38, (8), 861-9.

571. Kasten, P.; Vogel, J.; Luginbuhl, R.; Niemeyer, P.; Weiss, S.; Schneider, S.; Kramer, M.; Leo, A.; Richter, W., Influence of platelet-rich plasma on osteogenic differentiation of mesenchymal stem cells and ectopic bone formation in calcium phosphate ceramics. *Cells Tissues Organs* **2006,** 183, (2), 68-79.

572. Kasten, P.; Vogel, J.; Beyen, I.; Weiss, S.; Niemeyer, P.; Leo, A.; Luginbuhl, R., Effect of platelet-rich plasma on the in vitro proliferation and osteogenic differentiation of human mesenchymal stem cells on distinct calcium phosphate scaffolds: the specific surface area makes a difference. *J Biomater Appl* **2008,** 23, (2), 169-88.

573. Tasso, R.; Augello, A.; Boccardo, S.; Salvi, S.; Carida, M.; Postiglione, F.; Fais, F.; Truini, M.; Cancedda, R.; Pennesi, G., Recruitment of a host's osteoprogenitor cells using exogenous mesenchymal stem cells seeded on porous ceramic. *Tissue Eng Part A* **2009,** 15, (8), 2203-12.

574. Le Nihouannen, D.; Goyenvalle, E.; Aguado, E.; Pilet, P.; Bilban, M.; Daculsi, G.; Layrolle, P., Hybrid composites of calcium phosphate granules, fibrin glue, and bone marrow for skeletal repair. *J Biomed Mater Res A* **2007,** 81, (2), 399-408.

575. Ueno, T.; Honda, K.; Hirata, A.; Kagawa, T.; Kanou, M.; Shirasu, N.; Sawaki, M.; Yamachika, E.; Mizukawa, N.; Sugahara, T., Histological comparison of bone induced from autogenously grafted periosteum with bone induced from autogenously grafted bone marrow in the rat calvarial defect model. *Acta Histochem* **2008,** 110, (3), 217-23.

576. Becker, S.; Maissen, O.; Ponomarev, I.; Stoll, T.; Rahn, B.; Wilke, I., Osteopromotion by a beta-tricalcium phosphate/bone marrow hybrid implant for use in spine surgery. *Spine (Phila Pa 1976)* **2006,** 31, (1), 11-7.

577. Zhu, S. J.; Choi, B. H.; Jung, J. H.; Lee, S. H.; Huh, J. Y.; You, T. M.; Lee, H. J.; Li, J., A comparative histologic analysis of tissue-engineered bone using platelet-rich plasma and platelet-enriched fibrin glue. *Oral Surg Oral Med Oral Pathol Oral Radiol Endod* **2006,** 102, (2), 175-9.

578. Findikcioglu, K.; Findikcioglu, F.; Yavuzer, R.; Elmas, C.; Atabay, K., Effect of platelet-rich plasma and fibrin glue on healing of critical-size calvarial bone defects. *J Craniofac Surg* **2009,** 20, (1), 34-40.

579. Ito, K.; Yamada, Y.; Naiki, T.; Ueda, M., Simultaneous implant placement and bone regeneration around dental implants using tissue-engineered bone with fibrin glue, mesenchymal stem cells and platelet-rich plasma. *Clin Oral Implants Res* **2006,** 17, (5), 579-86.

580. Tsai, C. H.; Hsu, H. C.; Chen, Y. J.; Lin, M. J.; Chen, H. T., Using the growth factors-enriched platelet glue in spinal fusion and its efficiency. *J Spinal Disord Tech* **2009,** 22, (4), 246-50.

581. Lee, L. T.; Kwan, P. C.; Chen, Y. F.; Wong, Y. K., Comparison of the effectiveness of autologous fibrin glue and macroporous biphasic calcium phosphate as carriers in the osteogenesis process with or without mesenchymal stem cells. *J Chin Med Assoc* **2008,** 71, (2), 66-73.

582. Kalia, P.; Coathup, M. J.; Oussedik, S.; Konan, S.; Dodd, M.; Haddad, F. S.; Blunn, G. W., Augmentation of bone growth onto the acetabular cup surface using bone marrow stromal cells in total hip replacement surgery. *Tissue Eng Part A* **2009,** 15, (12), 3689-96.

583. Lucarelli, E.; Fini, M.; Beccheroni, A.; Giavaresi, G.; Di Bella, C.; Aldini, N. N.; Guzzardella, G.; Martini, L.; Cenacchi, A.; Di Maggio, N.; Sangiorgi, L.; Fornasari, P. M.; Mercuri, M.; Giardino, R.; Donati, D., Stromal stem cells and platelet-rich plasma improve bone allograft integration. *Clin Orthop Relat Res* **2005**, (435), 62-8.

584. Lei, H.; Xiao, R.; Tang, X. J.; Gui, L., Evaluation of the Efficacy of Platelet-Rich Plasma in Delivering BMSCs Into 3D Porous Scaffolds. *J Biomed Mater Res B Appl Biomater* **2009,** 91B, (2), 679-691.

585. Giannoni, P.; Scaglione, S.; Daga, A.; Ilengo, C.; Cilli, M.; Quarto, R., Short-time survival and engraftment of bone marrow stromal cells in an ectopic model of bone regeneration. *Tissue Eng Part A* **2009**.

586. Haasper, C.; Breitbart, A.; Hankemeier, S.; Wehmeier, M.; Hesse, E.; Citak, M.; Krettek, C.; Zeichen, J.; Jagodzinski, M., Influence of fibrin glue on proliferation and differentiation of human bone marrow stromal cells seeded on a biologic 3-dimensional matrix. *Technol Health Care* **2008,** 16, (2), 93-101.

587. Patel, V. V.; Zhao, L.; Wong, P.; Pradhan, B. B.; Bae, H. W.; Kanim, L.; Delamarter, R. B., An in vitro and in vivo analysis of fibrin glue use to control bone morphogenetic protein diffusion and bone morphogenetic protein-stimulated bone growth. *Spine J* **2006,** 6, (4), 397-403; discussion 404.

588. Woodruff, M. A.; Rath, S. N.; Susanto, E.; Haupt, L. M.; Hutmacher, D. W.; Nurcombe, V.; Cool, S. M., Sustained release and osteogenic potential of heparan sulfate-doped fibrin glue scaffolds within a rat cranial model. *J Mol Histol* **2007,** 38, (5), 425-33.

589. Hou, T.; Xu, J.; Li, Q.; Feng, J.; Zen, L., In vitro evaluation of a fibrin gel antibiotic delivery system containing mesenchymal stem cells and vancomycin alginate beads for treating bone infections and facilitating bone formation. *Tissue Eng Part A* **2008,** 14, (7), 1173-82.

590. Owens, B. D.; Kragh, J. F.; Wenke, J. C.; Macaitis, J.; Wade, C. E.; Holcomb, J. B., Combat wounds in operation Iraqi Freedom and operation Enduring Freedom. *J Trauma* **2008,** 64, (2), 295-9.

591. Wade, A. L.; Dye, J. L.; Mohrle, C. R.; Galarneau, M. R., Head, face, and neck injuries during Operation Iraqi Freedom II: results from the US Navy-Marine Corps Combat Trauma Registry. *J Trauma* **2007,** 63, (4), 836-40.

592. Champion, H. R.; Bellamy, R. F.; Roberts, C. P.; Leppaniemi, A., A profile of combat injury. *J Trauma* **2003,** 54, (5 Suppl), S13-9.

593. Kummoona, R., Posttraumatic missile injuries of the orofacial region. *J Craniofac Surg* **2008,** 19, (2), 300-5.

594. Koshima, I.; Nanba, Y.; Tsutsui, T.; Itoh, S., Sequential vascularized iliac bone graft and a superficial circumflex iliac artery perforator flap with a single source vessel for established mandibular defects. *Plast Reconstr Surg* **2004,** 113, (1), 101-6.

595. Rodriguez, E. D.; Martin, M.; Bluebond-Langner, R.; Manson, P. N., Multiplanar distraction osteogenesis of fibula free flaps used for secondary reconstruction of traumatic maxillary defects. *J Craniofac Surg* **2006,** 17, (5), 883-8.

596. Thorne, C. H., Gunshot wounds to the face. Current concepts. *Clin Plast Surg* **1992,** 19, (1), 233-44.

597. Gruss, J. S.; Antonyshyn, O.; Phillips, J. H., Early definitive bone and soft-tissue reconstruction of major gunshot wounds of the face. *Plast Reconstr Surg* **1991,** 87, (3), 436-50.

598. Kihtir, T.; Ivatury, R. R.; Simon, R. J.; Nassoura, Z.; Leban, S., Early management of civilian gunshot wounds to the face. *J Trauma* **1993,** 35, (4), 569-75; discussion 575-7.

599. Suominen, E.; Tukiainen, E., Close-range shotgun and rifle injuries to the face. *Clin Plast Surg* **2001,** 28, (2), 323-37.

600. Futran, N. D.; Farwell, D. G.; Smith, R. B.; Johnson, P. E.; Funk, G. F., Definitive management of severe facial trauma utilizing free tissue transfer. *Otolaryngol Head Neck Surg* **2005,** 132, (1), 75-85.

601. Goodger, N.; Wang, J.; Smagalski, G.; Hepworth, B., Methylmethacrylate as a space maintainer in mandibular reconstruction. *J Oral Maxillofac Surg* **2005,** 63, (7), 1048-1051.

602. Wright, S.; Bekiroglu, F.; Whear, N. M.; Grew, N. R., Use of Palacos R-40 with gentamicin to reconstruct temporal defects after maxillofacial reconstructions with temporalis flaps. *Br J Oral Maxillofac Surg* **2006,** 44, (6), 531-3.

603. Goode, R. L.; Reynolds, B. N., Tobramycin-impregnated methylmethacrylate for mandible reconstruction. *Arch Otolaryngol Head Neck Surg* **1992,** 118, (2), 201-4.

604. Brody, H. J., Complications of expanded polytetrafluoroethylene (e-PTFE) facial implant. *Dermatol Surg* **2001,** 27, (9), 792-4.

605. Shields, C. L.; Shields, J. A.; De Potter, P.; Singh, A. D., Problems with the hydroxyapatite orbital implant: experience with 250 consecutive cases. *Br J Ophthalmol* **1994,** 78, (9), 702-6.

606. Brown, A. E.; Banks, P., Late extrusion of alloplastic orbital floor implants. *Br J Oral Maxillofac Surg* **1993,** 31, (3), 154-7.

607. Hartman, E. H.; Vehof, J. W.; de Ruijter, J. E.; Spauwen, P. H.; Jansen, J., Ectopic bone formation in rats: the importance of vascularity of the acceptor site. *Biomaterials* **2004,** 25, (27), 5831-7.

608. Baran, C. N.; Celebioglu, S.; Sensöz, O.; Ulusoy, G.; Civelek, B.; Ortak, T., The behavior of fat grafts in recipient areas with enhanced vascularity. *Plast Reconstr Surg* **2002,** 109, (5), 1646-51; 1652.

609. van Gemert, J. T. M.; van Es, R. J. J.; Van Cann, E. M.; Koole, R., Nonvascularized Bone Grafts for Segmental Reconstruction of the Mandible– A Reappraisal. *J Oral Maxillofac Surg* **2009,** 67, (7), 1446-1452.

610. August, M.; Tompach, P.; Chang, Y.; Kaban, L., Factors influencing the long-term outcome of mandibular reconstruction. *J Oral Maxillofac Surg* **2000,** 58, (7), 731-737.

611. Vaandrager, J. M.; van Mullem, P. J.; de Wijn, J. R., Porous acrylic cement for the correction of craniofacial deformities and repair of defects, animal experimentation and two years of clinical application. *Biomaterials* **1983,** 4, (2), 128-30.

612. Zhang, S. M.; Chen, J. D., PMMA based foams made via surfactant-free high internal phase emulsion templates. *Chem Commun (Camb)* **2009**, (16), 2217-2219.

613. van Mullem, P.; de Wijn, J.; Vaandrager, J., Porous acrylic cement: evaluation of a novel implant material. *Ann Plast Surg* **1988,** 21, (6), 576.

614. van Mullem, P.; Vaandrager, J.; Nicolai, J.; De Wijn, J., Implantation of porous acrylic cement in soft tissues: an animal and human biopsy histological study. *Biomaterials* **1990,** 11, (5), 299.

615. Boger, A.; Bisig, A.; Bohner, M.; Heini, P.; Schneider, E., Variation of the mechanical properties of PMMA to suit osteoporotic cancellous bone. *J Biomater Sci Polym Ed* **2008,** 19, (9), 1125-42.

616. Hautamäki, M. P.; Aho, A. J.; Alander, P.; Rekola, J.; Gunn, J.; Strandberg, N.; Vallittu, P. K., Repair of bone segment defects with surface porous fiber-reinforced polymethyl methacrylate (PMMA) composite prosthesis: histomorphometric incorporation model and characterization by SEM. *Acta Orthop* **2008,** 79, (4), 555-64.

617. Young, S.; Bashoura, A. G.; Borden, T.; Baggett, L. S.; Jansen, J. A.; Wong, M.; Mikos, A. G., Development and characterization of a rabbit alveolar bone nonhealing defect model. *J Biomed Mater Res A* **2008,** 86, (1), 182-94.

618. van der Lubbe, H. B.; Klein, C. P.; de Groot, K., A simple method for preparing thin (10 microM) histological sections of undecalcified plastic embedded bone with implants. *Stain Technol* **1988,** 63, (3), 171-6.

619. Mellonig, J. T.; Nevins, M., Guided bone regeneration of bone defects associated with implants: an evidence-based outcome assessment. *Int J Periodontics Restorative Dent* **1995,** 15, (2), 168-85.

620. Behnia, H.; Motamedi, M. H., Reconstruction and rehabilitation of short-range, high-velocity gunshot injury to the lower face: a case report. *J Craniomaxillofac Surg* **1997,** 25, (4), 220-7.

621. Gasparini, G.; Boniello, R.; Moro, A.; Tamburrini, G.; Di Rocco, C.; Pelo, S., Cranial Reshaping Using Methyl Methacrylate: Technical Note. *J Craniofac Surg* **2009,** 20, (1), 184.

622. Tan, B. H.; Grijpma, D. W.; Nabuurs, T.; Feijen, J., Crosslinkable surfactants based on linoleic acid-functionalized block copolymers of ethylene oxide and epsilon-caprolactone for the preparation of stable PMMA latices. *Polymer* **2005,** 46, (4), 1347-1357.

623. Nathanson, D.; Gettleman, L.; Schnitman, P.; Shklar, G., Histologic response to porous PMMA implant materials. *J Biomed Mater Res* **1978,** 12, (1), 13-33.

624. McLaren, A. C.; McLaren, S. G.; Hickmon, M. K., Sucrose, xylitol, and erythritol increase PMMA permeability for depot antibiotics. *Clin Orthop* **2007,** 461, 60-3.

625. McLaren, A. C.; McLaren, S. G.; McLemore, R.; Vernon, B. L., Particle size of fillers affects permeability of polymethylmethacrylate. *Clin Orthop* **2007,** 461, 64-7.

626. De Wijn, J. R., Poly(methyl methacrylate)--aqueous phase blends: in situ curing porous materials. *J Biomed Mater Res* **1976,** 10, (4), 625-35.

627. Bruens, M. L.; Pieterman, H.; de Wijn, J. R.; Vaandrager, J. M., Porous polymethylmethacrylate as bone substitute in the craniofacial area. *J Craniofac Surg* **2003,** 14, (1), 63-8.

628. Meng, T.; Shi, B.; Lu, D.; Li, Y.; Wu, M., Roles of palatine bone denudation repairing with free buccal or palatal mucosal graft on maxillary growth: an experimental study in rabbits. *Ann Plast Surg* **2007,** 59, (3), 323.

629. Al-Asfour, A.; Al-Melh, M.; Andersson, L.; Joseph, B., Healing pattern of experimental soft tissue lacerations after application of novel topical anesthetic agents - an experimental study in rabbits. *Dent Traumatol* **2008,** 24, (1), 27-31.

630. Bronson, R. E.; Treat, J. A.; Bertolami, C. N., Fibroblastic subpopulations in uninjured and wounded rabbit oral mucosa. *J Dent Res* **1989,** 68, (1), 51-8.

631. Elshal, E. E.; Inokuchi, T.; Yoshida, S.; Sekine, J.; Sano, K.; Ninomiya, H.; Ikeda, H., A comparative study of epithelialization of subcutaneous fascial flaps

and muscle-only flaps in the oral cavity. A rabbit model. *Int J Oral Maxillofac Surg* **1998,** 27, (2), 141-8.

632. Fujisawa, K.; Miyamoto, Y.; Nagayama, M., Basic fibroblast growth factor and epidermal growth factor reverse impaired ulcer healing of the rabbit oral mucosa. *J Oral Pathol Med* **2003,** 32, (6), 358-66.

633. Onerci, M., The effects of lyophilized homograft amniotic membrane on wound healing on rabbits. *Acta Otorhinolaryngol Ital* **1991,** 11, (5), 491-6.

634. Levin, M. P.; Tsaknis, P. J.; Cutright, D. E., Healing of the oral mucosa with the use of collagen artificial skin. *J Periodontol* **1979,** 50, (5), 250-3.

635. Figueiredo, J. A.; Pesce, H. F.; Gioso, M. A.; Figueiredo, M. A., The histological effects of four endodontic sealers implanted in the oral mucosa: submucous injection versus implant in polyethylene tubes. *Int Endod J* **2001,** 34, (5), 377-85.

636. Bertolami, C. N.; Ellis, D. G.; Donoff, R. B., Healing of cutaneous and mucosal wounds grafted with collagen-glycosaminoglycan/silastic bilayer membranes: a preliminary report. *J Oral Maxillofac Surg* **1988,** 46, (11), 971-8.

637. Al Ruhaimi, K. A., Closure of palatal defects without a surgical flap: an experimental study in rabbits. *J Oral Maxillofac Surg* **2001,** 59, (11), 1319-25.

638. Ueda, M.; Ebata, K.; Kaneda, T., In vitro fabrication of bioartificial mucosa for reconstruction of oral mucosa: Basic research and clinical application. *Ann Plast Surg* **1991,** 27, (6), 540.

639. Williams, D. F., Introduction: Implantable materials and infection. *Injury* **1996,** 27, 1-4.

640. Depprich, R. A.; Handschel, J. G.; Meyer, U.; Meissner, G., Comparison of prevalence of microorganisms on titanium and silicone/polymethyl methacrylate obturators used for rehabilitation of maxillary defects. *J Prosthet Dent* **2008,** 99, (5), 400-5.

641. Cordero, J.; Munuera, L.; Folgueira, M. D., The influence of the chemical composition and surface of the implant on infection. *Injury* **1996,** 27, 34-37.

642. Pelissier, P.; Masquelet, A. C.; Bareille, R.; Pelissier, S. M.; Amedee, J., Induced membranes secrete growth factors including vascular and osteoinductive factors and could stimulate bone regeneration. *J Orthop Res* **2004,** 22, (1), 73-9.

643. Viateau, V.; Bensidhoum, M.; Guillemin, G.; Petite, H.; Hannouche, D.; Anagnostou, F.; Pelissier, P., Use of the induced membrane technique for bone tissue engineering purposes: animal studies. *Orthop Clin North Am* **2010,** 41, (1), 49-56.

644. Masquelet, A. C.; Begue, T., The concept of induced membrane for reconstruction of long bone defects. *Orthop Clin North Am* **2010,** 41, (1), 27-37.

645. Lenton, K. A.; Nacamuli, R. P.; Longaker, M. T., Porous polymethylmethacrylate as bone substitute in the craniofacial area. Bruens ML, Pieterman H, de Wijn JR, et al. J Craniofac Surg 2003; 14:63-68. *J Craniofac Surg* **2003,** 14, (4), 596-8.

646. de Jong, W. C.; Koolstra, J. H.; Korfage, J. A.; van Ruijven, L. J.; Langenbach, G. E., The daily habitual in vivo strain history of a non-weight-bearing bone. *Bone* **2009**.

647. Worley, R., The experimental use of poly (methyl methacrylate) implants in mandibular defects. *J Oral Surg* **1973,** 31, (3), 170.

648. Kangur, T. T.; Tolman, D. E.; Jowsey, J., The use of methylmethacrylate in the fixation of mandibular fractures in dogs. Experimental results. *Oral Surg Oral Med Oral Pathol* **1976,** 41, (5), 578-87.

649. Chiarini, L.; Figurelli, S.; Pollastri, G.; Torcia, E.; Ferrari, F.; Albanese, M.; Nocini, P. F., Cranioplasty using acrylic material: a new technical procedure. *J Craniomaxillofac Surg* **2004,** 32, (1), 5-9.

650. Lye, K. W.; Tideman, H.; Merkx, M. A.; Jansen, J., Bone cements and their potential use in a mandibular endoprosthesis. *Tissue Eng Part B Rev* **2009**.

651. Vaandrager, J.; van Mullem, P.; de Wijn, J., Craniofacial contouring and porous acrylic cement. *Ann Plast Surg* **1988,** 21, (6), 583.

652. Romo III, T.; Morris, L.; Reitzen, S.; Ghossaini, S.; Wazen, J.; Kohan, D., Reconstruction of Congenital Microtia-Atresia: Outcomes With the Medpor/Bone-Anchored Hearing Aid-Approach. *Ann Plast Surg* **2009,** 62, (4), 384.

653. Shirazi, M.; Marzo, S.; Leonetti, J., Perioperative complications with the bone-anchored hearing aid. *Otolaryngol Head Neck Surg* **2006,** 134, (2), 236-239.

654. Kiechel, S. F.; Rodeheaver, G. T.; Klawitter, J. J.; Edgerton, M. T.; Edlich, R. F., The role of implant porosity on the development of infection. *Surg Gynecol Obstet* **1977,** 144, (1), 58-62.

655. Sclafani, A. P.; Thomas, J. R.; Cox, A. J.; Cooper, M. H., Clinical and histologic response of subcutaneous expanded polytetrafluoroethylene (Gore-Tex) and porous high-density polyethylene (Medpor) implants to acute and early infection. *Arch Otolaryngol Head Neck Surg* **1997,** 123, (3), 328-36.

656. Padera, R. F.; Colton, C. K., Time course of membrane microarchitecture-driven neovascularization. *Biomaterials* **1996,** 17, (3), 277-84.

657. Beck, S.; Boger, A., Evaluation of the particle release of porous PMMA cements during curing. *Acta Biomater* **2009,** 5, (7), 2503-2507.

658. Yaszay, B.; Trindade, M. C.; Lind, M.; Goodman, S. B.; Smith, R. L., Fibroblast expression of C-C chemokines in response to orthopaedic biomaterial particle challenge in vitro. *J Orthop Res* **2001,** 19, (5), 970-6.

Chapter 10

Appendices

These appendices feature work in which the doctoral candidate participated and was a co-author on the resulting manuscript; however, the work was led by other researchers. Appendix A lists these publications and others that were not explicitly featured in this thesis. Appendices B and C are manuscripts that significantly influenced the work described in this thesis, in particular the study described in Chapter 4.

Appendix A: List of Manuscripts Co-Authored by the Doctoral Candidate During the Course of this Thesis

Kretlow, J. D.; Mikos, A. G., Review: mineralization of synthetic polymer scaffolds for bone tissue engineering. *Tissue Eng* **2007,** 13, (5), 927-38.

Kretlow, J. D.; Klouda, L.; Mikos, A. G., Injectable matrices and scaffolds for drug delivery in tissue engineering. *Adv Drug Deliv Rev* **2007,** 59, (4-5), 263-73.

Klouda, L.; Kretlow, J. D.; Mikos, A., Tailored Biomaterials for Tissue Engineering Needs and Their Clinical Translation. In *Translational Approaches in Tissue Engineering and Regenerative Medicine*, 1 ed.; Mao, J. J.; Vunjak-Novakovic, G.; Mikos, A. G.; Atala, A., Eds. Artech House: Boston, MA, 2008; Vol. 1, pp 325-337.

Hacker, M. C.; Klouda, L.; Ma, B. B.; Kretlow, J. D.; Mikos, A. G., Synthesis and Characterization of Injectable, Thermally and Chemically Gelable, Amphiphilic Poly(N-isopropylacrylamide)-Based Macromers. *Biomacromolecules* **2008,** 9, (3), 1558-1570.

Young, S.; Kretlow, J. D.; Nguyen, C.; Bashoura, A. G.; Baggett, L. S.; Jansen, J. A.; Wong, M.; Mikos, A. G., Microcomputed tomography characterization of neovascularization in bone tissue engineering applications. *Tissue Eng Part B Rev* **2008,** 14, (3), 295-306.

Kretlow, J. D.; Mikos, A. G., 2007 AIChE Alpha Chi Sigma Award: From Material to Tissue: Biomaterial Development, Scaffold Fabrication, and Tissue Engineering. *AIChE J* **2008,** 54, (12), 3048-3067.

Kasper F.K.; Liao J.; Kretlow J.D.; Sikavtsas V.I.; Mikos A.G., Flow Perfusion Culture of Mesenchymal Stem Cells for Bone Tissue Engineering. In *StemBook: Tissue Engineering*, 1 ed.; The Stem Cell Research Community, Ed. 2008.

Klouda, L.; Hacker, M. C.; Kretlow, J. D.; Mikos, A. G., Cytocompatibility evaluation of amphiphilic, thermally responsive and chemically crosslinkable macromers for in situ forming hydrogels. *Biomaterials* **2009,** 30, (27), 4558-66.

Young, S.; Patel, Z. S.; Kretlow, J. D.; Murphy, M. B.; Mountziaris, P. M.; Baggett, L. S.; Ueda, H.; Tabata, Y.; Jansen, J. A.; Wong, M.; Mikos, A. G., Dose effect of dual delivery of vascular endothelial growth factor and bone morphogenetic protein-2 on bone regeneration in a rat critical-size defect model. *Tissue Eng Part A* **2009,** 15, (9), 2347-62.

Guo, X.; Park, H.; Young, S.; Kretlow, J. D.; van den Beucken, J. J.; Baggett, L. S.; Tabata, Y.; Kasper, F. K.; Mikos, A. G.; Jansen, J. A., Repair of osteochondral defects with biodegradable hydrogel composites encapsulating marrow mesenchymal stem cells in a rabbit model. *Acta Biomater* **2010,** 6, (1), 39-47.

Shi, M; Kretlow, J. D.; Nguyen, A; Young, S.; Baggett, L. S.; Wong, M. E.; Kasper, F. K.; Mikos, A. G., Antibiotic-releasing porous polymethylmethacrylate constructs for osseous space maintenance and infection control. *Biomaterials* **2010,** in press.

Appendix B

Synthesis and Characterization of Injectable, Thermally and Chemically Gelable, Amphiphilic Poly(*N*-isopropylacrylamide)-Based Macromers[†]

Abstract

In this study, we synthesized and characterized a series of macromers based on poly(N-isopropylacrylamide) that undergo thermally induced physical gelation and, following chemical modification, can be chemically cross-linked. Macromers with number average molecular weights typically ranging from 2000 – 3500 Da were synthesized via free radical polymerization from, in addition to poly(*N*-isopropylacrylamide), pentaerythritol diacrylate monostearate, a bifunctional monomer containing a long hydrophobic chain, acrylamide, a hydrophilic monomer, and hydroxyethyl acrylate, a hydrophilic monomer used to provide hydroxyl groups for further chemical modification. Results indicated that the hydrophobic-hydrophilic balance achieved by varying the relative concentrations of comonomers used during synthesis was an important parameter in controlling the transition temperature of the macromers in solution and stability of the resultant gels. Storage moduli of the macromers increased over 4 orders of magnitude once gelation occurred above the transition temperature. Furthermore,

---

[†] This appendix was published as: Hacker, M. C.; Klouda, L.; Ma, B. B.; Kretlow, J. D.; Mikos, A. G., Synthesis and Characterization of Injectable, Thermally and Chemically Gelable, Amphiphilic Poly(N-isopropylacrylamide)-Based Macromers. *Biomacromolecules* **2008,** 9, (3), 1558-1570.

chemical cross-linking of these macromers resulted in gels with increased stability compared to uncross-linked controls. These results demonstrate the feasibility of synthesizing poly(*N*-isopropylacrylamide) based macromers that undergo tandem gelation and establish key criteria relating to the transition temperature and stability of these materials. The data suggest that these materials may be attractive substrates for tissue engineering and cellular delivery applications as the combination of mechanistically independent gelation techniques used in tandem may offer superior materials with regard to gelation kinetics and stability.

B.1 Introduction

One of the primary problems facing researchers and clinicians in the broad field of tissue engineering and regenerative medicine is the fabrication of biomaterial substrates that provide appropriate 3-dimensional architecture, mechanical support, and the ability to deliver both cells and growth factors tailored to a specific tissue of interest. *In situ* gel formation is a concept of great interest for tissue engineers as it enables the delivery of a hydrogel matrix encapsulating cells and/or growth factors to defects of any shape using minimally invasive surgical techniques.[1,2]

So far, no ideal technique towards achieving *in situ* gel formation exists. Various natural and synthetic polymers have been chemically modified with moieties for chemical cross-linking, including acrylic esters, methacrylic esters, cinnamoyl esters,[3] fumaric esters,[2] and vinylsulfone,[4] to yield injectable biodegradable matrices.[5] *In situ* gel formation by radical polymerization of electron-poor olefins can be induced photochemically or thermally without harming encapsulated cells.[6,7] However, only low concentrations of radical initiators and cross-linking agents are tolerated by encapsulated cells,[7,8] and thus certain important parameters such as gelation kinetics, cross-linking densities and resulting mechanical properties of the hydrogels can only be varied to a limited extent without compromising the cytocompatibility of the process.

Polymeric materials that respond to a variety of environmental stimuli such as changes in temperature, pH, osmotic pressure, ionic strength, pressure, and

electric or magnetic field[1,9,10] have become attractive materials in biotechnology and medicine[9] and represent a viable approach to developing *in situ* gelling biomaterials. Temperature-sensitive hydrogel-forming polymers are among the most common of such materials and have been extensively studied as temperature-regulated drug delivery systems[11-15] and injectable matrices for tissue engineering.[1,16,17] While soluble below a characteristic temperature, solutions of these polymers undergo thermally induced, entropically driven phase separation above their lower critical solution temperature (LCST).

Cytocompatible chemical gelation protocols typically yield firm hydrogels after several minutes, while thermally induced gelation of thermosensitive polymer solutions occurs almost instantaneously once the LCST is reached. For cell encapsulation applications, thermosensitive polymers must possess a LCST below 37 °C and the thermally aggregated polymer chains have to retain a significant amount of water. Polymer classes from which certain representatives have been shown to meet these characteristics include copolyethers of poly(ethylene glycol) (PEG) and poly(propylene glycol),[18] copolyesters of PEG and poly(lactic acid)[19] or poly(propylene fumarate),[20] homo- and copolymers of poly(organophosphazenes),[21] and copolymers of poly(*N*-isopropylacrylamide) (PNiPAAm).[22,23] PNiPAAm undergoes a sharp and reversible phase transition at a LCST of 32 °C, but when used at the physiological temperature of 37 °C, linear PNiPAAm collapses substantially and precipitates as a separate phase. PNiPAAm copolymers containing small amounts of hydrophilic molecules, such

as acrylic acid, PEG or hyaluronic acid, however, demonstrated reversible gelation around body temperature without significant syneresis.[24-26] Another method to stabilize PNiPAAm copolymers above the LCST is to copolymerize the monomers in the presence of a cross-linker to yield polymer networks,[17] which in part limits the injectability of the materials.[14] Despite this limitation, combining functional groups within a macromolecule such that in solution there is physical gelation in response to physiological temperature upon injection and radical cross-linking at a slower kinetic rate *in situ* is a concept that can yield superior materials with regard to gelation kinetics and ultimate mechanical properties. In addition, control over hydrogel properties might be improved through the combination of two mechanistically and kinetically independent gelation techniques additionally. The few studies that have explored such tandem gelation concepts for biomedical applications have used modified PNiPAAm-based and polyether-type thermogelling materials that were chemically cured after physical *in situ* gelation by Michael-type addition reactions between thiols and acrylates.[27-29]

This study describes the synthesis of novel injectable PNiPAAm-based thermogelling macromers that are modified with olefinic moieties available for chemical cross-linking *in vivo* and that contain biocompatible hydrophobic domains. This design is expected to yield novel water-soluble environmentally responsive amphiphiles that not only combine two independent gelation mechanisms but also incorporate hydrophobic domains for mechanical

reinforcement and increased hydrophobicity of the thermogelled and cross-linked hydrogel matrix. A radical polymerization strategy is proposed to copolymerize the thermosensitive component *N*-isopropylacrylamide (NiPAAm) with other acrylic monomers to yield the functional amphiphiles. Pentaerythritol diacrylate monostearate (PEDAS), a bifunctional monomer consisting of the biocompatible tetravalent alcohol pentaerythritol esterified with two acrylic acids and stearic acid, a natural, metabolically resorbable fatty acid, provides the hydrophobic domain and NiPAAm the thermogelling properties, while acrylamide (AAm) was selected as a hydrophilic comonomer to adjust the transition temperature of the macromer and 2-hydroxyethyl acrylate (HEA) was introduced to increase the number of hydroxyl groups available for chemical modification to yield chemically cross-linkable macromers. This study presents a protocol to yield water-soluble thermogelling amphiphilic macromers composed of PEDAS, NiPAAm, AAm, and HEA. Specifically, two series of macromers, one consisting of poly(PEDAS-*stat*-NiPAAm-*stat*-AAm) terpolymers and the other poly(PEDAS-*stat*-NiPAAm-*stat*-AAm-*stat*-HEA) copolymers, with different comonomer ratios were synthesized and characterized by nuclear magnetic resonance (NMR) spectroscopy and gel permeation chromatography (GPC). Solutions of the macromers were characterized for their phase transition properties by differential scanning calorimetry (DSC) and oscillation rheology. Macroscopic gelation studies were performed to identify the thermodynamic stability of the thermogels. Candidate amphiphiles were (meth)acrylated to yield chemically cross-linkable

thermogelling macromers, which were then analyzed for chemical composition and cross-linking characteristics. Thermally and chemically cross-linkable macromers are presented that are potential building blocks for novel hydrogel systems with improved mechanical properties for orthopedic applications.

B.2 Materials and Methods

B.2.1 Materials

Pentaerythritol diacrylate monostearate (PEDAS), octadecyl acrylate (ODA), *N*-isopropylacrylamide (NiPAAm), poly(NiPAAm) (PNiPAAm), acrylamide (AAm), 2-hydroxyethylacrylate (HEA), 2,2′-azobis(2-methylpropionitrile) (azobisisobutyronitrile, AIBN), acryloyl chloride (AcCl), methacryloyl chloride (MACl), anhydrous sodium carbonate, 4-methoxyphenol, ammonium persulfate (APS), and *N,N,N′,N′*-tetramethylethane-1,2-diamine (TEMED) were purchased from Sigma-Aldrich (Sigma, St. Louis, MO) and used as received. The solvents tetrahydrofuran (THF), diethyl ether and acetone were obtained from Fisher Scientific (Pittsburgh, PA) in analytical grade and were used as received unless stated differently. THF used during macromer (meth)acrylation was dried by refluxing over a potassium/sodium alloy for 3 days under nitrogen and distilled prior to use.

B.2.2 Methods

Macromer synthesis

Statistical copolymers were synthesized from PEDAS, NiPAAm, AAm, and HEA using free radical polymerization (Scheme B.1). Thermogelling macromers (TGMs) of various compositions were obtained by dissolving the acrylic monomers at corresponding molar comonomer ratios in THF at 60 °C under nitrogen and initiating polymerization through the addition of AIBN (1.5 mol%). In a typical experiment, 3 g of PEDAS and corresponding amounts of comonomers were dissolved in 250 mL THF. The reaction was continuously stirred at 60 °C over 16 - 18h and then refluxed for an additional 2h while the nitrogen atmosphere was maintained. The product was isolated by rotoevaporation and precipitation in cold diethyl ether. The filtrate was dried, dissolved in THF for a second time and again precipitated in diethyl ether. Precipitating the product in ether twice has been shown efficient to remove unreacted monomers and low molecular weight oligomers during method development. The final filtrate was vacuum dried at ambient temperature and ground to a fine powder. Table B.1 summarizes the different TGMs that were synthesized and characterized.

Macromer (meth)acrylation

Methacrylated TGMs (TGM-MA) or acrylated TGMs (TGM-Ac) were obtained through the conversion of TGMs with MACl or AcCl in anhydrous THF in the presence of anhydrous sodium carbonate as scavenger for any acidic by-products. In a typical reaction, 5 g of vacuum dried TGM, 2.5 g of sodium

carbonate, and approximately 120 mg of 4-methoxy phenol as radical inhibitor were weighed into a three neck flask, which was subsequently purged with nitrogen and sealed against moisture. The nitrogen stream was maintained throughout the entire reaction. THF (75 mL) was added through a septum and the polymer was dissolved under vigorous stirring. Thereafter, the reaction was chilled to below -10 °C using an ice-sodium chloride bath. As soon as the temperature dropped below -10 °C, the (meth)acrylation agent (MACl or AcCl) was added dropwise by means of a plastic syringe with needle through the septum. This addition step was controlled by the reaction temperature, which was maintained below -10 °C at any time. Following the addition of the (meth)acrylation agent, the mixture was stirred for another 16 - 18 h during which the ice was allowed to melt and the mixture warmed up to ambient temperature. The reaction mixture was filtered to remove any salt. Subsequently, the polymer solution was carefully concentrated by rotoevaporation, diluted with acetone, and again concentrated until almost dry. Enough acetone was added to redissolve the polymer. The solution was precipitated in cold diethyl ether. This step allows also for the removal of the radical inhibitor 4-methoxy phenol which is soluble in diethyl ether. The (meth)acrylated TGM was isolated by vacuum filtration and finally dried under vacuum at ambient temperature.

Proton nuclear magnetic resonance spectroscopy (^{1}H-NMR)

^{1}H-NMR spectra were obtained using a 400 MHz spectrometer (Bruker, Switzerland). Sample materials were dissolved in $CDCl_3$ (typical concentration:

20 mg/mL) that contained 0.05 % tetramethylsilane (TMS) as internal shift reference. All postacquisition data processing was performed with the MestRe-C NMR software package (Mestrelab Research S.L., Spain). The free induction decay (FID) was Fourier transformed, manually phased, referenced using the TMS signal, baseline corrected, and integrated. To improve signal-to-noise, line broadening of 1.5 Hz was applied during transformation of the FID when meth(acrylated) TGMs were analyzed. To determine the comonomer composition of the macromers relative to PEDAS, the spectra were typically integrated between 0.85 and 0.94 ppm (I1), 0.95 and 1.24 ppm (I2), 1.25 and 1.34 ppm (I3), 1.35 and 2.45 ppm (I4), and between 3.50 and 4.50 ppm (I5) (Fig. B.1). I3, which was attributed to 28 (b in Fig. B.1) out of the 32 methylene protons of the stearate chain in PEDAS was set to 28. Consequently, I1, which represents the methyl protons in PEDAS (a in Fig. B1.), yielded values ranging between 2.8 and 3.4. It was found that the use of I3 instead of I1 as internal standard yielded more accurate results because I3 comprises a higher number of protons. The relative molar contents of the comonomers NiPAAm, AAm and HEA were calculated from the values obtained for I2, I4, and I5 according to the following equations (indices m, n, and o refer to Scheme B.1):

$$I2 = 6 \cdot n_m(\text{NiPAAm}) \quad (1)$$

$$I4 = 11 + 3 \cdot n_m(\text{NiPAAm}) + 3 \cdot n_n(\text{AAm}) + 3 \cdot n_o(\text{HEA}) \quad (2)$$

$$I5 = 8 + n_m(\text{NiPAAm}) + 5 \cdot n_o(\text{HEA})$$

(3)

Integral I2 comprises the 6 methyl protons of the N-isopropyl group of NiPAAm (p in Fig. B.1) (equation 1). I5 measures the methine proton of the latter functional group (i in Fig. B.1), the 8 methylene protons of pentaerythrityl core in PEDAS (e,f in Fig. B.1) as well as the 5 protons of the hydroxyethyl residue of HEA (l,m,h in Fig. B.1) (equation 3). I4 summarizes the 4 methylene protons on C2 and C3 of the fatty acid in PEDAS (c,d in Fig. B.1), the free hydroxyl proton in PEDAS (g in Fig. B.1), the 6 protons of the polymerized acrylic moieties of PEDAS, as well as 3 protons from each of the other copolymerized monomers NiPAAm, AAm, and HEA (x,y in Fig. B.1) (equation 2).

TGM conversion upon (meth)acylation was also determined relative to PEDAS. The integral I3 (1.25 - 1.34 ppm) was set to equal 28 protons. The signals derived from the olefinic protons of the acrylate (typically: 5.9 ppm, 6.2 ppm, and 6.5 ppm) or methacrylate groups (typically: 5.6 ppm, 6.15 ppm) were integrated individually and the upfield signal (5.9 ppm (TGM-Ac) or 5.6 ppm (TGM-MA)) was quantified to obtain the degree of (meth)acrylation relative to PEDAS. The olefinic signals located further downfield often overlapped with the broad signal of the -NHR proton (6 - 7 ppm) of NiPAAm, which lead to falsely increased signal integrals.

Gel Permeation Chromatography (GPC)

Molecular weight distributions of the different TGMs and (meth)acrylated TGMs were determined by GPC. A GPC system consisting of an HPLC pump (Waters, model 510, Milford, MA), an autosampler/injector (Waters, model 717) and a differential refractometer (Waters, model 410) equipped with a series of analytical columns (Styragel® guard column 20 mm, 4.6 x 30 mm; Styragel® HR3, 5 mm, 4.6 x 300 mm; Styragel® HR1 column, 5 mm, 4.6 x 300 mm (all Waters) was used with degassed chloroform (HPLC grade, Sigma) as the eluent at a flow rate of 1.0 mL/min. Samples were prepared in chloroform at a concentration of 25 mg/mL and filtered prior to analysis. Macromer number average molecular weight (Mn), weight average molecular weight (Mw), and polydispersity index (PI) were determined relative to polystyrene. Three samples of each material were prepared and analyzed.

Rheological characterization

All rheological measurements were performed on a thermostated oscillating rheometer (Rheolyst AR1000, TA Instruments, New Castle, DE, USA) equipped with a 6 cm steel cone (1 degree). TGMs were dissolved at the desired concentration, 10% (w/v) unless otherwise stated, in sterile minimum essential media (α modification; α-MEM) (Sigma) and kept on an orbital shaker over 24h at room temperature. In case the transition temperature of the macromer solution was below 25 °C, samples were shaken in a cold room (4 °C) until the polymers were dissolved. The dynamic viscoelastic properties of the solutions, namely the

dynamic moduli, storage modulus (G') and loss modulus (G"), complex viscosity ($|\eta^*|$), and loss angle (δ), were recorded using the TA Rheology Advantage™ software (TA Instruments) at a gap size of 26 μm.

Gelation properties and transition temperatures

In a typical experiment, TGM and control samples were loaded, cooled to 5 °C, pre-sheared at a rate of 1 s^{-1} for 1 min, and equilibrated for 15 min at 5 °C. The viscoelastic properties of the samples were then recorded during a temperature sweep from 5 °C to 65 °C at a rate of 1 °C/min at an observing frequency of 1 Hz and a displacement of $1x10^{-4}$ rad. To characterize the phase transition temperature of the TGM solution, different characteristic temperatures were determined. Upon thermogelation different rheological properties show characteristic changes during the temperature sweep. The initial change in viscoelastic properties is characterized by an increase of G' over G" resulting in a decrease of the phase angle δ. T_s characterizes the temperature at the first inflection point of the temperature-phase angle curve. During thermogel formation the viscosity of the system increased notably. T_η describes the location of the inflection point of the temperature-complex viscosity curve.

Reversibility of the thermogelation

Samples were loaded, cooled to 10 °C, pre-sheared at a rate of 1 s^{-1} for 1 min, and equilibrated for 5 min at 10 °C. The viscoelastic properties of the samples were then recorded during a set of different steps with a solvent trap installed. To gel the samples, a temperature sweep from 10 °C to 37 °C was

performed at a rate of 4 °C/min with a frequency of 1 Hz and a displacement of $1x10^{-4}$ rad (step I). The samples were kept at 37 °C for 2 min while maintaining frequency and displacement at 1 Hz and $1x10^{-4}$ rad, respectively (step II). For the next 2 min at 37 °C the displacement was increased to $1.5x10^{-3}$ rad (step III). Thereafter, the temperature setting was automatically changed to 15 °C and a time sweep was recorded over 90 min at a frequency of 1 Hz and a displacement of $1.5x10^{-3}$ rad (step IV). In a typical experiment, the temperature had equilibrated at 15 °C after around 2.0 min into the time sweep. G' and $|\eta^*|$ were analyzed at 15 °C in step I, at the end of step II and after 60' during step IV.

Macromer cross-linking

The cone-plate setup described above including the solvent trap was used to compare the gelation properties of solutions from (meth)acrylated TGMs with and without chemical initiation. Solutions of different (meth)acrylated TGMs with a concentration of 10% (m/v) were prepared in α-MEM and loaded on the rheometer at 15 °C. Before the geometry was lowered to gap size, TEMED and APS solution (100 mg/mL in water) were added to reach final concentrations of 20 mM each. In control samples without chemical initiation, equal amounts of TEMED and water were added. The samples were pre-sheared at a rate of 1 s^{-1} for 1 min at 15 °C before the viscoelastic properties were recorded in a two-step protocol. A temperature sweep from 15 °C to 37 °C was performed at a rate of 5 °C/min with a frequency of 1 Hz and a displacement of $1x10^{-4}$ rad (step I). Thereafter, the thermogel properties were monitored at 37 °C over 30 min while

maintaining oscillation frequency and displacement (step II). For samples with a transition temperature below 20 °C, the temperature sweep (step I) was started at 10 °C. For sample comparison the complex viscosities of the different samples were determined at 15 °C during step I and at the end of step II (30' at 37 °C).

Differential Scanning Calorimetry (DSC)

The transition temperature of different TGM solutions was also determined by DSC. Solutions of different macromers (10% w/v) were prepared in sterile α-MEM as described for the rheology samples and 20 μL were pipetted in an aluminum sample pan (TA Instruments, Newcastle, DE) and capped. Thermograms were recorded on a TA Instruments DSC 2920 equipped with a refrigerated cooling system against an empty sealed pan as reference. In a typical run, the oven was equilibrated at 5 °C for 10 min and then heated to 80 °C at a heating rate of 5 °C/min. For samples with a transition temperature below 20 °C, the measurements were performed between -5 °C and 50 °C. The transition temperature (T_{DSC}) of the TGM solution was determined as the "onset at inflection" of the endothermic peak in the thermogram using the Universal Analysis 2000 software provided with the DSC system. DSC has been shown to yield phase separation temperatures that are comparable to values obtained by optical cloud point measurements and UV turbidimetry;[30,31] methods that are typically used to determine the LCST of a polymer solution. All DSC experiments were performed in triplicate.

Thermogel stability

TGM solutions (10% m/v) in α-MEM were prepared as described above, pipetted (450 μL) into glass vials, which were finally capped airtight. The vials were placed in an incubator at 37 °C and analyzed after 2h and 24h. Following macroscopic observation of the thermogels, any supernatant was removed carefully using a syringe with needle. The amount of aspirated solvent was determined gravimetrically on an analytical scale and recorded relative to the amount of media that could be removed from control vials that had been filled with 450 μL plain α-MEM. The relative amount of supernatant represents a means to characterize the amount of syneresis of the corresponding thermogel.

Statistics

Unless otherwise stated, all experiments were conducted in triplicate and the data were expressed as mean ± standard deviation (SD). Single-factor analysis of variance (ANOVA) in conjunction with Tukey's Post Hoc test was performed to assess the statistical significance ($p < 0.05$) within data sets.

B.3 Results & Discussion

B.3.1 Macromonomer design

Statistical copolymers of different comonomer ratios were synthesized from PEDAS, NiPAAm, AAm, and HEA in a free radical polymerization reaction initiated by AIBN in THF (Scheme B.1). The main design criteria behind the amphiphilic NiPAAm-based macromers were the incorporation of a hydrophobic

moiety to improve intermolecular cohesion and hydrogel mechanics in the long run; the introduction of hydrolytically labile bonds to foster macromer biodegradability; the presence of thermoresponsive domains and of functional groups that can be modified to enable chemical cross-linking of the macromers. Hydrophobicity has been described as an important design criterion for polymers in bone tissue engineering.[32] Hydrophobic domains also contribute to cell-biomaterial interactions and can improve the mechanical properties of a material. Lipids and fatty acids are hydrophobic building blocks that have become popular in biomaterial research due to their biocompatibility, metabolic elimination and renewability.[33-35] PEDAS was selected as a hydrophobic building block as it contains the natural fatty acid stearic acid. Further components of PEDAS are the biocompatible alcohol pentaerythritol and two acrylic moieties that allow for the incorporation of PEDAS in copolymers synthesized by radical polymerization. The ester functionalities in PEDAS are potentially prone to hydrolysis. Other polymeric pentaerythritol esters have shown reasonable tissue compatibility and biodegradation,[36] PEDAS, therefore, was intended to function as a hydrophobic acrylic building block that mediates degradability to the copolymers. NiPAAm served as a well established building block for thermoresponsive polymers.[25] PNiPAAm is characterized by a LCST around 32 °C and is known to show extensive phase separation at higher temperatures. To form stable hydrogels, NiPAAm has been copolymerized with hydrophilic comonomers or cross-linked.[16] Since copolymerization with the hydrophobic comonomer PEDAS would

decrease the transition temperature, AAm was selected as a non-ionic, hydrophilic acrylic monomer to compensate for the hydrophobic contribution of PEDAS and adjust the hydrophilic-hydrophobic balance of the resulting macromer. Through HEA, free hydroxyl groups can be introduced into the macromer that are available for chemical modification. Acrylation or methacrylation of the hydroxyl group would lead to cross-linkable macromers in which the (meth)acrylate functionalities are connected to the polymer backbone via hydrolysable hydroxyethyl esters, a design that fosters degradability of the cross-linked hydrogels.

Initial experiments identified THF as a more suitable solvent for the synthesis of uncross-linked low-molecular weight macromers than toluene (data not shown). The reaction protocol described in the "Materials and Methods" section yielded copolymers that remained dissolved in the reaction mixture without increasing its viscosity significantly. The copolymers were precipitated out in diethyl ether and a colorless water- and chloroform-soluble powder was obtained after vacuum drying at yields around 80% - 85%. Initial studies further identified a 1:20 ratio of bifunctional PEDAS to the monofunctional acrylic comonomers to yield copolymers of reproducible molecular weight and promising hydrophilic-hydrophobic balance (data not shown). In order to establish the synthetic protocol and identify structure-property relations, terpolymers of PEDAS, NiPAAm and AAm were first synthesized and characterized. Since PEDAS contains a free hydroxyl group, such terpolymers technically already fulfill

the design criteria. Copolymers that contain HEA as a fourth comonomer were later synthesized with the objective to increase the number of free nucleophilic moieties for chemical modification. All copolymers are referred to with their theoretical comonomer composition throughout this study.

B.3.2 Synthesis and structural characterization of thermogelling poly(PEDAS-*stat*-NiPAAm-*stat*-AAm) terpolymers

Statistical copolymers were synthesized from PEDAS, NiPAAm and AAm with the content of hydrophilic AAm varying between 0% and 30% (Table B.1). Qualitative ^{1}H-NMR analysis of the purified polymers revealed the absence of any olefinic signals (5 - 7 ppm) from unreacted monomers (data not shown) and the presence of all characteristic signals derived from the copolymerized monomers (Fig. B.1, trace a). Aliphatic signals derived from the stearic acid chain of PEDAS were found at 0.9 ppm (-CH_3, 3H, triplet) and around 1.3 ppm (-CH_2-, 28H, broad signal). The integral of the signal between 1.25 and 1.34 ppm was set to 28 and used as internal reference to calculate comonomer composition relative to PEDAS. Further signals were derived from the N-isopropyl group in NiPAAm and found at 1.15 ppm (-NH-CH(C**H**$_3$)$_2$) and 4 ppm (-NH-C**H**(CH$_3$)$_2$), and the methine and methylene groups of the polyacrylate backbone together with some functionalities in PEDAS between 1.4 and 2.4 ppm. The signals at 2.9 ppm (Fig. B.1, trace a) and 2.5 ppm (trace b) were attributed to residual water. Due to interactions of the moisture with the macromer molecules in $CDCl_3$, the signal was found to vary in intensity and chemical shift dependent on macromer

composition and concentration (data not shown). With increasing AAm content and correspondingly decreasing NiPAAm content (Table B.1), the relative signal intensities of the aliphatic signals at around 1.15 and 1.3 ppm accordingly shifted towards the signal at 1.3 ppm indicating the varied comonomer composition in the copolymer (Fig. B.2A). Quantitative analysis of the NMR spectra revealed that copolymers at the desired comonomer ratios could be synthesized with appropriate control (Table B.1).

With regard to the applicability of these macromers as injectable materials, control over macromer molecular weight and branching is critical, especially since PEDAS is a bifunctional monomer. The free radical polymerization protocol was optimized to allow for the synthesis of macromers that contain one to two PEDAS molecules and comprise the other comonomers at the feed ratio. In any case, the formation of branched, high molecular weight products should be avoided. Living radical polymerization techniques, such as group transfer polymerization (GTP) or reversible addition-fragmentation chain transfer (RAFT), may likely provide better control over macromer composition and molecular weight, but the requirements towards comonomer chemistry and purity (GTP) and catalyst chemistry (RAFT) are far more specific [37]. Using these techniques, a systematic screening of different comonomer compositions as presented here would involve laborious adaptation of the protocol to the different comonomer compositions. The versatility of a free radical polymerization protocol appeared

advantageous for this study especially when control of macromer composition and weight can be achieved.

GPC analysis of the PEDAS-NiPAAm-AAm terpolymers with AAm contents up to 20% revealed number average molecular weights ranging between 1690 and 2250 Da (Table B.1). These values correlate well with theoretical molecular weights calculated for macromers that consist of one to two PEDAS precursors and the corresponding comonomers. The observed trend of decreasing molecular weights with increasing AAm and correspondingly decreasing NiPAAm content correlates with the difference in molecular weight between NiPAAm and AAm. Polydispersity indices between 2.3 and 2.7 were calculated. Figure B.3 shows representative chromatograms of different TGMs and precursors as obtained by GPC in chloroform. The polymer chromatograms were free of monomer signals at around 25 min, the elution time of NiPAAm monomers (Fig. B.3, trace a). PEDAS yielded a broad signal for which a PI of around 2 was determined (Fig. B.3, trace b). The copolymer chromatograms were characterized by a broad signal with a significant tail (Fig. B.3, trace c-e). As a similar shape was found for a control polymer containing ODA, a monofunctional lipophilic monomer, instead of the bifunctional PEDAS (Fig. B.3, trace c), the broad distribution was not attributed to macromer branching but to the amphiphilic properties and resulting possible interactions with the chromatographic system. Extensive branching, indicated by a high molecular weight peak at low retention time (Fig. B.3, trace f) was however observed for

poly(PEDAS$_1$-*stat*-NiPAAm$_{14}$-*stat*-AAm$_6$), the terpolymers with the highest AAm content. Quantitative analysis consequently revealed a low Mn with a high PI of almost 7 (Table B.1). Further studies revealed that macromer molecular weight and branching increased with increasing reactant concentrations and decreasing initiator concentration (data not shown). From the above described results one can conclude that good control over macromer architecture can be achieved with the established synthesis protocol for different comonomer compositions with AAm contents of up to 20%.

B.3.4 Thermogelation properties of poly(PEDAS-*stat*-NiPAAm-*stat*-AAm) terpolymers

The thermogelation properties of solutions of the synthesized macromers (10% (m/v)) were analyzed by oscillation rheology. It is known that thermally induced phase separation is strongly affected by solution pH and ionic strength. Therefore, cell culture medium (α-MEM) was used as solvent during these experiments to simulate physiological and *in vitro* cell culture conditions. Figure B.4 shows a typical rheogram of a TGM, here poly(PEDAS$_1$-*stat*-NiPAAm$_{15}$-*stat*-AAm$_{3.5}$-*stat*-HEA$_{1.5}$). The temperature dependent profiles observed for the complex moduli G' (storage modulus) and G" (loss modulus), the complex viscosity $|\eta^*|$ and the phase angle δ are typical for thermogelling materials.[22,38] At low temperatures, G" far exceeded G', which was indicated by a phase angle δ >> 45°, a property characteristic of viscous liquids (Fig. B.4). For temperatures below 25 °C, the storage modulus of the displayed TGM was below the detection

limit of the instrument. At temperatures below the phase transition, complex moduli and complex viscosity of the polymer solution decreased slightly with temperature, which is a typical behaviour of viscoelastic polymer solutions. Upon further heating and thermogelation (here past 26 °C), G' and G" both increased drastically with G' finally exceeding G" ($\delta < 45°$), which indicated the formation of a viscoelastic hydrogel. The complex viscosity of the system increased by almost five orders of magnitude during this transition. Characteristic temperatures that were determined from the rheograms of different TGMs for sample comparison are the temperatures at the first inflection point of the temperature-phase angle curve (T_s) and the inflection point of the temperature-complex viscosity curve (T_η). While T_s represents the onset of phase transition that is associated with colloidal aggregation of the macromers and clouding of the solution, T_η depicts the temperature at which the molecules have aggregated into a coherent network and form a hydrogel. The transition temperatures determined for poly(PEDAS$_1$-*stat*-NiPAAm$_{20}$) and the different PEDAS-NiPAAm-AAm terpolymers are summarized in Figure B.5A. The figure also contains the transition temperatures as obtained by DSC (T_{DSC}) for the different TGM solutions (10% (w/v) in α-MEM). The characteristic temperatures determined for PNiPAAm are displayed in Figure B.5B, I. Almost identical transition temperatures T_s (27.4 ± 1.2 °C) and T_η (27.4 ± 1.3 °C) were obtained for PNiPAAm by rheology. DSC analysis yielded a transition temperature of 30.7 ± 0.1 °C. The discrepancy between the different temperatures likely has methodical reasons especially since T_{DSC} is derived from

a calorimetric signal and the other two temperatures are derived from viscoelastic parameters relevant for material application. Poly(PEDAS$_1$-*stat*-NiPAAm$_{20}$) was characterized by significantly lower values for T_s (25.7 ± 0.1 °C) and T_n (26.8 ± 0.0 °C) (Fig. B.5A). T_{DSC} (23.5 ± 0.6 °C) confirmed the shift towards a lower phase transition temperature, which is caused by the hydrophobic structures in PEDAS. Increasing contents of the hydrophilic comonomer AAm in PEDAS-NiPAAm-AAm terpolymers compensated for the hydrophobic effect of PEDAS and the characteristic temperatures increased above the values of PNiPAAm. For poly(PEDAS$_1$-*stat*-NiPAAm$_{14}$-*stat*-AAm$_6$), the terpolymer with the highest AAm content investigated, transition temperatures of 34.7 ± 2.4 °C (T_s), 43.5 ± 2.3 °C (T_n), and 36.6 ± 1.4 °C (T_{DSC}) were measured. A similar correlation between TGM composition and the different transition temperatures was found. For all TGMs a difference between T_s and T_n was observed, which typically increased with AAm content. In comparison to pure PNiPAAm, for which identical values for T_s and T_n were obtained, the TGMs are amphiphilic molecules and the formation of micellar aggregates is likely involved in the colloidal aggregation of the macromers during phase transition.[39] Upon thermogelation the micelles aggregate and packing interactions increase to form dense gels. As the NiPAAm residues of the amphiphilic TGMs drastically change their interactions with solvent molecules during thermogelation, the hydrophilic-hydrophobic balance of the micelle-forming macromers is also altered significantly and micelle structure affected. Complex structural changes of the TGM solution are expected during

thermogelation that involve micelle formation, aggregation and vesicle shrinkage upon macromer dehydration. With this transition, T_s depicts the onset of colloidal aggregation and sol-gel transition, while T_n describes the temperature at which the macromers finally assemble into a coherent physical network and a dense gel is formed. For hydrophobic monomers (systems with low phase transition temperatures), the calorimetric transition (T_{DSC}) appears to correlate with the onset of phase transition T_s. With increasing hydrophilicity of the macromers, T_{DSC} shifts closer towards T_n (Fig. B.5 A,C). Since the different transition temperatures depend on solution concentration, trends between T_{DSC}, T_s and T_n might differ at different concentrations. The relatively low T_{DSC} observed for poly(PEDAS$_1$-*stat*-NiPAAm$_{14}$-*stat*-AAm$_6$) is likely attributed to the extensive branching of this macromer (Fig. B.5A, Table B.1).

Due to thermodynamic instability, PNiPAAm-based thermogels show considerable syneresis and possibly full phase separation when the temperature is increased above the phase transition temperature.[22,40] With regard to biomedical applications, it has been shown that the extent of phase separation correlates with the difference between transition temperature, commonly the LCST, and 37 °C. In order to test for the thermodynamic stability of thermogels formed by the different TGMs, solutions (10% (w/v) were incubated at a constant temperature of 37 °C and the extent of syneresis was determined after 1h, 2h and 24h. The results from the 2h time point are summarized in Figure B.6. Part A depicts the gross view of the thermogels after 2h at 37 °C. The residual gel mass

is summarized in part B (Fig. B.6). The solutions were prepared and pipetted into glass vials at ambient temperature below the transition temperature of the TGM solution. In a typical experiment thermogel formation occurred approximately 10 min after the vials were placed into the incubator. Immediately after gelation, the gel volume equalled the volume of the polymer solution (450 μL). After 24h, the residual gel fractions of all thermogels ranged around 10 - 15%, which was assumed to correlate with full syneresis and phase separation (data not shown). In accordance with the literature, PNiPAAm solutions (Fig. B.6, sample a) show extensive syneresis and phase separation at 37 °C. Solutions of poly($PEDAS_1$-*stat*-$NiPAAm_{20}$), which gelled at a lower temperature then PNiPAAm, shrunk to a comparable extent after 2h (sample b). With increasing AAm content, improved stability was observed for PEDAS-NiPAAm-AAm terpolymers (sample c, d) with poly($PEDAS_1$-*stat*-$NiPAAm_{16}$-*stat*-AAm_4) forming stable thermogels at 37 °C for 2h (sample d). Solutions of poly($PEDAS_1$-*stat*-$NiPAAm_{14}$-*stat*-AAm_6) (T_n = 43.5 ± 2.3 °C) did not gel at 37 °C; correspondingly, no gel fraction could be quantified after 2h (sample e).

These results show that amphiphilic terpolymers were synthesized with controlled molecular composition and structure. TGM structure, especially the hydrophobic-hydrophilic balance, controlled the thermally induced gelation of corresponding aqueous macromer solutions. The thermodynamic stability of the resulting thermogels correlated with transition temperature. With regard to the intended chemical modification of the macromers, initial tests revealed that the

free hydroxyl group in PEDAS (Scheme B.1) was not sufficiently accessible for (meth)acrylation reaction possibly due to steric hindrance (data not shown). In order to incorporate additional hydroxyl groups, HEA was introduced as comonomer and initially copolymerized with PEDAS and NiPAAm. HEA is known as a hydrophilic monomer and was therefore considered as a building block that could provide chemically accessible hydroxyl groups in combination with a potential to balance the hydrophobicity of PEDAS and control the transition temperature of the macromers. Analogous to the synthesis of poly($PEDAS_1$-*stat*-$NiPAAm_{16}$-*stat*-AAm_4), poly($PEDAS_1$-*stat*-$NiPAAm_{16}$-*stat*-HEA_4) was synthesized at the desired composition and molecular weight (Table B.1). Analysis of the transition temperatures revealed values below 25 °C for T_n, T_n and T_{DSC} (Fig. B.5B, II). As a result of intra- or intermolecular hydrogen bond formation the hydroxyl group of HEA did not fully interact with water and the expected hydrophilic effect of HEA was diminished in solution. Correspondingly, extensive syneresis was observed for the corresponding thermogels (Fig. B.6, sample h). Consequently, copolymers of PEDAS, NiPAAm, AAm, and HEA were synthesized for further experiments. The molar ratio of PEDAS to NiPAAm + AAm + HEA was maintained at 1:20.

B.3.5 Synthesis and characterization of thermogelling poly(PEDAS-*stat*-NiPAAm-*stat*-AAm-*stat*-HEA) copolymers

Copolymers containing 1 mol PEDAS, 15.4 mol NiPAAm and varying ratios of AAm and HEA (poly($PEDAS_1$-*stat*-$NiPAAm_{15.4}$-*stat*-AAm_m-*stat*-HEA_n))

were synthesized at the desired composition and molecular weight distribution (Table B.1, Fig. B.3). A trend between molecular weight and HEA content as a result of the molecular weight difference of AAm and HEA was observed. ^{1}H-NMR analysis confirmed the presence of HEA specific protons in the copolymers (l,h,m in Fig. B.1, trace b). The intensities of these signals were found to increase relative to the methine signal (4.0 ppm) of the *N*-isopropyl group of NiPAAm with increasing comonomer contents of HEA (Fig. B.2B). Figure B.3 compares the molecular weight distribution of poly(PEDAS$_1$-*stat*-NiPAAm$_{15.4}$-*stat*-AAm$_3$-*stat*-HEA$_{1.6}$) (trace d) and poly(ODA$_1$-*stat*-NiPAAm$_{15.4}$-*stat*-AAm$_3$-*stat*-HEA$_{1.6}$) (trace c). This comparison was motivated by the concern of network formation due to the use of the bifunctional monomer PEDAS. ODA is a monofunctional monomer comprising stearic alcohol and acrylic acid making the lipophilic component comparable to the stearic acid domain in PEDAS. The results illustrate that the molecular weight distributions of the different macromers do not differ significantly which indicates that PEDAS-containing TGMs are most likely branched but not networked and still contain individual macromers of controllable molecular weight (Mn) in the range of 2000 - 3500 Da (Fig. B.3, Table B.1). Despite its bifunctionality, PEDAS is considered advantageous over ODA because the lipophilic domain of PEDAS, stearic acid, can be metabolized following ester hydrolysis in contrast to stearic alcohol. Comparison of the transition temperatures of both copolymers (Fig B.5; B, III vs. C, data set on far left), revealed significantly higher values for poly(PEDAS$_1$-*stat*-NiPAAm$_{15.4}$-*stat*-

AAm_3-*stat*-$HEA_{1.6}$), which likely indicates that the hydrophilic pentaerythrityl core of PEDAS positively affects the hydrophobic-hydrophilic balance within the macromer. Within the set of poly($PEDAS_1$-*stat*-$NiPAAm_{15.4}$-*stat*-AAm_m-*stat*-HEA_n) copolymers, the transition temperatures follow the structure-property relations established in PEDAS-NiPAAm-AAm terpolymers (Fig. B.5C). With increasing HEA and decreasing AAm contents, the transition temperatures decrease. T_{DSC} again approaches T_c with increasing hydrophobicity of the TGMs. In correlation with the transition temperatures, the thermogel stability of poly($PEDAS_1$-*stat*-$NiPAAm_{15.4}$-*stat*-AAm_m-*stat*-HEA_n) copolymers at 37 °C decreased with increasing n/m ratio (Fig. B.6, samples f and g).

B.3.6 Thermogel stability of amphiphilic NiPAAm-based macromers

The TGMs were designed to contain hydrophobic domains to promote disperse interactions among the macromers and potentially increase mechanical stability of a TGM-based hydrogel. With regard to the thermogelation properties, these domains necessitated the incorporation of hydrophilic domains to adjust transition temperature and thermodynamic stability of thermally gelled TGM solutions. To test for any effects of the resulting amphiphilic design on the stability of corresponding thermogels, rheological experiments investigating the reversibility of the physical gelation were performed with PNiPAAm as control polymer (Fig. B.7). Two TGMs, poly($PEDAS_1$-*stat*-$NiPAAm_{14}$-*stat*-AAm_3-*stat*-HEA_3) and poly($PEDAS_1$-*stat*-$NiPAAm_{15.4}$-*stat*-AAm_2-*stat*-$HEA_{2.6}$), with calorimetric transition temperatures (T_{DSC}) surrounding the value determined for

PNiPAAm were selected considering the structure property relation established for TGM hydrogels. Comparison of PNiPAAm with the two TGMs that were characterized by comparable transition temperatures revealed significant differences for the gel-sol transition upon cooling below transition temperature. During the rheometric experiment, the macromers were first gelled during a controlled temperature sweep to 37 °C. After an isothermal phase of 2 min, the shear stress was increased and maintained for another 2 min before the temperature was set to 15 °C and changes in the complex viscosity were monitored (Fig. B.7). All systems underwent thermogelation upon heating to 37 °C, which was associated with an increase in complex viscosity by 3-4 orders of magnitude. The PNiPAAm solution showed the highest complex viscosity at 5 °C and after 2 min at 37 °C. This can likely be attributed to the higher molecular weight of the PNiPAAm (Mn of 20 - 25 kDa according to manufacturer) as compared to the TGMs. In response to the temperature decrease to 15 °C, the PNiPAAm system degelled almost instantly into a solution with a complex viscosity as at the start of the experiment. Both TGM hydrogels, in contrast, maintained a significantly elevated complex viscosity for 60 min at 15 °C, while the systems became translucent once the temperature dropped below the transition temperature. Macroscopic observations revealed the full reversibility of the thermogelation for the TGM gels after 2-3 days at 20 °C and below (data not shown). This indicates that during thermally induced gelation of amphiphilic NiPAAm-based macromers colloids are formed, which are stabilized by additional

intermolecular forces than those arising from the entropically driven aggregation of PNiPAAm domains. PNiPAAm-based amphiphiles appear advantageous over pure PNiPAAm hydrogels when increased hydrogel stability is warranted and the kinetics of the gel-sol transition is of minor importance.

B.3.7 TGMs with optimized composition and gelation properties

In view of the established structure property correlations and the design objective to optimize the thermodynamic stability of the TGMs and to provide a sufficient number of hydroxyl groups available for chemical modification per macromer, TGMs with high AAm and HEA contents and reduced NiPAAm comonomer contents were synthesized and analyzed (Table B.1). Poly(PEDAS$_1$-*stat*-NiPAAm$_{14}$-*stat*-AAm$_3$-*stat*-HEA$_3$) could be synthesized at the desired composition and molecular weight. The NMR analysis of poly(PEDAS$_1$-*stat*-NiPAAm$_{13.5}$-*stat*-AAm$_{3.5}$-*stat*-HEA$_3$) revealed overly high AAm contents and low NiPAAm contents, a phenomenon also observed for poly(PEDAS$_1$-*stat*-NiPAAm$_{14}$-*stat*-AAm$_6$). These findings are attributed to likely colloid formation of these strongly amphiphilic macromers in the NMR solvent $CDCl_3$ and shielding of PEDAS and NiPAAm protons. Increased branching was observed for poly(PEDAS$_1$-*stat*-NiPAAm$_{15}$-*stat*-AAm$_{3.5}$-*stat*-HEA$_{1.5}$), which was designed to contain half of the HEA compared to poly(PEDAS$_1$-*stat*-NiPAAm$_{14}$-*stat*-AAm$_3$-*stat*-HEA$_3$) and keep the molar AAm comonomer content below 4 (relative to PEDAS). Poly(PEDAS$_1$-*stat*-NiPAAm$_{14}$-*stat*-AAm$_3$-*stat*-HEA$_3$) solutions were characterized by a T_c of 33.7 ± 0.2 °C more than 5 °C above the T_c determined

for PNiPAAm (Fig. B.5C, I). The stability of thermogels formed from this TGM were also significantly increased (Fig. B.6, sample i). A further increase in AAm content resulted in a TGM (poly(PEDAS$_1$-*stat*-NiPAAm$_{13.5}$-*stat*-AAm$_{3.5}$-*stat*-HEA$_3$)) that yielded even more stable thermogels (Fig. B.6, sample k). The chemical characteristics of the macromers, however, were less definite (Table B.1), which explains the disperse results obtained for T_s, T_g and T_{DSC} (Fig. B.5D, V). Another well balanced TGM was synthesized with poly(PEDAS$_1$-*stat*-NiPAAm$_{15}$-*stat*-AAm$_{3.5}$-*stat*-HEA$_{1.5}$), which was characterized by T_s and T_g comparable to poly(PEDAS$_1$-*stat*-NiPAAm$_{14}$-*stat*-AAm$_3$-*stat*-HEA$_3$) but a significantly increased T_{DSC} (35.6 ± 0.5 °C) (Fig. B.5C, VI) and formed thermogels of appropriate stability (Fig. B.6, sample l). In view of their favorable thermogelation properties, poly(PEDAS$_1$-*stat*-NiPAAm$_{14}$-*stat*-AAm$_3$-*stat*-HEA$_3$) and poly(PEDAS$_1$-*stat*-NiPAAm$_{15}$-*stat*-AAm$_{3.5}$-*stat*-HEA$_{1.5}$) were chemically modified to yield chemically cross-linkable TGMs (Scheme B.1, step II).

B.3.8 Synthesis and structural characterization of chemically crosslikable TGMs

With the objective to introduce chemically cross-linkable domains into the TGMs to yield macromers that can be gelled both physically and chemically, TGMs were reacted with AcCl or MACl. Anhydrous sodium carbonate was used to scavenge any acidic by-products during the reaction and upon termination any salt was removed by filtration.[41] Triethylamine, which is a commonly used base to catalyze such (meth)acrylation reactions, could not be effectively removed from

the reaction products due to the lack of a suitable extraction solvent that would precipitate the amphiphilic macromers. As described for the hydroxyl group methacrylation of other molecules,[42] the molar excess of the acrylation or methacrylation agent, AcCl or MACl, controlled the extent of hydroxyl group conversion (Table B.2, Fig. B.8). Figure B.8 shows representative ^{1}H-NMR traces of poly(PEDAS$_1$-*stat*-NiPAAm$_{14}$-*stat*-AAm$_3$-*stat*-HEA$_3$) as well as two acrylated and one methacrylated derivative. Characteristic changes of the proton signal indicate successful (meth)acrylation of the TGM. Upon (meth)acrylation, characteristic olefinic proton signals appear between 5.6 and 6.6 ppm representing three (TGM-Ac) or two (TGM-MA) olefinic protons per (meth)acrylic ester. In addition, a downfield shift of the methylene protons in α-position to the newly formed (meth)acrylic ester was observed (signal at 4.3 ppm). A signal at 1.9 - 2.0 ppm representing the methyl group of the methacrylate ester group was found in the spectrum of TGM-MA. The conversion was calculated relative to the PEDAS molecules per TGM and an increased conversion was found with higher feeds of (meth)acryloyl chloride. Poly(PEDAS$_1$-*stat*-NiPAAm$_{14}$-*stat*-AAm$_3$-*stat*-HEA$_3$), the TGM with the higher HEA content per macromer, showed a higher conversion relative to PEDAS. A maximum of 1.25 acrylic groups per macromer subunit identified by one PEDAS block was achieved with an acryloyl chloride excess of 2.5 (relative to the theoretical number of hydroxyl groups per macromer subunit). This means that 1.25 out of the 4 theoretical hydroxyl groups per macromer subunit (3 in HEA and one in PEDAS) were acrylated. Additional

experiments revealed that the hydroxyl group of PEDAS was not accessible for (meth)acrylation under the applied conditions (data not shown). Due to the lower reactivity of methacrylic chloride, a likely consequence of steric limitations, a lower conversion was found for the methacrylated TGMs as compared to the acrylation products at corresponding molar feeds of the reactive chlorides (Table B.2). The transition temperatures of the (meth)acrylated macromers, here T_{DSC}, were found to decrease with the extent of (meth)acrylation. As hydrophilic hydroxyl functionalities are turned into considerably less hydrophilic (meth)acrylic esters, the hydrophilic-hydrophobic balance of the macromer was changed towards increased hydrophobicity and the phase transition temperature decreased. A stronger effect of macromer derivatization on transition temperature was found for TGM-MA, which is explained by the stronger hydrophobicity of the methacrylic ester as compared to an acrylic ester.

B.3.9 Gelation properties of chemically crosslinkable TGMs

Results of rheological experiments performed with solutions of the (meth)acrylated TGMs (10% (w/v)) with and without the presence of the thermal initiator system APS/TEMED (25mM each) are summarized in Figure B.9. Redox initiator system and concentration have been shown suitable and sufficiently biocompatible for direct cell encapsulation with *in situ* cross-linked hydrogels.[7,43] All (meth)acrylated TGMs except acrylated (Ac 2.5x) poly($PEDAS_1$-*stat*-$NiPAAm_{14}$-*stat*-AAm_3-*stat*-HEA_3) showed thermogelation during the initial temperature sweep to 37 °C, which was associated with a significant increase in

complex viscosity for samples with (APS/TEMED) and without (H_2O/TEMED) chemical initiation (Fig. B.9A,B). Acrylated (2.5x) poly(PEDAS$_1$-*stat*-NiPAAm$_{14}$-*stat*-AAm$_3$-*stat*-HEA$_3$), which showed the highest degree of acrylation, had likely partially cross-linked during preparation of rheological samples. The high complex viscosity values determined for this sample at the beginning of the rheological experiment confirmed this assumption. For the other samples, low complex viscosities below 0.1 Pa•s were determined for the solutions at 15 °C and no significant differences were found between the APS containing samples and the control samples (H_2O/TEMED) at 15 °C (Fig. B.9B,C). At 37 °C, higher complex viscosity values were typically determined for initiated samples (APS/TEMED) compared to the non-initiated controls (Fig. B.9A). During the subsequent time sweep at 37 °C, the complex viscosity was monitored for 30 min at 37 °C. While the APS/TEMED groups typically maintained the values for complex viscosity during this time, decreasing complex viscosity values due to the thermodynamic instability of the physical gels were recorded for the H_2O/TEMED groups (Fig. B.9A). This result indicates thermally initiated cross-linking of the (meth)acrylated TGMs in the presence of APS/TEMED during the temperature sweep within a few minutes. Based on these findings, that show that physical and chemical cross-linking occurred almost simultaneously, the tested initiator concentration appears high. If slower cross-linking kinetics are desired to achieve successive thermogelation and chemical cross-linking, a lower initiator concentration would be recommended. Comparison of the complex viscosities

after 30 min at 37 °C revealed a significant difference between the cross-linked macromers and the physically gelled systems (Fig. B.9B,C). The viscosities determined for the highly acrylated poly(PEDAS$_1$-*stat*-NiPAAm$_{15}$-*stat*-AAm$_{3.5}$-*stat*-HEA$_{1.5}$) were comparable to those achieved for poly(PEDAS$_1$-*stat*-NiPAAm$_{14}$-*stat*-AAm$_3$-*stat*-HEA$_3$) acrylated using a low AcCl feed (0.75x). For this polymer higher acrylation rates could be achieved with AcCl feeds of 1.25x and 2.5x (Table B.2), but the viscosity of gels cross-linked from these macromers was decreased likely due to extensive phase separation of these hydrophobic macromers at 37 °C (Fig. B.9B). In general, high viscosities were reached by cross-linking the methacrylated macromers but their low transition temperatures significantly impair polymer processing with regard to biomedical applications. Macroscopically, the APS/TEMED systems remained as a coherent hydrogel film on the geometry upon disassembly of the rheometer, while the non-initiated samples resembled a highly viscous liquid (data not shown). The cross-linking density and (meth)acrylate conversion of the cross-linked hydrogels could be determined by total hydrolysis of the gels and subsequent chromatographic analysis.[44] For all experiments, macromer solutions with a concentration of 10% (w/v) have been used. This concentration is comparably low with regard to other injectable hydrogels based on synthetic polymers such as poly(ethylene glycol), which typically range from 20 - 25%.[43,45,46] The use of macromer concentrations higher than 10% is expected to yield TGM hydrogels with increased cros-linking densities.

B.4 Conclusions

Amphiphilic TGMs with controlled polymer architecture and low molecular weight (~2 - 3.5 kDa) were synthesized from PEDAS, NiPAAm, AAm, and HEA at different compositions and selected macromers were subsequently (meth)acrylated to yield chemically cross-linkable thermogelling materials for biomedical applications. Structure-property correlations for non-modified TGMs were established and the hydrophilic-hydrophobic balance was characterized as an important design criterion to adjust the gelation temperature of TGM solutions and thermodynamic stability of the resulting thermogels. The amphiphilic design was shown to support intermolecular interactions, a property which could improve the mechanical stability of cross-linked TGM-based gels. (Meth)acrylated TGMs were synthesized and the combination of thermogelation and thermally induced chemical cross-linking was shown to improve hydrogel stability. The experiments further suggest that degree of acrylation and hydrophilic-hydrophobic balance of the macromers have to be well-adjusted to yield hydrogels of optimal stability. The synthesis of chemically cross-linkable, thermogelling, and potentially biodegradable macromers was realized and promising macromers for the design of injectable drug and/or cell delivery systems with improved properties and stability are presented.

B.5 References

1. Gutowska, A.; Jeong, B.; Jasionowski, M. Injectable gels for tissue engineering. *Anat Rec* **2001,** *263* (4), 342-349.

2. Temenoff, J. S.; Mikos, A. G. Injectable biodegradable materials for orthopedic tissue engineering. *Biomaterials* **2000,** *21* (23), 2405-2412.

3. Nguyen, K. T.; West, J. L. Photopolymerizable hydrogels for tissue engineering applications. *Biomaterials* **2002,** *23* (22), 4307-4314.

4. Lutolf, M. P.; Weber, F. E.; Schmoekel, H. G.; Schense, J. C.; Kohler, T.; Muller, R.; Hubbell, J. A. Repair of bone defects using synthetic mimetics of collagenous extracellular matrices. *Nat Biotechnol* **2003,** *21* (5), 513-518.

5. Ifkovits, J. L.; Burdick, J. A. Review: Photopolymerizable and Degradable Biomaterials for Tissue Engineering Applications. *Tissue Eng* **2007,** *13* (10), 2369-2385.

6. Elisseeff, J.; Anseth, K.; Sims, D.; McIntosh, W.; Randolph, M.; Langer, R. Transdermal photopolymerization for minimally invasive implantation. *Proc Natl Acad Sci USA* **1999,** *96* (6), 3104-3107.

7. Temenoff, J. S.; Shin, H.; Conway, D. E.; Engel, P. S.; Mikos, A. G. In vitro cytotoxicity of redox radical initiators for cross-linking of oligo(poly(ethylene glycol) fumarate) macromers. *Biomacromolecules* **2003,** *4* (6), 1605-1613.

8. Shin, H.; Temenoff, J. S.; Mikos, A. G. In vitro cytotoxicity of unsaturated oligo[poly(ethylene glycol)fumarate] macromers and their cross-linked hydrogels. *Biomacromolecules* **2003,** *4* (3), 552-560.

9. Galaev, I. Y.; Mattiasson, B. `Smart' polymers and what they could do in biotechnology and medicine. *Trends Biotechnol* **1999,** *17* (8), 335-340.

10. Qiu, Y.; Park, K. Environment-sensitive hydrogels for drug delivery. *Adv Drug Deliv Rev* **2001,** *53* (3), 321-339.

11. Gutowska, A.; Seok Bark, J.; Chan Kwon, I.; Han Bae, Y.; Cha, Y.; Wan Kim, S. Squeezing hydrogels for controlled oral drug delivery. *J Control Release* **1997,** *48* (2-3), 141-148.

12. Dong, L. c.; Hoffman, A. S. Synthesis and application of thermally reversible heterogels for drug delivery. *J Control Release* **1990,** *13* (1), 21-31.

13. Ruel-Gariepy, E.; Leroux, J. C. In situ-forming hydrogels--review of temperature-sensitive systems. *Eur J Pharm Biopharm* **2004,** *58* (2), 409-426.

14. Bromberg, L. E.; Ron, E. S. Temperature-responsive gels and thermogelling polymer matrices for protein and peptide delivery. *Adv Drug Deliv Rev* **1998,** *31* (3), 197-221.

15. Klouda, L.; Mikos, A. G. Thermoresponsive hydrogels in biomedical applications. *Eur J Pharm Biopharm* **2008,** *68* (1), 34-45.

16. Hoffman, A. S. Hydrogels for biomedical applications. *Adv Drug Deliv Rev* **2002,** *54* (1), 3-12.

17. Stile, R. A.; Healy, K. E. Thermo-responsive peptide-modified hydrogels for tissue regeneration. *Biomacromolecules* **2001,** *2* (1), 185-194.

18. Saim, A. B.; Cao, Y.; Weng, Y.; Chang, C. N.; Vacanti, M. A.; Vacanti, C. A.; Eavey, R. D. Engineering autogenous cartilage in the shape of a helix using an injectable hydrogel scaffold. *Laryngoscope* **2000,** *110* (10 I), 1694-1697.

19. Jeong, B.; Lee, K. M.; Gutowska, A.; An, Y. H. Thermogelling biodegradable copolymer aqueous solutions for injectable protein delivery and tissue engineering. *Biomacromolecules* **2002,** *3* (4), 865-868.

20. Fisher, J. P.; Jo, S.; Mikos, A. G.; Reddi, A. H. Thermoreversible hydrogel scaffolds for articular cartilage engineering. *J Biomed Mater Res A* **2004,** *71* (2), 268-274.

21. Seong, J. Y.; Jun, Y. J.; Jeong, B.; Sohn, Y. S. New thermogelling poly(organophosphazenes) with methoxypoly(ethylene glycol) and oligopeptide as side groups. *Polymer* **2005,** *46* (14), 5075-5081.

22. Stile, R. A.; Burghardt, W. R.; Healy, K. E. Synthesis and characterization of injectable poly(N-isopropylacrylamide)-based hydrogels that support tissue formation in vitro. *Macromolecules* **1999,** *32* (22), 7370-7379.

23. Ibusuki, S.; Iwamoto, Y.; Matsuda, T. System-Engineered Cartilage Using Poly(N-isopropylacrylamide)-Grafted Gelatin as in Situ-Formable Scaffold: In Vivo Performance. *Tissue Eng* **2003,** *9* (6), 1133-1142.

24. Vernon, B.; Kim, S. W.; Bae, Y. H. Thermoreversible copolymer gels for extracellular matrix. *J Biomed Mater Res* **2000,** *51* (1), 69-79.

25. Gil, E. S.; Hudson, S. M. Stimuli-reponsive polymers and their bioconjugates. *Progr Polym Sci* **2004,** *29* (12), 1173-1222.

26. Ohya, S.; Nakayama, Y.; Matsuda, T. Thermoresponsive artificial extracellular matrix for tissue engineering: Hyaluronic acid bioconjugated with poly(N-isopropylacrylamide) grafts. *Biomacromolecules* **2001,** *2* (3), 856-863.

27. Cellesi, F.; Tirelli, N.; Hubbell, J. A. Materials for cell encapsulation via a new tandem approach combining reverse thermal gelation and covalent crosslinking. *Macromol Chem Phys* **2002,** *203* (10-11), 1466-1472.

28. Lee, B. H.; West, B.; McLemore, R.; Pauken, C.; Vernon, B. L. In-Situ Injectable Physically and Chemically Gelling NIPAAm-Based Copolymer System for Embolization. *Biomacromolecules* **2006,** *7* (6), 2059-2064.

29. Robb, S. A.; Lee, B. H.; McLemore, R.; Vernon, B. L. Simultaneously Physically and Chemically Gelling Polymer System Utilizing a Poly(NIPAAm-co-cysteamine)-Based Copolymer. *Biomacromolecules* **2007,** *8* (7), 2294-2300.

30. Boutris, C.; Chatzi, E. G.; Kiparissides, C. Characterization of the LCST behaviour of aqueous poly(N-isopropylacrylamide) solutions by thermal and cloud point techniques. *Polymer* **1997,** *38* (10), 2567-2570.

31. Schild, H. G. Poly(N-isopropylacrylamide): experiment, theory and application. *Progr Polym Sci* **1992,** *17* (2), 163-249.

32. Jansen, E. J. P.; Sladek, R. E. J.; Bahar, H.; Yaffe, A.; Gijbels, M. J.; Kuijer, R.; Bulstra, S. K.; Guldemond, N. A.; Binderman, I.; Koole, L. H. Hydrophobicity as a design criterion for polymer scaffolds in bone tissue engineering. *Biomaterials* **2005,** *26* (21), 4423-4431.

33. Guse, C.; Koennings, S.; Maschke, A.; Hacker, M.; Becker, C.; Schreiner, S.; Blunk, T.; Spruss, T.; Goepferich, A. Biocompatibility and erosion behavior of implants made of triglycerides and blends with cholesterol and phospholipids. *Int J Pharm* **2006,** *314* (2), 153-160.

34. Seniha Guner, F.; Yagci, Y.; Tuncer Erciyes, A. Polymers from triglyceride oils. *Progr Polym Sci* **2006,** *31* (7), 633-670.

35. Lindblad, M. S.; Liu, Y.; Albertsson, A. C.; Ranucci, E.; Karlsson, S. Polymers from renewable resources. *Adv Polym Sci* **2002,** *157*, 139-161.

36. Fulzele, S. V.; Satturwar, P. M.; Dorle, A. K. Study of the biodegradation and in vivo biocompatibility of novel biomaterials. *Eur J Pharm Sci* **2003,** *20* (1), 53-61.

37. Braunecker, W. A.; Matyjaszewski, K. Controlled/living radical polymerization: Features, developments, and perspectives. *Progr Polymer Sci* **2007,** *32* (1), 93-146.

38. Yoshioka, H.; Mori, Y.; Tsukikawa, S.; Kubota, S. Thermoreversible gelation on cooling and on heating of an aqueous gelatin-poly(N-isopropylacrylamide) conjugate. *Polym Adv Technol* **1998,** *9* (2), 155-158.

39. Shim, M. S.; Lee, H. T.; Shim, W. S.; Park, I.; Lee, H.; Chang, T.; Kim, S. W.; Lee, D. S. Poly(D,L-lactic acid-co-glycolic acid)-b-poly(ethylene glycol)-b-poly (D,L-lactic acid-co-glycolic acid) triblock copolymer and thermoreversible phase transition in water. *J Biomed Mater Res* **2002,** *61* (2), 188-196.

40. Pelton, R. Temperature-sensitive aqueous microgels. *Adv Colloid Interface Sci* **2000,** *85* (1), 1-33.

41. Peter, S. J.; Suggs, L. J.; Yaszemski, M. J.; Engel, P. S.; Mikos, A. G. Synthesis of poly(propylene fumarate) by acylation of propylene glycol in the presence of a proton scavenger. *J Biomater Sci Polym Ed* **1999,** *10* (3), 363-373.

42. Hu, X.; Zhang, Z.; Zhang, X.; Li, Z.; Zhu, X. X. Selective acylation of cholic acid derivatives with multiple methacrylate groups. *Steroids* **2005,** *70* (8), 531-537.

43. Park, H.; Temenoff, J. S.; Holland, T. A.; Tabata, Y.; Mikos, A. G. Delivery of TGF-[beta]1 and chondrocytes via injectable, biodegradable hydrogels for cartilage tissue engineering applications. *Biomaterials* **2005,** *26* (34), 7095-7103.

44. Timmer, M. D.; Jo, S.; Wang, C.; Ambrose, C. G.; Mikos, A. G. Characterization of the Cross-Linked Structure of Fumarate-Based Degradable Polymer Networks. *Macromolecules* **2002,** *35* (11), 4373-4379.

45. Elisseeff, J.; McIntosh, W.; Anseth, K.; Riley, S.; Ragan, P.; Langer, R. Photoencapsulation of chondrocytes in poly(ethylene oxide)-based semi-interpenetrating networks. *J Biomed Mater Res* **2000,** *51* (2), 164-171.

46. Mann, B. K.; Gobin, A. S.; Tsai, A. T.; Schmedlen, R. H.; West, J. L. Smooth muscle cell growth in photopolymerized hydrogels with cell adhesive and proteolytically degradable domains: Synthetic ECM analogs for tissue engineering. *Biomaterials* **2001,** *22* (22), 3045-3051.

B.6 Figures

Table B.1. Compositions and molecular weight characteristics of thermogelling macromers.

theoretical composition	actual comonomer feed [mol] (based on 1 mol PEDAS)	^{1}H NMR results (based on 1 mol PEDAS)	GPC results	
PEDAS/NiPAAm/AAm/HEA	NiPAAm/AAm/HEA (b/c/d in Scheme 1)	NiPAAm/AAm/HEA (m/n/o in Scheme 1)	Mn [Da]	PI
		Effect of AAm Content		
1/20/-/-	20.0/-/-	20.7/-/-	2660 ± 130	3.4 ± 0.2
1/18.5/1.5/-	18.6/1.6/-	19.1/2.1/-	2450 ± 280	2.6 ± 0.2
1/18/2/-	18.0/2.0/-	18.9/2.4/-	1870 ± 130	2.5 ± 0.3
1/17/3/-	17.0/3.0/-	16.4/2.1/-	1860 ± 260	2.7 ± 0.2
1/16/4/-	16.0/4.1/-	13.3/4.2/-	1690 ± 80	2.7 ± 0.1
1/14/6/-	13.9/6.0/-	10.0/5.2/-	1470 ± 250	6.9 ± 2.1
		Effect of HEA Content		
1/16/-/4	15.9/-/4.0	17.5/-/5.8	3050 ± 140	2.9 ± 0.2
1/15.4/1/3.6	15.4/1.0/4.2	17.0/1.3/3.2	3810 ± 260	3.0 ± 0.3
1/15.4/2/2.6	15.3/2.0/2.6	17.4/1.8/2.0	2070 ± 90	2.7 ± 0.1
1/15.4/2.6/2	15.4/2.7/2.2	15.0/3.1/2.8	2030 ± 190	2.9 ± 0.2
1/15.4/3/1.6	15.1/3.0/1.9	14.0/4.0/0.9	1930 ± 120	2.9 ± 0.4
1/15/3.5/1.5	15.2/3.5/1.5	15.8/3.1/2.0	2110 ± 60	3.7 ± 0.6
1/14/3/3	14.0/3.0/3.0	15.2/2.0/3.4	2630 ± 200	2.9 ± 0.0
1/13.5/3.5/3	13.4/3.5/3.0	11.6/6.6/2.2	2770 ± 80	2.7 ± 0.2
	Control (composition, comonomer feed and NMR data are based on 1 mol ODA)			
ODA/15.4/3/1.6	15.4/3.1/1.7	15.5/5.1/1.8	2450 ± 80	2.1 ± 0.0

Table B.2. Methacrylated (TGM-MA) or acrylated (TGM-Ac) macromers synthesized from two different TGMs at increasing molar rations of the (meth)methacrylation reagents (XCl) methacryloyl chloride or acryloyl chloride, respectively. Conversion of TGM hydroxyl groups into (meth)acrylate esters as determined by ^{1}H-NMR per PEDAS molecule (n_{olefin}/n_{PEDAS}) and corresponding transition temperature of a 10% macromer solution as determined by DSC (n = 3).

TGM (PEDAS/NiPAAm/AAm/HEA)		1:14:3:3		1:15:3.5:1.5	
modification	reagent feed (n_{XCl}/n_{OH})	^{1}H NMR (n_{olefin}/n_{PEDAS})	T_{DSC} [°C]	^{1}H NMR (n_{olefin}/n_{PEDAS})	T_{DSC} [°C]
unmodified	n/a	n/a	33.1 ± 0.4	n/a	35.6 ± 0.5
methacrylation	1.25	0.55	13.6 ± 1.1	0.19	24.1 ± 0.6
	2.5	1.12	13.8 ± 0.5	0.57	15.2 ± 0.9
acrylation	0.75	0.27	25.1 ± 0.6	0.15	31.2 ± 0.2
	1.25	1.01	22.3 ± 1.2	0.64	24.6 ± 0.3
	2.5	1.25	19.6 ± 0.7	0.98	20.8 ± 0.9

[a] Conversion of TGM hydroxyl groups into (meth)acrylate esters, as determined by ^{1}H-NMR per PEDAS molecule (n_{olefin}/n_{PEDAS}) and corresponding transition temperature of a 10% macromer solution as determined by DSC ($n = 3$).

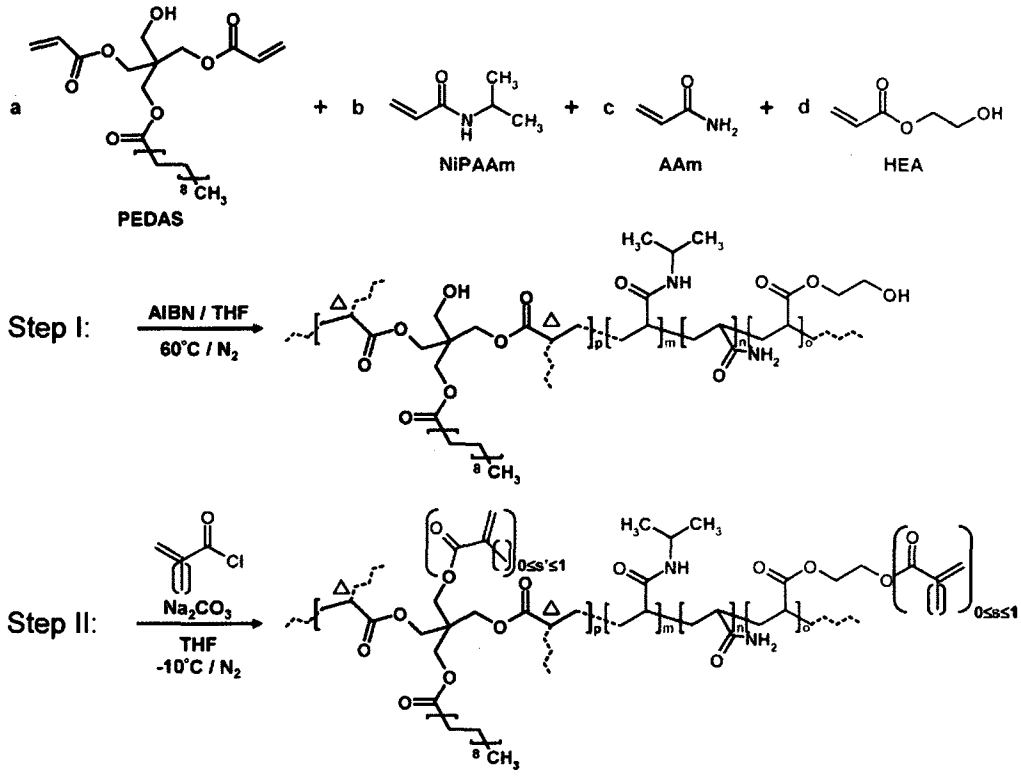

Scheme B.1. Synthetic scheme for thermogelling macromers (TGM) from the bifunctional monomer pentaerythritol diacrylate monostearate (PEDAS) and the acrylic monomers *N*-isopropylacrylamide (NiPAAm), acrylamide (AAm), and 2-hydroxyethylacrylate (HEA) by radical copolymerization (Step I). The resulting macromer is a branched statistical copolymer. The schematic illustration of its structure is very simplified recognizing that a PEDAS repeating unit can be part of two linear chains thus contributing to the branched structure of the macromer (Δ indicates possible branching sites). All copolymers in this study are synthesized from a comonomer ratio of a:(b+c+d) = 1:20. Theoretically, three out of four indices (p,m,n,o) could equal zero in possible products. In the ideal case, the ratio p:m:n:o equals a:b:c:d. (Meth)acrylate moieties that enable chemical crosslinking of the macromer are introduced in the second reaction step. Pendant hydroxyl groups that can be reacted in this methacrylation step are found in the PEDAS and HEA repeating units of the macromer and will be converted to different degrees (s, s').

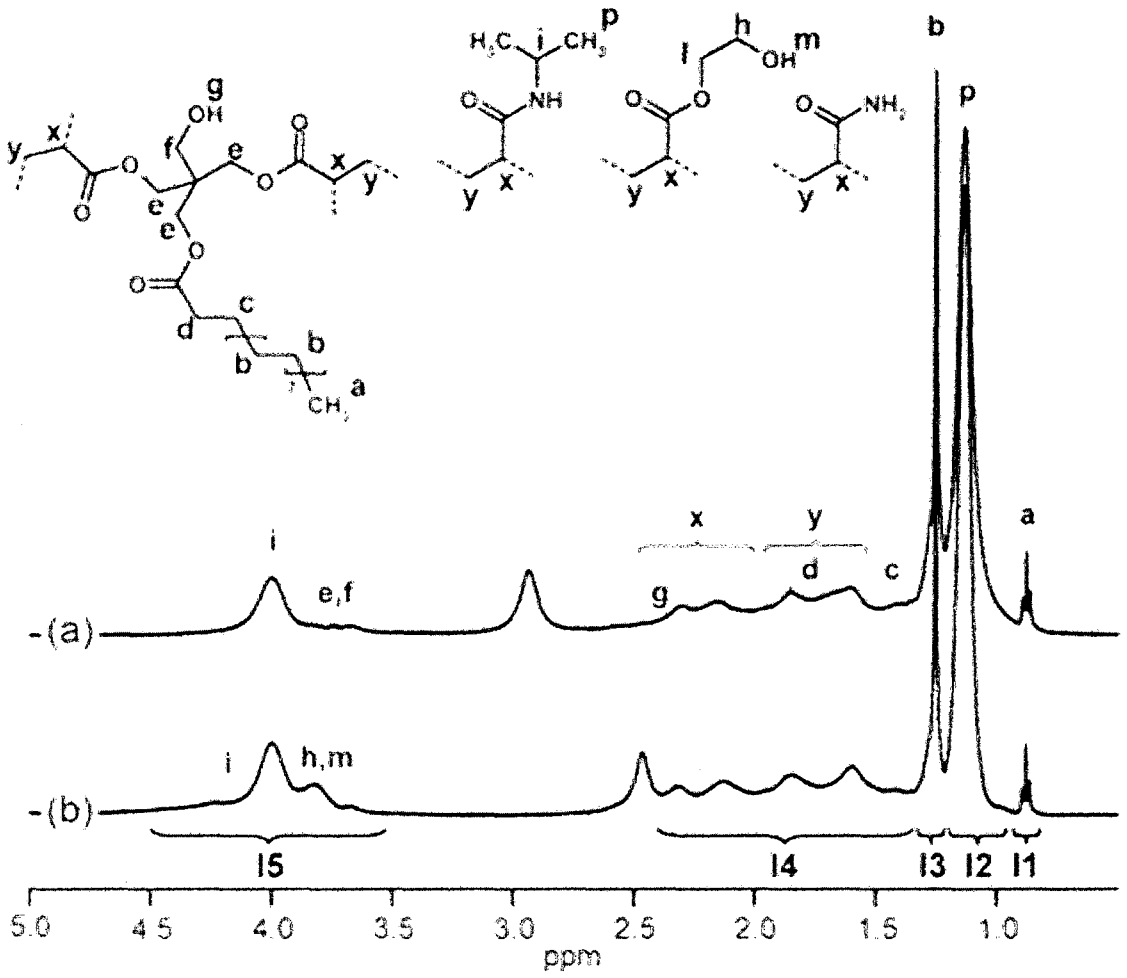

Figure B.1. ^{1}H-NMR spectra of (a) poly(PEDAS$_1$-*stat*-NiPAAm$_{16}$-*stat*-AAm$_4$) and (b) poly(PEDAS$_1$-*stat*-NiPAAm$_{16}$-*stat*-HEA$_4$). The letters assigned to the peaks correspond to the protons at the positions labeled in the structural elements of the copolymers. I1 - I5 represent the integrals used to determine macromer composition.

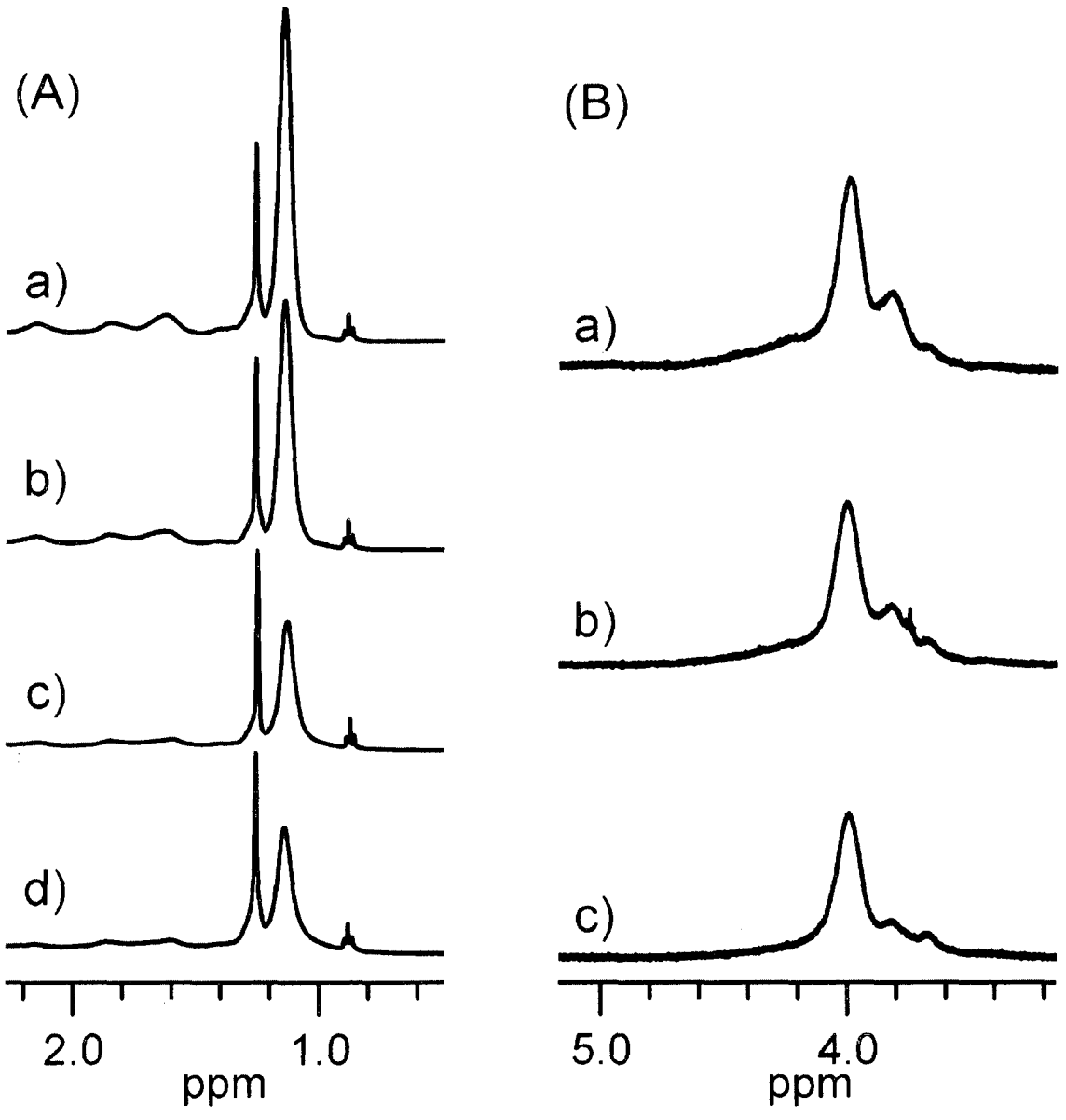

Figure B.2. Close-ups of ^{1}H-NMR spectra for different TGMs illustrating qualitative changes in signal intensities with changing comonomer ratios. (A) Poly(PEDAS$_1$-*stat*-NiPAAm$_{(20-m)}$-*stat*-AAm$_m$) with m = 0, 2, 4, 6 (a-d). (B) Poly(PEDAS$_1$-*stat*-NiPAAm$_{(20-m-n)}$-*stat*-AAm$_m$-*stat*-HEA$_n$) with m/n = 1/3.6 (a), 2/2.6 (b), and 3/1.6 (c).

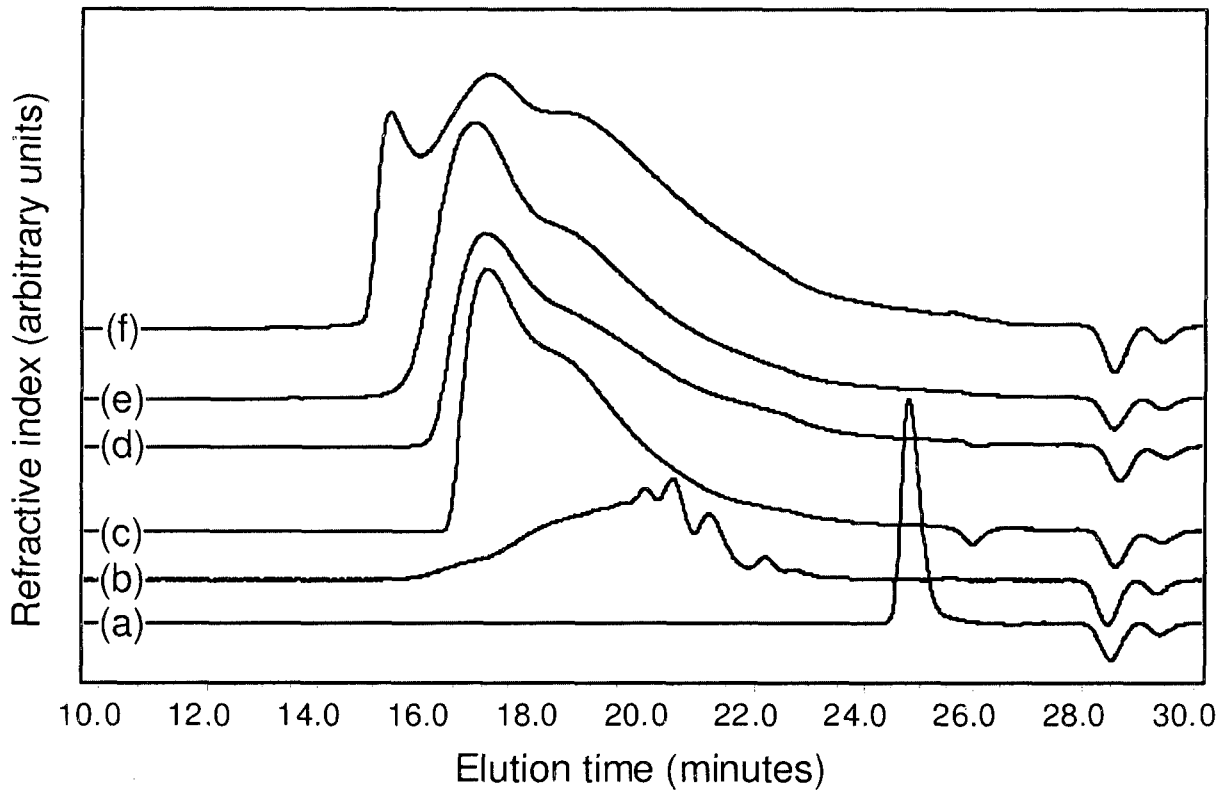

Figure B.3. GPC traces of (a) NiPAAm, (b) PEDAS, (c) poly(ODA_1-*stat*-$NiPAAm_{15.4}$-*stat*-AAm_3-*stat*-$HEA_{1.6}$) (control synthesized with monofunctional monomers only), (d) poly($PEDAS_1$-*stat*-$NiPAAm_{15.4}$-*stat*-AAm_3-*stat*-$HEA_{1.6}$), (e) poly($PEDAS_1$-*stat*-$NiPAAm_{16}$-*stat*-AAm_4), and (f) poly($PEDAS_1$-*stat*-$NiPAAm_{14}$-*stat*-AAm_6) (macromer that showed formation of branched networks).

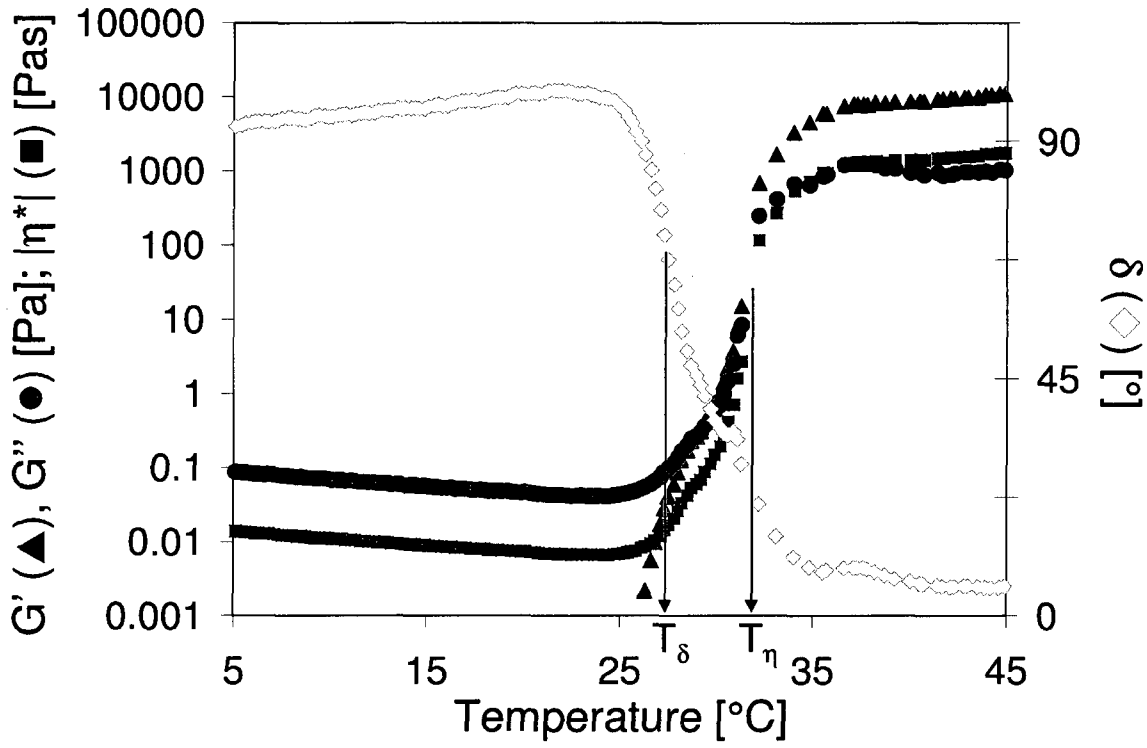

Figure B.4. Representative rheogram of poly(PEDAS$_1$-*stat*-NiPAAm$_{15}$-*stat*-AAm$_{3.5}$-*stat*-HEA$_{1.5}$) obtained during a temperature sweep between 5 and 45°C at 1 Hz. The complex moduli (G' and G'') and the complex viscosity |η*| are displayed on the left y-axis, while the right y-axis refers to the loss angle (δ). The locations of the characteristic temperatures T_δ and T_η are indicated by arrows.

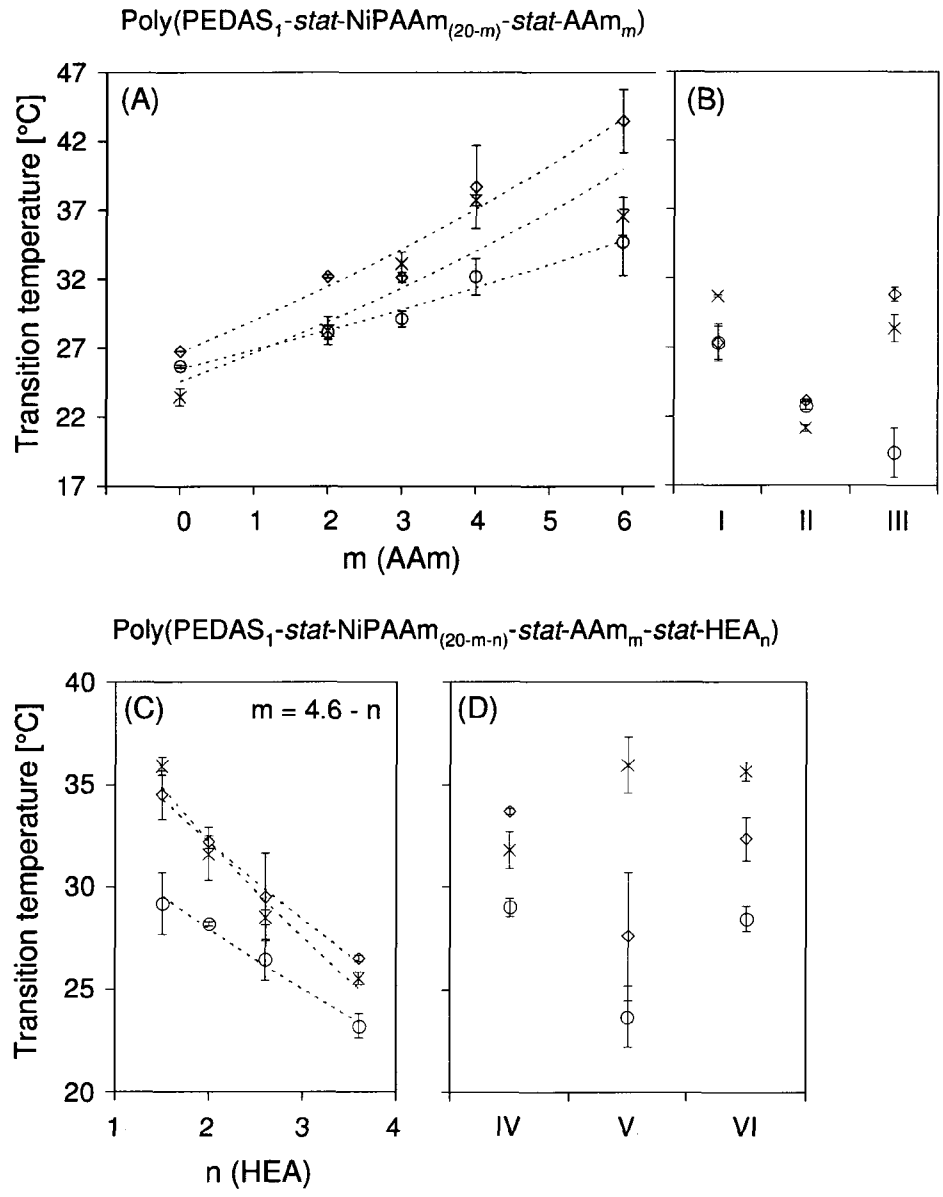

Figure B.5. Phase transition temperatures determined from rheology (T_δ, T_η) and differential scanning calorimetry (T_{DSC}) for different TGMs. (A) Co- and terpolymers composed of PEDAS, NiPAAm and different contents of AAm (m = 0-6). (B) Polymeric controls: (I) PNiPAAm, (II) poly(PEDAS$_1$-*stat*-NiPAAm$_{16}$-*stat*-HEA$_4$) and (III) poly(ODA$_1$-*stat*-NiPAAm$_{15.4}$-*stat*-AAm$_3$-*stat*-HEA$_{1.6}$). (C) Poly(PEDAS1-*stat*-NiPAAm$_{15.4}$-*stat*-AAm$_{(4.6-n)}$-*stat*-HEA$_n$) with differents contents of HEA (n = 1.6, 2, 2.6, 3.6) (D) TGMs with different NiPAAm:AAm:HEA comonomer ratios, (IV) 14:3:3, (V) 13:4:3, (VI) 15:3.5:1.5.

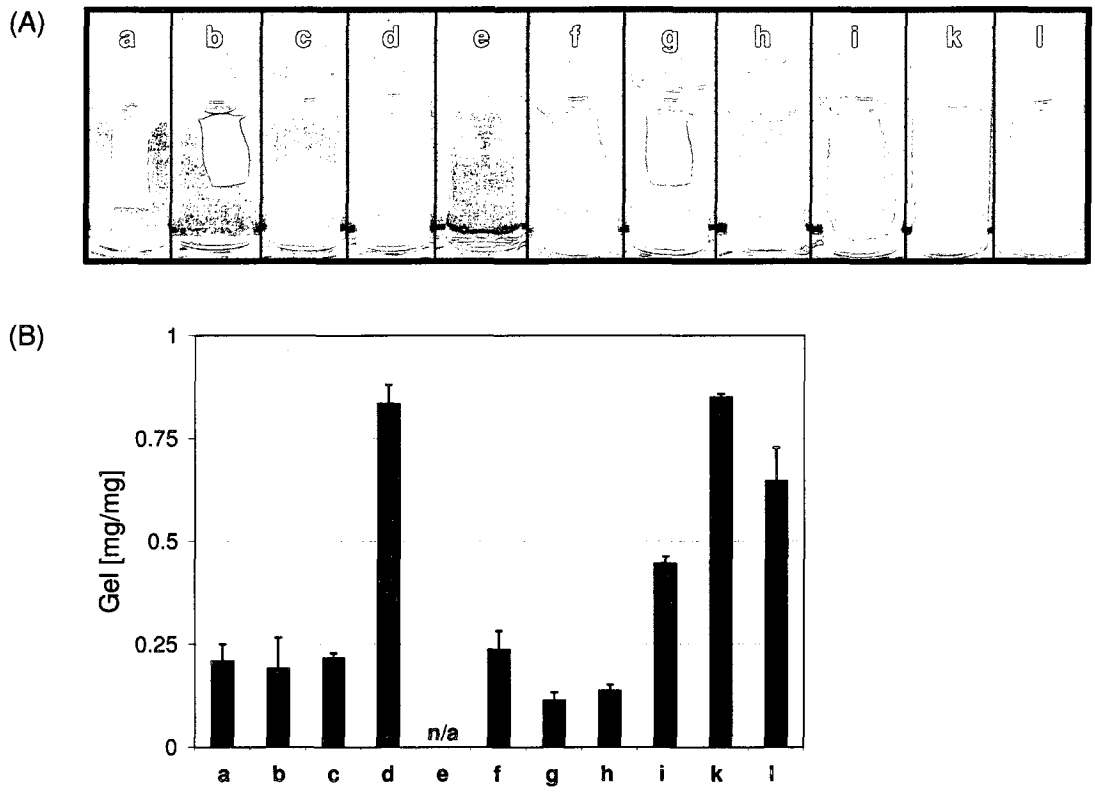

Figure B.6. Stability of thermogels of different comonomer composition at 37 °C. (A) Macroscopic images of thermogels after 2 h of incubation. (B) Mass fraction of thermogels after 2 h. Columns and error bar represent means ± standard deviation for *n* = 3. Samples: (*a*) PNiPAAm; poly(PEDAS$_1$-*stat*-NiPAAm$_{(20-m)}$-*stat*-AAm$_m$) with m = 0, 3, 4, 6 (b-e); poly(PEDAS$_1$-*stat*-NiPAAm$_{(20-m-n)}$-*stat*-AAm$_m$-*stat*-HEA$_n$) with m/n = 2/2.6 (f), 1/3.6 (g), 0/4 (h), 3/3 (i), 3.5/3 (k), and 3.5/1.5 (l).

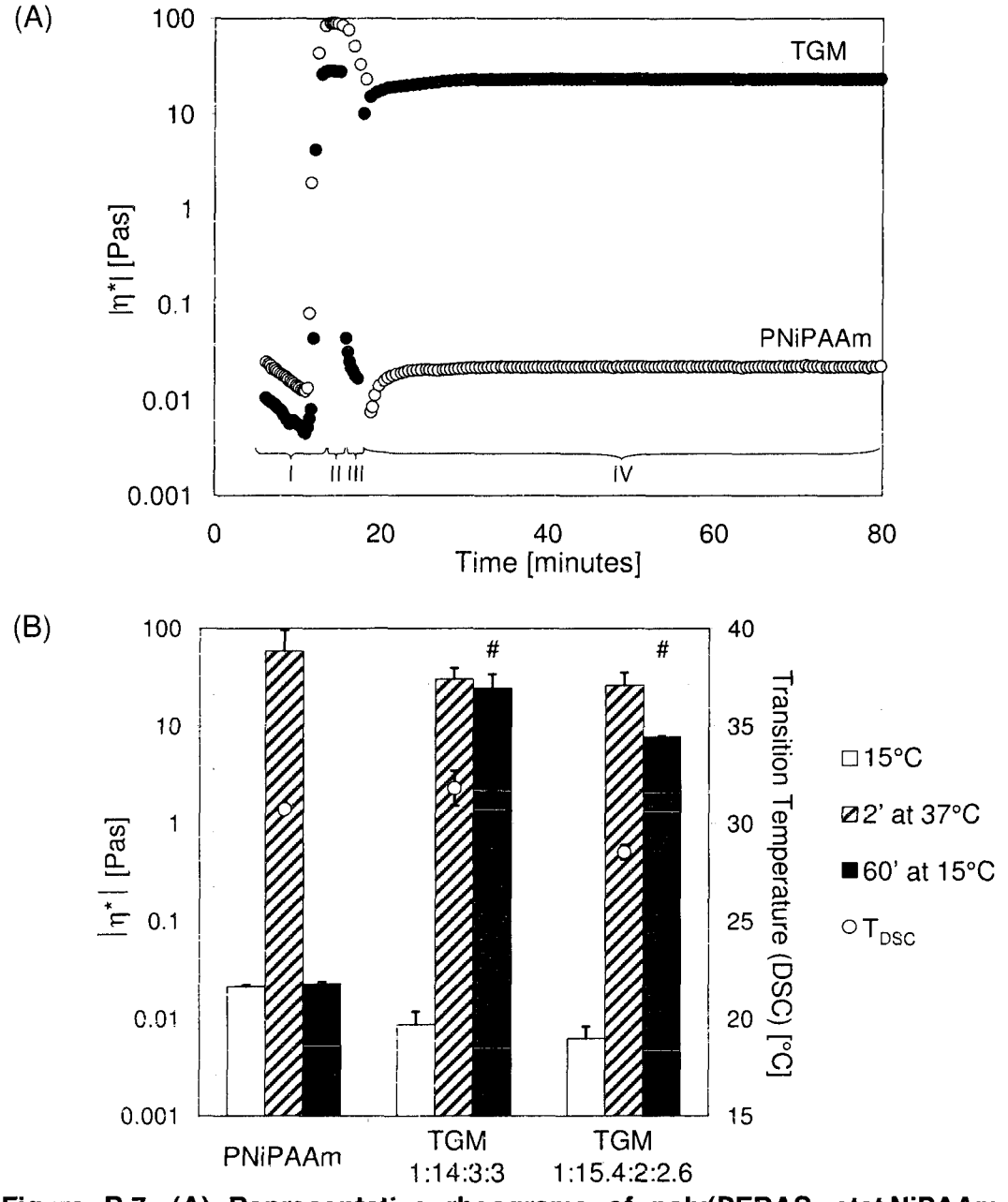

Figure B.7. (A) Representative rheograms of poly(PEDAS$_1$-*stat*-NiPAAm$_{14}$-*stat*-AAm$_3$-*stat*-HEA$_3$) (TGM) and PNiPAAm as recorded during a test for reversibility of the thermogelation. For experimental conditions during steps I - IV please refer to the *Methods* section. (B) Values for complex viscosity |η*| (left y-axis) for PNiPAAM, poly(PEDAS$_1$-*stat*-NiPAAm$_{14}$-*stat*-AAm$_3$-*stat*-HEA$_3$) and poly(PEDAS$_1$-*stat*-NiPAAm$_{15.4}$-*stat*-AAm$_2$-*stat*-HEA$_{2.6}$) as determined at 15 °C during step I (15 °C), after 2 min at 37 °C, and after 60' into step IV at 15 °C. Transition temperatures as determined by DSC (TDSC) of the different polymers are assigned to the right y-axis. Columns and error bar represent means + standard deviation for n = 3. Statistically significant differences between the complex viscosities of the TGM samples (60 min at 15°C) as compared to the corresponding value for PNiPAAm is denoted by #.

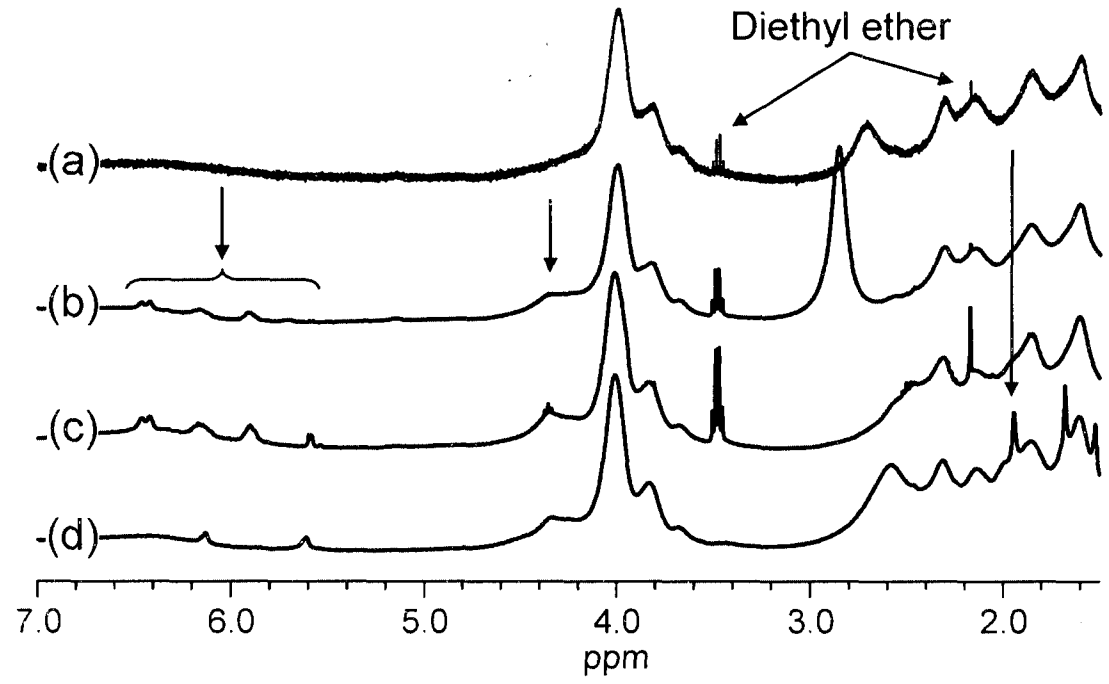

Figure B.8. Close up (1.5 - 7 ppm) of 1H-NMR spectra obtained for (a) poly(PEDAS$_1$-*stat*-NiPAAm$_{14}$-*stat*-AAm$_3$-*stat*-HEA$_3$) (TGM) and (b-d) (meth)acrylated poly(PEDAS$_1$-*stat*-NiPAAm$_{14}$-*stat*-AAm$_3$-*stat*-HEA$_3$) at different molar excesses of (meth)acryloyl chloride: (b) TGM-Ac (0.75x), (c) TGM-Ac (2.5x), and (d) TGM-MA (2.5x). Proton signal derived from the (meth)acrylate groups are indicated by arrows.

(A)

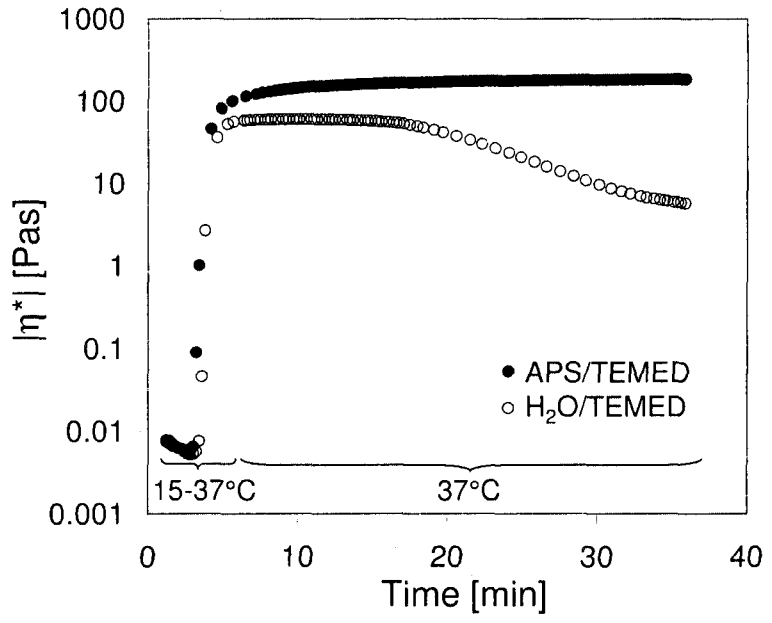
1000
100
10
1
0.1
0.01
0.001
|η*| [Pas]
APS/TEMED
H2O/TEMED
15-37°C
37°C
0
10
20
30
40
Time [min]

(B)

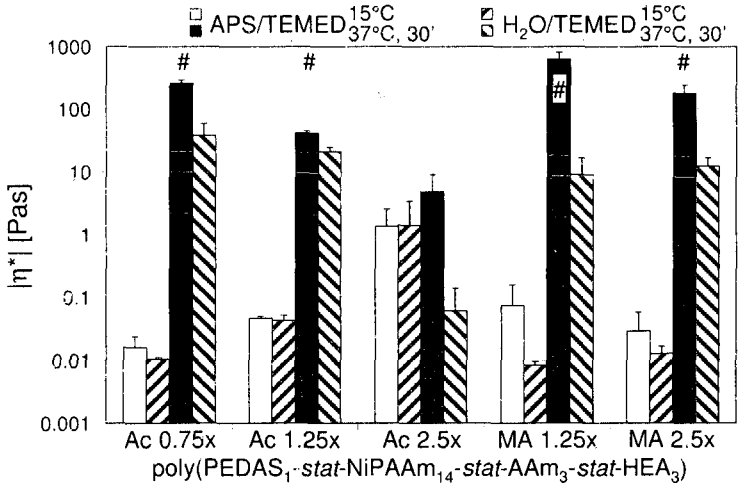
APS/TEMED 15°C 37°C, 30'
H2O/TEMED 15°C 37°C, 30'
1000
100
10
1
0.1
0.01
0.001
|η*| [Pas]
#
Ac 0.75x
Ac 1.25x
Ac 2.5x
MA 1.25x
MA 2.5x
poly(PEDAS1-stat-NiPAAm14-stat-AAm3-stat-HEA3)

(C)

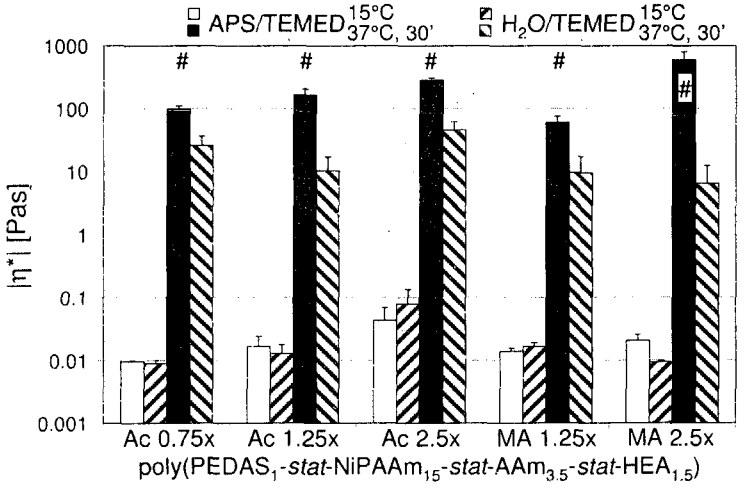
APS/TEMED 15°C 37°C, 30'
H2O/TEMED 15°C 37°C, 30'
1000
100
10
1
0.1
0.01
0.001
|η*| [Pas]
#
Ac 0.75x
Ac 1.25x
Ac 2.5x
MA 1.25x
MA 2.5x
poly(PEDAS1-stat-NiPAAm15-stat-AAm3.5-stat-HEA1.5)

Figure B.9. Rheological characterization of solutions of different (meth)acrylated TGMs with (APS/TEMED) and without (H_2O/TEMED) chemical initiation. (A) Representative rheograms of acrylated (0.75x) poly(PEDAS$_1$-*stat*-NiPAAm$_{15}$-*stat*-AAm$_{3.5}$-*stat*-HEA$_{1.5}$) (10% (m/v)) with and without chemical initiation during the combined temperature-time experiment. Complex viscosity $|\eta^*|$ at 15 °C and after 30' at 37 °C as determined for macromer solutions of (A) different (meth)acrylated poly(PEDAS$_1$-*stat*-NiPAAm$_{14}$-*stat*-AAm$_3$-*stat*-HEA$_3$) and (B) different (meth)acrylated poly(PEDAS$_1$-*stat*-NiPAAm$_{15}$-*stat*-AAm$_{3.5}$-*stat*-HEA$_{1.5}$) with (APS/TEMED) and without (H_2O/TEMED) chemical initiation. Columns and error bar represent means + standard deviation for n = 3. A statistically significantly increased complex viscosity for the APS/TEMED samples after 30 min at 37 °C as compared to the H_2O/TEMED samples at the same time point is denoted by #.

Appendix C

Cytocompatibility evaluation of amphiphilic, thermally responsive and chemically crosslinkable macromers for *in situ* forming hydrogels[†]

Abstract

The cytocompatibility of a new type of amphiphilic, thermoresponsive and chemically crosslinkable macromers was examined *in vitro*. Macromers synthesized from pentaerythritol diacrylate monostearate, *N*–isopropylacrylamide, acrylamide and hydroxyethyl acrylate in different molar ratios and with varying molecular weights and lower critical solution temperatures were evaluated for cytocompatibility with rat fibroblasts. Cell viabilities of over 60% percent for all and over 80% for most formulations were observed after 24-h incubation with macromers with molecular weights in the range of approximately 1500 to 3000 Da. The chemical modification of the macromers with a (meth)acrylate group was shown to have a time- and dose-dependent effect on cell viability. Uncrosslinked macromers with lower degrees of (meth)acrylation allowed for cell viability of over 60% for up to 6 h. (Meth)acrylated macromers with lower critical solution temperature (LCST) closer to physiological temperature allowed for higher cell viabilities as opposed to those with lower

[†] This appendix was published as: Klouda, L.; Hacker, M. C.; Kretlow, J. D.; Mikos, A. G., Cytocompatibility evaluation of amphiphilic, thermally responsive and chemically crosslinkable macromers for in situ forming hydrogels. *Biomaterials* **2009,** 30, (27), 4558-66.

LCST. The data suggest that when the (meth)acrylated macromers are assembled into a physical gel, their cytotoxicity is diminished. After gel phase separation, cytotoxicity increased. This study gives information on the parameters that enable viable cell encapsulation for *in situ* forming hydrogel systems.

C.1 Introduction

Injectable, *in situ* forming materials represent an attractive option for cellular delivery in tissue engineering. Hydrogels in particular are excellent extracellular matrix equivalents due to their highly hydrated nature[1] and can be delivered in liquid form and then solidify *in situ*. It is highly important that the solidification takes place in a clinically relevant time frame so that the material is localized at the point of interest. The solidification mechanism should be selected as not to cause necrosis to surrounding tissue by excessive heat formation and to be tolerated by encapsulated cells and/or any potentially sensitive molecules that are encapsulated for delivery. Moreover, fast solidification allows for homogeneous cell dispersion within the hydrogel matrix.[2-5] Thermally responsive hydrogels, materials that solidify upon temperature change, form *in situ* in a mild and fast manner, but they often possess insufficient mechanical properties and stability.[6] To circumvent this problem, thermogelling polymers have been modified by the addition of reactive groups that allow for covalent crosslinking. These polymers exhibit physical gelation triggered by temperature increase, followed by an irreversible chemical crosslinking after a Michael-type addition[7-9] or a photoinitiated polymerization reaction.[10]

Our group has recently proposed a new type of thermally responsive, chemically crosslinkable macromer for the fabrication of *in situ* forming hydrogels based on *N*-isopropylacrylamide.[11] These macromers employ a hydrophobic core

molecule that increases cohesive interactions of polymeric chains, augmenting the mechanical stability of the resulting hydrogel. The addition of a methacrylate or acrylate group enables chemical crosslinking with the use of a biocompatible, water-soluble thermal initiator system. The macromers are designed to exhibit a rapid thermal gelation at temperatures slightly below physiological temperature, followed by a slower chemical crosslinking *in situ*. The advantage of this approach is that fast solidification is achieved in a mild process through thermal gelation, with the subsequent slow chemical crosslinking not requiring high amounts of initiator. The rate of the chemical crosslinking reaction is dependent on the amount of initiator used, and it has been shown that thermal initiator systems are less cytocompatible above a certain concentration.[12-14]

The macromers are synthesized from pentaerythritol diacrylate monostearate, a bifunctional monomer containing a natural fatty acid as hydrophobic chain, *N*–isopropylacrylamide, which provides thermoresponsive properties, acrylamide, a hydrophilic monomer, and hydroxyethyl acrylate, a hydrophilic monomer which provides hydroxyl groups for further chemical modification.[11] The lower critical solution temperature (LCST) of macromer solutions and the resultant gel stability are shown to be a function of the comonomer ratios in the composition and the amphiphilicity of the macromers. As a further step, the modification of the macromers with the addition of a (meth)acrylate group allows for covalent crosslinking of gels with higher stability as compared to physically gelled, uncrosslinked controls.

The scope of this study is to evaluate the *in vitro* cytocompatibility of this novel type of macromer. Specifically, properties of unmodified macromers such as the molecular weight, the composition and the transition temperature are assessed for their effect on cytocompatibility. After chemical modification, (meth)acrylated macromers are evaluated to determine the optimal variables for viable cell delivery. The degree of modification, the concentration and the effects of acrylation versus methacrylation on cell viability are examined. Furthermore, cell viability is examined at intervals over 24 h in order to determine the length of exposure to (meth)acrylated macromers tolerable by cells.

C.2 Materials and Methods

C.2.1 Unmodified thermogelling macromers

Amphiphilic, water-soluble thermogelling macromers (TGMs) were synthesized from pentaerythritol monostearate diacrylate (PEDAS), *N*-isopropylacrylamide (NiPAAm) and varying contents of acrylamide (AAm) and 2-hydroxyethyl acrylate (HEA) via a free radical polymerization reaction as previously described.[11] The macromers were subsequently purified by precipitation in diethyl ether and were characterized by gel permeation chromatography (GPC), proton nuclear magnetic resonance spectroscopy (^{1}H-NMR), rheology and differential scanning calorimetry (DSC).[11] Table C.1 summarizes the composition of the macromers evaluated in the study, denoted by their molar feed composition, and their respective properties. The number-average molecular weights (M_n) and polydispersity indices (PI) were obtained by

GPC for n=3. The lower critical solution temperature (T_η) had been previously determined rheologically as the inflection point of the temperature-complex viscosity curve (n=3). The structure of the TGMs is illustrated in Figure C.1.

C.2.2 Cell culture

A rat fibroblast cell line (ATCC, CRL-1764) was cultured on T-75 flasks using Dulbecco's modified Eagle medium (DMEM; Gibco Life, Grand Island, NY) supplemented with 10 % (v/v) fetal bovine serum (FBS; Cambrex BioScience, Walkersville, MD) and 1% (v/v) antibiotics containing penicillin, streptomycin and amphotericin (Gibco Life). Cells were cultured in a humidified incubator at 37 °C and 5% CO_2. Cells of passage numbers 7-9 were used in this study.

C.2.3 Cytocompatibility assays of unmodified thermogelling macromers

Leachables assay

Solutions of thermogelling macromers were prepared at a 10% (w/v) concentration in cell culture media (DMEM, supplemented with antibiotics) without the addition of serum. The solutions were left on a shaker table overnight to dissolve. In the case of macromer solutions with LCST below room temperature, the solutions were left to dissolve at a temperature of 4 °C. After dissolution, macromer solutions were incubated at 37 °C for 24 h. During this time interval, the solutions first gel and subsequently phase-separate and collapse. After 24 h in the incubator, the supernatant of the macromer solutions was aspirated, sterile-filtered through a Nalgene 0.2 μm filter (Nalge, Rochester, NY) and diluted 10 times in cell culture media. Cells were seeded on a 96-well plate at a density of 28,300 cells/cm^2 using a working volume of 100 μL cell

suspension per well. The cells were incubated for 24 hours to achieve 80-90% confluence and were then exposed to 100 µL of the solution supernatant. Two experimental groups were used, one without and one with 10-fold dilution (n=5). Following 24 h of incubation, the macromer-conditioned media were removed, and the cells were rinsed three times with phosphate-buffered saline (PBS, Gibco), followed by the addition of calcein AM and ethidium homodimer-1 in 2 µM and 4 µM concentrations in PBS, respectively (Live/Dead viability/cytoxicity kit, Molecular Probes, Eugene, OR). The cells were incubated with the Live/Dead reagents for 30 min in the dark at room temperature. Cell viability was quantified using a fluorescence plate reader (Biotek Instrument FLx800, Winooski, VT) equipped with filter sets of 485/528 nm (excitation/emission) for calcein AM (live cells) and 528/620 nm (excitation/emission) for EthD-1 (dead cells). Untreated cells that were cultured with primary media only served as the positive (live) control, whereas cells exposed to 70% ethanol for 15 min served as the negative (dead) control. The fluorescence of the cell populations was recorded and the fractions of live and dead cells were calculated according to the following equations:[14]

(1) Fraction of live cells $= \frac{F_{LS}}{F_{LC}}$

(2) Fraction of dead cells $= \frac{F_{DS}}{F_{DC}}$

with

(4) F_{LS} = fluorescence $_{sample}$ - average background fluorescence $_{(no\ cells)}$

(5) F_{LC} = average (fluorescence $_{\text{live control}}$ - (average background fluorescence $_{\text{(no cells)}}$))

and

(6) F_{DS} = fluorescence $_{\text{sample}}$ - average background fluorescence $_{\text{(no cells)}}$

(7) F_{DC} = average (fluorescence $_{\text{dead control}}$ - (average background fluorescence $_{\text{(no cells)}}$))

Following quantification, images of the cells were obtained with a fluorescence microscope (LSM 510 META, Carl Zeiss, Germany).

Direct contact assay

The macromers were vacuum-dried and sterilized under UV irradiation for 3 h. Macromer solutions were prepared in 10% (w/v) concentration in DMEM without FBS as described above. Cells were seeded on 48-well plates at a seeding density of 28,300 cells/ cm^2 with a working volume of 500 µL cell suspension per well. After 24-h incubation, the media were aspirated and 150 µL of macromer solution was added to the cells (n=4-5). This quantity was calculated so that after gelation, a thin gel film would form above the cells. After 30-minute incubation at 37 °C to ensure gel formation, 300 µL DMEM without FBS was carefully added on top of the gel and the cells were incubated with the macromers for 24 h. Following this incubation period, the gel pellet was carefully removed with tweezers, and cells were rinsed three times with PBS before adding the Live/Dead reagents and evaluating cell viability as described above.

C.2.4 Modified (acrylated and methacrylated) thermogelling macromers

In order to add chemically crosslinkable domains, the purified macromers were modified with the addition of an acrylate or methacrylate group through a reaction between the hydroxyl group of 2-hydroxyethyl acrylate (HEA) and (meth)acryloyl chloride. The hydroxyl group on PEDAS was not modified during this reaction. The reaction, purification and characterization processes were performed as previously described by Hacker *et al.*[11] The structure of modified macromers can be seen in Figure C.1. Macromers with varying acrylate or methacrylate group contents were synthesized by feeding different volumes of acryloyl chloride or methacryloyl chloride respectively. Table C.2 denotes the composition of the modified TGMs and the conversion of the hydroxyls to (meth)acrylate groups as determined by ^{1}H-NMR. The thermal transition temperatures are also included in Table C.2, as the substitution of the hydroxyl group of HEA by the more hydrophobic (meth)acrylate moieties has an effect on the lower critical solution temperature of these macromers. LCST was previously obtained by differential scanning calorimetry for n=3.

C.2.5 Cytocompatibility of modified (acrylated and methacrylated) thermogelling macromers

The macromers were vacuum-dried and sterilized under UV irradiation for 3 h. Macromer solutions were prepared in 10, 1 and 0.1% (w/v) concentrations in DMEM without FBS as described above, which will be denoted throughout the text also as 100, 10 and 1 mg/mL respectively. Cells were seeded on 96-well plates at a seeding density of 28,300 cells/cm^2. After 24-h incubation, the media were aspirated. For the 1 and 0.1% solutions, 100 µL of macromer solution was

added to the cells. These concentrations showed minimal gel formation at 37 °C and therefore the addition of media for nutrient supply was not required. For the 10% solutions, 40 µL of macromer solution was applied, followed by 30-min incubation at 37 °C to ensure gel formation, and 60 µL DMEM without FBS was carefully added on top of the gel. For all groups, a sample size of five was used (n=5). Cell viability was evaluated after 2, 6 and 24-hour incubation using the Live/Dead assay as described above.

C.2.6 Osmolality measurements

The osmolality of the solutions was measured with an Osmette automatic osmometer (Precision Systems, Natick, MA). In order to create a standard curve for cell viability versus osmolality of solution, the osmolalities of dextran (average molecular weight 68.8 kDa, Sigma, St. Louis, MO) solutions in concentrations from 0 to 30% (w/v) in DMEM were measured. Cells were then incubated with dextran solutions in that concentration range for 24 h, and their viability was recorded. Dextran was chosen because it is a known biocompatible polysaccharide and thus in case any toxic effects were observed, they would be due to changes in osmolality of the solution and not molecular composition.

The osmolality of the 10% (w/v) macromer solutions as used in the study was measured. Moreover, the osmolality of the supernatant solutions was measured. The supernatant was obtained after incubating the macromer solutions for 24 h at 37 °C and following gel phase separation in order to simulate the properties of the solutions to which cells are exposed during the direct contact assay.

C.2.7 Statistical analysis

Statistical analysis of the data was performed with a single-factor analysis of variance (ANOVA) with a 95% confidence interval ($p<0.05$). In the case of statistically significant differences, Tukey's *post hoc* test was conducted. Data are expressed as mean ± standard deviation.

C.3 Results

C.3.1 Effect of molecular weight on unmodified macromer cytocompatibility

Viability of over 80% was observed for cells incubated with the supernatant of hydrogels composed of macromers with number-average weights ranging from 1750 to 2830 Da and polydispersity indices from 2.9 to 3.6 (Figure C.2A). In this experimental group, no statistically significant differences were found between undiluted and 10-fold diluted samples. For the direct contact assay, viabilities of above 80% were found for the lower molecular weight groups (Figure C.2B). The higher molecular weight group showed cell viability of 69±3 %.

C.3.2 Effect of composition on unmodified macromer cytocompatibility

Cells incubated with hydrogel supernatant showed high viabilities (above 75%) for all but one formulation, with a decrease in live cells with increasing acrylamide content in the composition (Figure C.3A). The formulation with the highest acrylamide content in the composition (20%) and no 2-hydroxyethyl acrylate showed lower viability values of 55±2%. No statistically significant difference was noted between undiluted and 10-fold diluted supernatant. When

cells were exposed to the thermogelling macromers in a direct contact assay, cell survival was above 80% (Figure C.3B).

C.3.3 Effect of LCST on unmodified macromer cytocompatibility

Among the formulations tested, lower cell viability was observed for the formulations with transition temperatures of 38.7 and 40.8 °C, both in the leachables (55±2% and 61±5% respectively) as well as in the direct contact assay (81±19% and 60±22%) (Figure C.4). Macromer solutions with lower or higher transition temperatures than the aforementioned showed viabilities of 70% or more for their leachable components and the direct contact assay. Characteristic fluorescence microscopy images of the cells after incubation with these macromers can be seen in Figure C.5. High densities of live cells (stained green) with morphology similar to the positive control were observed for most formulations, and no obvious damage to cells that were in direct contact with the hydrogel was noted. The composition with an LCST of 40.8 °C (molecular composition $PEDAS_1NiPAAm_{16}AAm_4$) showed an increased number of dead cells (stained red).

C.3.4 Effect of macromer solution osmolality on cytocompatibility

Cell viability showed a decreasing trend after 24-h incubation with increasing osmolalities of dextran solutions in various concentrations; differences, however, were not statistically significant (Figure C.6). For a solution osmolality of 451 mOsm/kg, cell viability was 85±7%. Thermogelling macromer solutions in 1% (w/v) concentration in cell culture media showed similar osmolalities to that of DMEM (330 mOsm/kg). Solutions of 10% (w/v)

concentration had osmolalities on the order of 406-462 mOsm/kg. The supernatant of gels after 24-h incubation at 37 °C and full phase separation showed even lower values (340-408 mOsm/kg).

C.3.5 Cytocompatibility of (meth)acrylated thermogelling macromers

Effect of macromer concentration

At the 2 h time interval, most formulations had similar cell viabilities in 1, 10 and 100 mg/mL concentrations or showed trends of decreasing viability (Figure C.7). A formulation with a 32% degree of acrylation showed values of 0.95±0.09, 0.71±0.08 and 0.68±0.10 at 1, 10 and 100 mg/mL respectively. A formulation with a 49% acrylation had cell viabilities of 1.23±0.06, 0.99±0.05 and 0.12±0.01 at the above concentrations. The effect of concentration was even more pronounced with decreasing trends in viability at the 6- and 24-h intervals. At 24 h, the cell viabilities for the 32% acrylated formulation decreased from 0.75±0.02 at the 1 mg/mL concentration to 0.16±0.05 at 100 mg/mL.

Effect of time

In addition to the aforementioned results, the effect of incubation time on cell viability can be seen in Figure C.8 for a concentration of 100 mg/mL. An unmodified composition showed a statistically significant decrease in viability at 6 h. The fraction of live cells at 24 h was 0.61±0.05, which did not change from the viability at 6 h. For all acrylated formulations, a statistically significant decrease in viability was observed after 24 h. At 6 h, the compositions with lower degrees of acrylation showed cell viabilities of 60% and higher. A composition with low methacrylation also showed a statistically significant decrease in

cytocompatibility at 24 h, whereas the macromers with higher methacrylation exhibited high toxicity as soon as 6 h after incubation.

Effect of modification

The macromers were rendered less cytocompatible with increasing degrees of modification. Figure C.9 depicts cell viability after 24-h incubation with 100 mg/mL macromer solutions. Unmodified macromers showed a viability of 61±5%, which was very similar for macromers with 8% acrylation. For macromers with higher acrylation degrees of 32% and 49%, only 16±6% and 2±1% of the cells respectively were viable after 24 h. Methacrylation seemed to be less tolerable by the cells from these results. After 24-h incubation, cell viability was only 3±1% for both formulations, which had methacrylation degrees of 10% and 29%, respectively.

C.4 Discussion

The evaluation of cytocompatibility is a crucial step in the characterization of every new class of biomaterials. In the case of *in vitro* testing of hydrogels, prior to performing a viability assay where cells are in direct contact with the material, an assay with the hydrogel leachable products in the supernatant phase is often included. This experiment allows for the identification of any potential toxicity caused by leachable substances after syneresis of the hydrogel. In our case of physical, uncrosslinked hydrogels, there was substantial phase separation of the hydrogels over 24 h. For the leachables assay, cells were exposed to undiluted supernatant as well as its 10-fold dilution. Preliminary

results showed no difference in cytocompatibility between 10-fold and 100-fold dilution of supernatant liquid (data not shown), therefore the higher dilutions were omitted from subsequent studies. Dilution of the supernatant allows for the evaluation of concentration effects and accounts also for osmotic effects. Cell viability was compared to a positive control, which was untreated cells cultured on tissue-culture polystyrene wells. A negative control, cells treated with 70% ethanol, was also included in order to confirm trends obtained by the live assay.[13] The numbers of dead cells are not reported in these studies, as dead cells tend to detach from the culture plates, making their count inaccurate.

The effects of molecular weight, monomer ratios in the composition and solution thermal transition temperature were the parameters investigated for their effect on macromer cytocompatibility. A second set of studies examines the cytocompatibility of the macromers after the addition of a reactive (meth)acrylate group over time and for different compositions and concentrations. Although these macromers can be physically gelled and chemically crosslinked, all experiments were performed with the non-crosslinked macromers to evaluate toxicity of the reactive groups and macromer composition, mainly hydrophilic-hydrophobic balance.

C.4.1 Cytocompatibility of unmodified thermogelling macromers

Macromer molecular weight is a factor that influences the compatibility of hydrogels with cells. Low-molecular weight oligomers are often associated with toxicity issues in hydrogels.[1] Generally, hydrogels for cell encapsulation are fabricated with macromers of molecular weights above 3000 Da,[15] as they

otherwise may enter the cell. The cytocompatibility of macromers with same composition but different molecular weights was assessed in this study. No adverse effects of thermogelling macromers of all molecular weights, ranging from 1750 to 2830 Da, were observed on cell viability. Cell viability was over 80% for most formulations, both in the leachables as well as in the direct contact assay. Moreover, broad molecular weight distributions as indicated by polydispersity indices of 2.9-3.6 suggested that the presence of any lower-molecular weight chains in this composition did not prove to be overly cytotoxic.

As for the macromer composition evaluation, it had been shown previously[11] that increasing acrylamide contents correlates with higher transition temperatures of the macromer solutions (Table C.1). Therefore, whether the decreasing cytocompatibility observed with increasing acrylamide in the formulation was an effect of transition temperature rather than composition had to be evaluated. Macromers with transition temperatures higher than the incubation temperature stay in solution or show minimal gel formation as opposed to those with transition temperatures close to physiological temperature which gel rapidly at 37 °C. It was hypothesized that due to their amphiphilic nature, solubilized macromers could potentially interact with the cell membrane. This effect was expected to be diminished when polymer chains do not stay in solution for a long time and form a gel. The experimental data showed a decrease in cell viability for the macromer solutions with transition temperatures of 38.7 and 40.8 °C. Interestingly, a macromer solution with a transition temperature of 43.5 °C, which

did not gel after 24-h incubation at 37 °C, allowed for cell viability of over 70%, whereas solutions with transition temperatures significantly lower than physiological temperature (27.2 and 30.6 °C respectively) showed similar cell survival values. The differences in the relative amphiphilicity may explain these observations. The lower critical phase separation phenomenon is imparted by hydrophobic interactions between macromolecular chains.[16] Macromers with transition temperatures lower than the incubation temperature of 37 °C had more hydrophobic compositions. Associations between polymer chains were more pronounced, leading to gel formation. On the other hand, increase in the hydrophilicity of the macromers facilitated polymer-water interactions, not allowing gel formation at this temperature. The macromers with the highest transition temperature have also the highest content of hydrophilic acrylamide. This hydrophilic structure, as suggested by the viability data, caused minimal interactions with the cells. The macromers with transition temperatures around physiological temperature exhibited such a hydrophilic/hydrophobic balance at 37 °C that might have caused increasing interactions with the cell membrane and could explain the lower cell viability values observed.

Another possible source of toxicity evaluated, solution osmolality, does not seem to be a contributing factor in these studies. Cells would be first exposed to the macromer solution until the gelation takes place and later to the supernatant solution after gel syneresis. Even though high osmotic stress has been shown to suppress growth[17] and induce apoptosis[18] in mammalian cells, the osmolality of

solutions was within the range tolerable by cells as suggested the dextran osmolality-cell viability curve (Figure C.6). This is in accordance with the observations of Zhu *et al.*[19] No obvious changes in viable density of CHO cells were noted when medium osmolality was increased to 400-450 mOsm/kg, but a further increase in osmolality to 460-500 mOsm/kg led to an 8% decrease in cell viability as compared to the control.

C.4.2 Cytocompatibility of modified thermogelling macromers

Some of the macromer solutions were too viscous for sterilization by filtration. Therefore, the macromers were dried in a vacuum oven and sterilized under UV irradiation for 3 h. In order to assess the effect of UV sterilization of the macromers, the presence of the olefinic protons was confirmed by ^{1}H-NMR, indicating that after UV irradiation the structure of the (meth)acrylated macromers was preserved (data not shown). The macromers selected for (meth)acrylation were chosen based on their amphiphilic character and lower critical solution properties, and their molecular composition prior to modification was found to be cytocompatible. The parameters tested in this study were concentration, time, degree of modification and modification type (acrylation or methacrylation) on their effect on cytocompatibility. It is valuable to obtain correlations between cell viability, concentration and chemical structure of the macromers as a function of time if the hydrogel is used for cell encapsulation, as cells will be in direct contact with the macromer chains until the crosslinking of the hydrogel is completed.[13] This study was designed to answer questions about the optimal variables for cell delivery.

Exposure to (meth)acrylated macromers was shown to have a dose-dependent effect on cell viability (Figure C.7). This effect was more pronounced with higher modification and after longer exposure. The cytotoxicity of hydrogel-forming macromers is often reported in concentrations of up to 1 mg/mL in cell culture media.[20, 21] We have opted to evaluate higher concentrations, since a relevant polymer concentration for hydrogel fabrication is on the order of 100 mg/mL. In this study, when the direct contact assay was performed, cell culture medium was added on top of the hydrogel layer after its solidification. In the course of the 24-h incubation, the hydrogel was phase-separated, which means that the addition of medium diluted down the supernatant solution. This step was however required to ensure nutrient delivery to the cells. Solutions of lower concentrations did not show significant gel formation. Since the solutions were made in cell culture medium, no further addition for nutrient supply was deemed necessary. The cytotoxicity of the macromers also showed a time-dependent behavior (Figure C.8). Acrylated macromers all showed statistically significant higher cytotoxicity at the 24 h time interval compared to 2 and 6-h exposure. The same correlation was observed for the methacrylated macromers with lower (10%) modification. Macromers with a higher degree of methacrylation (29%) showed significantly higher toxicity already after 6-h incubation compared to 2 h. This study seems to be a good indicator for determining the kinetics of the crosslinking reaction by establishing the tolerable time of exposure of cells to the (meth)acrylated macromers. It represents the worst-case scenario, since within

the time frame examined, chains would have already started to crosslink with the addition of an initiator system. If the toxicity of the macromers is low for up to 6 hours, cells can be exposed to them for that time interval, during which crosslinking will be completed and the detrimental effects of the (meth)acrylate end groups should be eliminated. The presence of reactive end groups, such as the (meth)acrylate groups, contributes to the toxicity of materials. Increasing degrees of modification drastically reduce cell viability, as can be seen in Figure C.9.

To the best of our knowledge, there are only a few studies that investigate the cytocompatibility of (meth)acrylated, uncrosslinked macromers. De Groot *et al.*[22] showed that methacrylate- and hydroxyethyl methacrylate-derivatized dextran had comparably low toxicity with unmodified dextran over an incubation period of 72 h at a 100 mg/mL concentration. Poly(ethylene glycol) diacrylate (PEG-DA) (molecular weight 3.4 kDa) showed similar cytotoxicity patterns at 24 h as the higher modified (meth)acrylated thermogelling macromers in our study, whereas PEG-DA of lower molecular weight (575 Da) showed high toxicity already after 2-h incubation.[13] Extracts of the crosslinker propylene fumarate diacrylate, a low molecular weight and comparably hydrophobic macromer, were found to be very toxic on cells.[23] Many studies have been carried out to elucidate the cytotoxic effects of acrylic and methacrylic monomers as these materials are extensively used in dentistry. In general, acrylic monomers have been reported to be more toxic than corresponding methacrylic analogues.[24, 25] Some researchers

suggested that toxicity correlates with monomer lipophilicity, and that cytotoxic effects of (meth)acrylates are exerted through reacting with and disrupting the lipid bilayer in cell membranes.[26, 27] Other researchers did not find toxicity related to hydrophobicity and identified a mechanism involving the covalent binding of electrophilic reactive (meth)acrylates to cellular targets such as thiol groups on proteins through a Michael-type reaction.[28, 29] In the present case, we found acrylated macromers to be more cytotoxic than methacrylated ones after 2-h incubation, which is in agreement with the statements presented above. However, after 24 hours, this phenomenon seemed to have reversed. Figure C.10 shows the fraction of live cells at 2 and 24 hours as a function of transition temperature of the macromer solutions. Our previous studies[11] showed that the hydrogel stability at 37 °C is proportional to the LCST of the macromer solutions. Hydrogels fabricated of macromers with low transition temperatures tend to phase-separate and precipitate faster. This offers an explanation for the higher toxicity observed for methacrylates as compared to acrylates with the same degree of modification after 24-h incubation. At 2 hours, the gels are still stable, but the precipitation over the 24-h time interval happens sooner for macromers with lower transition temperatures, as in the case of methacrylates. A lower transition temperature and faster precipitation prolongs the period in which non-gelled, (meth)acrylated, reactive macromer chains interact directly with structures of the cells, such as membranes, as opposed to chains that are fully assembled into a gel. This increased contact enhances the toxic action of the methacrylated

macromers after 24 hours. The results suggest that when (meth)acrylates form a gel, their cytotoxic effects are diminished. Macromer toxicity seems to be associated with their soluble form, or in this specific case, precipitated, and not when the macromolecular chains are assembled in a physical network. These findings may have important implications with regard to hydrogel use for cell encapsulation.

C.5 Conclusions

This study demonstrated the good cytocompatibility properties of a novel type of thermally responsive, chemically crosslinkable macromers. It was found that unmodified macromers with number-average molecular weights in the range of approximately 1500 to 3000 Da with varying molecular compositions allowed for high cell viability over a 24-h time interval. The chemical modification with an acrylate or methacrylate group enables the chemical crosslinking of the macromers. We investigated the effect of the (meth)acrylate derivatization on the toxicity of uncrosslinked macromers and determined that a 6-h time frame for crosslinking completion would allow for viable cell encapsulation. Increased degrees of modification were shown to decrease the thermal transition temperature as well as the cytocompatibility of the macromers. Formulations with the parameters established in this study will be used towards the fabrication of injectable, thermoresponsive, *in situ* forming hydrogel systems for cell and drug delivery.

C.6 References

1. Peppas, N. A.; Bures, P.; Leobandung, W.; Ichikawa, H., Hydrogels in pharmaceutical formulations. *Eur J Pharm Biopharm* **2000,** 50, (1), 27-46.

2. Bryant, S. J.; Anseth, K. S., The effects of scaffold thickness on tissue engineered cartilage in photocrosslinked poly(ethylene oxide) hydrogels. *Biomaterials* **2001,** 22, (6), 619-26.

3. Kretlow, J. D.; Klouda, L.; Mikos, A. G., Injectable matrices and scaffolds for drug delivery in tissue engineering. *Adv Drug Deliv Rev* **2007,** 59, (4-5), 263-73.

4. Temenoff, J. S.; Mikos, A. G., Injectable biodegradable materials for orthopedic tissue engineering. *Biomaterials* **2000,** 21, (23), 2405-12.

5. Temenoff, J. S.; Park, H.; Jabbari, E.; Conway, D. E.; Sheffield, T. L.; Ambrose, C. G.; Mikos, A. G., Thermally cross-linked oligo(poly(ethylene glycol) fumarate) hydrogels support osteogenic differentiation of encapsulated marrow stromal cells in vitro. *Biomacromolecules* **2004,** 5, (1), 5-10.

6. Klouda, L.; Mikos, A. G., Thermoresponsive hydrogels in biomedical applications. *Eur J Pharm Biopharm* **2008,** 68, (1), 34-45.

7. Cellesi, F.; Tirelli, N.; Hubbell, J. A., Towards a fully-synthetic substitute of alginate: development of a new process using thermal gelation and chemical cross-linking. *Biomaterials* **2004,** 25, (21), 5115-24.

8. Lee, B. H.; West, B.; McLemore, R.; Pauken, C.; Vernon, B. L., In-situ injectable physically and chemically gelling NIPAAm-based copolymer system for embolization. *Biomacromolecules* **2006,** 7, (6), 2059-64.

9. Robb, S. A.; Lee, B. H.; McLemore, R.; Vernon, B. L., Simultaneously physically and chemically gelling polymer system utilizing a poly(NIPAAm-co-cysteamine)-based copolymer. *Biomacromolecules* **2007,** 8, (7), 2294-300.

10. Vermonden, T.; Fedorovich, N. E.; van Geemen, D.; Alblas, J.; van Nostrum, C. F.; Dhert, W. J.; Hennink, W. E., Photopolymerized thermosensitive hydrogels: synthesis, degradation, and cytocompatibility. *Biomacromolecules* **2008,** 9, (3), 919-26.

11. Hacker, M. C.; Klouda, L.; Ma, B. B.; Kretlow, J. D.; Mikos, A. G., Synthesis and characterization of injectable, thermally and chemically gelable, amphiphilic poly(N-isopropylacrylamide)-based macromers. *Biomacromolecules* **2008,** 9, (6), 1558-70.

12. Betz, M. W.; Modi, P. C.; Caccamese, J. F.; Coletti, D. P.; Sauk, J. J.; Fisher, J. P., Cyclic acetal hydrogel system for bone marrow stromal cell encapsulation and osteodifferentiation. *J Biomed Mater Res A* **2008,** 86, (3), 662-70.

13. Shin, H.; Temenoff, J. S.; Mikos, A. G., In vitro cytotoxicity of unsaturated oligo[poly(ethylene glycol) fumarate] macromers and their cross-linked hydrogels. *Biomacromolecules* **2003,** 4, (3), 552-60.

14. Temenoff, J. S.; Shin, H.; Conway, D. E.; Engel, P. S.; Mikos, A. G., In vitro cytotoxicity of redox radical initiators for cross-linking of oligo(poly(ethylene glycol) fumarate) macromers. *Biomacromolecules* **2003,** 4, (6), 1605-13.

15. Nicodemus, G. D.; Bryant, S. J., Cell encapsulation in biodegradable hydrogels for tissue engineering applications. *Tissue Eng Part B Rev* **2008,** 14, (2), 149-65.

16. Southall, N. T.; Dill, K. A.; Haymet, A. D. J., A View of the Hydrophobic Effect. *Journal of Physical Chemistry B* **2002,** 106, (3), 521-533.

17. Kim, N. S.; Lee, G. M., Response of recombinant Chinese hamster ovary cells to hyperosmotic pressure: effect of Bcl-2 overexpression. *J Biotechnol* **2002,** 95, (3), 237-48.

18. Mockridge, J. W.; Benton, E. C.; Andreeva, L. V.; Latchman, D. S.; Marber, M. S.; Heads, R. J., IGF-1 regulates cardiac fibroblast apoptosis induced by osmotic stress. *Biochem Biophys Res Commun* **2000,** 273, (1), 322-7.

19. Zhu, M. M.; Goyal, A.; Rank, D. L.; Gupta, S. K.; Vanden Boom, T.; Lee, S. S., Effects of elevated pCO2 and osmolality on growth of CHO cells and production of antibody-fusion protein B1: a case study. *Biotechnol Prog* **2005,** 21, (1), 70-7.

20. Kaihara, S.; Matsumura, S.; Fisher, J. P., Cellular responses to degradable cyclic acetal modified PEG hydrogels. *J Biomed Mater Res A* **2008**.

21. Du, J. Z.; Sun, T. M.; Weng, S. Q.; Chen, X. S.; Wang, J., Synthesis and characterization of photo-cross-linked hydrogels based on biodegradable polyphosphoesters and poly(ethylene glycol) copolymers. *Biomacromolecules* **2007,** 8, (11), 3375-81.

22. De Groot, C. J.; Van Luyn, M. J.; Van Dijk-Wolthuis, W. N.; Cadee, J. A.; Plantinga, J. A.; Den Otter, W.; Hennink, W. E., In vitro biocompatibility of biodegradable dextran-based hydrogels tested with human fibroblasts. *Biomaterials* **2001,** 22, (11), 1197-203.

23. Timmer, M. D.; Shin, H.; Horch, R. A.; Ambrose, C. G.; Mikos, A. G., In vitro cytotoxicity of injectable and biodegradable poly(propylene fumarate)-based networks: unreacted macromers, cross-linked networks, and degradation products. *Biomacromolecules* **2003,** 4, (4), 1026-33.

24. Yoshii, E., Cytotoxic effects of acrylates and methacrylates: relationships of monomer structures and cytotoxicity. *J Biomed Mater Res* **1997,** 37, (4), 517-24.

25. Atsumi, T.; Fujisawa, S.; Tonosaki, K., (Meth)acrylate monomer-induced cytotoxicity and intracellular Ca(2+) mobilization in human salivary gland carcinoma cells and human gingival fibroblast cells related to monomer hydrophobicity. *Biomaterials* **2006,** 27, (34), 5794-800.

26. Fujisawa, S.; Atsumi, T.; Kadoma, Y., Cytotoxicity of methyl methacrylate (MMA) and related compounds and their interaction with dipalmitoylphosphatidylcholine (DPPC) liposomes as a model for biomembranes. *Oral Dis* **2000,** 6, (4), 215-21.

27. Fujisawa, S.; Kadoma, Y.; Komoda, Y., 1H and 13C NMR studies of the interaction of eugenol, phenol, and triethyleneglycol dimethacrylate with phospholipid liposomes as a model system for odontoblast membranes. *J Dent Res* **1988,** 67, (11), 1438-41.

28. Schweikl, H.; Spagnuolo, G.; Schmalz, G., Genetic and cellular toxicology of dental resin monomers. *J Dent Res* **2006,** 85, (10), 870-7.

29. Chan, K.; O'Brien, P. J., Structure-activity relationships for hepatocyte toxicity and electrophilic reactivity of alpha,beta-unsaturated esters, acrylates and methacrylates. *J Appl Toxicol* **2008,** 28, (8), 1004-15.

C.7 Figures

Table C.1. Molecular composition, molecular weight characteristics and transition temperature of unmodified thermogelling macromers[a]

Molecular weight group

Molar Composition	M_n [Da]	PI	T_η [°C]
PEDAS/NiPAAm/AAm/HEA			
1/15.4/2.6/2	1750±370	3.4±0.6	31.6±0.3
1/15.4/2.6/2	2300±140	2.9±0.3	32.7±0.8
1/15.4/2.6/2	2440±420	3.0±0.8	32.6±0.2
1/15.4/2.6/2	2830±170	3.6±0.5	31.5±1.2

Composition group

Molar Composition	Acrylic Monomer Ratios (%HEA/%AAm)	M_n [Da]	PI	T_η [°C]
PEDAS/NiPAAm/AAm/HEA				
1/16/0/4	20/0	3050±140	2.9±0.2	23.2±0.1
1/15.4/1/3.6	18/5	3810±260	3.0±0.3	26.5±0.1
1/15.4/2.6/2	10/13	1750±370	3.4±0.6	31.6±0.3
1/14/3/3	15/15	2700±120	2.7±0.1	33.7±0.2
1/16/4/0	0/20	1700±80	2.7±0.1	38.7±3.0

LCST group

Molar Composition	M_n [Da]	PI	T_η [°C]
PEDAS/NiPAAm/AAm/HEA			
1/20/0/0	2560±250	2.7±0.1	27.2±0.2
1/18.5/1.5/0	2450±280	2.6±0.2	30.6±0.4
1/16/4/0	1700±80	2.7±0.1	38.7±3.0
1/16/4/0	1370±100 [b]	2.9±0.1 [b]	40.8±1.4
1/14/6/0	1470±250	6.9±2.1	43.5±2.3

[a] Molecular weight characteristics were obtained by gel permeation chromatography. The transition temperature T_η was determined from rheological measurements of 10% (w/v) macromer solutions as the inflection point of the temperature-complex viscosity curve. Values represent means ± standard deviation for a sample size of n=3. Table is adapted from [11].

[b] The average and range for this formulation were determined for n=2.

Table C.2. Acrylated or methacrylated thermogelling macromers with varying degrees of modification and their transition temperatures [c]

Molar Composition: PEDAS/NiPAAm/AAm/HEA : 1/15/3.5/1.5		
Modification	**% of hydroxyls modified**	**T_{DSC} [°C]**
No modification	0	35.6 ± 0.5
Acrylation	8	31.2 ± 0.2
Acrylation	32	24.6 ± 0.3
Acrylation	49	20.8 ± 0.9
Methacrylation	10	24.1 ± 0.6
Methacrylation	29	15.2 ± 0.9

[c] The degree of hydroxyl group conversion was determined by ^{1}H-NMR. The transition temperature T_{DSC} was obtained by differential scanning calorimetry (DSC) for 10% (w/v) macromer solutions. Values represent means ± standard deviation for a sample size of n=3. Table is adapted from [11].

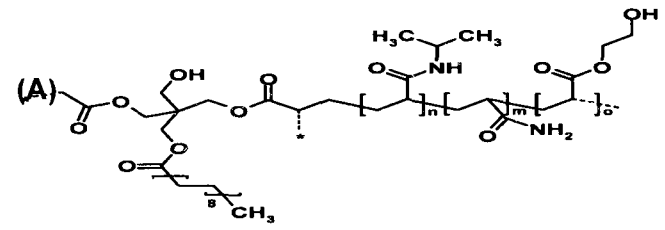
(A)
OH
O
O
O

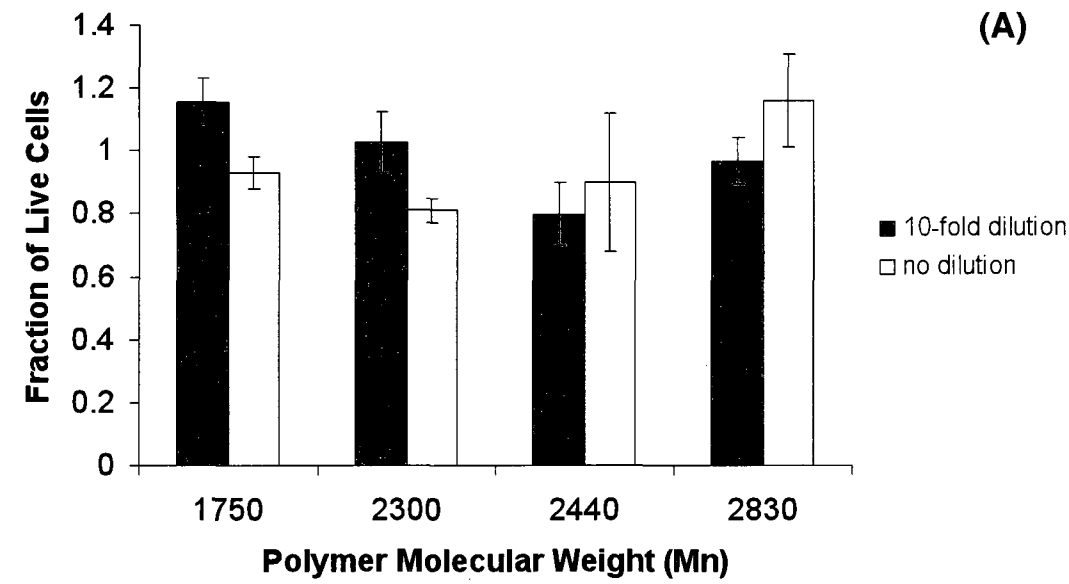

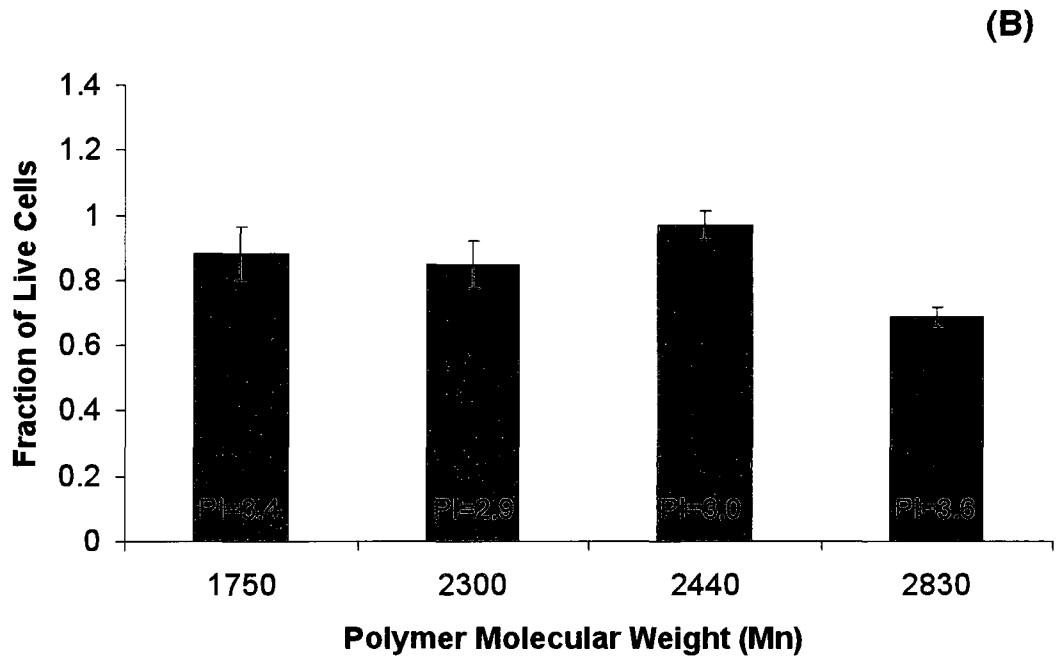

Figure C.2. Cell viability after 24-h incubation with macromers of different number-average molecular weights and polydispersity indices (PI). A) Leachables assay: incubation with hydrogel supernatant B) Direct contact assay: incubation with hydrogel. Error bars represent standard deviation; n= 3-5.

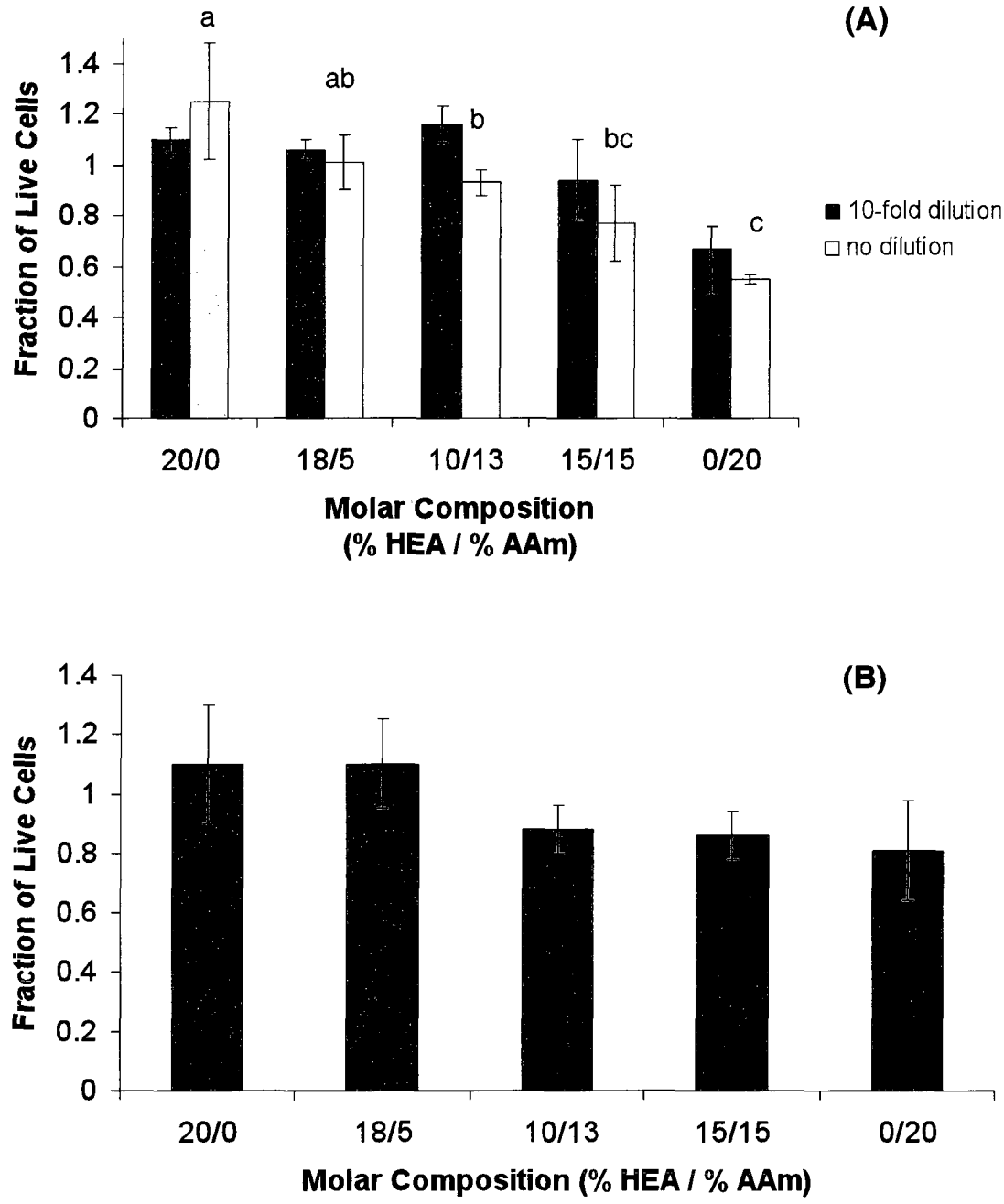

Figure C.3. Cell viability after 24-h incubation with macromers of different molecular ratios of 2-hydroxyethyl acrylate (HEA) and acrylamide (AAm) in their compositions. A) Leachables assay: incubation with hydrogel supernatant B) Direct contact assay: incubation with hydrogel. Error bars represent standard deviation; n= 3-5. Characters on experimental groups indicate statistically significant differences when groups are not marked with the same letter ($p<0.05$).

For clarity purposes, in figure (A) differences are marked for undiluted group only.

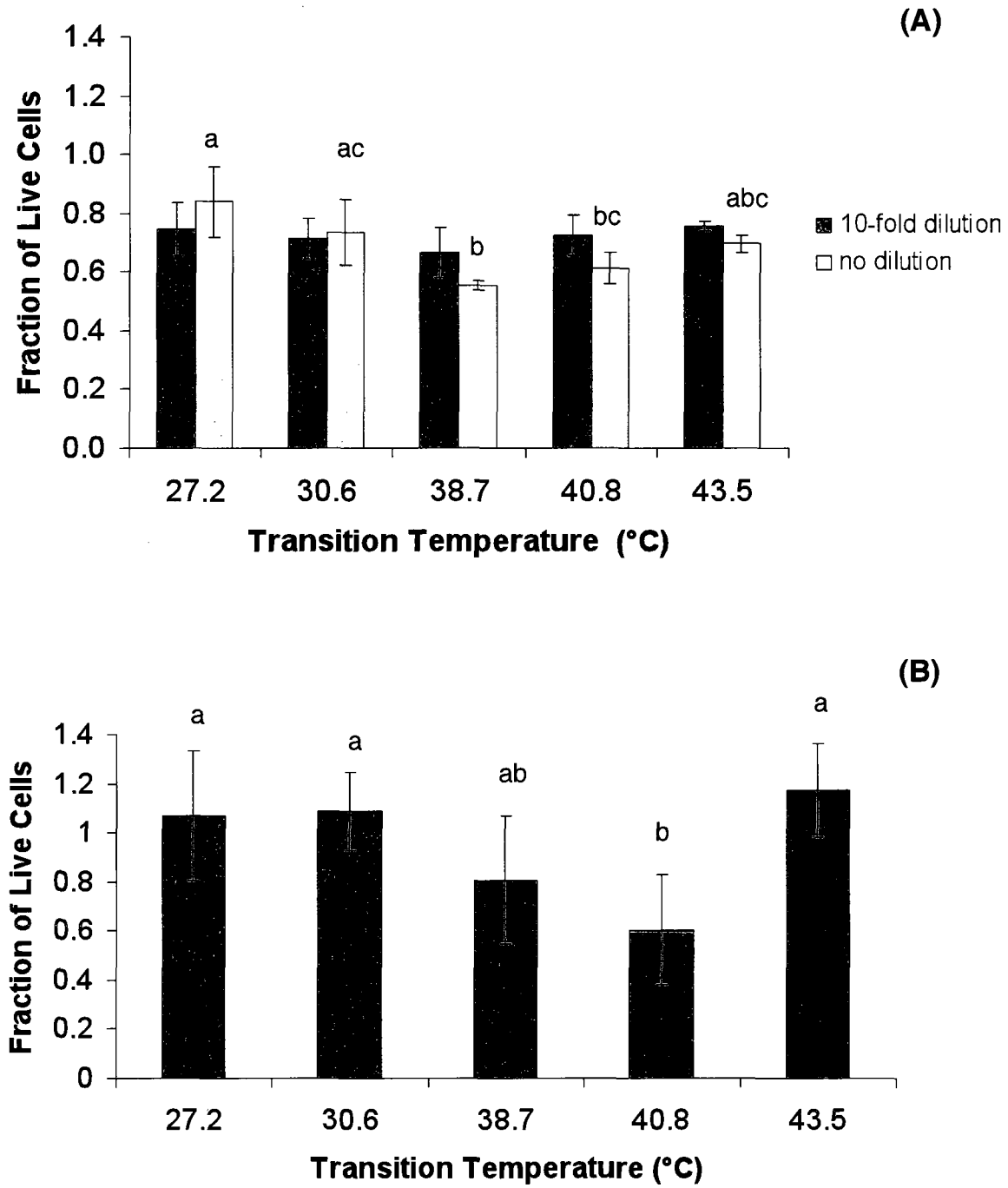

Figure C.4. Cell viability after 24-h incubation with macromers of different transition temperatures (T_n). A) Leachables assay: incubation with hydrogel supernatant B) Direct contact assay: incubation with hydrogel. Error bars represent standard deviation; n= 5. Experimental groups denoted by different

letters show statistically significant differences ($p<0.05$). For clarity purposes, in figure (A) differences are marked for undiluted group only.

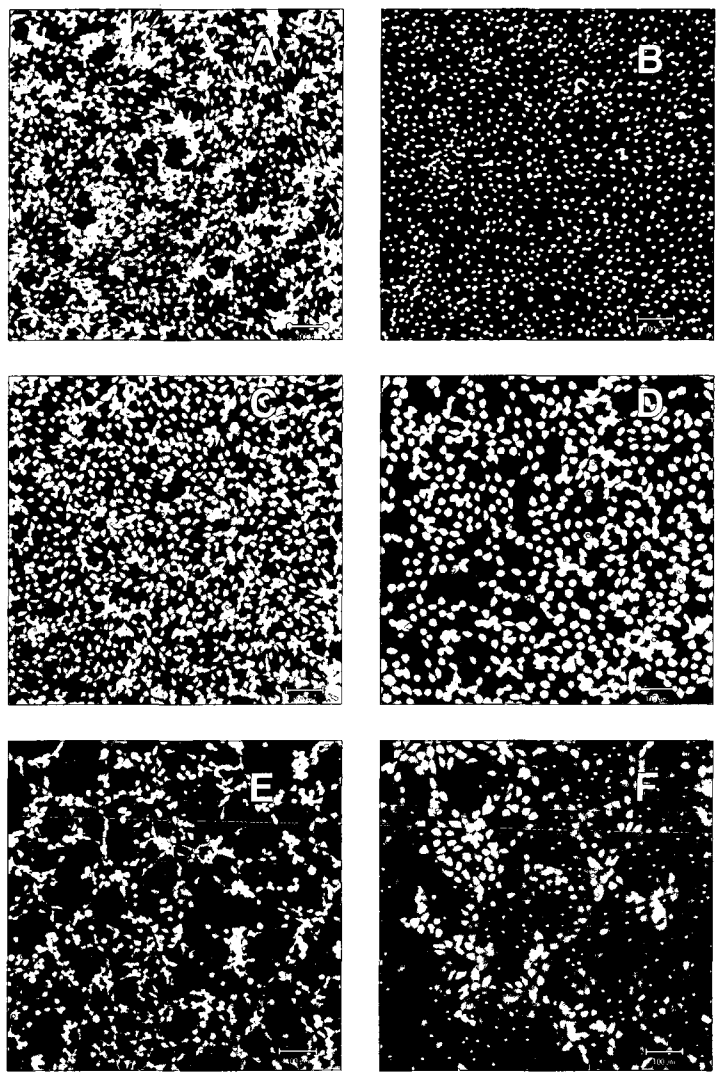

Figure C.5. Fluorescence microscopy images of fibroblasts after 24-h exposure to hydrogel leachables or in direct contact with hydrogel and treatment with Live/Dead reagent. Letters denote the positive control (A), negative control (B), treatment with a formulation composed of $PEDAS_1NiPAAm_{20}$ in leachables assay (C) and direct contact (D), treatment with a formulation composed of $PEDAS_1NiPAAm_{16}AAm_4$ in polymer-conditioned media (E) and direct contact (F). Scale bar indicates 100 μm.

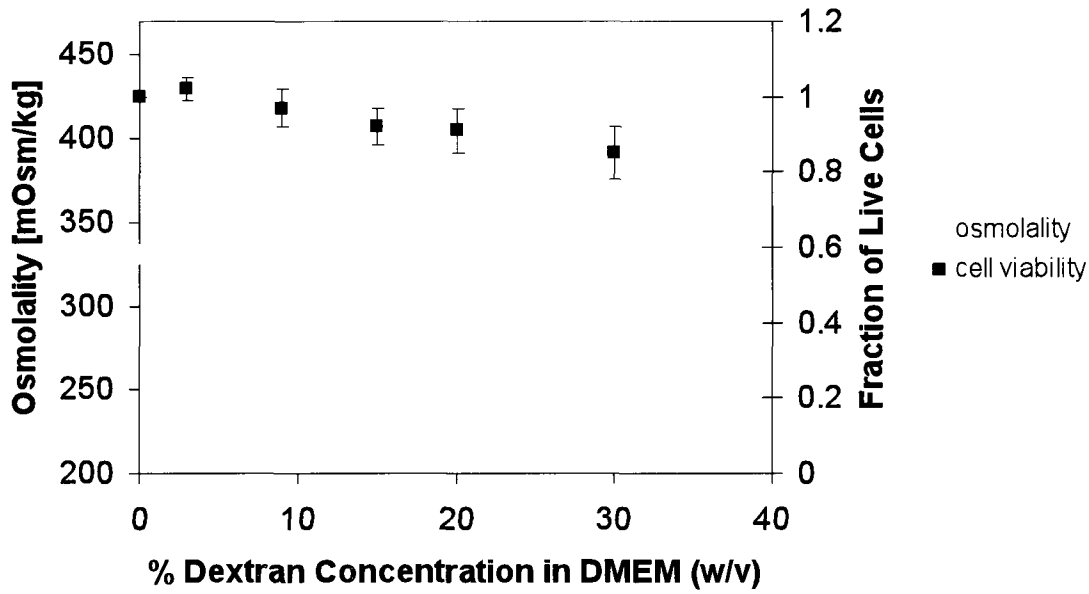

Figure C.6. Osmolality of dextran solutions of different concentrations and cell viability values after 24-h incubation with these solutions. Differences in cytocompatibility are not statistically significant ($p<0.05$).

(A)

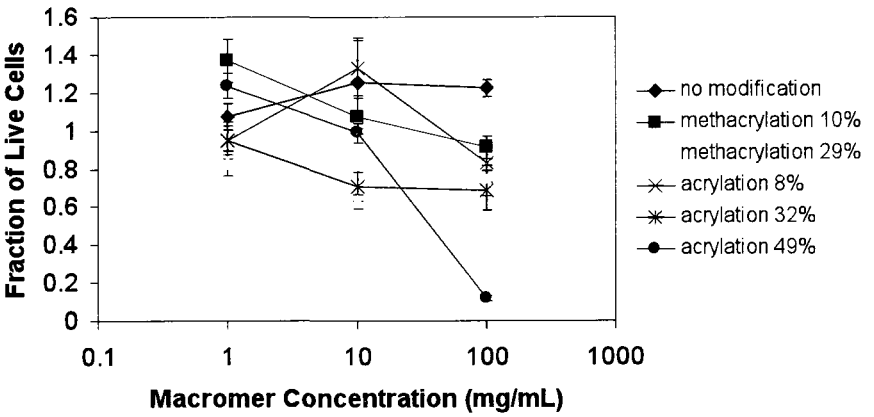
Fraction of Live Cells
1.6
1.4
1.2
1
0.8
0.6
0.4
0.2
0
0.1
1
10
100
1000
Macromer Concentration (mg/mL)
no modification
methacrylation 10%
methacrylation 29%
acrylation 8%
acrylation 32%
acrylation 49%

(B)

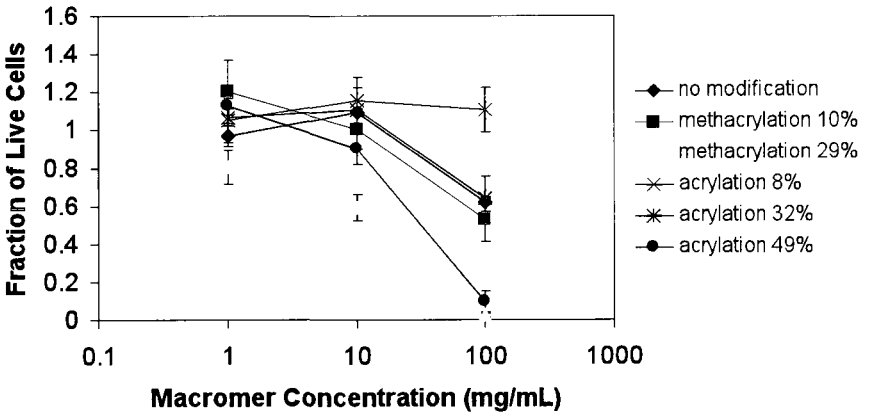
Fraction of Live Cells
1.6
1.4
1.2
1
0.8
0.6
0.4
0.2
0
0.1
1
10
100
1000
Macromer Concentration (mg/mL)
no modification
methacrylation 10%
methacrylation 29%
acrylation 8%
acrylation 32%
acrylation 49%

(C)

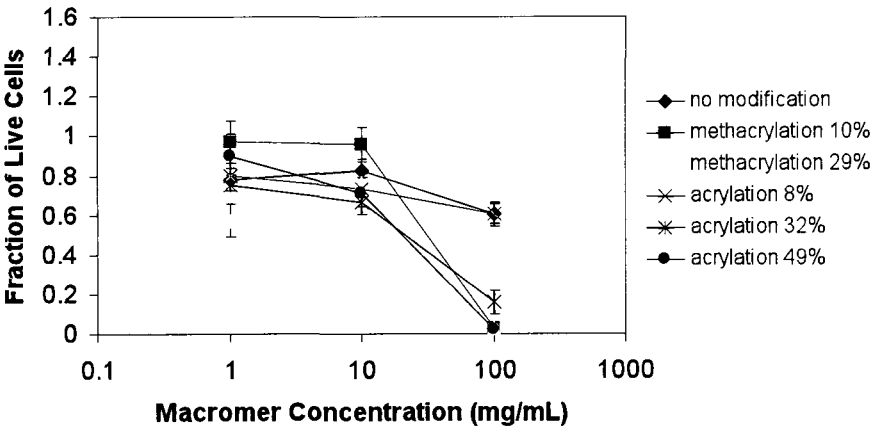
Fraction of Live Cells
1.6
1.4
1.2
1
0.8
0.6
0.4
0.2
0
0.1
1
10
100
1000
Macromer Concentration (mg/mL)
no modification
methacrylation 10%
methacrylation 29%
acrylation 8%
acrylation 32%
acrylation 49%

Figure C.7. Cell viability after (A) 2-h, (B) 6-h and (C) 24-h incubation with various concentrations of (meth)acrylated macromers with a theoretical composition of $PEDAS_1$ $NiPAAm_{15}$:$AAm_{3.5}HEA_{1.5}$. Error bars represent standard deviation for n=3-5.

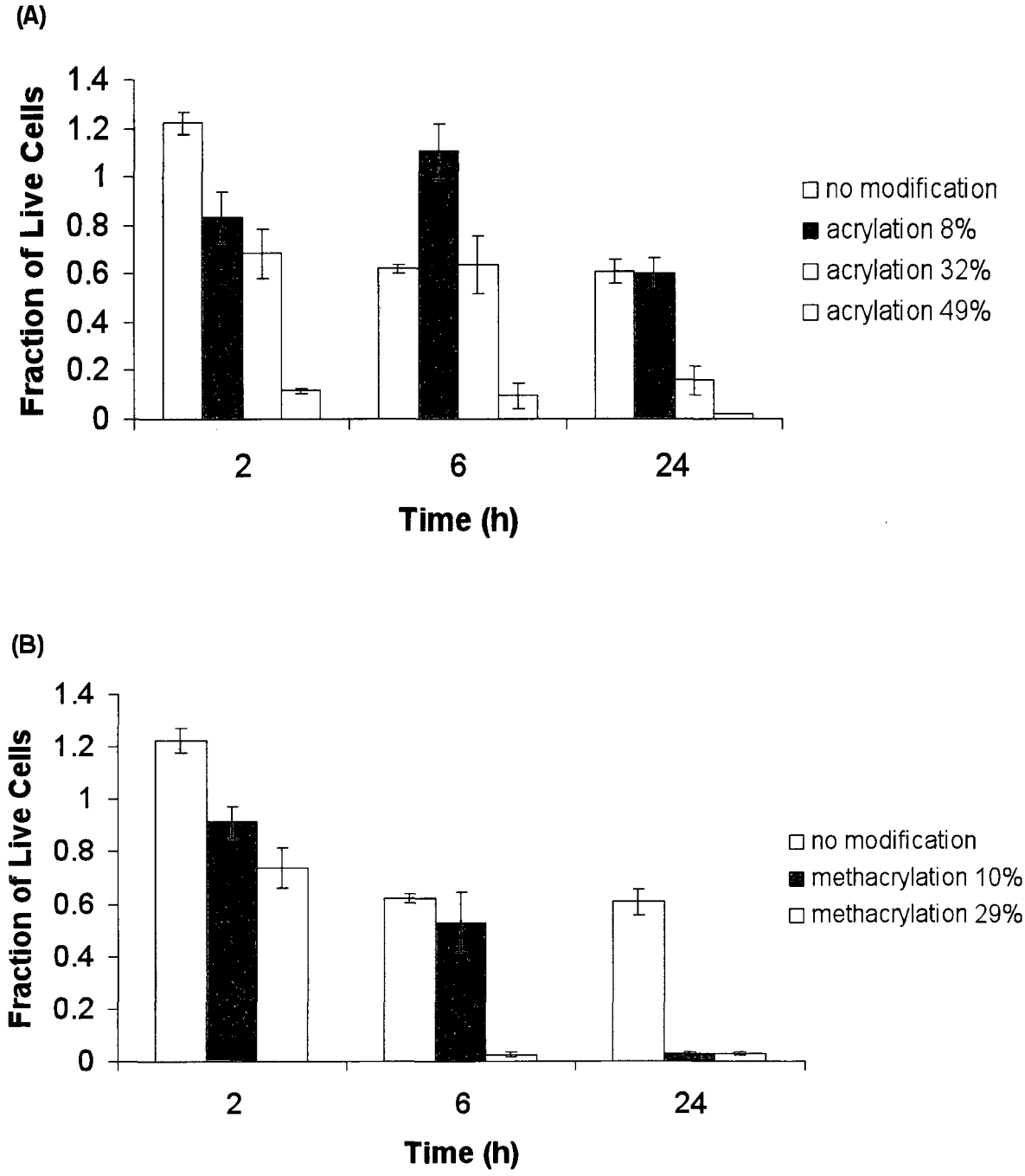

Figure C.8. Cell viability over time after exposure to 100 mg/mL solutions of (A) acrylated and (B) methacrylated macromers, with an unmodified composition as a control. Error bars represent standard deviation for n=3-5. Statistically significant

differences over time within one composition group are marked with an asterisk ($p<0.05$).

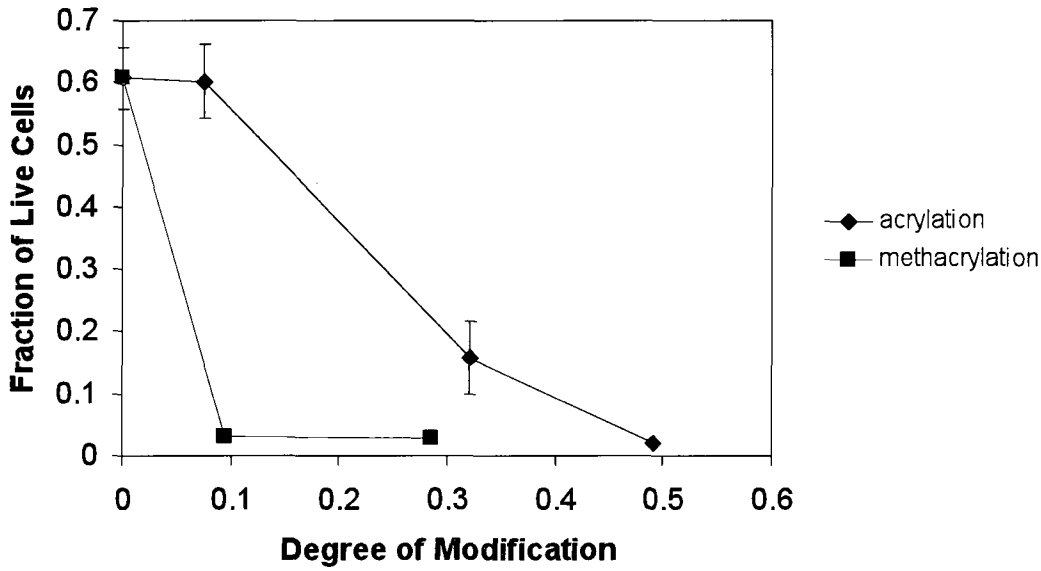

Figure C.9. Cell viability after 24-h incubation with 100 mg/mL solutions of acrylated and methacrylated macromers with different degrees of modification. Modification is expressed as the fraction of hydroxyl moieties substituted by (meth)acrylate groups. Error bars represent standard deviation for n=3-5.

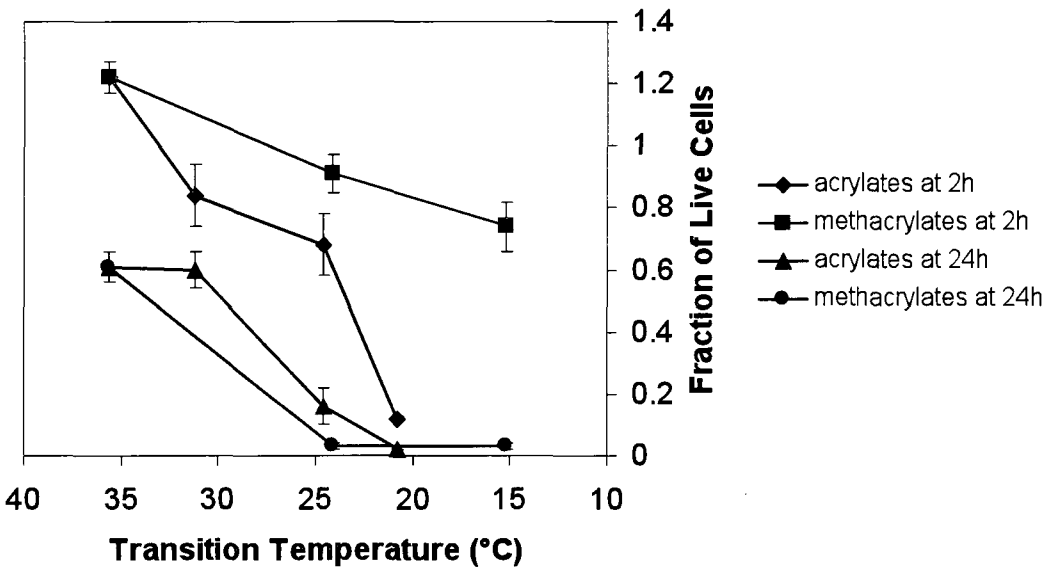

Figure C.10. Cell viability after 2 and 24-h incubation with 100 mg/mL solutions of acrylated and methacrylated macromers as a function of their thermal transition temperature. Error bars represent standard deviation for n=3-5.